Minna Hakkarainen   *Editor*

Mass Spectrometry of Polymers – New Techniques

Springer

248
Advances in Polymer Science

Advances in Polymer Science

Recently Published and Forthcoming Volumes

Mass Spectrometry of Polymers – New Techniques

Volume Editor: Minna Hakkarainen

With contributions by

N. Aminlashgari · W. Buchberger · J. Hacaloglu ·
M. Hakkarainen · P. Mischnick · M. Stiftinger

Editor
Prof. Minna Hakkarainen
Department of Fibre and Polymer Technology
Royal Institute of Technology (KTH)
Teknikringen 56-58
100 44 Stockholm
Sweden
minna@polymer.kth.se

Printed on acid-free paper

Advances in Polymer Sciences
Also Available Electronically

Advances in Polymer Sciences is included in Springer's eBook package *Chemistry and Materials Science*. If a library does not opt for the whole package the book series may be bought on a subscription basis. Also, all back volumes are available electronically.

For all customers who have a standing order to the print version of *Advances in Polymer Sciences*, we offer free access to the electronic volumes of the Series published in the current year via SpringerLink.

If you do not have access, you can still view the table of contents of each volume and the abstract of each article by going to the SpringerLink homepage, clicking on "Browse by Online Libraries", then "Chemical Sciences", and finally choose *Advances in Polymer Science*.

You will find information about the

– Editorial Board
– Aims and Scope
– Instructions for Authors
– Sample Contribution

at springer.com using the search function by typing in *Advances in Polymer Sciences*.

Color figures are published in full color in the electronic version on SpringerLink.

Aims and Scope

The series presents critical reviews of the present and future trends in polymer and biopolymer science including chemistry, physical chemistry, physics and material science. It is addressed to all scientists at universities and in industry who wish to keep abreast of advances in the topics covered.

Review articles for the topical volumes are invited by the volume editors. As a rule, single contributions are also specially commissioned. The editors and publishers will, however, always be pleased to receive suggestions and supplementary information. Papers are accepted for *Advances in Polymer Science* in English.

In references *Advances in Polymer Sciences* is abbreviated as *Adv Polym Sci* and is cited as a journal.

Special volumes are edited by well known guest editors who invite reputed authors for the review articles in their volumes.

Impact Factor in 2010: 6.723; Section "Polymer Science": Rank 3 of 79

Preface

Mass spectrometry has become an irreplaceable tool for the characterization of ever more advanced polymer structures and polymer compositions. Considering the rapid developments in the field of mass spectrometry and the appearance of new interesting techniques, I am sure that in the coming years mass spectrometry will even further strengthen its position as an invaluable polymer characterization tool. The potential is still far from being fully exploited. Chapter 1 of this book reviews newer mass spectrometric techniques that are emerging or being established as polymer characterization tools. Here, ambient desorption ionization-mass spectrometry techniques, which offer intriguing new possibilities for direct analysis of polymer surfaces, are typical examples.

Chapter 2 presents liquid chromatography–mass spectrometry and capillary electrophoresis–mass spectrometry techniques for analysis of low-molecular weight additives and impurities in polymeric materials. This is an important area as we become more and more aware of our environment and the potential influence of chemicals. The total composition and possible migration of additives and unknown degradation products from polymers is thus of outmost interest. Many regulations already exist concerning the composition of, for example, food contact materials and medical materials, and new regulations can be expected in an increasing number of fields. Chapter 3 concerns direct insertion probe-mass spectrometry of polymers. Many characterization techniques require dissolution of the sample. Some polymers are, however, not soluble. In Chap. 3, examples of the application of direct insertion probe-mass spectrometry for structural and compositional analysis of cross-linked, or for other reasons, insoluble polymers are given. In addition, applications for thermal stability and decomposition mechanism studies are demonstrated.

Mass spectrometry is also an increasingly important technique for structural characterization of biomolecules. With the ongoing change from petroleum-based to bio-based materials, the proper characterization of biomolecules, as well as various monomers and intermediates from renewable resources, is an area of increasing importance. Chapter 4 summarizes the current knowledge in mass spectrometric characterization of oligo-and polysaccharides and their chemical

modifications. The last chapter explores the potential of electrospray ionization-mass spectrometry in revealing the molecular level reactions and changes taking place during polymer degradation. The improved understanding of degradation reactions is crucial for the development of more stable and inert polymeric materials, as well as for the development of truly environmentally benign degradable materials with controlled degradation mechanisms. Finally, I would like to thank all the authors who contributed to this book. I am convinced that a wider use of mass spectrometry in polymer analysis will increase our understanding of these fascinating materials with enormous structural variety. This in turn will lead to faster development of better functioning and more sustainable polymer products. I hope this book will inspire more people to explore the world of mass spectrometry for molecular level understanding of the multilevel complexity of polymeric materials.

November, 2011   Minna Hakkarainen

Contents

Emerging Mass Spectrometric Tools for Analysis of Polymers and Polymer Additives

Nina Aminlashgari and Minna Hakkarainen

Abstract The field of mass spectrometry has experienced enormous developments in the last few years. New interesting mass spectrometric techniques have arrived and there have been further developments in the existing methods that have opened up new possibilities for the analysis of increasingly complex polymer structures and compositions. Some of the most interesting emerging techniques for polymer analysis are briefly reviewed in this paper. These include new developments in laser desorption ionization techniques, like solvent-free matrix-assisted laser desorption ionization (solvent-free MALDI) and surface-assisted laser desorption ionization (SALDI) mass spectrometry, and the developments in secondary ion mass spectrometry (SIMS), such as gentle-SIMS and cluster SIMS. Desorption electrospray ionization (DESI) mass spectrometry and direct analysis in real time (DART) mass spectrometry offer great possibilities for analysis of solid samples in their native form, while mobility separation prior to mass spectrometric analysis in ion mobility spectrometry (IMS) mass spectrometry further facilitates the analysis of complex polymer structures. The potential of these new developments is still largely unexplored, but they will surely further strengthen the position of mass spectrometry as an irreplaceable tool for polymer characterization.

Keywords Additives · Degradation products · Desorption ionization mass spectrometry · Laser desorption ionization mass spectrometry · Mass spectrometry · Polymer analysis · Secondary ion mass spectrometry

N. Aminlashgari and M. Hakkarainen (✉)
Department of Fibre and Polymer Technology, School of Chemical Science and Engineering,
Royal Institute of Technology (KTH), 100 44 Stockholm, Sweden
e-mail: minna@polymer.kth.se

Contents

Abbreviations

APCI	Atmospheric pressure chemical ionization
APPI	Atmospheric pressure photoionization
BFRs	Brominated flame retardants
CHCA	α-Cyano-4-hydroxycinnamic acid
CID	Collision-induced dissociation
CNTs	Carbon nanotubes
DART	Direct analysis in real time
DBP	Dibutyl phthalate
DEHP	Di-2-ethylhexyl phthalate
DESI	Desorption electrospray ionization
DHB	2,5-Dihydroxybenzonic acid
DIDP	Diisodecyl phthalate
DINP	Diisononyl phthalate
DIOS	Desorption ionization on porous silicon
DNOP	Di-n-octyl phthalate
ECD	Electron-capture dissociation
ERM	European Reference Material
ESI-MS	Electrospray ionization-mass spectrometry
FTICR-MS	Fourier transform ion cyclotron resonance- mass spectrometry
FTMS	Fourier transform mass spectrometry
GC-MS	Gas chromatography–mass spectrometry
HDPE	High density polyethylene

HPLC-UV	High performance liquid chromatography–ultraviolet
ICP-MS	Inductive coupled plasma–mass spectrometry
IMS-MS	Ion mobility spectrometry–mass spectrometry
LC	Liquid chromatography
LDI-MS	Laser desorption ionization–mass spectrometry
LOD	Limits of detection
m/z	Mass-to-charge ratio
MALDI-MS	Matrix-assisted laser desorption ionization–mass spectrometry
MS	Mass spectrometry
MS/MS	Tandem mass spectrometry
NaI	Sodium iodide
PAE	Phthalic acid esters
PALDI-MS	Polymer-assisted laser desorption ionization–mass spectrometry
PAM	Polyacrylamide
PBBs	Polybrominated biphenyls
PBDEs	Polybrominated diphenyl ethers
PDMS	Poly(dimethyl siloxane)
PEG	Poly(ethylene glycol)
PET	Poly(ethylene terephthalate)
PGS	Pyrolytic highly oriented graphite polymer film
PLA	Polylactide
PMMA	Polymethylmethacrylate
PMS	Poly(α-methyl styrene)
PP	Polypropylene
ppb	Parts per billion
PPEs	Polyphosphoesters
PPG	Poly(propylene glycol)
PS	Polystyrene
PTMG	Poly(tetramethylene glycol)
PVC	Polyvinyl chloride
S/N	Signal-to-noise ratio
SALDI-MS	Surface-assisted laser desorption ionization-mass spectrometry
SIMS	Secondary ion mass spectrometry
TFA	Trifluoroacetic acid
TOF	Time-of-flight
VOCs	Volatile organic compounds

1   Introduction

Soft ionization mass spectrometric techniques have become dominant tools for analysis of polymers and polymer additives. Matrix-assisted laser desorption ionization–mass spectrometry (MALDI-MS) together with electrospray ionization–mass spectrometry (ESI-MS) have been two preeminent techniques for

the analysis of higher molecular mass synthetic compounds. The difficulty with ESI-MS is the multiply charged ion adducts when dealing with polymers with high molar mass distribution. Industrial polymeric materials contain several low molecular weight compounds, i.e., additives to enhance properties such as durability, thermo-oxidative stability, or processability. The drawback with MALDI is the difficulty in studying these low molecular weight compounds. The matrix applied in MALDI interferes with the low mass range and often makes it impossible to detect low molecular weight compounds. Two approaches have been to use high molecular weight matrices or to pick a matrix that does not interfere with the analyte signal [1].

The analysis of low molecular weight compounds in polymers is important for many applications to ensure the safe use of plastic products. For example, in the food industry, the quality, environmental, and health controls are important and are followed by agencies such as the US Food and Drug Administration. Moreover, the US Environmental Protection Agency is concerned with the presence of compounds such as bisphenol A and brominated flame retardants (BFRs) in the plastic materials. Different extraction methods combined with gas chromatography–mass spectrometry (GC-MS) and liquid chromatography–mass spectrometry (LC-MS) have been employed with excellent results in many studies of low molecular weight compounds such as additives and polymer degradation products. However, these techniques are often time-consuming because of long sample preparation steps prior to analysis and they have limitations concerning the volatility, solubility, or thermal stability of the analytes.

In order to overcome all these problems, a new generation of mass spectrometric techniques has been developed for analysis of small molecules. This chapter will introduce emerging mass spectrometric tools that do not need a matrix, such as desorption ionization on porous silicon (DIOS) and surface-assisted laser desorption ionization–mass spectrometry (SALDI-MS). The similarity of these two techniques is that they use a surface instead of a matrix as a target for the analysis. Another approach in mass spectrometry has been the direct analysis of solid, liquid, and gas samples with new ambient techniques. These techniques, including direct analysis in real time (DART) and desorption electrospray ionization (DESI), will be further described in Sect. 3. These ambient techniques have especially facilitated the sample preparation step as, in most cases, no sample preparation is needed at all. The possibility of analyzing samples in their untreated, native form introduces a new level of analysis in mass spectrometry.

In this chapter, alternative emerging techniques for mass spectrometric analysis of polymer and polymer additives are introduced and discussed. For instance, another important tool that often contributes to limitations in mass spectrometric analysis is the mass analyzer. Fourier transform ion cyclotron resonance–mass spectrometry (FTICR-MS) provides higher resolving power and higher mass accuracy. Ion mobility spectrometry–mass spectrometry (IMS-MS) on the other hand introduces mobility separation before mass spectrometric analysis, which enhances the possibility of performing structural analysis of complex polymeric materials. In addition, inductive coupled plasma–mass spectrometry (ICP-MS) is a technique that has been used for screening of heavy metal elements or BFRs in polymeric materials.

2 Laser Desorption Ionization Techniques

MALDI-MS is a routine tool for analysis of high molecular mass compounds such as synthetic polymers and biopolymers. Until now it has not been widely applied for the analysis of low molecular mass compounds. However, there has been increased interest in matrix-free methods for laser desorption ionization–mass spectrometry (LDI-MS) during the past decade to enable analysis of low molecular mass compounds. The main reason for this development is the difficulty in analyzing low molecular mass compounds ($<1,000$ m/z) with the traditional MALDI-MS due to matrix cluster ions that tend to interfere with the low mass range of the spectrum. These matrix limitations have led to the introduction of several LDI techniques for the analysis of small molecules.

2.1 Desorption Ionization on Silicon

Siuzdak and coworkers [2] developed one of the first LDI technique without matrix assistance, called DIOS. The porous silicon target is produced by etching silicon wafers to form a nanostructure surface, an effective semiconductive platform for desorption/ionization. The preparation of a DIOS plate is very important since the shape and pore size can influence the efficiency of the LDI. An efficient surface should have high porosity and pore size in order to increase the surface area for energy transfer from the surface to the analyte molecules [3].

DIOS has been successfully applied for the analysis of low molecular mass polymers such as polyesters [4]. Polyesters are common synthetic polymers widely used in industry. Polyesters often have high polydispersity. The presence of low molecular mass components can affect the physical properties of the polyester and therefore it is important to identify these compounds. MALDI measurements with two different matrices, the traditional α-cyano-4-hydroxycinnamic acid (CHCA) and 10,15,20-tetrakis(pentafluorophenyl)porphyrin F20TPP, were compared with the DIOS mass spectrum. The DIOS mass spectrum of the polyester was easier to evaluate because of the absence of interfering matrix cluster ions (see Fig. 1). The signals at $m/z > 2,500$ in the DIOS mass spectrum are more abundant, indicating a smaller mass discrimination in DIOS than in MALDI. The calculation of the average molecular mass for synthetic polymers might, thus, be more accurate with DIOS than with MALDI. Polyethers are also well-known polymers used as lubricants, stabilizers, removers, antifoaming agents, and raw materials for polyurethanes. DIOS has also been successfully applied for the quantitative analysis of polyethers in the form of diol and triol mixtures of poly(propylene glycol) (PPG) [5] and poly(ethylene glycol) (PEG) [6, 7]. This technique also permits the identification of polymer degradation products from, for example, poly(ethylene terephthalate) (PET) [8].
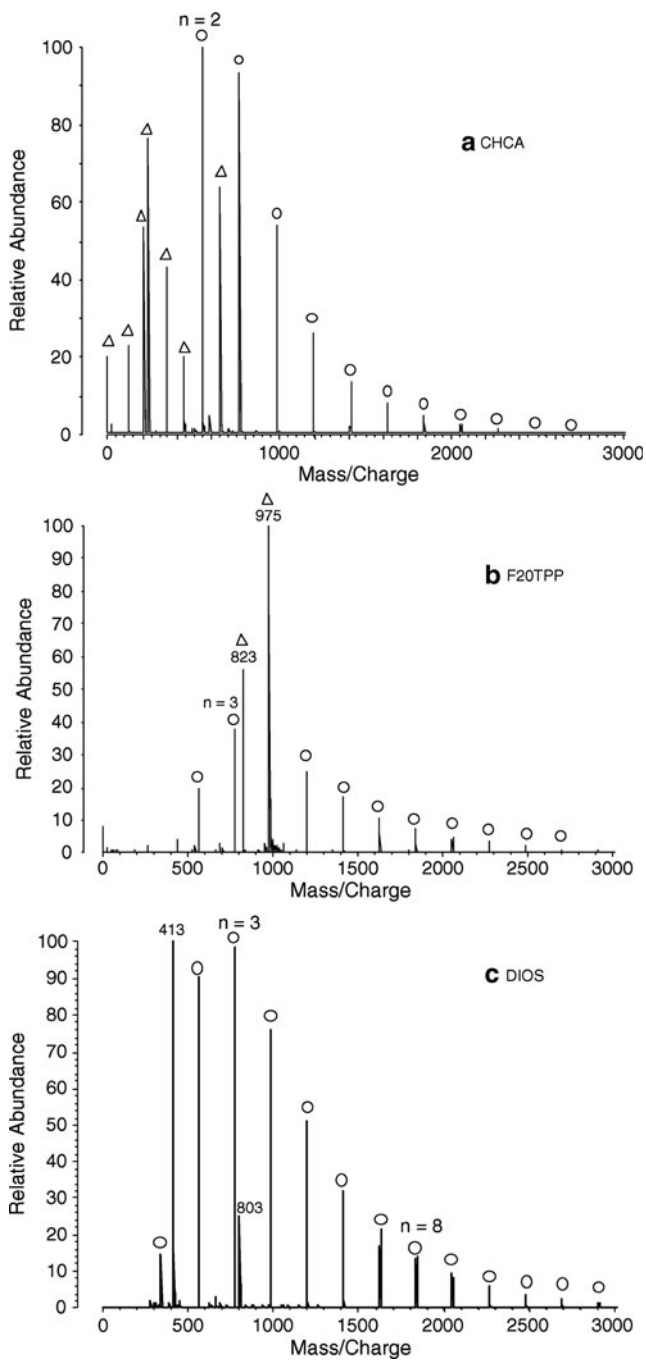
Fig. 1 Mass spectra of a low molecular mass polyester ($M_n = 600$) obtained by different methods: (**a**) MALDI spectrum with CHCA as matrix, (**b**) MALDI spectrum with F20TPP as matrix, and (**c**) DIOS using NaI as cationizing agent. The *circles* and *triangles* represent polyester ions and matrix-related ions respectively. Reprinted from [4] with permission of John Wiley and Sons. Copyright John Wiley and Sons (2004)

2.2 Surface-Assisted Laser Desorption Ionization–Mass Spectrometry

SALDI was originally developed by Tanaka et al. [9] who used cobalt nanoparticles in glycerol to analyze lysozyme and synthetic polymers. However, the method was first named by Sunner et al. [10] who used graphite powder as a matrix. The principal concept of the technique is a solid surface where analytes are deposited and ionized from. The traditional organic matrices in MALDI were replaced with a surface that is tailored to absorb the laser energy and transfer it to the analyte molecules in order to desorb them. The sensitivity and molecular weight distribution of SALDI is comparable with MALDI mass spectra [11]. The solid surfaces used in SALDI are not ionized, which makes it a good technique for analysis of small molecules. The physical and chemical properties of the applied surface have an important role in the desorption and ionization processes and it was soon concluded that carbon was a unique material and that surface roughness was essential. One of the most important features with SALDI is that, in contrast to MALDI, no interference of surface cluster ions is observed in the low mass region, which makes it easier to detect low molecular weight compounds (50–500 m/z).

2.2.1 SALDI Surfaces

Since the development of SALDI a number of materials have been studied for their function as surfaces, ranging from nano- to macroscaled materials. The majority of SALDI substrates can be divided into three different groups: carbon-based materials, silicon-based materials, and metal particle-based substrates. Inorganic nanoparticles have been utilized a lot because they offer a high surface area, simple sample preparation, and flexible deposit of samples under different conditions. The type, form, and size (micro- or nanosized particles) of the SALDI substrates have an important impact on the analytical performance. Among suitable SALDI surfaces are metals [12], metal oxides [13], carbon nanotubes [14], activated carbon [15], graphitized carbon black [16], silicon nitride nanoparticles [17], inorganic materials [18], surfactant-suppressed matrices [19], and some polymers such as poly(glycidyl methacrylate/divinylbenzene) [20].

Recently, gold and platinum metal nanoparticles were utilized as SALDI substrates for analysis of synthetic polymers [21]. Low molecular weight PEG (400, 1,000, 2,000, and 3,000 g mol^{-1}) and poly(methyl methacrylate) (PMMA) (1,890 g mol^{-1}) were analyzed with SALDI and the spectra compared with those from conventional MALDI using the organic matrix CHCA and 2,5-dihydroxybenzonic acid (DHB). It could be observed that gold and platinum nanoparticles yielded a better spectrum with almost no noise in the low mass range. In contrast, the quality of the spectrum obtained with CHCA was not as good. Additionally, it was confirmed that the particle size of the nanoparticles could affect the peak intensities in the mass spectrum. The peak shapes obtained after using platinum nanoparticles

as surfaces or CHCA as an organic matrix are quite similar, whereas the peak shapes for PEG 400 g mol^{-1} analyzed on gold nanoparticle surfaces are more intensive in the low mass range. PMMA was also analyzed on gold nanoparticles and by using a traditional DHB matrix. The same trend was seen, i.e., the intensities of the SALDI spectrum are higher compared to the MALDI spectrum. This phenomena of higher signal intensity of the analytes in the low mass region was in agreement with an earlier study by Hillenkamp [22]. Here, it is interesting to consider the polymer–surface interactions that tend to be weak. However, polymers with higher molecular weight are not easily detached from a surface because there are more binding sites. Therefore, a higher energy may be necessary for the LDI process for higher molecular weight compounds, resulting in a mass spectrum containing a lot of fragmentation.

SALDI-MS with titanium dioxide nanoparticles (TiO$_2$), MALDI-MS, and DIOS-MS were examined as possible methods for analysis of the antioxidant Irganox 1010 in polypropylene (PP) materials [23]. TiO$_2$ nanoparticles were suspended with 2-propanol to a concentration of 0.33 wt%. Comparison of the mass spectra of standard solutions consisting of the internal standard Irganox 1098 and the analyte Irganox 1010 obtained by using the three different method showed that the background noise, below 500 m/z, is much higher for the MALDI- and DIOS-MS than for SALDI-MS. However, the ion intensity of Irganox 1098 after SALDI-MS was less sensitive compared to Irganox 1010. Additionally, quantitative analysis by the different techniques was also compared. For MALDI, the ionization efficiency was strongly dependent on the ratio of the analyte and matrix concentrations and therefore was not considered a suitable technique for quantitative analysis. Quantitative analysis by DIOS and SALDI could, however, be possible. Commercial and laboratory-produced PP materials were evaluated with SALDI-MS for quantitative analysis of antioxidants. The amount of Irganox 1010 in the PP samples was determined to be 0.51 wt% for the commercial and 0.48 wt% for the laboratory-produced PP compared to the actual content of 0.5 wt%. Irganox 1076 and calcium stearate were also added to the commercial PP but they were not detectable by the SALDI method used. The authors concluded that SALDI-MS with TiO$_2$ nanoparticles could be used for quantitative analysis of antioxidants within the range 0.01–2.00 wt% in PP.

Zinc oxide (ZnO) nanoparticles were evaluated for their potential to function as SALDI substrates for low molecular weight synthetic polymers of PPG 400 g mol^{-1} with aminopropyl ether endgroups, PEG 6,000 g mol^{-1}, polystyrene (PS) 2,400 g mol^{-1}, and PMMA 1,890 g mol^{-1} [11]. ZnO particles were suspended in methanol to achieve a concentration of 0.17–1.0 wt%. A MALDI mass spectrum with DHB as matrix and a SALDI mass spectrum with TiO$_2$ and ZnO nanoparticles of PEG 6,000 g mol^{-1} is shown in Fig. 2. The results from TiO$_2$-SALDI showed generated fragment ions and no ions at around 6,000 g mol^{-1}. TiO$_2$ is known to have strong UV photocatalytic activity and this could be the reason for the observed degradation of PEG. In contrast, the molecular weight distribution for ZnO-SALDI was comparable to MALDI with DHB, and no fragmentation was observed because the photocatalytic activity of ZnO is not strong enough. The number average
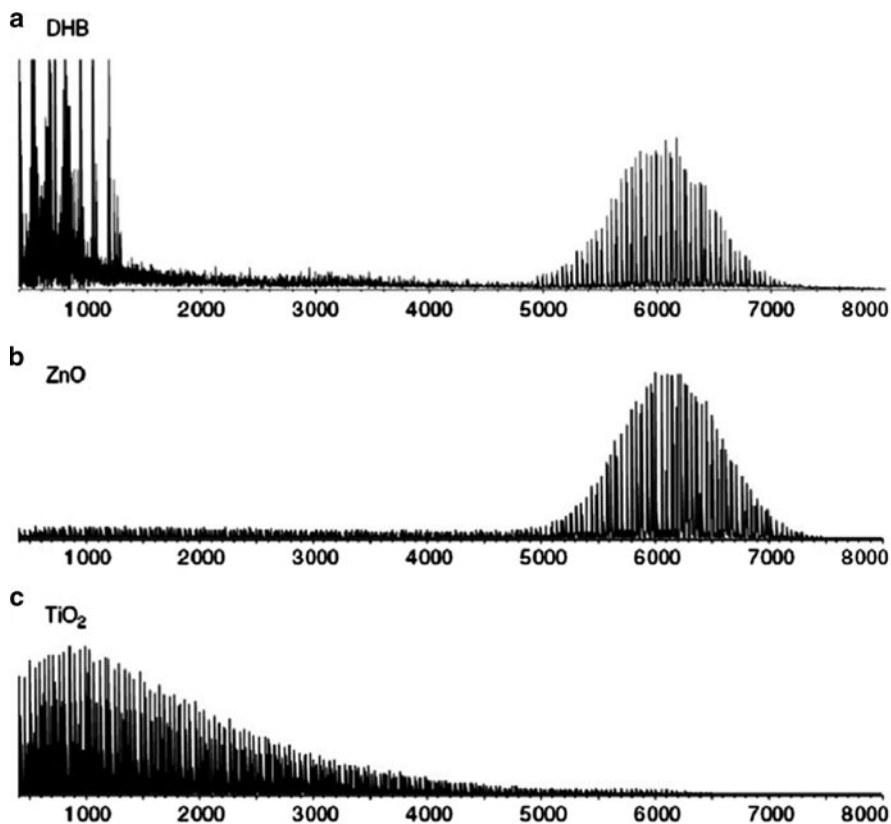
Fig. 2 LDI-MS of polyethylene glycol 6000 obtained with (**a**) DHB as a matrix, (**b**) ZnO nanoparticles as a surface, and (**c**) TiO$_2$ nanoparticles as a surface. Reprinted from [11] with permission of John Wiley and Sons. Copyright John Wiley and Sons (2008)

molecular weight (M_n) and the polydispersity index (PDI) was similar for SALDI and MALDI: for PS, $M_n = 2,380$ and PDI $= 1.03$ for ZnO, and $M_n = 2,245$ and PDI $= 1.04$ for DHB; for PMMA, $M_n = 1,755$ and PDI $= 1.09$ for ZnO, and $M_n = 1,773$ and PDI $= 1.10$ for DHB. ZnO showed great potential as SALDI substrate for analysis of synthetic polymers. More studies are, however, needed to conclude whether it can be used as a more general matrix or if it is limited to the type of polymer. For example, it was also possible to obtain a mass spectrum for higher molecular weight PEG (10,000 g mol^{-1}) but not for PS (9,000 g mol^{-1}). In Fig. 3, the mass spectra for PS and PMMA obtained by ZnO-SALDI are shown.

Drawbacks with nanoparticles as SALDI substrates are possible instrument contamination and the difficulty in handling free nanoparticles. In a recent study, nanoparticles were immobilized into polylactide (PLA) and evaluated as SALDI substrates for detection of drugs for human use: propanolol, acebutolol, and carba-mazepine [24]. Nanocomposite films were made of PLA blend mixed with eight
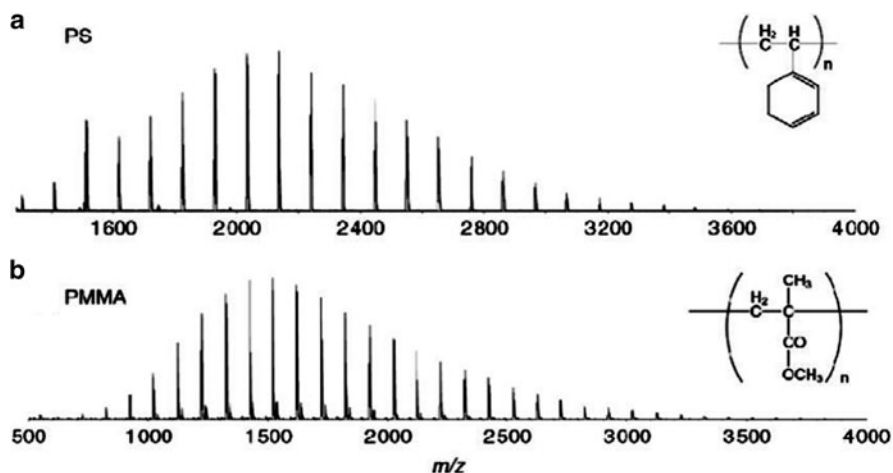
Fig. 3 ZnO-SALDI-MS spectra of (**a**) polystyrene and (**b**) polymethylmethacrylate. Reprinted from [11] with permission of John Wiley and Sons. Copyright John Wiley and Sons (2008)

different nanoparticles: TiO_2, magnesium oxide, silicon nitride, graphitized carbon black, silicon dioxide, halloysite nanoclay, montmorillonite nanoclay, and hydroxyapatite. The concentrations of nanoparticles in the polymer matrix were 5, 10, 20, and 30 wt%. These nanocomposites could provide a new strategy of easy-to-handle surfaces for rapid SALDI-MS analysis. The background noise of a blank nanocomposite spot was determined for all surfaces to see if the low mass range was clean, without any interference from surface cluster ions. The background spectrum corresponding to the PLA containing 10% TiO_2 is demonstrated in Fig. 4. A clean background is shown except for the peak at 64.1 m/z, which corresponds to the fragment TiO. Pure PLA surface was compared with surfaces containing nanoparticles and it was obvious that the contribution of nanoparticles affected the ionization/desorption process and a higher signal-to-noise (S/N) ratio was obtained after addition of nanoparticles. The percentage of nanoparticles could also affect the results and most surfaces containing 10 wt% nanoparticles gave better S/N values than the surfaces containing 30% nanoparticles. The spectrum of carbamazepine spotted on the PLA with 10 wt% TiO_2 is shown in Fig. 5. A certain amount of nanoparticles could enhance the S/N ratio. However, a larger amount of nanoparticles led to a lower S/N ratio, which could be to do with the hydrophobicity of the surface, as seen from the contact angle measurements. The analyte hydrophobicity was also considered; acebutolol was the least hydrophobic analyte and generally gave the highest S/N ratio. Propanolol was the most hydrophobic analyte and gave the lowest S/N ratios. The limits of detection (LOD) for all the surfaces were 1.7–56.3 ppm. However, the best surface was the one containing 10 wt% silicon nitride, giving relative standard deviations for the S/N values of 20–30%. In an earlier study, silicon nitride was used as pure nanoparticles and showed excellent results as a SALDI medium for analysis of drugs [17].
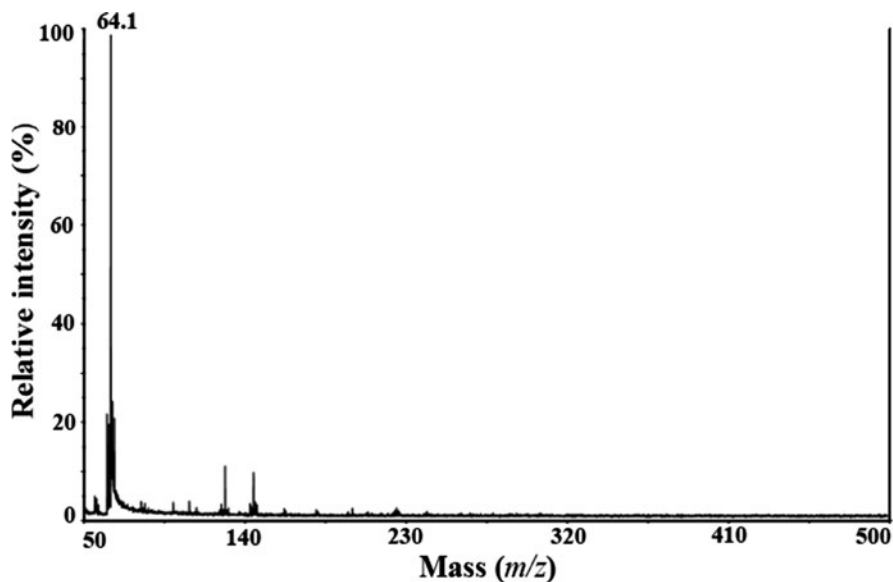
Fig. 4 SALDI-MS background spectrum of PLA surface containing 10% TiO_2. Reprinted from [24] with permission of The Royal Society of Chemistry. Copyright The Royal Society of Chemistry (2011)
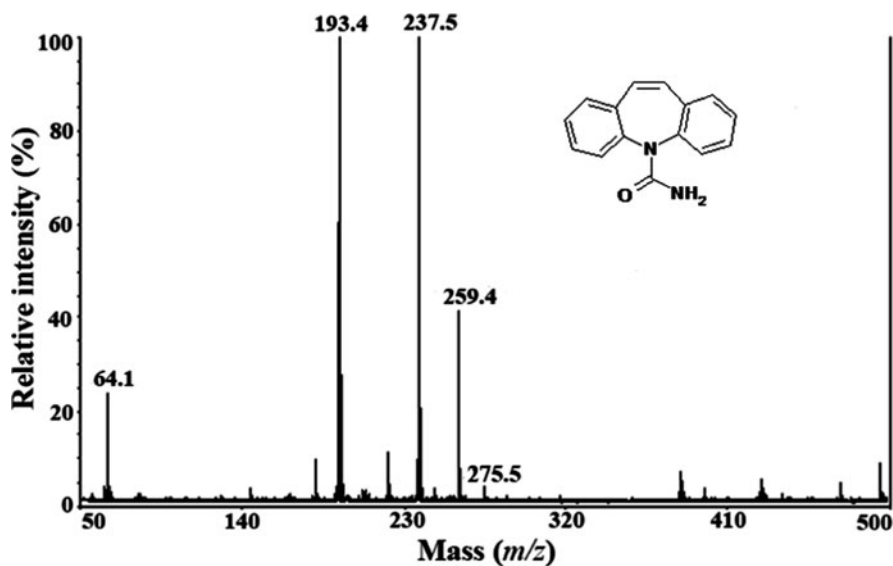
Fig. 5 SALDI-MS spectrum of carbamazepine on the surface of PLA containing 10% TiO_2. The proton adduct, sodium adduct, and potassium adduct together with a fragment ion is observed at m/z 237.5, 259.4, 275.5, and 193.4 respectively. Reprinted from [24] with permission of The Royal Society of Chemistry. Copyright The Royal Society of Chemistry (2011)

Polymer degradation products are typically analyzed with ESI-MS [25, 26] and GC-MS [27, 28], however, extraction methods are often necessary prior to analysis. Recently, SALDI-MS has shown great potential for analysis of polyester degradation products. Three different polycaprolactones (PCLs) with molecular weights of 900, 1,250, and 2,000 g mol^{-1} were employed for development of a SALDI-MS method for analysis of degradation products. The method development was carried out with different combinations of nanoparticles, solvents, and cationizing agents. Graphitizied carbon black, silicon nitride, TiO_2, halloysite nanoclay, and magnesium hydroxide were employed as potential surfaces. However, the most promising surfaces were halloysite nanoclay and magnesium hydroxide. Figure 6 shows the analysis of PCL 900 g mol^{-1} with magnesium hydroxide surface and either conventional trifluoroacetic acid (TFA) or sodium iodide (at two different concentrations). The spectra show the increased intensities using sodium iodide over the conventional TFA. In addition, compared to MALDI-MS, the resolution was better and the background noises were reduced. The ability to employ SALDI-MS for analysis of polymer degradation products would reduce sample preparation.

An essential property for a SALDI substrate is conductivity, i.e., the ability to transfer laser energy along the surface to obtain an efficient LDI. Pyrolytic highly
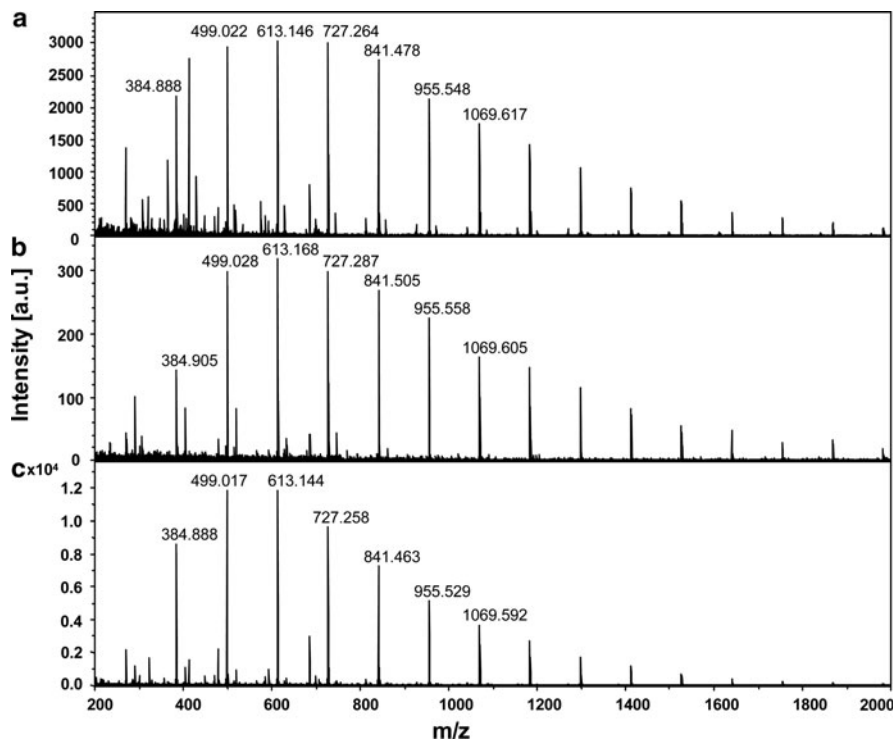
Fig. 6 Mass spectra of polycaprolactone oligomer obtained with magnesium hydroxide as a surface and (**a**) 0.1% TFA (**b**) NaI 1 mg/mL, and (**c**) NaI 10 mg/mL as cationizing agent

oriented graphite polymer film (PGS) is a highly conductive material that has been employed for environmental analysis of low molecular weight compounds by SALDI-MS [29]. In addition, it is a highly oriented graphite film with submicrometer surface roughness. The advantage of PGS is the simple sample preparation, as mentioned earlier for the nanocomposites. Modification of PGS could yield different surface properties and thereby be able to target the analytes of interest. In this study, the surface of PGS was oxidized and modified with the cationic polymer polyethyleneimine in order to improve the sensitivity for detection of environmental compounds. Environmental analysis of perfluorinated acids such as perfluorooctanesulfonic acid, perfluorooctanoic acid, pentachlorophenol, bisphenol A, benzo[α]pyrene, and 4-hydroxy-2-chlorobiphenyl was possible by using PGS SALDI-MS. The PGS SALDI performance was also tested for different carbon chain lengths of perfluoroalkylcarboxylic acid, from C5 to C14. A difference in chain length will also change the hydrophobic properties and may influence the LDI process. The signal intensities decreased as the carbon chain length increased. This could be to do with the hydrophobic chains, because intermolecular forces might be stronger between the surface and the analyte or between the carbon chains and thereby inhibit desorption. For good results, chain lengths below C6 were believed to be suitable for PGS SALDI-MS. Quantitative analysis showed that PGS SALDI-MS allowed the detection of several tens of parts per billion (ppb).

2.2.2 Polymeric Materials

Using polymers and oligomers as surfaces for LDI-MS could be referred to as polymer-assisted laser desorption ionization–mass spectrometry (PALDI-MS) or, as earlier, SALDI-MS [30–33]. Small oligomers have been used for LDI-MS analysis, similar to the matrix in MALDI, of small molecules and no fragmentation or suppression of the mass spectrum was observed (<350 Da). An advantage of this surface technique using polymeric materials is the possibility to characterize nonpolar compounds, since the mechanism involves a charge transfer instead of protonation or metal ion adducts like other surface LDI techniques in positive ion mode. Alkyl-substituted thiophene polymers have been used for analysis of small aromatic complexes, with a sensitivity of 10 nmol. Copolymers and polymer blends of porous monolith structures have been used for matrix-free methods. These are rigid polymers with both micropores and mesopores. Poly(butyl methacrylate-*co*-ethylene dimethacrylate), poly(styrene-*co*-divinyl benzene), and poly(benzyl methacrylate-*co*-ethylene dimethacrylate) monoliths were compared and the latter showed the best potential for LDI analysis. The desorption and ionization of the monolithic polymers depends on the laser power, solvent for the sample preparation, and the pore size of the monoliths. The polymers were effective in laser powers used for typical MALDI analysis. An optimal pore size was approximately 200 nm. In addition, the polymer samples could be stored for a month in ambient conditions without change in the analyte signals. Carbon nanotubes (CNTs) have recently been immobilized in a polyurethane adhesive in order to improve the

sample deposition step. The immobilized form of CNTs showed equal SALDI performance as the pure CNTs [34]. Naifion is another carbon-based material incorporated into a polymer matrix [35]. Microparticles of carbon graphite are added to the Naifion polymer. The role of the particles is to absorb the energy and transfer it to the analytes while the polymer donates protons to promote ionization of the analytes.

2.3   *Solvent-Free Matrix-Assisted Laser Desorption Ionization–Mass Spectrometry*

Solvent-free MALDI methods provide advantages for analyzing polymers that are insoluble such as polyfluorene [36] and large aromatic hydrocarbons [37]. The sample preparation step is simplified and problems that are caused by the solvent are reduced. Compared to the solvent-based methods, a more homogeneous analyte/matrix mixture and higher shot-to-shot and sample-to-sample reproducibility can be obtained with the solvent-free methods [38, 39]. However, this method is still less efficient for samples for which the solvent is not an issue. Also, a lower laser power is applied, which results in milder conditions with less fragmentation compared to the conventional solvent-based methods. The background signals are reduced and the resolution of the analyte signals is improved. The analyte, matrix, and salt are usually mixed by grinding [39, 40] (mortar and pestle), ball-mill, or vortexing [41]. In addition, an enhanced method for sample preparation is the multisample method that is derived from the vortex method. This is a method that facilitates sample preparation and has been used for the evaluation of numerous polymers such as PEG, PS, and PMMA with different molecular weights, and also of polymer additives [42, 43]. However, the transfer of the sample mixture to the MALDI plate is generally made in one of two ways: by pressing a pellet that is affixed to the plate with an adhesive tape, or by transferring the sample with a small spatula and pressing it on the plate to a thin film. The solvent-free MALDI method opens up investigation of new matrices without dependence on the compatibility with the solvent system. In a recent work, analysis of PLA with this method gave very good results and it was possible to follow up the interactions between the matrix and analyte by solid state nuclear magnetic resonance spectroscopy [44].

3   Ambient Desorption Ionization–Mass Spectrometry

One of the most challenging parts of traditional atmospheric pressure ionization sources for analysis of polymer or polymer additives is the requirement of sometimes extensive sample preparation steps prior to analysis. This is the case for ESI, MALDI, atmospheric pressure chemical ionization (APCI) and atmospheric

pressure photoionization (APPI). During the last few years, a new generation of ionization methods known as 'ambient MS' and 'direct ionization MS' have been developed and are summarized in many reviews [45–47]. The specialty of these new ambient techniques is that they do not require any sample preparation so that samples can be directly analyzed in their native, untreated forms. Ambient desorption ionization mass spectrometry operates in open air and is well suited for surface analysis and in situ studies of any size and shape. There exist nearly 30 different ambient techniques today and they are divided into ESI-related techniques and APCI-related techniques. However, the two most emerging tools in ambient ionization mass spectrometry are DESI and DART. These two similar techniques offer qualitative and semi-quantitative analysis, the main difference being the sample preparation. In DESI, liquid samples have to be deposited on a suitable surface, after which they are allowed to dry. Gas samples on the other hand have to be adsorbed into materials. However, no sample preparation is required for solid samples. In DART, no sample preparation is necessary at all.

3.1   Desorption Electrospray Ionization–Mass Spectrometry

DESI was developed in 2004 by Cooks [48] and, as mentioned earlier, is analogous to electrospray ionization, i.e., it is an ESI-related technique. It is a simple and straightforward technique and well-suited for solid samples. It already has a wide applicability, from small molecules to proteomics, and has especially been applied for analysis of polymer surfaces and their surface-active additives. The detection limit for this technique is very low and can be in the order of attomoles [49]. DESI has been combined with different mass analyzers, including quadropoles, triple quadropoles [50], quadrupole time-of-flight [51], and a hybrid quadrupole linear ion trap [52]. Additionally, DESI has been combined with FTICR [53] and an Orbitrap instrument [54]. In DESI, a solid-phase sample surface is bombarded with a spray of charged microdroplets from an electrospray needle in an ambient environment. The surface is first pre-wetted by initial droplets that will impact the surface; analytes are desorbed and collected from the surface into the droplets. Subsequent droplets will hit these first droplets and break them up and transfer the new droplets containing the analyte molecules to the mass spectrometer inlet for detection. The mass spectrum observed is similar to that in ESI, with both multiple and single charged molecular ions.

3.1.1   Analysis of Polymer Additives

Polymeric materials contain wide range of different additives, some of them added to protect the polymer from degradation or decomposition. Recently, a qualitative and semiquantitative analysis of four common polymer additives (Chimassorb 81, Tinuvin 328, Tinuvin 326, and Tinuvin 770) in concentrations between 0.02% and

0.2% in PP samples was performed with DESI-TOF-MS [55]. DESI parameters such as heating of the polymer and different spray solutions were tested and optimized before analysis. The polymers were heated using a heat gun before analysis to 400 °C for 2–5 s. It was shown that longer heating times increased the signal intensities; however, 5 s of heating could lead to deformation of the sample and thereby decrease the reproducibility. The decomposition and voltage of the DESI solvent spray is another important parameter. The selection depends on the ability to act as a good solvent for the specific analytes in question and on the robustness of spray performance. In this study and for these special analytes, the spray voltage was set to 3,400 V and the solvent was a mixture of methanol, water, and formic acid (80:20:0.1 vol/vol). The investigated polymer samples were used as a liner for an in-ground swimming pool. Calibration curves were constructed for different concentrations for the quantitative analysis. Quantitative analysis of Chimassorb 81 in a liner for an in-ground swimming pool showed a concentration of 0.082%. The result was in accordance with a high performance liquid chromatography–ultraviolet (HPLC-UV) method that was employed in an earlier study and showed a concentration of 0.080% of Chimassorb 81. In addition, quantitative analysis of PP granules was tested, and Tinuvin 770 was found at a concentration of 0.150%. However, HPLC-UV could not be used for verification since it does not work for Tinuvin 770. Instead, another technique, TDS-GC-MS, was tested and the concentration was determined to be 0.148%, verifying the earlier results.

3.1.2 Polymer Samples and Surfaces for DESI

In 2006, the first industrial polymers, such as PEG, poly(tetramethylene glycol) (PTMG) and polyacrylamide (PAM) were analyzed using DESI in solid phase [56]. A paper surface was employed for the analysis of polymer materials. The mass spectrum of PEG showed multiple charged molecular ions with Gaussian distribution. The average molecular weight was calculated to be 3,146, which is in good agreement with the expected value of 3,000. The study of hydrophobic polymers such as PTMG by ESI [57] is very challenging, and since DESI is an ESI-related technique the same results were expected here. Dissolution systems are usually required for the spray solvent in order to avoid discrimination between oligomers with different molecular weights. Also, a low polarity solvent decreases multiple charged molecular ions and thereby limits the mass range. The results reflect these drawbacks; the calculated average molecular weight was 1,412 and the value reported by the manufacturer was 2,900. For the hydrophilic polymer PAM, the same drawback resulted in a measured average molecular weight of 500 that should have been 1,500. The challenges in DESI analysis of higher molecular weight polymers are the discrimination of molecules, the reduction of multiple charged analytes in low polarity solvents, and overlapping peaks.

Structural information on the low molecular weight synthetic polymers PEG, PPG, PMMA, poly(α-methyl styrene) (PMS), and poly(dimethyl siloxane) (PDMS)

was obtained with DESI combined with tandem mass spectrometry (MS/MS) [58]. This combination works well and is comparable with ESI, MALDI, and MS/MS ionization techniques. The advantage with DESI over earlier systems is the short time and reduced sample preparation required for studies. Additionally, pharmaceutical tablets made of PDMS can be directly introduced into the DESI source and analyzed in tablet form.

3.1.3   DESI Surfaces

For studies of liquids by DESI-MS, a surface is employed where the analytes are deposit. The quality of the surface in terms of potential, chemical composition, and temperature limits can affect the ionization mechanism. Since charged particles are in contact with the surface, neutralization must be avoided. Neutralization occurs for conductive materials such as graphite and metal materials. However, if the materials are isolated or a voltage is applied on the surface that is equal or lower than the spray voltage, then these materials can be used as substrates. The signal stability is also affected by the electrostatic properties of the surface, whether the surface prefers the polarity of the spray solvent or not.

Polymers have been applied as surfaces, e.g., polytetraflouroethylene [59] is an electronegative polymer that gives high signal stability in negative-ion mode whereas PMMA performs better in positive-ion mode. Additionally, the chemical composition of a surface can affect the crystallization of the analytes when deposited from a solution, resulting in an uneven distribution. The analyte molecules should not have high affinity towards the surface since sensitivity could be lost. Surface roughness is another important parameter that could affect the ionization efficiency. Cooks and coworkers tried microscope glass slides as surfaces before and after HF etching and the results showed that etching increased the signal stability and reduced sweet spot effects. Therefore, a rough surface such as paper is one of the best substrates for DESI. A surface that can work at higher temperatures is preferred because it can increase the ion yield and increase the signal stability; however, this could be analyte-dependent and therefore an optimal temperature should be chosen for the specific study.

3.2   Direct Analysis in Real Time Mass Spectrometry

In 2005, DART was developed as an atmospheric pressure ion source that is suitable for direct analysis of solids, liquids, and gasses in open air conditions [60]. This became one of the first ambient ionization techniques that allow a new source of detection of compounds without the need for sample preparation. The technique is very similar to APCI and APPI but DART-MS offers direct input of samples as mentioned earlier. A unique application of DART has been for direct analysis of chemicals on surfaces without any sample preparation, such as the solvent extraction that is necessary for GC-MS or HPLC before analysis. Among

many interesting and successful studies, DART has been employed especially for analysis of additives, stabilizers, and polymer degradation products.

The analysis of samples is based on a reaction between a gas stream, usually helium or nitrogen, and sample molecules at atmospheric pressure. The reaction is initiated in a discharge chamber containing a cathode and an anode where the gas will be exposed to electrical potential and produce electronic or vibronic excited-state species (metastable molecules or atoms). These species can directly interact, desorb, and ionize the sample molecules on the surface. The mass spectrum obtained is usually dominated by protonated molecules in positive-ion mode or deprotonated molecules in negative-ion mode. The advantages of DART are that samples can be desorbed and ionized directly from surfaces and provide real-time information, and that no radioactive components are involved.

3.2.1   Identification of Polymer Additives

Additives are divided into low and high molecular weight compounds with different physiochemical and chemical properties. Therefore, different analytical methods need to be applied. The volatile compounds are usually detected with gas chromatography combined with mass spectrometry (GC-MS) and the nonvolatile compounds with liquid chromatography combined with mass spectrometry (LC-MS). Polymeric food packaging materials contain many different additives such as UV stabilizers, plasticizers, antioxidants, colorants, and grease-proofers that are desirable for the packaging characteristics. Migration of these additives but also monomers and degradation products from the polymeric packaging material to the foodstuff is possible. Therefore, a simple quality control method for screening the presence of undesirable compounds in contact with food would be useful. Different extraction methods in combination with gas chromatography have been used for analysis of migrants; however, some of these can be problematic and time-consuming because the analytes need to be separated from the polymer matrix before analysis. Extraction of chemicals can be selective and competitive displacement could easily occur between the analytes of interest. Another feature is that extraction methods such as headspace GC-MS do not provide surface analysis. An ideal tool for identification of surface contamination by additives is DART-MS. This technique allows direct introduction of solid samples and provides a fast and simple detection of polymer additives.

DART-MS has been successfully applied for the screening of common additives such as Tinuvin 234, di-2-ethylhexyl phthalate (DEHP), di-2-ethylhexyl adipate, Irganox (1076, 1010), Irgafos 168, and Chimassorb 81 from commercially available packaging materials such as PP, low density polyethylene, high density polyethylene (HDPE), PET, polyvinyl chloride (PVC), and polyvinylidene chloride (PVDC) [61]. The spectra of packaging additives produced predominately protonated molecular ions and matched the spectra from standard additives very well. Product ion spectra, DART-MS/MS, were also obtained for the different additives and these matched the standard additive spectra even better. Figure 7 compares the mass
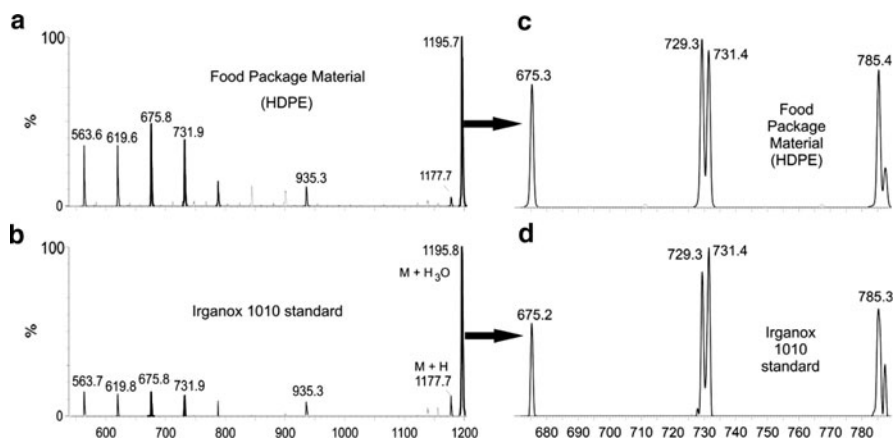
Fig. 7 DART-MS spectra of (a) food-packaging material (HDPE) (b) Irganox 1010 standard, and (c, d) corresponding MS/MS product ion spectra. Reprinted from [61] with permission of Springer. Copyright Springer (2009)

spectrum of the food packaging material of HDPE and the spectrum of the Irganox 1010 standard, and also compares the respective product ion spectra. In another similar study, 21 different stabilizers used for PP were detected with DART-MS. The additives were analyzed both from liquid samples mixed with toluene, and solid polymer samples [62]. The stabilizers analyzed were different Irganox (1010, 1330, 3114, 1035, 1076, 1081, MD 1024, E201, PS 800, and PS 802), Irgafos (126, 38, 168, HP 136, PEP 36, and Chimassorb 81), and Tinuvin (234, 326, 327, 328, and 770) compounds. The study showed that some stabilizers tend to decompose when exposed to high temperatures, high pressures, or oxidizing atmosphere. This led to a reduction of signal intensities, as seen in Fig. 8, and the intensity of some common stabilizers decreased with increasing temperature. This result confirmed that applying high temperatures during polymer processing could lead to a lower additive concentration in the final product. DART-MS also allowed the identification of degradation products from some additives. For example, a spectrum of the polymer sample containing Irgafos 126 and its degradation products such as 2,4-di-*tert* butylphenol were detectable.

Phthalic acid esters (PAE) are common plasticizers used for materials made of PVC. Toys and childcare articles could be made of PVC and there is concern about the migration of these PAE and their effect on human health. There exist different types of PAE and the challenge is to distinguish between the different phthalates. It is essential to be able to distinguish a sample mixture of DEHP, dibutyl phthalate (DBP), and benzyl butyl phthalate from diisononyl phthalate (DINP), diisodecyl phthalate (DIDP), and di-*n*-octyl phthalate (DNOP) because European legislation treats these compounds differently. Recently, toy materials made of PVC were analyzed with DART-MS in order to develop a rapid method for screening of PAE [63]. Figure 9 shows typical DART-MS spectra for DINP, DIDP, and DBP. Toy
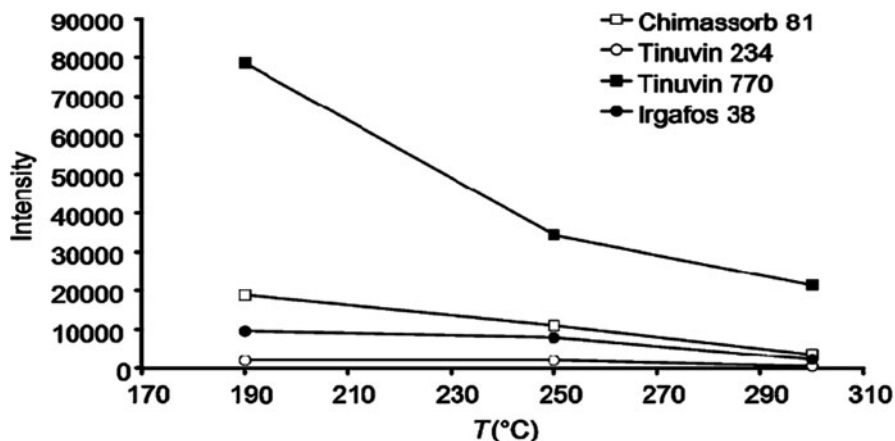
Fig. 8 Degradation of antioxidants due to high temperatures during polymer processing is shown by the reduced signal intensities for some common stabilizers. Reprinted from [62] with permission of The Royal Society of Chemistry. Copyright The Royal Society of Chemistry (2010)

samples were manually introduced in the DART source and the LODs for the protonated phthalate molecules were $\leq$ 0.1%. It was also possible to differentiate between the isomers DEHP and DNOP by their different fragmentation pathways. The same authors have studied lid gaskets of glass jars made of PVC containing diverse plasticizers and other additives, also called plastisols [64]. An interesting finding was the ability to study complex mixtures of polyadipates (PADs) from food packaging materials. PADs are very complex polyester additives and, usually, their identification in foodstuff needs a lot of pre-preparation before mass spectrometry. However, a successful DART-MS analysis was possible.

Chewing gums are delivery systems typically made of polybutadiene or polyvinyl acetate containing several flavor compounds. The volatile flavor compounds are usually studied with GC-MS and the nonvolatile analytes by LC-MS after a sample extraction step. Recently, DART-MS has been applied for the kinetic release study of an apolar cooling agent cyclohexanecarboxamide, *N*-ethyl-5-methyl-2-(1-methylethyl) (WS-3) from chewing gum in saliva [65]. Quantitative analysis of WS-3 in saliva by DART-MS and LC-MS was compared and a good agreement was achieved between the two methods. The DART-MS method could, therefore, become a fundamental technique for investigating delivery systems.

Moreover, DART-MS could be applied for the analysis of insoluble samples that are difficult to analyze with liquid-based methods such as ESI, APCI, and APPI. These techniques require samples to be dissolved in a solvent. During the last few years, solvent-free methods such as solvent-free MALDI have been applied for the analysis of insoluble compounds. However, they are time-consuming and there is a high risk of contaminating the ion source. In a recent study, DART-MS was capable of analyzing insoluble polycyclic aromatic hydrocarbons [66]. It should also be possible to apply this method for analysis of insoluble polymer samples used for food packaging or environmental materials.

Fig. 9 DART-MS spectra for PAE in toluene: (**a**) DINP, (**b**) DIDP, and (**c**) DBP. The adducts (proton and ammonium) are marked with an *asterisk*. Reprinted from [63] with permission of Springer. Copyright Springer (2009)
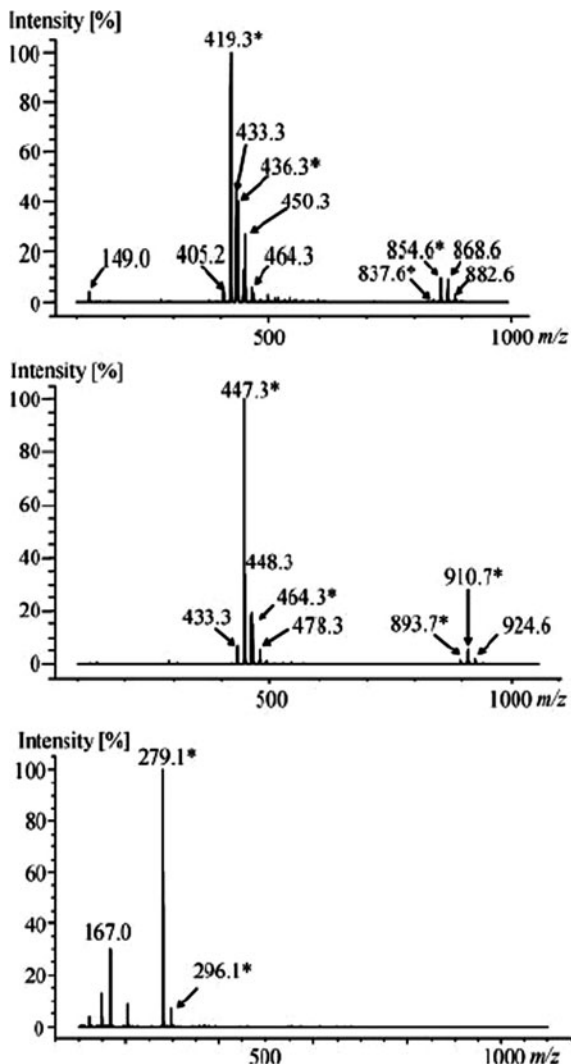
4 Fourier Transform Mass Spectrometry and FTICR-MS

In mass spectrometry, the quality and performance of a mass analyzer is very important for analysis of high molecular weight compounds such as polymers. TOF mass analyzers have been used for analysis of synthetic polymers because of their high sensitivity and the wide mass range that can be obtained. However, for analysis of complex polymer samples a mass analyzer such as those used for FTICR-MS or FTMS, with higher resolving power and high mass accuracy, is an advantage. This technique combined with tandem mass spectrometry techniques

could offer oligomer determination [67], molecular weight distribution [68], and endgroup analysis [69]. FTMS is usually combined with two tandem mass spectrometry techniques: collision-induced dissociation (CID) and electron-capture dissociation (ECD) [70]. The two fragmentation techniques, CID and ECD, are usually used in combination since they give complementary information. In CID, a selected ion is excited to a higher cyclotron radius (higher kinetic energy) and allowed to collide with a neutral gas (helium, nitrogen or argon). Collisions will lead to a transfer of kinetic energy from the ions to the neutral gas and conversion to internal energy, which will result in bond breakage and fragmentation. There are different ways to increase the kinetic energy of ions but the most common method used in combination with FTICR-MS is sustained off-resonance ion excitation. The ions accelerate in a cyclotron motion and the increased pressure results in CID fragmentation. In coating characterization, complex polymer compositions like copolymers are dominant and mass spectrometry is a routine tool for obtaining information about polydispersity, molecular weight distribution of polymers, and also structural and elemental composition such as repeating units and endgroups. However, for these complex structures a high resolution FTMS combined with tandem mass spectrometry is fundamental [69]. Polyesters are used in automotive coatings and their function is to prevent pigment aggregation and to maintain viscosity.

4.1 Polyphosphoesters in Biomedical Applications

Polyphosphoesters (PPEs) are polymers used in many biological and pharmaceutical applications in drugs, gene delivery, and tissue engineering because of their chemical properties, biocompatibility, and biodegradability. These polymer have structural versatility, and modification in the backbone of PPEs could introduce new bioactive molecules. However, only a small variation in structure can change their interaction with biological systems. PPEs are biodegradable polymers and their performance in biomedical application depends on their properties. They can only be applied if the degradation products are known and nontoxic. Recently and for the first time, FT-ICR mass spectrometry and tandem mass spectrometry (CID and ECD) were applied for the analysis of the polyphosphoester poly[1,4-bis (hydroxyethyl)terephthalate-*alt*-ethyloxyphosphate] [71]. Valuable information on the structure and degradation products was obtained. The polyphosphoester was dissolved in a chloroform/methanol/acetic acid (30:70:2, vol/vol) solution and electrospray ionization was performed. The resulting spectrum was mainly dominated by single charged ions (see Fig. 10). The first spectrum (Fig. 10a) is divided into four different areas $1 \times P$, $2 \times P$, $3 \times P$, and $4 \times P$ and these represent the number of phosphate groups for each degradation product. The Fig. 10b shows an expanded version of the $1 \times P$ region, with belonging single charged adducts, and Fig. 10c shows the first part of the $2 \times P$ region. For CID and ECD fragmentation analysis, cationization was promoted with sodium iodide (NaI) added to the final
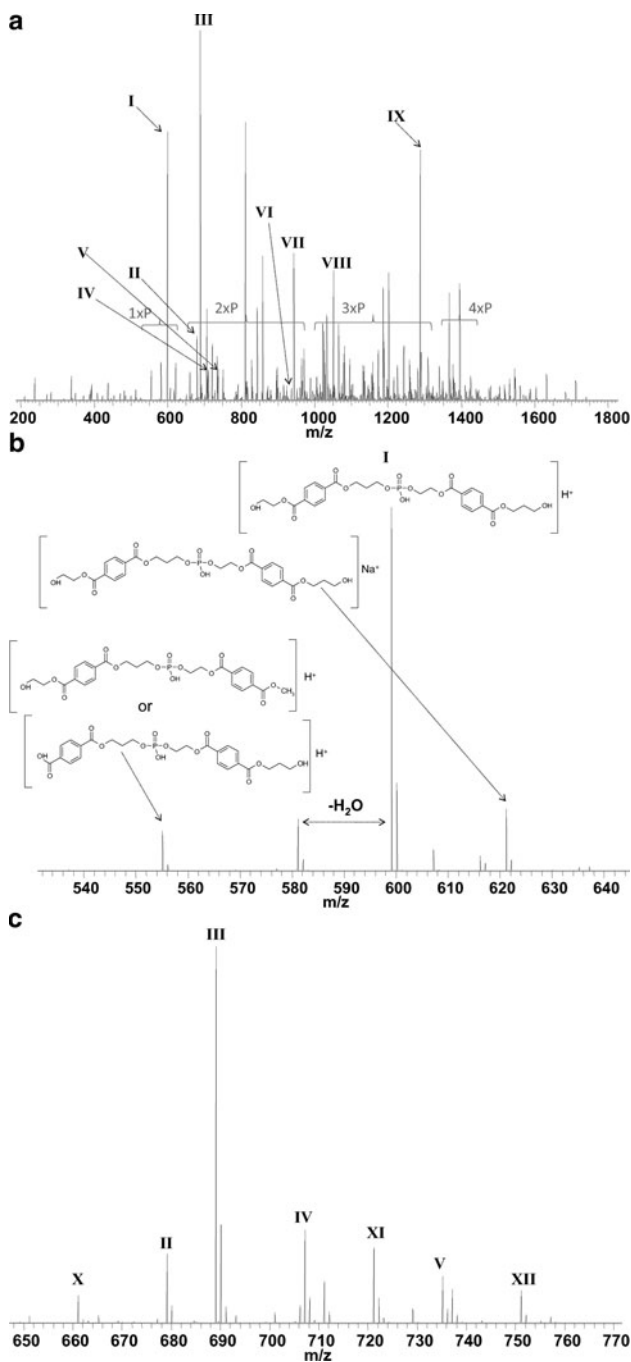
Fig. 10 Electrospray FT-ICR mass spectrum of (**a**) poly[1,4-bis(hydroxyethyl)terephthalate-*alt*-ethyloxyphosphate] in a solution of chloroform/methanol/acetic acid, (**b**) enlarged *m/z* region 550–650 and (**c**) enlarged *m/z* region 650–770. Reprinted from [71] with permission of Springer. Copyright Springer (2009)
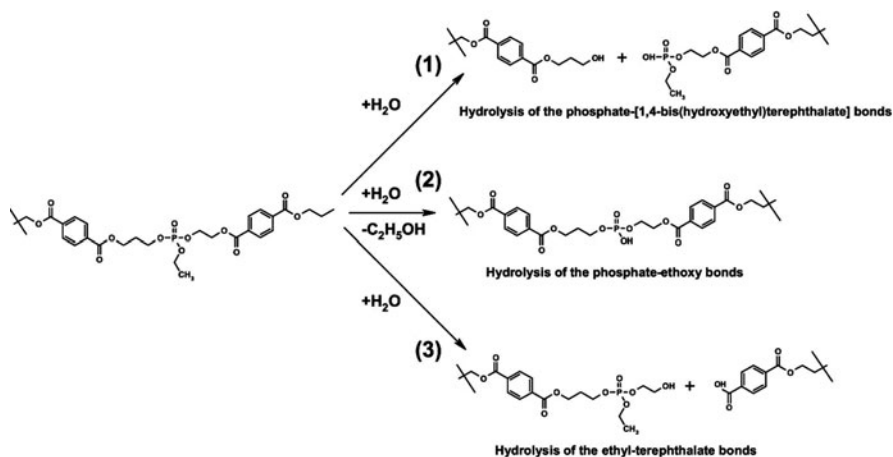
Fig. 11 Degradation scheme of poly[1,4-bis(hydroxyethyl)terephthalate-*alt*-ethyloxyphosphate]. Reprinted from [71] with permission of Springer. Copyright Springer (2009)

electrospray solution: polyphosphoester in chloroform, NaI in water, NaI in methanol, and NaI in acetic acid (30:10:70:2, vol/vol). The molar ratio between polyphosphoester and NaI was approximately 1:1. Additionally, the two fragmentation methods gave detailed information about the structure and the degradation products; see Fig. 11 for the degradation pathway of polyphosphoester poly[1,4-bis(hydroxyethyl)terephthalate-*alt*-ethyloxyphosphate]. The degradation occurred through hydrolysis at phosphate–[1,4-bis(hydroxyethyl)terephthalate] bonds, phosphate–ethoxy bonds, and ethyl–terephthalate bonds. In CID, both single protonated and sodiated PPE ions were observed due to cleavage of backbone C–C bonds. This could also be observed in ECD; however, a larger number of other fragments could be observed, such as cleavage of CH_2–O bonds closest to the terephthalate.

4.2   FTMS Versus TOF

The mass analyzer used plays an important role in the detection of a polymer spectrum. In a recent study, the spectrum of nonpolar polymers with narrow molecular weight distribution such as polyethylene 2,000 (the number is the average molecular weight), polybutadiene 8,300, polyisoprene 8,000 and polystyrene 10,000 were compared [72]. The spectra from a MALDI instrument coupled to either a FTMS or a reflectron TOF mass spectrometer were compared. Low mass fragment ions were found in the spectrum for polyethylene using TOF whereas no fragmentation occurred in the same FTMS spectrum. It was believed that the results were related to the time frame of each mass analyzer, ca. 100 μs/spectrum for TOF and 100–1,000 s of ms per spectrum for FTMS measurements. The fragment ions might
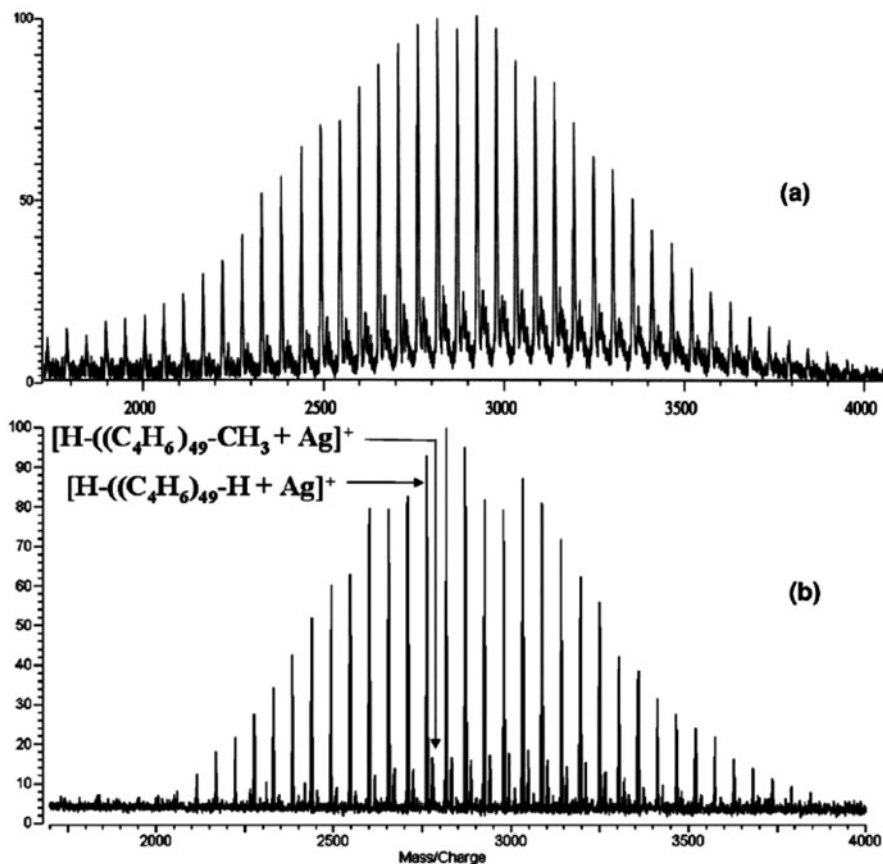
Fig. 12 (**a**) MALDI-TOF spectrum and (**b**) MALDI-FTMS spectrum of polybutadiene (M_n ~2,800) with two distributions of the oligomers having different endgroups. Reprinted from [72] with permission of Springer. Copyright Springer (2005)

not be observed in FTMS because they are often short-lived ions and therefore only seen by the faster TOF. This trend can be observed in Fig. 12 for polybutadiene with average molecular weight of 2,800 in a MALDI-TOF spectrum and a MALDI-FTMS spectrum. Moreover, the other spectra for nonpolar polymers showed better results using MALDI-FTMS with regard to mass accuracy and resolving power compared to MALDI-TOF.

4.3 Analysis of Polymers

A polymer consists of molecules with different molecular weights, and the properties of a polymer can be affected by the width of the molecular weight

distribution and also by the composition of endgroups. Characterization of synthetic polymers has been performed by MALDI FTICR-MS [73]. However, the feature with this combination is the single charged peaks and therefore it is limited to polymeric systems with lower molecular weight. Another ionization technique that would overcome this problem is the combination of ESI with FTICR-MS. In ESI, multiple charged ions are formed, enabling detection at lower mass-to-charge values, which is advantage. This combination also provides a higher accuracy and a high resolution in order to distinguish between the isotopic peaks of the oligomers in different charged states. Molecular weights up to 23,000 could be observed with a setup of ESI with FTICR-MS [74]. Monomer and endgroup characterization of PEG, PPG, and poly(tetrahydrofuran) were also studied by ESI FTICR-MS [75]. Two methods were developed in order to evaluate the monomer and endgroup compositions: a linear regression method and an averaging method for ESI FTICR-MS. The results showed a threefold increase in accuracy with this new combination of ESI with FTICR-MS compared to earlier MALDI FTICR-MS. ESI-FTICR-MS has also been applied for fragmentation observations of homopolyester oligomers, poly (dipropoxylated bisphenol A/isophthalic acid) and poly(dipropoxylated bisphenol A/acipic acid) and the copolyester poly(diproxylated bisphenol A/isophthalic acid/ adipic acid) [76].

Oxidation reactions in polymeric materials are important to understand because they could affect the mechanical properties of materials. The concern in these reactions is the release of toxic volatile organic compounds (VOCs). The reaction pathway of thermal oxidation of PP is of high interest, and proton transfer reactions combined with FTICR are a suitable tool for the analysis of complex mixtures of VOCs in air. Recently, thermal degradation of PP samples were studied for real time characterization and quantification of emitted VOCs [77]. The four VOCs found were acetone, formaldehyde, acetaldehyde, and methylacrolein. The advantage of this technique over GC is the detection of very volatile compounds, such as formaldehyde, and of course the rapid real time analysis.

5 Inductively Coupled Plasma–Mass Spectrometry

ICP-MS is a multi-element detection technique that is sensitive and specific. It can detect analytes at very low detection limits, from sub-parts per billion to sub-parts per trillion. This is a practical technique used for analysis of elements, such as heavy metals, in polymers.

5.1 *Brominated Flame Retardants*

BFRs have been widely used as additives in commercial materials to prevent fire in building materials, textiles, paintings, and electrical components [78]. These

compounds could be aromatic, aliphatic, or cycloaliphatic with different bromine content. BFRs could seriously impact our environment and human health. Therefore, a rapid method for analyzing traces of bromine is essential. BFRs such as polybrominated biphenyls (PBBs) and polybrominated diphenyl ethers (PBDEs) are examples of BFRs used to prevent fire in different materials. The Restriction of Hazardous Substances Directive (2002/95/EC) has limited the concentration of maximum BFRs to 0.1 wt% of homogenous material.

A flow-injection ICP-MS has recently been applied for the screening of polyurethanes containing different concentrations of bromine [79]. An advantage of ICP-MS is that there is no need for a matrix calibration, whereas many other techniques require a matrix-matched standard. Here, a low-cost bromide salt is used for calibration. The analytical performance demonstrated that the detection limit for bromine was 4 mg kg^{-1}. Flow-injected ICP-MS is a fundamental technique for screening of bromine-positive samples. Techniques such as GC-MS could provide more information and the exact identity of the additives or additive degradation products [80]; however, ICP-MS is a faster option just for detection proposes as the sample preparation needed in GC-MS is avoided.

The major separation techniques used for analysis of BFRs are GC and HPLC coupled to different detectors (MS, ECD, DAD/UV) [81–88]. However, using ICP-MS as a detection tool is a great advantage since this technique offers a compound-independent response. This method does not experience any interference from other co-eluted halogenated compounds (non-bromine). Therefore, it is not necessary to resolve the chromatogram of the BFRs from other interfering halogenated compounds. Both GC-ICP-MS and HPLC-ICP-MS have been applied for the analysis of BFRs. However, thermal degradation of brominated compounds is a concern when using GC-MS and GC-ECD. PBDEs have been successfully determined with GC-ICP-MS [89] but thermal degradation of highly brominated compounds is still a concern. HPLC-ICP-MS could be a promising method since it overcomes these degradation problems and the injection is done at room temperature. This accurate method for detection of BFRs in polymers has recently been demonstrated [90]. An ultrasonic-assisted extraction (UAE) was employed before introduction to HPLC-ICP-MS for detection of PBDEs and PBB additives in HDPE, PS, acrylonitrile-butadiene-styrene copolymer (ABS), and PP. Solutions of different PBDEs were analyzed: PBDE-47, PBDE-99, PBDE-100, PBDE-153, PBDE-154, PBDE-183, PBDE-196, PBDE-197, PBDE-203, PBDE-206, and PBDE-207 and also PBB-209. However, the LOD and the limits of quantification (LOQ) with this method were higher compared to the earlier GC-ICP-MS, GC-ECD, and GC-MS methods but still within the range that is required from the Restriction of Hazardous Substances Directive (2002/95/EC). But, thermal degradation of the highly brominated compound, PBDE-209 in this case, was not observed.

Another concern when analyzing polymeric materials is traces of inorganic compounds, such as heavy metals (Cd, Cr, Hg, and Pb) that can originate from additives, fillers, colorants, stabilizers, plasticizers, anti-oxidizing agents, and catalyst residues due to toxicity of these elements. Wet chemical analysis is the most

common method for determination of metal concentration in products. However, digestion may lead to loss of elements and is therefore a time-consuming method. During the last decade, laser ablation–inductive coupled plasma–mass spectrometry (LA-ICP-MS) has been used for bulk analysis of plastic materials. Also, two suitable polyethylene reference materials containing several heavy metals have been developed for calibration (European Reference Material (ERM)-EC680 and ERM-EC681), which could improve the analysis. In a recent study, ERM was utilized for analysis of real samples such as polyethylene bags, ABS, and plastic toy bricks [91]. LA-ICP-MS was found to be a suitable technique for tracing metal elements in polymeric materials with a concentration level of sub-micrograms per gram to tens of thousands of micrograms per gram. Besides the ERM, internal standards may also be required if the composition of the sample of interest differs from polyethylene. Waste polymer materials, glass, and polyethylene-based materials have also been studied with LA-ICP-MS using external standards [92].

6   Secondary Ion Mass Spectrometry

Secondary ion mass spectrometry (SIMS) is a surface-sensitive analysis technique for composition analysis of the uppermost atomic layer of thin films. The conventional SIMS can operate in two different modes: static mode or dynamic mode. The static SIMS mode provides information about molecular composition whereas the dynamic mode gives elemental and isotopic information. A target plate containing a polymer is bombarded by a primary ion beam (argon or cesium ions) and secondary ions are produced from the surface. The secondary ions are positive ions, negative ions, electrons, and neutral species. TOF-SIMS is a promising method for polymer surface analysis and has been widely used for characterization of molecular weight and endgroups of ethylene–propylene polymers [93], surface crystallization of poly (ethylene terephthalate) [94], specific interactions at the polymer surface [95], modifications of polymer surface [96], contaminants [97], polymer additives [98], detailed structural analysis [99], and surface quantitative analysis of degradation products [100]. Interesting research has been carried out to understand physio-chemical surface interactions between degradable biopolymers and biological environments. Hydrolytic degradation of poly(α-hydroxy acid)s such as poly (glycolic acid) (PGA), poly(L-lactide acid) (PLLA) and poly(lactide-co-glycolic acid) (PLGA) in different pH buffers were analyzed with TOF-SIMS. It was possible to distinguish and identify the degradation products by their characteristic ion fragmentation patterns. In addition, the interpretation of static SIMS mass spectra can be challenging due to many peaks from fragmented species and therefore depends on making comparisons with spectra from library databases. The chance to find a similar spectrum is low because of library limitations. Recently, an emerging tool known as gentle-SIMS (G-SIMS) has been employed for easier interpretation of static SIMS spectra. The mass spectrum of static SIMS contains mass peaks from degraded and rearranged fragments with high intensities,

thus, the identification of the surface becomes difficult. Using G-SIMS, most of these mass peaks can be removed and a cleaner spectrum obtained. Details of G-SIMS can be found elsewhere and its capability has been described for different materials including polymers and Irganox 1010 [101–103]. In a recent study, static SIMS and G-SIMS have been compared for studies of related biodegradable homo-polyesters including PGA, PLA, poly-β-(hydroxybutyrate) (PHB), and PCL [104]. However, in spite of the difficulties of the static SIMS it has been the method of choice for surface analysis of polymers. Recently, qualitative and quantitative surface analysis of individual PCL nanofibers was performed in detail [105].

Besides a range of studies using static SIMS, the dynamic SIMS has shown great potential to increase the understanding of stabilization of polymeric dispersions. Polymer surfactants can be used to stabilize polymer blends since polymers are often immiscible in one another. A copolymer surfactant or compatibilizer at a polymer–polymer interface of two homopolymers of polybutadiene has been investigated, with focus on the adsorption and desorption dynamics of the copolymer [106]. Another limitation or challenge with SIMS is the yield of secondary ions. During the last two decades, researchers have tried to develop ways of increasing the yield of secondary ions. The different methods to enhance this have been polyatomic projectiles [107], matrix-enhanced SIMS [108], use of noble metal substrates, and metal-assisted SIMS [109].

6.1 Cluster Secondary Ion Mass Spectrometry

Cluster SIMS introduces new molecular sources (C_{60}^+, Au_3^+, Bi_3^+) compared to the conventional ion beam in SIMS (Ar^+, Cs^+, Ga^+). Polymer analysis by cluster beams is a successful method within SIMS that provides in-depth molecular information; the procedure of cluster SIMS is explained elsewhere [110]. The first molecular depth profiling was carried out on PMMA samples. Cluster ions compared to the conventional ion beam could increase the molecular signal for analysis of polymer-based systems. This has recently been demonstrated in a study of drug-loaded cardiac stents based on poly(styrene-*co*-isobutylene) doped with paclitaxel [111]. It was actually impossible to observe any signals with the conventional SIMS. The molecular signals could also be improved in cluster SIMS by applying a thin layer of a metal such as Au or Ag, a technique known as metal-assisted SIMS [112, 113]. Matrix-enhanced SIMS is another way to enhance the signal by placing the sample in a matrix such as sinapic acid, similarly to MALDI [114, 115]. The metal-assisted SIMS has recently been employed on the surface of polymer-based systems including PS, PE, and PP [116–118]. Cluster SIMS has been used for cleaning of contaminants from the surface. Several studies have demonstrated the ability to remove polydimethylsiloxane from contaminated samples including PLA [119] and PLGA [120]. It is also a promising technique for molecular depth profiling of drug delivery systems. In addition, cluster ions could be used to remove damage created by atomic ion beams [121].

7 Ion Mobility Spectrometry–Mass Spectrometry

Complexity of polymer structures has increased in order to tailor desirable properties and functions for ever more demanding applications [122]. However, the complexity also results in more challenging structural analysis. The introduction of mobility separation prior to mass spectrometric analysis facilitates the analysis of more complex polymer systems [123]. IMS-MS has the ability to extend the dynamic range and separate isomeric compositions and therefore has an advantage over many high-resolution mass spectrometers. Ion sources such as ESI could be combined with IMS-MS to detect more complex chemistries such as copolymers. This combination has been employed for analysis of biomolecules and biopolymers [124, 125]. IMS-MS has recently been combined with ESI to examine distributions of PEG with masses of 6,550 and 17,900 Da and to evaluate the existing oligomers within the polymer matrix [126]. PEG has also been analyzed with IMS-MS in other studies [127, 128]. Furthermore, high resolution IMS-MS has been employed for analysis of PMMA [129]. It was possible to obtain detailed endgroup information, and discrimination of molecules with same nominal masses was possible without time-consuming LC separation prior to analysis. A benefit with IMS is the possible combination with a solvent-free sample preparation, as described for solvent-free MALDI (Sect. 2.3), since IMS is a solvent-free gas-phase separation.

8 Future Perspectives

Mass spectrometry has in recent years become an irreplaceable tool for characterization of increasingly advanced polymer structures, polymer additives, and degradation products. However, we are still far from utilizing the full potential of mass spectrometry in the structural analysis of polymers and their multidimensional complexity. The field of mass spectrometry has experienced enormous development in the last years, with several highly interesting mass spectrometric techniques arriving and being applied for polymer analysis. Some of the most interesting techniques with huge potential in polymer analysis include new developments in LDI techniques, like solvent-free MALDI and SALDI-MS. Another highly attractive possibility is to analyze solid samples in their native form by techniques like DESI-MS and DART-MS. Mass spectrometry already has its given place in the analysis of chemical structures, endgroups, copolymer compositions, molecular masses, and polymer compositions including additives and degradation products. In the future it will surely further strengthen its position as a polymer characterization tool.

References

1. Cohen L, Gusev A (2002) Small molecule analysis by MALDI mass spectrometry. Anal Bioanal Chem 373(7):571–586
2. Wei J, Buriak JM, Siuzdak G (1999) Desorption-ionization mass spectrometry on porous silicon. Nature 399(6733):243–246
3. Kruse RA, Li X, Bohn PW, Sweedler JV (2001) Experimental factors controlling analyte Ion generation in laser desorption/ionization mass spectrometry on porous silicon. Anal Chem 73(15):3639–3645
4. Arakawa R, Shimomae Y, Morikawa H, Ohara K, Okuno S (2004) Mass spectrometric analysis of low molecular mass polyesters by laser desorption/ionization on porous silicon. J Mass Spectrom 39(8):961–965
5. Okuno S, Wada Y, Arakawa R (2005) Quantitative analysis of polypropyleneglycol mixtures by desorption/ionization on porous silicon mass spectrometry. Int J Mass Spectrom 241(1):43–48
6. Shen Z, Thomas JJ, Averbuj C, Broo KM, Engelhard M, Crowell JE, Finn MG, Siuzdak G (2000) Porous silicon as a versatile platform for laser desorption/ionization mass spectrometry. Anal Chem 73(3):612–619
7. Thomas JJ, Shen Z, Blackledge R, Siuzdak G (2001) Desorption-ionization on silicon mass spectrometry: an application in forensics. Anal Chim Acta 442(2):183–190
8. Ladasiu Ciolacu FC, Choudhury NR, Dutta N, Voelcker NH (2006) MALDI-TOF MS and DIOS-MS investigation of the degradation and discoloration of poly(ethylene terephthalate). Macromolecules 39(23):7872–7881
9. Tanaka K, Waki H, Ido Y, Akita S, Yoshida Y, Yoshida T, Matsuo T (1988) Protein and polymer analyses up to m/z 100 000 by laser ionization time-of-flight mass spectrometry. Rapid Commun Mass Spectrom 2(8):151–153
10. Sunner J, Dratz E, Chen Y-C (1995) Graphite surface-assisted laser desorption/ionization time-of-flight mass spectrometry of peptides and proteins from liquid solutions. Anal Chem 67(23):4335–4342
11. Watanabe T, Kawasaki H, Yonezawa T, Arakawa R (2008) Surface-assisted laser desorption/ionization mass spectrometry (SALDI-MS) of low molecular weight organic compounds and synthetic polymers using zinc oxide (ZnO) nanoparticles. J Mass Spectrom 43(8):1063–1071
12. Schürenberg M, Dreisewerd K, Hillenkamp F (1999) Laser desorption/ionization mass spectrometry of peptides and proteins with particle suspension matrixes. Anal Chem 71(1):221–229
13. Hua L, Chen J, Ge L, Tan S (2007) Silver nanoparticles as matrix for laser desorption/ionization mass spectrometry of peptides. J Nanopart Res 9(6):1133–1138
14. Pan C, Xu S, Hu L, Su X, Ou J, Zou H, Guo Z, Zhang Y, Guo B (2005) Using oxidized carbon nanotubes as matrix for analysis of small molecules by MALDI-TOF MS. J Am Soc Mass Spectrom 16(6):883–892
15. Chen Y-C, Shiea J, Sunner J (2000) Rapid determination of trace nitrophenolic organics in water by combining solid-phase extraction with surface-assisted laser desorption/ionization time-of-flight mass spectrometry. Rapid Commun Mass Spectrom 14(2):86–90
16. Shariatgorji M, Amini N, Thorsen G, Crescenzi C, Ilag LL (2008) m-trap for the SALDI-MS screening of organic compounds prior to LC/MS analysis. Anal Chem 80(14):5515–5523
17. Shariatgorji M, Amini N, Ilag L (2009) Silicon nitride nanoparticles for surface-assisted laser desorption/ionization of small molecules. J Nanopart Res 11(6):1509–1512
18. Kinumi T, Saisu T, Takayama M, Niwa H (2000) Matrix-assisted laser desorption/ionization time-of-flight mass spectrometry using an inorganic particle matrix for small molecule analysis. J Mass Spectrom 35(3):417–422
19. Grant DC, Helleur RJ (2007) Surfactant-mediated matrix-assisted laser desorption/ionization time-of-flight mass spectrometry of small molecules. Rapid Commun Mass Spectrom 21(6):837–845

20. Feuerstein I, Najam-ul-Haq M, Rainer M, Trojer L, Bakry R, Aprilita NH, Stecher G, Huck CW, Bonn GK, Klocker H, Bartsch G, Guttman A (2006) Material-enhanced laser desorption/ionization (MELDI)–a New protein profiling tool utilizing specific carrier materials for time of flight mass spectrometric analysis. J Am Soc Mass Spectrom 17 (9):1203–1208
21. Tetsu YHK, Akira T, Takehiro W, Ryuichi A, Toshihiro S, Fumitaka M (2009) Detailed investigation on the possibility of nanoparticles of various metal elements for surface-assisted laser desorption/ionization mass spectrometry. Anal Sci 25(339–346)
22. Schurenberg M, Dreisewerd K, Hillenkamp F (1998) Laser desorption/ionization mass spectrometry of peptides and proteins with particle suspension matrixes. Anal Chem 71(1): 221–229
23. Osaka I, Okumura K, Miyake N, Watanabe T, Nozaki K, Kawasaki H, Arakawa R (2010) Quantitative analysis of an antioxidant additive in insoluble plastics by surface-assisted laser desorption/ionization mass spectrometry (SALDI-MS) using TiO_2 nanoparticles. J Mass Spectrom Soc Jpn 58(4):123–127
24. Aminlashgari N, Shariatgorji M, Ilag LL, Hakkarainen M (2011) Nanocomposites as novel surfaces for laser desorption ionization mass spectrometry. Analytical Methods 3(1): 192–197
25. Hakkarainen M, Adamus G, Höglund A, Kowalczuk M, Albertsson A-C (2008) ESI-MS reveals the influence of hydrophilicity and architecture on the water-soluble degradation product patterns of biodegradable homo- and copolyesters of 1,5-dioxepan-2-one and ε-caprolactone. Macromolecules 41:3547–3554
26. Andersson SR, Hakkarainen M, Inkinen S, Södergård A, Albertsson A-C (2010) Polylactide stereocomplexation leads to higher hydrolytic stability but more acidic hydrolysis product pattern. Biomacromolecules 11:1067–1073
27. Hakkarainen M, Höglund A, Odelius K, Albertsson A-C (2007) Tuning the release rate of acidic degradation products through macromolecular design of caprolactone-based copolymers. J Am Chem Soc 129:6308–6312
28. Gröning M, Hakkarainen M, Albertsson A-C (2008) Quantitative determination of volatiles in polymers and quality control of recycled materials by static headspace techniques. Adv Polym Sci 211:51–84
29. Kawasaki H, Takahashi N, Fujimori H, Okumura K, Watanabe T, Matsumura C, Takemine S, Nakano T, Arakawa R (2009) Functionalized pyrolytic highly oriented graphite polymer film for surface-assisted laser desorption/ionization mass spectrometry in environmental analysis. Rapid Commun Mass Spectrom 23(20):3323–3332
30. Woldegiorgis A, Fv K, Dahlstedt E, Hellberg J, Brinck T, Roeraade J (2004) Polymer-assisted laser desorption/ionization analysis of small molecular weight compounds. Rapid Commun Mass Spectrom 18(8):841–852
31. Woldegiorgis A, Löwenhielm P, Björk A, Roeraade J (2004) Matrix-assisted and polymer-assisted laser desorption/ionization time-of-flight mass spectrometric analysis of low molecular weight polystyrenes and polyethylene glycols. Rapid Commun Mass Spectrom 18(23): 2904–2912
32. Peterson DS, Luo Q, Hilder EF, Svec F, Fréchet JMJ (2004) Porous polymer monolith for surface-enhanced laser desorption/ionization time-of-flight mass spectrometry of small molecules. Rapid Commun Mass Spectrom 18(13):1504–1512
33. Soltzberg LJ, Patel P (2004) Small molecule matrix-assisted laser desorption/ionization time-of-flight mass spectrometry using a polymer matrix. Rapid Commun Mass Spectrom 18(13): 1455–1458
34. S-f R, Zhang L, Z-h C, Y-l G (2005) Immobilized carbon nanotubes as matrix for MALDI-TOF-MS analysis: applications to neutral small carbohydrates. J Am Soc Mass Spectrom 16(3):333–339

35. Kalkan AK, Fonash SJ (2004) Carbon/Nafion ® nanocomposite thin films as potential matrix-free laser desorption-ionization mass spectroscopy substrates. Mater Res Soc Proc 788:L8.49
36. Trimpin S, Grimsdale AC, Räder HJ, Müllen K (2002) Characterization of an insoluble poly (9,9-diphenyl-2,7-fluorene) by solvent-free sample preparation for MALDI-TOF mass spectrometry. Anal Chem 74(15):3777–3782
37. Simpson CD, Mattersteig G, Martin K, Gherghel L, Bauer RE, Räder HJ, Müllen K (2004) Nanosized molecular propellers by cyclodehydrogenation of polyphenylene dendrimers. J Am Chem Soc 126(10):3139–3147
38. Trimpin S, Keune S, Räder HJ, Müllen K (2006) Solvent-free MALDI-MS: developmental improvements in the reliability and the potential of MALDI in the analysis of synthetic polymers and giant organic molecules. J Am Soc Mass Spectrom 17(5):661–671
39. Trimpin S, Rouhanipour A, Az R, Räder HJ, Müllen K (2001) New aspects in matrix-assisted laser desorption/ionization time-of-flight mass spectrometry: a universal solvent-free sample preparation. Rapid Commun Mass Spectrom 15(15):1364–1373
40. Skelton R, Dubois F, Zenobi R (2000) A MALDI sample preparation method suitable for insoluble polymers. Anal Chem 72(7):1707–1710
41. Hanton SD, Parees DM (2005) Extending the solvent-free MALDI sample preparation method. J Am Soc Mass Spectrom 16(1):90–93
42. Trimpin S, McEwen CN (2007) Multisample preparation methods for the solvent-free MALDI-MS analysis of synthetic polymers. J Am Soc Mass Spectrom 18(3):377–381
43. Trimpin S, Wijerathne K, McEwen CN (2009) Rapid methods of polymer and polymer additives identification: multi-sample solvent-free MALDI, pyrolysis at atmospheric pressure, and atmospheric solids analysis probe mass spectrometry. Anal Chim Acta 654(1): 20–25
44. Sroka-Bartnicka A, Ciesielski W, Libiszowski J, Duda A, Sochacki M, Potrzebowski MJ (2009) Complementarity of solvent-free MALDI TOF and solid-state NMR spectroscopy in spectral analysis of polylactides. Anal Chem 82(1):323–328
45. Venter A, Nefliu M, Graham Cooks R (2008) Ambient desorption ionization mass spectrometry. Trends Analyt Chem 27(4):284–290
46. Harris GA, Nyadong L, Fernandez FM (2008) Recent developments in ambient ionization techniques for analytical mass spectrometry. Analyst 133(10):1297–1301
47. Weston DJ (2010) Ambient ionization mass spectrometry: current understanding of mechanistic theory; analytical performance and application areas. Analyst 135(4):661–668
48. Zn T, Wiseman JM, Gologan B, Cooks RG (2004) Mass spectrometry sampling under ambient conditions with desorption electrospray ionization. Science 306(5695):471–473
49. Bereman M, Muddiman D (2007) Detection of attomole amounts of analyte by desorption electrospray ionization mass spectrometry (DESI-MS) determined using fluorescence spectroscopy. J Am Soc Mass Spectrom 18(6):1093–1096
50. Leuthold LA, Mandscheff J-F, Fathi M, Giroud C, Augsburger M, Varesio E, Hopfgartner G (2006) Desorption electrospray ionization mass spectrometry: direct toxicological screening and analysis of illicit Ecstasy tablets. Rapid Commun Mass Spectrom 20(2):103–110
51. Williams JP, Scrivens JH (2005) Rapid accurate mass desorption electrospray ionisation tandem mass spectrometry of pharmaceutical samples. Rapid Commun Mass Spectrom 19(24):3643–3650
52. Van Berkel GJ, Ford MJ, Deibel MA (2005) Thin-layer chromatography and mass spectrometry coupled using desorption electrospray ionization. Anal Chem 77(5):1207–1215
53. Bereman MS, Williams TI, Muddiman DC (2007) Carbohydrate analysis by desorption electrospray ionization fourier transform Ion cyclotron resonance mass spectrometry. Anal Chem 79(22):8812–8815
54. Hu Q, Talaty N, Noll RJ, Cooks RG (2006) Desorption electrospray ionization using an Orbitrap mass spectrometer: exact mass measurements on drugs and peptides. Rapid Commun Mass Spectrom 20(22):3403–3408

55. Reiter S, Buchberger W, Klampfl C (2011) Rapid identification and semi-quantitative determination of polymer additives by desorption electrospray ionization/time-of-flight mass spectrometry. Anal Bioanal Chem 400:2317–2322

56. Nefliu M, Venter A, Cooks RG (2006) Desorption electrospray ionization and electrosonic spray ionization for solid- and solution-phase analysis of industrial polymers. Chem Commun 2006(8):888–890

57. Latourte L, Blais J-C, Tabet J-C, Cole RB (1997) Desorption behavior and distributions of fluorinated polymers in MALDI and electrospray ionization mass spectrometry. Anal Chem 69(14):2742–2750

58. Jackson AT, Williams JP, Scrivens JH (2006) Desorption electrospray ionisation mass spectrometry and tandem mass spectrometry of low molecular weight synthetic polymers. Rapid Commun Mass Spectrom 20(18):2717–2727

59. Ifa DR, Manicke NE, Rusine AL, Cooks RG (2008) Quantitative analysis of small molecules by desorption electrospray ionization mass spectrometry from polytetrafluoroethylene surfaces. Rapid Commun Mass Spectrom 22(4):503–510

60. Cody RB, Laramée JA, Durst HD (2005) Versatile new ion source for the analysis of materials in open air under ambient conditions. Anal Chem 77(8):2297–2302

61. Ackerman LK, Noonan GO, Begley TH (2009) Assessing direct analysis in real-time-mass spectrometry (DART-MS) for the rapid identification of additives in food packaging. Food Addit Contam Part A Chem Anal Control Expo Risk Assess 26(12):1611–1618

62. Haunschmidt M, Klampfl CW, Buchberger W, Hertsens R (2009) Rapid identification of stabilisers in polypropylene using time-of-flight mass spectrometry and DART as ion source. Analyst 135(1):80–85

63. Rothenbacher T, Schwack W (2009) Rapid and nondestructive analysis of phthalic acid esters in toys made of poly(vinyl chloride) by direct analysis in real time single-quadrupole mass spectrometry. Rapid Commun Mass Spectrom 23(17):2829–2835

64. Rothenbacher T, Schwack W (2009) Rapid identification of additives in poly(vinyl chloride) lid gaskets by direct analysis in real time ionisation and single-quadrupole mass spectrometry. Rapid Commun Mass Spectrom 24(1):21–29

65. Jeckelmann N, Haefliger OP (2010) Release kinetics of actives from chewing gums into saliva monitored by direct analysis in real time mass spectrometry. Rapid Commun Mass Spectrom 24(8):1165–1171

66. Domin MA, Steinberg BD, Quimby JM, Smith NJ, Greene AK, Scott LT (2010) Routine analysis and characterization of highly insoluble polycyclic aromatic compounds by direct analysis in real time mass spectrometry (DART). Analyst 135(4):700–704

67. Dey M, Castoro JA, Wilkins CL (1995) Determination of molecular weight distributions of polymers by MALDI-FTMS. Anal Chem 67(9):1575–1579

68. Miladinovic S, Robotham S, Wilkins C (2008) Wide mass range trapping using a 7-T internal source matrix-assisted laser desorption/ionization Fourier transform mass spectrometer. Anal Bioanal Chem 392(4):585–594

69. Simonsick W, Petkovska V (2008) Detailed structural elucidation of polyesters and acrylates using Fourier transform mass spectrometry. Anal Bioanal Chem 392(4):575–583

70. Heeren RMA, Kleinnijenhuis AJ, McDonnell LA, Mize TH (2004) A mini-review of mass spectrometry using high-performance FTICR-MS methods. Anal Bioanal Chem 378(4):1048–1058

71. Kaczorowska MA, Cooper HJ (2009) Characterization of polyphosphoesters by fourier transform Ion cyclotron resonance mass spectrometry. J Am Soc Mass Spectrom 20(12):2238–2247

72. Jaber AJ, Wilkins CL (2005) Hydrocarbon polymer analysis by external MALDI fourier transform and reflectron time of flight mass spectrometry. J Am Soc Mass Spectrom 16(12):2009–2016

73. van Rooij G, Duursma M, Heeren R, Boon J, de Koster C (1996) High resolution end group determination of low molecular weight polymers by matrix-assisted laser desorption

ionization on an external ion source fourier transform ion cyclotron resonance mass spectrometer. J Am Soc Mass Spectrom 7(5):449–457

74. O'Connor PB, McLafferty FW (1995) Oligomer characterization of 4–23 kDa polymers by electrospray fourier transform mass spectrometry. J Am Chem Soc 117(51):12826–12831

75. Koster S, Duursma MC, Boon JJ, Heeren RMA (2000) Endgroup determination of synthetic polymers by electrospray ionization Fourier transform ion cyclotron resonance mass spectrometry. J Am Soc Mass Spectrom 11(6):536–543

76. Koster S, Duursma MC, Boon JJ, Nielen MWF, de Koster CG, Heeren RMA (2000) Structural analysis of synthetic homo- and copolyesters by electrospray ionization on a Fourier transform ion cyclotron resonance mass spectrometer. J Mass Spectrom 35(6): 739–748

77. Sarrabi S, Colin X, Tcharkhtchi A, Heninger M, Leprovost J, Hln M (2009) Real time analysis of volatile organic compounds from polypropylene thermal oxidation using chemical ionization fourier transform Ion cyclotron resonance mass spectrometry. Anal Chem 81(15): 6013–6020

78. Eljarrat E, Barceló D (2004) Sample handling and analysis of brominated flame retardants in soil and sludge samples. Trends Analyt Chem 23(10–11):727–736

79. Vázquez AS, Costa-Fernandez JM, Encinar JR, Pereiro R, Sanz-Medel A (2008) Bromine determination in polymers by inductively coupled plasma-mass spectrometry and its potential for fast first screening of brominated flame retardants in polymers and paintings. Anal Chim Acta 623(2):140–145

80. Hakkarainen M, Gröning M, Albertsson A-C (2003) Solid-phase microextraction (SPME) in polymer characterization—long-term properties and quality control of polymeric materials. J Appl Polym Sci 89(3):867–873

81. Schlummer M, Brandl F, Mäurer A, van Eldik R (2005) Analysis of flame retardant additives in polymer fractions of waste of electric and electronic equipment (WEEE) by means of HPLC-UV/MS and GPC-HPLC-UV. J Chromatogr A 1064(1):39–51

82. Pöhlein M, Llopis AS, Wolf M, Rv E (2005) Rapid identification of RoHS-relevant flame retardants from polymer housings by ultrasonic extraction and RP-HPLC/UV. J Chromatogr A 1066(1–2):111–117

83. Dirtu AC, Ravindra K, Roosens L, van Grieken R, Neels H, Blust R, Covaci A (2008) Fast analysis of decabrominated diphenyl ether using low-pressure gas chromatography-electron-capture negative ionization mass spectrometry. J Chromatogr A 1186(1–2):295–301

84. Vilaplana F, Karlsson P, Ribes-Greus A, Ivarsson P, Karlsson S (2008) Analysis of brominated flame retardants in styrenic polymers: comparison of the extraction efficiency of ultrasonication, microwave-assisted extraction and pressurised liquid extraction. J Chromatogr A 1196–1197:139–146

85. Hosaka A, Watanabe C, Tsuge S (2005) Rapid determination of decabromodiphenyl ether in polystyrene by thermal desorption-GC/MS. Anal Sci 21(10):1145–1147

86. Ranz A, Maier E, Trampitsch C, Lankmayr E (2008) Microwave-assisted extraction of decabromodiphenylether from polymers. Talanta 76(1):102–106

87. Am A, Wolf M, van Eldik R (2003) Extraction of brominated flame retardants from polymeric waste material using different solvents and supercritical carbon dioxide. Anal Chim Acta 491(1):111–123

88. Pöhlein M, Bertran RU, Wolf M, van Eldik R (2008) Versatile and fast gas chromatographic determination of frequently used brominated flame retardants in styrenic polymers. J Chromatogr A 1203(2):217–228

89. Vonderheide AP, Montes-Bayon M, Caruso JA (2002) Development and application of a method for the analysis of brominated flame retardants by fast gas chromatography with inductively coupled plasma mass spectrometric detection. J Anal At Spectrom 17(11): 1480–1485

90. Mingwu S, Chao W, Yongjuan J, Xinhua D, Xiang F (2010) Determination of selected polybrominated diphenylethers and polybrominated biphenyl in polymers by ultrasonic-

assisted extraction and high-performance liquid chromatography − inductively coupled plasma mass spectrometry. Anal Chem 82(12):5154–5159

91. Resano M, García-Ruiz E, Vanhaecke F (2005) Laser ablation-inductively coupled plasma-dynamic reaction cell-mass spectrometry for the multi-element analysis of polymers. Spectrochimica Acta Part B: Atomic Spectroscopy 60(11):1472–1481

92. Stehrer T, Heitz J, Pedarnig J, Huber N, Aeschlimann B, Günther D, Scherndl H, Linsmeyer T, Wolfmeir H, Arenholz E (2010) LA-ICP-MS analysis of waste polymer materials. Anal Bioanal Chem 398(1):415–424

93. Galuska AA (1997) Quantitative surface analysis of ethylene–propylene polymers using ToF-SIMS. Surf Interface Anal 25(1):1–4

94. Reichlmaier S, Bryan SR, Briggs D (1995) Surface trimer crystallization on poly (ethylene terephthalate) studied by time-of-flight secondary ion mass spectrometry. In: Proceedings of the 41st National Symposium of the American Vacuum Society, Denver, CO. AVS, pp 1217–1223

95. Li L, Chan C-M, Weng L-T, Xiang M-L, Jiang M (1998) Specific interaction between poly(styrene-co-4-vinylphenol) and poly(styrene-co-4-vinylpyridine) studied by X-ray photoelectron spectroscopy and time-of-flight secondary Ion mass spectrometry. Macromolecules 31(21):7248–7255

96. Bletsos IV, Hercules DM, Magill JH, VanLeyen D, Niehuis E, Benninghoven A (1988) Time-of-flight secondary ion mass spectrometry: detection of fragments from thick polymer films in the range m/z.Ltoreq. 4500. Anal Chem 60(9):938–944

97. Lub J, van Vroonhoven FCBM, van Leyen D, Benninghoven A (1988) Static secondary ion mass spectrometry analysis of polycarbonate surfaces. Effect of structure and of surface modification on the spectra. Polymer 29(6):998–1003

98. Lub J, van Velzen PNT, van Leyen D, Hagenhoff B, Benninghoven A (1988) TOF-SIMS analysis of the surface of insulators. Examples of chemically modified polymers and glass. Surf Interface Anal 12(1):53–57

99. Bletsos IV, Hercules DM, VanLeyen D, Benninghoven A, Karakatsanis CG, Rieck JN (1989) Structural characterization of model polyurethanes using time-of-flight secondary ion mass spectrometry. Anal Chem 61(19):2142–2149

100. Lee J-W, Gardella JA (2002) Quantitative TOF-SIMS analysis of oligomeric degradation products at the surface of biodegradable poly([alpha]-hydroxy acid)s. J Am Soc Mass Spectrom 13(9):1108–1119

101. Gilmore IS, Seah MP (2000) Static SIMS: towards unfragmented mass spectra – the G-SIMS procedure. Appl Surf Sci 161(3–4):465–480

102. Gilmore IS, Seah MP (2003) G-SIMS of crystallisable organics. Appl Surf Sci 203–204:551–555

103. Gilmore IS, Seah MP (2004) Organic molecule characterization–G-SIMS. Appl Surf Sci 231–232:224–229

104. Ogaki R, Green FM, Li S, Vert M, Alexander MR, Gilmore IS, Davies MC (2008) A comparison of the static SIMS and G-SIMS spectra of biodegradable homo-polyesters. Surf Interface Anal 40(8):1202–1208

105. Van Royen P, Boschmans B, dos Santos A, Schacht E, Dubruel P, Cornelissen R, Beenaerts L, Van Vaeck L (2011) Static secondary ion mass spectrometry for the surface characterisation of individual nanofibres of polycaprolactone functionalised with an antibacterial additive. Anal Bioanal Chem 399(3):1163–1172

106. Reynolds BJ, Ruegg ML, Mates TE, Radke CJ, Balsara NP (2006) Diblock copolymer surfactant transport across the interface between two homopolymers. Langmuir 22(22):9192–9200

107. Kollmer F (2004) Cluster primary ion bombardment of organic materials. Appl Surf Sci 231–232:153–158

108. Delcorte A (2006) Matrix-enhanced secondary ion mass spectrometry: the Alchemist's solution? Appl Surf Sci 252(19):6582–6587

109. Adriaensen L, Vangaever F, Gijbels R (2004) Metal-assisted secondary ion mass spectrometry: influence of Ag and Au deposition on molecular ion yields. Anal Chem 76(22):6777–6785

110. Gillen G, Roberson S (1998) Preliminary evaluation of an SF5+ polyatomic primary ion beam for analysis of organic thin films by secondary ion mass spectrometry. Rapid Commun Mass Spectrom 12(19):1303–1312

111. Braun RM, Cheng J, Parsonage EE, Moeller J, Winograd N (2006) Surface and depth profiling investigation of a drug-loaded copolymer utilized to coat Taxus Express2 stents. Anal Chem 78(24):8347–8353

112. Grade H, Cooks RG (1978) Secondary ion mass spectrometry. Cationization of organic molecules with metals. J Am Chem Soc 100(18):5615–5621

113. Linton RW, Mawn MP, Belu AM, DeSimone JM, Hunt MO, Menceloglu YZ, Cramer HG, Benninghoven A (1993) Time-of-flight secondary ion mass spectrometric analysis of polymer surfaces and additives. Surf Interface Anal 20(12):991–999

114. Wu KJ, Odom RW (1996) Matrix-enhanced secondary Ion mass spectrometry: a method for molecular analysis of solid surfaces. Anal Chem 68(5):873–882

115. Wittmaack K, Szymczak W, Hoheisel G, Tuszynski W (2000) Time-of-flight secondary ion mass spectrometry of matrix-diluted oligo- and polypeptides bombarded with slow and fast projectiles: Positive and negative matrix and analyte ion yields, background signals, and sample aging. J Am Soc Mass Spectrom 11(6):553–563

116. Delcorte A, Poleunis C, Bertrand P (2006) Stretching the limits of static SIMS with C60+. Appl Surf Sci 252(19):6494–6497

117. Delcorte A, Garrison BJ (2007) keV fullerene interaction with hydrocarbon targets: projectile penetration, damage creation and removal. Nucl Instr Meth Phys Res B 255(1):223–228

118. Delcorte A, Yunus S, Wehbe N, Nieuwjaer N, Poleunis C, Felten A, Houssiau L, Pireaux JJ, Bertrand P (2007) Metal-assisted secondary Ion mass spectrometry using atomic (Ga+, in+) and fullerene projectiles. Anal Chem 79(10):3673–3689

119. Mahoney CM, Roberson SV, Gillen G (2004) Depth profiling of 4-acetamindophenol-doped poly(lactic acid) films using cluster secondary Ion mass spectrometry. Anal Chem 76(11):3199–3207

120. Mahoney CM, Fahey AJ, Belu AM (2008) Three-dimensional compositional analysis of drug eluting stent coatings using cluster secondary Ion mass spectrometry. Anal Chem 80 (3):624–632

121. McMahon J, Dookeran N, Todd P (1995) Organic ion imaging beyond the limit of static secondary ion mass spectrometry. J Am Soc Mass Spectrom 6(11):1047–1058

122. Ober CK (2000) Shape persistence of synthetic polymers. Science 288(5465):448–449

123. Trimpin S, Clemmer DE (2008) Ion mobility spectrometry/mass spectrometry snapshots for assessing the molecular compositions of complex polymeric systems. Anal Chem 80 (23):9073–9083

124. Fenn L, McLean J (2008) Biomolecular structural separations by ion mobility–mass spectrometry. Anal Bioanal Chem 391(3):905–909. doi:10.1007/s00216-008-1951-x

125. Kanu AB, Dwivedi P, Tam M, Matz L, Hill HH (2008) Ion mobility–mass spectrometry. J Mass Spectrom 43(1):1–22

126. Trimpin S, Plasencia M, Isallovic D, Clemmer DE (2007) Resolving oligomers from fully grown polymers with IMS/MS. Anal Chem 79(21):7965–7974

127. Bagal D, Zhang H, Schnier PD (2008) Gas-phase proton-transfer chemistry coupled with TOF mass spectrometry and Ion mobility-MS for the facile analysis of poly(ethylene glycols) and PEGylated polypeptide conjugates. Anal Chem 80(7):2408–2418

128. Hilton GR, Jackson AT, Thalassinos K, Scrivens JH (2008) Structural analysis of synthetic polymer mixtures using Ion mobility and tandem mass spectrometry. Anal Chem 80(24): 9720–9725

129. Song J, Grün CH, Heeren RMA, Janssen H-G, van den Brink OF (2010) High-resolution Ion mobility spectrometry–mass spectrometry on poly(methyl methacrylate). Angew Chem Int Ed Engl 49(52):10168–10171

Analysis of Polymer Additives and Impurities by Liquid Chromatography/Mass Spectrometry and Capillary Electrophoresis/Mass Spectrometry

Wolfgang Buchberger and Martin Stiftinger

Abstract The analysis of polymeric materials can be quite challenging because such samples are often of complex nature due to the presence of various groups of additives, compounding ingredients, and fillers. Of special importance are stabilizers that protect the material from degradation by thermal stress during manufacture or from environmental impact during use. Apart from intact stabilizers, the degradation products of stabilizers should also be identified to understand the reactions occurring in a polymeric material. In all cases, the optimization of performance of a polymer as well as the reduction of production costs requires adequate analytical methods, whereby high-performance liquid chromatography plays a major role. As outlined in this review, mass spectrometry with atmospheric pressure ionization has become state-of-the-art for identification of components in polymeric materials after separation by liquid chromatography. These ionization techniques include electrospray ionization, atmospheric pressure chemical ionization, and atmospheric pressure photoionization. The latter technique shows various advantages such as low detection limits and applicability to a wide range of structurally different polymer additives. Besides chromatography, capillary electrophoresis has demonstrated some potential for separation of polymer stabilizers and for characterization of polymers, but its importance is still limited in comparison with liquid chromatography. As an alternative to the combination of chromatography with mass spectrometric detection, direct mass spectrometric techniques for solid polymer samples are emerging. These techniques provide new tools for quick screening procedures at the same time as avoiding tedious sample preparation.

W. Buchberger (✉) and M. Stiftinger
Johannes-Kepler-University Linz, Institute of Analytical Chemistry, Altenbergerstrasse 69, 4040 Linz, Austria
e-mail: wolfgang.buchberger@jku.at

Contents

Abbreviations

APCI   Atmospheric pressure chemical ionization
APPI   Atmospheric pressure photoionization
ASAP   Atmospheric solid analysis probe
CE   Capillary electrophoresis
CZE   Capillary zone electrophoresis
DART   Direct analysis in real time
DESI   Desorption electrospray ionization
EOF   Electroosmotic flow
ESI   Electrospray ionization
GC   Gas chromatography
HALS   Hindered amine light stabilizers
HPLC   High-performance liquid chromatography
MALDI   Matrix-assisted laser desorption/ionization
MEEKC   Microemulsion electrokinetic chromatography
MEKC   Micellar electrokinetic chromatography
MS   Mass spectrometry
NP   Normal phase
RP   Reversed phase
SEC   Size-exclusion chromatography

SFC   Supercritical fluid chromatography
SIMS   Secondary ion mass spectrometry
TOF   Time-of-flight
UHPLC   Ultrahigh-performance liquid chromatography

1 Introduction

The importance of polymeric materials for various applications in everyday life
has continuously increased over the last decades. These materials provide sig-
nificant benefits, such as being durable and lightweight with an excellent cost/
performance ratio. At a first glance, many technical polymers may seem to be of
chemically simple composition, but polymeric materials can be complex samples
containing numerous additives that are responsible for the final physical and
chemical properties as well as for the long-term behavior. Among these additives
are nucleating agents that provide control over the formation of crystals; antistatics
that prevent build-up of static electricity by interacting with atmospheric mois-
ture; slip and antiblocking agents for easier manipulation of the polymer; acid
scavengers that protect manufacturing devices from corrosion; flame retardants;
compounding ingredients including mineral fillers or glass fibers; color pigments;
and stabilizers. Stabilizers are of utmost importance because several polymers
would be significantly impaired by degradation processes if no stabilizers were
added. Typical stabilizers include phenolic antioxidants that scavenge radicals,
organophosphites that decompose peroxides, and light stabilizers such as benzo-
phenone derivatives, benzotriazol compounds, and hindered amine light stabilizers
(HALS) that protect the material against photooxidation. The structures of a few
typically employed stabilizers are given in Fig. 1 together with common trade
names (although these compounds may also be available under different trade
names).

The analysis of additives (and especially of stabilizers) can be approached at in
two different ways. On the one hand, there is an obvious need for target analysis
(quantitative determination of known additives) for quality control during the
production process of polymers and polymeric materials, as the lifetime of a plastic
component may be directly related to the presence of a sufficiently high concen-
tration of a certain stabilizer. On the other hand, non-target analysis (qualitative
and quantitative analysis of unknown species) becomes a matter of concern when
products of competitors must be characterized or when degradation pathways of
additives (stabilizers) are investigated in order to obtain a better understanding of
the reaction mechanisms of stabilizers in a polymer. A better knowledge of degra-
dation products helps to avoid an insufficient stabilizer performance and to select
the most appropriate ones for a certain application.

Generally, the determination of additives and possibly unknown degradation
products in plastic materials is a challenging task in analytical chemistry due to the
widely differing chemical structures of additives. From the practical point of view,
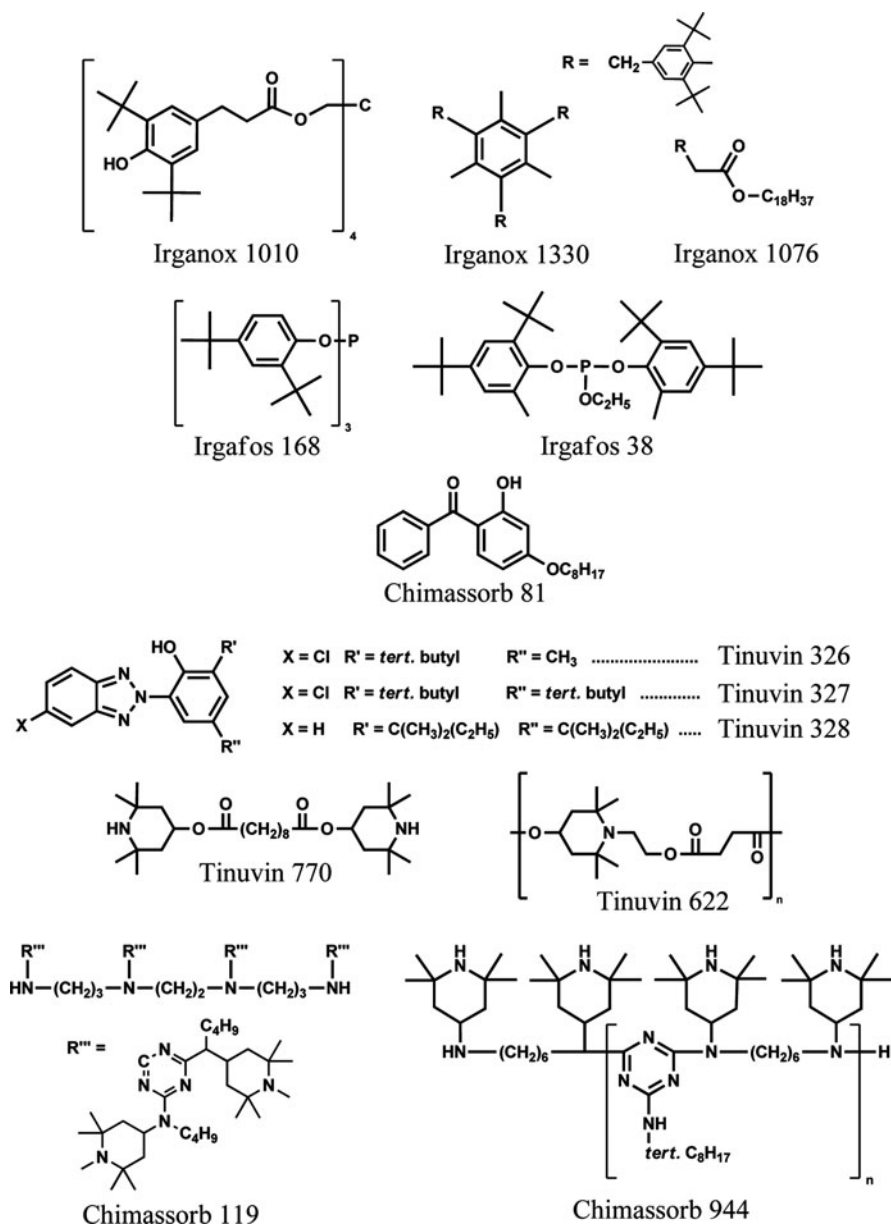
Fig. 1 Structures of various antioxidants (Irganox 1010, Irganox 1330, Irganox 1076), organophosphite process stabilizers (Irgafos 168, Irgafos 38), a benzophenone-type light stabilizer (Chimasorb 81), benzotriazole-type light stabilizers (Tinuvin 326, Tinuvin 327, Tinuvin 328), and hindered amine light stabilizers (Tinuvin 770, Tinuvin 622, Chimassorb 119, Chimasorb 944)

methods that can directly analyze additives in the solid sample without sample preparation would be most attractive. Unfortunately, such methods are not yet widely available or may not be sensitive enough to measure stabilizers typically present at concentration levels of a few tenths of a percent. In many cases, extraction of the analytes from the polymeric material or dissolution of the whole sample may be necessary. Due to the superior chemical stability of various technical polymeric materials, dissolution can become a main obstacle within the analysis. Also, extraction processes without dissolution of the whole sample can be quite tricky, and it may be difficult to prove that the extraction of the analyte is indeed quantitative. Even if sample preparation steps are available to get the analytes into solution, the subsequent determination step, typically based on chromatographic procedures, is far from trivial. Most additives are only slightly volatile and therefore not suitable for gas chromatographic (GC) analysis. Consequently, separation techniques operating in the liquid phase, including high-performance liquid chromatography (HPLC) and capillary electrophoresis (CE), are preferred. Although HPLC methods have become a routine tool for determination of additives in technical polymers, there is still no single stationary phase or single detection mode that allows simultaneous separation of the whole range of chemically different additives typically used for polymers.

This review deals with novel HPLC and CE methods for analysis and determination of additives in polymers. The possibilities of their use in conjunction with mass spectrometry (MS) are presented, with emphasis on achieving confirmation of additive identity, improving detection limits in the case of target analysis, and structure elucidation for unknown chromatographic peaks in the case of non-target analysis. Special attention will be paid to stabilizers, which are the additives most frequently analyzed for routine purposes.

2 Sample Preparation Prior to Chromatographic Analysis

As mentioned in the Introduction, a common approach to sample preparation for chromatographic analysis of additives is the dissolution of the total polymeric matrix, with all the different components present. Subsequently, the polymer can be precipitated by addition of an appropriate solvent that decreases the solubility of the polymer but still acts as a good solvent for the additives so that quite clean solutions for analysis are obtained. Depending on the chemical nature of the polymer, good solvents for dissolution of the whole sample may be difficult to find. Furthermore, polymers sometimes become strongly swollen rather than completely dissolved when treated with an organic solvent.

A typical procedure based on dissolution and precipitation for determination of stabilizers in polyolefins [1] includes the treatment of a 500 mg sample with 50 mL

toluene by refluxing. Subsequently, the solution is cooled and mixed with 25–50 mL of methanol. After filtration, an aliquot of the filtrate is evaporated to dryness and reconstituted in 0.5 mL of appropriate solvent for chromatographic analysis. Various similar procedures can be found in the literature for polyolefins using xylene or toluene for dissolution and methanol for precipitation [2, 3]. Depending on the type of polymer, other more aggressive solvents such as chloroform [4] or hexafluoropropanol/dichloromethane [5] have been suggested for dissolution, followed by precipitation using methanol or acetone. Such sample preparation strategies have been used for many years and are included in a review by Vandenburg et al. [6] prepared almost 15 years ago. More recently, it has been demonstrated that this dissolution/precipitation approach can also be miniaturized and applied to depth-profiling of stabilizers in polymeric materials using microtome slices [7].

In the case of HALS, the polymer can be completely dissolved in an appropriate solvent, followed by a liquid–liquid extraction step with aqueous sulfuric acid, which allows selective extraction of the analytes into the aqueous phase (see for example [8]).

Instead of using the total dissolution/precipitation approach, additives may also be extracted in a more selective way from the polymer by solid–liquid extraction using various techniques. In these cases, it is essential to decrease the particle size of the sample by grinding down to approximately 0.5 mm, preferentially with cooling by liquid nitrogen to avoid thermal degradation of the analytes. Traditional reflux or Soxhlet extraction, ultrasonic extraction, and more recent techniques like accelerated solvent extraction (sometimes called pressurized fluid extraction or enhanced solvent extraction) [9–12] and microwave-assisted extraction [12–14] have been applied for analysis of additives in polymer materials and have found their way into standard methods such as ASTM D7210-06. Supercritical fluid extraction has also demonstrated its potential for extraction of additives from polymers [15–17], although it requires equipment that is more expensive in comparison with other techniques.

3 HPLC/MS of Additives in Polymers

MS detection after liquid chromatographic separation is state-of-the art in modern instrumental analysis. Among the various interfaces and ionization sources developed over the last few decades for combination of HPLC with MS, only ionization sources working at atmospheric pressure, like electrospray ionization (ESI), atmospheric pressure chemical ionization (APCI), and atmospheric pressure photoionization (APPI), are nowadays used in routine analysis. Generally, the compatibility of mobile phases with the various ionization sources must be critically evaluated and optimization of mobile phase composition must be done with respect to both maximum separation selectivity/efficiency as well as maximum MS response.

3.1 HPLC Separation Modes for Additives in Polymers

Reversed-phase (RP)-HPLC using alkyl-modified silica as stationary phase has been the most widely used chromatographic system for the separation of various additives in polymers, particularly stabilizers. This is underlined by the fact that RP-HPLC is recommended in standard methods such as ASTM D6042-09. Typically, acetonitrile/water gradients are used. A comparison of acetonitrile/water and methanol/water gradients [18] indicated that the latter yields somewhat poorer separations, although this is not necessarily the case for every application. The main point in optimizing such separations is the optimization of the gradient conditions (time, steepness), which strongly depend on the type of RP material used (C18-materials from different manufacturers exhibit somewhat different separation selectivities so that gradient conditions must be adjusted accordingly). Some attempts have also been made to optimize the separation by using the column at elevated temperatures or applying thermal gradients [19].

Current trends in RP-HPLC of polymer additives point to the use of ultrahigh-performance liquid chromatography (UHPLC) using stationary phase particles of about 1.7 μm diameter (see for example [20]). Thereby, the efficiency (number of theoretical plates) is significantly increased and shorter columns leading to shorter analysis times can be employed. The disadvantage is the fact that the backpressure generated by UHPLC columns is considerably higher, which necessitates adequate hardware. Furthermore, UHPLC requires the strict elimination of dead volumes in the system. This may be less difficult if a UV detector is used, but ionization sources for MS may contribute to extra-column peak dispersion so that all the benefits of UHPLC columns are not fully available. As an alternative, particles with a nonporous core and a porous shell (core–shell particles, also known under the trade name Fused-Core particles) lead to less backpressure but still are more efficient than traditional particles used in HPLC. The advantages of such core–shell particles for routine analysis of various stabilizers of polymeric materials have recently been investigated [18].

Besides RP-HPLC, normal-phase (NP)-HPLC has also been used for separation of stabilizers (see for example [10, 21]). Although this approach may be advantageous as most stabilizers are easily soluble in typical NP mobile phases, its importance seems to be minor. In addition, NP-HPLC is not fully compatible with some ion sources nowadays used for MS detection.

Supercritical fluid chromatography (SFC) may also have some potential for separation of polymer additives both in the capillary column as well as in the packed column format, as demonstrated several years ago [22, 23]. Nevertheless, this technique has not fully found its way into routine analysis.

3.2 Detection by Electrospray Ionization/Mass Spectrometry

In many cases, polymer additives are nonpolar substances that are less suitable for ESI. An exception is the group of HALS compounds that are readily detected by

ESI in the positive mode due to the presence of protonable nitrogen atoms in the molecule structure. Andersen et al. [24] developed a RP separation of two HALS compounds by capillary RP-HPLC with time-of-flight (TOF) MS detection using a mobile phase consisting of ethylacetate/acetonitrile/triethylamine/acetic acid (45:44.9:10:0.1 v/v/v/v). The use of an amine in the mobile phase to block active sites on silica-based RP stationary phases in order to achieve good peak shapes may lead to ionization suppression in ESI. Therefore, mobile phases without the addition of an amine might be an advantage. Recently, Noguerol-Cal et al. reported the use of HPLC with a mobile phase consisting of water and methanol with 1% formic acid [25] for coupling with an Orbitrap MS. Unfortunately, under such chromatographic conditions the separation performance deteriorates considerably. An alternative to the use of mobile phases containing an amine would be the use of mobile phases at high pH, above the pK_a values of the HALS compounds. Reasonable peak shapes can indeed be achieved under such conditions with a gradient of an aqueous phosphate solution adjusted to pH 11 and acetonitrile [25], but these conditions are hardly compatible with ESI. Reisinger [26] has demonstrated that even a gradient of 0.005 M KOH in methanol and aqueous 0.01 M KOH can achieve a separation of HALS analytes on a stationary phase based on pH-stable methacrylate functionalized with C18 groups. In this case it would be possible to use a suppressor (well-known from suppressed conductivity detection in ion chromatography [27]) between the column and the ESI so that KOH is converted to water prior to entering the ion source. So far, this approach has not yet been investigated in detail but is an attractive approach to be studied in future work.

In the case of Tinuvin 770, which is a relatively simple HALS, Gill et al. [28] developed a RP-HPLC-ESI/MS method using a mobile phase of aqueous ammonium acetate and methanol under gradient conditions, and validated this method for quantitation in migration studies of the stabilizer from a polymeric material into water.

Another area where ESI may be appropriate is the characterization of antistatic additives such as glycerol monostearates, sorbitan fatty acid esters, or ethoxylated alkyl amines. These additives are typically used in polymeric materials as complex mixtures, so that appropriate methods based on HPLC/MS are required for quality control of the additives. Methods have been recently developed for such purposes [29], although applications regarding the quantitation of the additives in polymeric materials are still missing.

HPLC-ESI/MS may also be the method of choice for detection of perfluorooctanoic acid in polytetrafluoroethylene polymers [30]. In this case, perfluorooctanoic acid may occur as an impurity rather than an additive.

Himmelsbach et al. [31] have systematically compared the ESI behavior of various phenolic antioxidants, organophosphites, and benzotriazole light stabilizers with their behavior in APCI and APPI. ESI turned out, as expected, to be inferior to APCI and APPI. On the other hand, the poorer detection limits of ESI do not necessarily exclude its suitability for certain applications such as the analysis of antioxidants in insulation cladding of copper wire [32].

A way around the poor response of nonpolar compounds in the ESI mode is the use of coordination ion spray (CIS). In this case, a common ESI source is used, but after the HPLC column the addition of ions, typically Ag^+, leads to the formation of stable complexes with the analytes and to the ionization. An application to polymer analysis has been reported by Hayen et al. [33] who investigated the behavior of bis-(3-triethoxysilylpropyl) tetrasulfide, a widely used coupling reagent for silica-reinforced rubber materials, and related compounds as well as their reaction products during rubber vulcanization processes.

3.3 Detection by Atmospheric Pressure Chemical Ionization/Mass Spectrometry

In most cases, when MS detection has been employed for determination of additives in polymeric materials, APCI has been used. Its advantages for additives like phenolic antioxidants, organophosphites, benzotriazole compounds, erucamide, oleamide, and oleylpalmitamide have been demonstrated by Block et al. [34] who were able to compile a library of MS spectra of polymer additives. The response of brominated and phosphate-based flame retardants has been studied by Schlummer et al. [35] using RP-HPLC as well as size-exclusion chromatography (SEC) coupled to RP-HPLC. The wide field of applications of APCI in polymer analysis, including even NP chromatography, has recently been outlined by Desmazieres et al. [36], although the focus of that paper was on the polymers and not on the additives. APCI/MS detection has also been successfully applied to separations done by SFC [23].

Duderstadt and Fischer [37] have investigated the impact of the composition of the mobile phase typically employed in RP chromatography on the signal intensities achieved by APCI/MS for selected additives used in polyalkenes. For the positive ionization mode, they tested gradients of water with acetonitrile, methanol, or acetone. In addition, acetonitrile-based mobile phases with post-column addition of methanol were investigated. In the negative ionization mode, the same mobile phases as for positive ionization were employed with the exception of post-column addition of methanol. For the analytes responding in the positive mode, mobile phases based on methanol demonstrated the highest universality, and at the same time yielded the highest response in nearly all cases. In the negative ionization mode, the number of detectable analytes was generally lower, but again methanol-based mobile phases turned out to be best suited. Post-column addition of methanol to mobile phases based on acetonitrile did not lead to results as good as those for mobile phases based on methanol. It should be noted that these investigations primarily focused on a maximum in signal intensities. Highest signal intensity does not necessarily lead to lowest detection limits because the noise of APCI detection must be taken into account and signal/noise ratios do not necessarily depend in the same way on mobile phase composition as signal intensities.

A detailed study of detection limits for polymer additives using APCI/MS detection has been carried out by Himmelsbach et al. [31] and data have been compared with APPI/MS (see discussion in the next section).

3.4 Detection by Atmospheric Pressure Photoionization/Mass Spectrometry

APPI is the latest technology introduced for atmospheric pressure ionization MS [38] and has expanded the range of analytes accessible to HPLC/MS considerably. In many cases, both polar and nonpolar analytes can be analyzed with satisfactory efficiency so that this ionization source has become increasingly popular over the last few years in various application areas [39, 40].

APPI is achieved by photons emitted from a krypton lamp that can interact with the vaporized mobile phase of the HPLC and with the analytes. In the positive ionization mode, direct ionization of the analyte is possible by the photons. Alternatively, a dopand can be added to the mobile phase that is preferentially ionized and, in a second step, ionizes the analyte via charge transfer or proton transfer. Furthermore, the ionized dopand can react with solvent molecules of the mobile phase, thereby forming protonated solvent clusters that ionize the analyte via proton transfer. In the negative ionization mode, direct ionization of the analyte by electron capture is possible. Alternatively, the electrons generated during dopant photoionization may interact with oxygen and yield superoxide ions that can ionize the analyte via deprotonation or by electron transfer. Superoxide ions may also react with analytes in a way that H, Cl, Br, or NO_2 is split off and oxygen is attached. Details of the ionization mechanisms can be found in the recent literature [39]. In addition to photoionization, thermospray ionization can also occur in APPI sources currently in use [41].

The applicability of APPI to a series of stabilizers including phenolic antioxidants (Irganox MD1024, Irganox 1081, Irganox 1035, Irganox 3114, Irganox 1010, Irganox 1330, Irganox 1076), a benzophenone-type UV absorber (Chimassorb 81), benzotriazol-type UV absorbers (Tinuvin 234, Tinuvin 326, Tinuvin 327, Tinuvin 328), and organophosphite processing stabilizers (Irgafos 126, Irgafos 38, Irgafos 168) has been studied by Himmelsbach et al. [31] using RP-HPLC with mobile phases of acetonitrile and water. Figure 2 shows the comparison of HPLC with UV detection at 200 nm and detection by APPI/MS of a standard solution of these stabilizers. The chromatogram clearly demonstrates the improvement made with APPI/MS detection in comparison with commonly employed UV detection. The results were also compared with APCI and ESI. Table 1 summarizes the detection limits of HPLC/MS with different ionization techniques. In the case of phenolic antioxidants, negative ionization is generally favored over the positive mode, as can be expected from the presence of phenolic groups in these molecules. Overall, APPI performs better for phenolic antioxidants than does APCI and ESI. Also, the UV
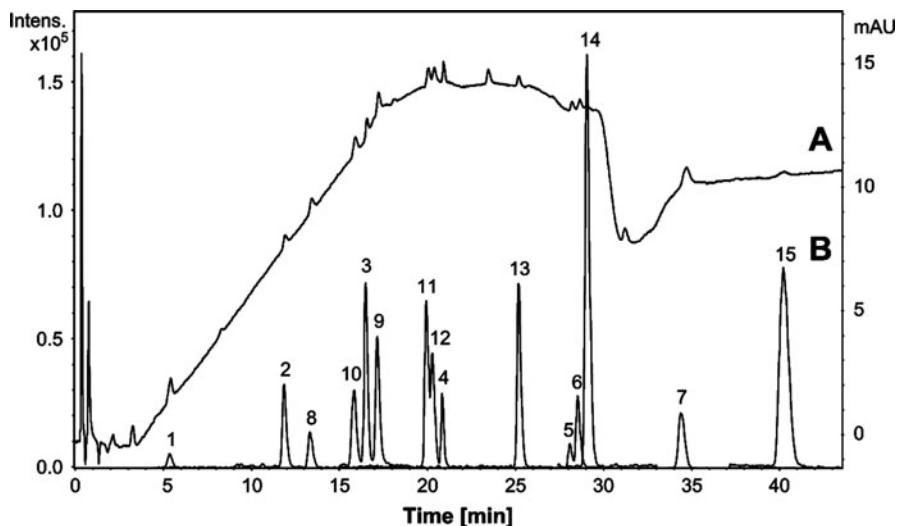
Fig. 2 HPLC separation of stabilizers with UV detection at 200 nm (*A*) and an APPI/MS extracted ion chromatogram (*B*) of a standard solution containing 0.07 mg L^{-1} of each analyte. Peaks: *1* Irganox MD1024, *2* Irganox 1081, *3* Irganox 1035, *4* Irganox 3114, *5* Irganox 1010, *6* Irganox 1330, *7* Irganox 1076, *8* Chimassorb 81, *9* Tinuvin 234, *10* Tinuvin 326, *11* Tinuvin 327, *12* Tinuvin 328, *13* Irgafos 126, *14* Irgafos 38, *15* Irgafos 168. Reprinted from [31] with permission from Elsevier

Table 1 Detection limits (mg L^{-1}) of polymer stabilizers in RP-HPLC/MS using a methanol/water gradient elution with different ionization techniques (data taken from [31])

Analyte	APPI positive	APPI positive with dopant toluene	APPI negative	APPI negative with dopant toluene	APCI positive	APCI negative	ESI positive with formic acid	ESI negative with ammonia
Irganox MD 1024	0.100	0.038	0.022	0.010	0.100	0.040	0.004	0.033
Irganox 1081	0.078	0.700	0.009	0.035	0.900	0.021	0.180	0.011
Irganox 1035	0.008	0.039	0.001	0.002	0.057	0.018	0.003	0.002
Irganox 3114	0.370	1.300	0.007	0.033	0.200	0.067	0.240	0.023
Irganox 1010	0.035	0.030	0.012	0.065	0.032	0.110	0.400	0.022
Irganox 1330	0.013	0.077	0.009	0.009	0.045	0.027	0.049	0.300
Irganox 1076	>10	>10	0.002	0.029	>10	0.015	>10	0.017
Chimassorb 81	0.019	0.060	0.014	0.069	0.290	0.022	0.060	0.038
Tinuvin 234	0.001	0.009	0.001	0.015	0.016	0.011	0.060	0.090
Tinuvin 326	0.100	0.560	0.011	0.110	0.310	0.030	0.070	0.072
Tinuvin 327	0.054	0.710	0.005	0.037	0.400	0.068	0.046	0.051
Tinuvin 328	0.006	0.090	0.005	0.054	0.057	0.042	0.043	0.070
Irgafos 126	0.003	0.008	>10	>10	0.013	>10	0.044	>10
Irgafos 38	0.001	0.005	>10	>10	0.010	>10	0.017	>10
Irgafos 168	0.001	0.018	>10	6.000	0.012	>10	0.028	2.100

absorbers showed lower detection limits in the negative ionization mode than in the positive mode, with APPI outperforming the other ionization techniques. Organophosphite compounds can only be analyzed at sufficiently low concentrations in the positive ionization mode, whereby protonated species are generated. Again, APPI yields the lowest detection limits.

In this context, the behavior of Tinuvin 326 and Tinuvin 327 is interesting. The chemical structures of these two stabilizers contain a chlorine atom. When comparing the APPI responses of Tinuvin 326 and 327 with those of structurally analogous Tinuvin 234 or 328 (which do not contain a chlorine atom), it is evident that in the negative mode the detection limits are quite similar, whereas in the positive mode the detection limits of Tinvin 326 and 327 are considerably worse. This behavior is even more pronounced when looking at the response of the analyte instead of the detection limits. From these results it can be concluded that analogous structures may result in quite different ionization efficiencies if an electronegative group is present or absent in the molecule.

As can be seen from Table 1, the use of a dopant does not improve the detection limits on average. Nevertheless, it is interesting to compare the signal intensities (peak areas) for APPI with and without dopant. Table 2 summarizes the signal intensity enhancement factors obtained by dividing the signal intensity by the peak intensity for APPI without dopant. All data in Fig. 2 refer to the results in the negative ionization mode, except for the Irgafos-type stabilizers for which results from the positive ionization mode are used. Toluene as dopant increases signal intensities by up to a factor of 6.6 (but no signal enhancement is achieved for

Table 2 Signal intensity enhancement in APPI resulting from the use of a dopant, relative to APPI without dopant

Analyte	Enhancement factor		
	APPI	APPI with dopant toluene	APPI with dopant acetone
Irganox MD 1024	1.0	4.8	12.9
Irganox 1081	1.0	6.6	21.9
Irganox 1035	1.0	2.1	9.8
Irganox 3114	1.0	2.0	3.9
Irganox 1010	1.0	1.1	6.4
Irganox 1330	1.0	1.5	7.7
Irganox 1076	1.0	2.9	21.5
Chimassorb 81	1.0	5.3	21.3
Tinuvin 234	1.0	2.2	12.3
Tinuvin 326	1.0	6.1	36.4
Tinuvin 327	1.0	3.4	22.1
Tinuvin 328	1.0	5.3	28.6
Irgafos 126	1.0	1.0	3.6
Irgafos 38	1.0	1.0	4.5
Irgafos 168	1.0	1.0	4.1

All data refer to the negative ionization mode except for the Irgafos-type analytes, which were measured in the positive mode (data taken from [31])
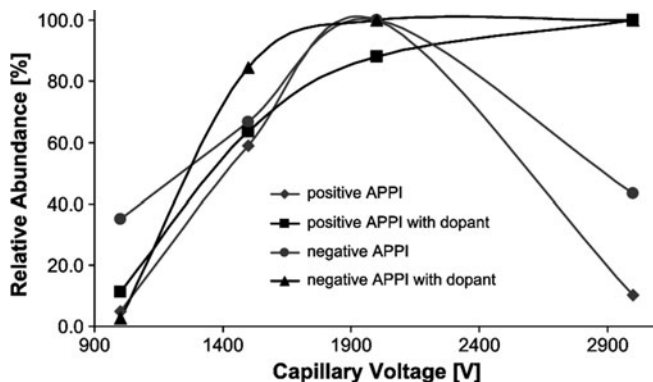
Fig. 3 Effect of MS capillary voltage on the signal intensity of Tinuvin 234 in positive and negative APPI both with and without toluene as dopant. The maximum intensity obtained in each mode is normalized to 100%. Reprinted from [31] with permission from Elsevier

Irgafos-type analytes). Nevertheless, noise also increases so that no significant improvement in the detection limits can be achieved. Even higher enhancement factors of up to 36.4 are observed for acetone as dopant, but again the increasing baseline noise cancels the positive effect of signal enhancement. In this context it is important to be aware of the fact that APPI without or with a dopant may require somewhat different operating parameters, such as the MS capillary voltage. As shown in Fig. 3 for Tinuvin 234, a narrow maximum at about 2,000 V is encountered for the ionization process without a dopant, whereas in case of toluene as dopant a wide range of between 2,000 V and 3,000 V can be used.

3.5 Analysis of Degradation Products of Stabilizers by HPLC/MS

Degradation products of stabilizers can be generated due to oxidative processes and/or heat during processing of the polymeric material, or during use of the material due to environmental impact. Such degradation reactions are typically related to the protection of the polymer by the stabilizer. On the other hand, stabilizers can be degraded by reactions that are not related to their consumption during stabilization, such as by interactions with other additives used in the polymeric material. Whatever the reasons for degradation might be, a decrease in the concentration of intact stabilizer is undesired, and information on the formation of degradation products is required to clarify degradation pathways and to avoid major degradation reactions. On the other hand, HALS stabilizers are recycled during stabilization of the polymer. Therefore, no accumulation of stable degradation products is observed, but intermediate products may occur. Their analysis would be an even more challenging task because their concentrations stay quite low.

Some information about the degradation pathways of stabilizers can be obtained from the results of emission measurements, which are necessary for quality control of polymeric materials with respect to the final application. It is well known that, for example, industrial-grade polypropylene can emit compounds like di-*tert*-butylphenol (the hydrolysis product of phosphite-type stabilizers), *tert*-butylphenol and phenol (generated from di-*tert*-butylphenol), and di-*tert*-butylcresol or di-*tert*-butylbenzoquinone (both generated from phenolic antioxidants). Emission measurements are typically performed by well-established GC methods in combination with MS detection and are not discussed further in this review.

The fragmentation patters observed in mass spectra of pure stabilizers can provide some suggestions about how stabilizers can degrade. Nevertheless, conditions of fragmentation during MS ionization are still significantly different from real-world conditions so that the relevance of MS fragmentation patterns must be critically checked in all cases. Therefore, degradation experiments under controlled conditions must be carried out. A recent review [42] summarizes the degradation products observed so far under controlled conditions. Both GC and HPLC methods have been applied for analysis of degradation products, but HPLC approaches published so far have included MS detection only in a very limited number of cases.

Reingruber et al. [1] have undertaken investigations on the degradation products of pure antioxidants generated under thermal stress, and have extended these studies to mixtures of pure antioxidants and talcum commonly used as inorganic filler in polypropylene. Figure 4 shows the HPLC chromatograms with APPI/MS detection (negative ionization mode) of various stabilizers treated at 115 °C for 24 h in the presence of talcum. The amount of some degradation products generated under these conditions was quite small, but identification of several peaks was still possible. The results of this study are summarized in Table 3. A comparison of APPI with APCI or ESI, showed that APPI is a quite universal detection technique, whereas ESI yielded a much lower number of peaks in the chromatogram.

Besides thermal stress, the impact of chlorinated water on the degradation pathways of stabilizers is of considerable fundamental interest. Various preliminary experiments using HPLC with APPI/MS were carried out by Pan [43]. As an example, the chromatogram of Irganox 1035 after exposure to chlorinated water is given in Fig. 5. During model experiments, this stabilizer underwent quick oxidation at its sulfur atom (besides additional degradation reactions).

4 CE/MS of Additives in Polymers

CE has become a well-established high-performance separation technique that is complementary to liquid chromatography. With respect to the determination of analytes of low to medium molecular weight, capillary zone electrophoresis (CZE) and micellar electrokinetic chromatography (MEKC) as well as microemulsion electrokinetic chromatography (MEEKC) are the most promising techniques. In CZE, the application of a high voltage leads to separation of the analytes due
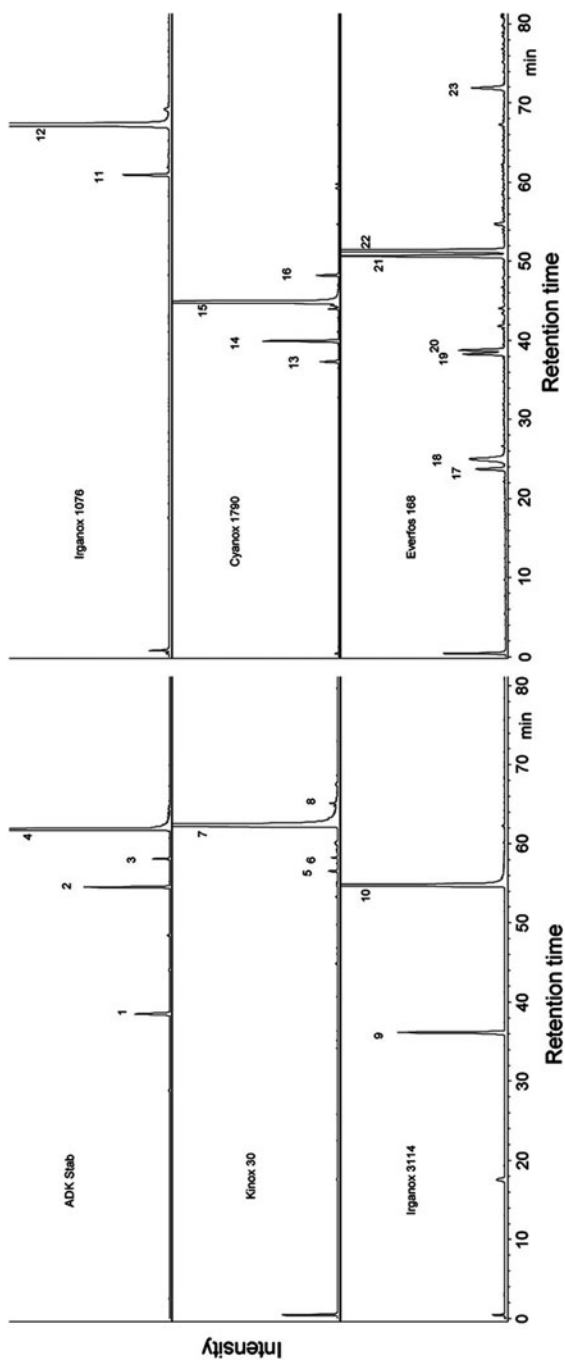
Fig. 4 HPLC-APPI/MS (negative mode) of extracts from model mixtures of different stabilizers with talcum (ADK Stab and Kinox 30 refer to the stabilizers Irganox 1010 and Irganox 1330). Peak numbering see Table 3. Reprinted from [1] with permission from Elsevier

Table 3 Peaks identified in the chromatograms shown in Fig. 4 (adapted from [1])

Peak number	Molecular formula	Identified substances
1	$C_{39}H_{60}O_8$	Irganox 1010, two ester bonds hydrolyzed
2	$C_{56}H_{84}O_{10}$	Irganox 1010, one ester bonds hydrolyzed
3	$C_{69}H_{100}O_{12}$	Irganox 1010, one *tert*-butyl group split off
4	$C_{73}H_{108}O_{12}$	Irganox 1010
5	$C_{39}H_{56}O_2$	Irganox 1330, one di-*tert*-hydroxy-toluene group split off
6	$C_{50}H_{70}O_3$	Irganox 1330, one *tert*-butyl group split off
7	$C_{54}H_{78}O_3$	Irganox 1330
8	$C_{54}H_{76}O_3$	Irganox 1330, one hydroxy group oxidized
9	$C_{33}H_{47}N_3O_5$	Irganox 3114, one di-*tert*-butyl-phenol group split off
10	$C_{33}H_{47}N_3O_5$	Irganox 3114, detected as a fragment with one di-*tert*-butyl-phenol group split off
11	$C_{31}H_{54}O_3$	Irganox 1076, one *tert*-butyl group split off
12	$C_{35}H_{62}O_3$	Irganox 1076
13	$C_{42}H_{57}N_3O_7$	Hydroxylated Cyanox 1790
14	$C_{42}H_{55}N_3O_7$	Oxidized Cyanox 1790
15	$C_{42}H_{57}N_3O_6$	Cyanox 1790
16	$C_{42}H_{57}N_3O_6$	Cyanox 1790 with *tert*-butyl and methyl groups rearranged
17	$C_{14}H_{22}O$	Di-*tert*-butyl-phenol
18	$C_{20}H_{26}O_2$	Reaction product of two mono-*tert*-butyl-phenols
19	$C_{18}H_{30}O$	Tri-*tert*-butyl-phenol
20	$C_{24}H_{34}O_2$	Reaction product of a mono- with a di-*tert*-butyl-phenol
21	$C_{28}H_{43}O_3P$	Irgafos 168, one di-*tert*-butyl-phenol group split off
22	$C_{28}H_{42}O_2$	Reaction product of two di-*tert*-butyl-phenols
23	$C_{28}H_{43}O_4P$	Irgafos 168, detected as an oxidized fragment with one-di-*tert*-butyl-phenol group split off

to migration in a suitable carrier electrolyte according to their electrophoretic mobilities, which depend on their charge/size ratio. Fused silica capillaries generally used in CE provide a negative charge at the inner surface as a result of the dissociation of silanol groups, thereby generating an electroosmotic flow (EOF), also called electroosmotic mobility, that is normally directed towards the cathode and superimposes the electrophoretic mobility of analytes. Therefore, the total mobility of an analyte is the vector sum of the electrophoretic mobility and the electroosmotic mobility.

Besides CZE, CE techniques involving a pseudostationary phase such as micelles or a microemulsion in the carrier electrolyte are frequently applied. If micelles consisting of an anionic surfactant are employed, their electrophoretic mobility will be directed to the anode, whereas the electroosmotic mobility is directed towards the cathode. In the case of an alkaline carrier electrolyte that produces a relatively high EOF, the total mobility of the micelles will be directed towards the cathode but will be smaller than the EOF. A neutral hydrophilic analyte will move with the velocity of the EOF. Hydrophobic analytes will also undergo a partitioning equilibrium with the pseudostationary phase and will move at a lower
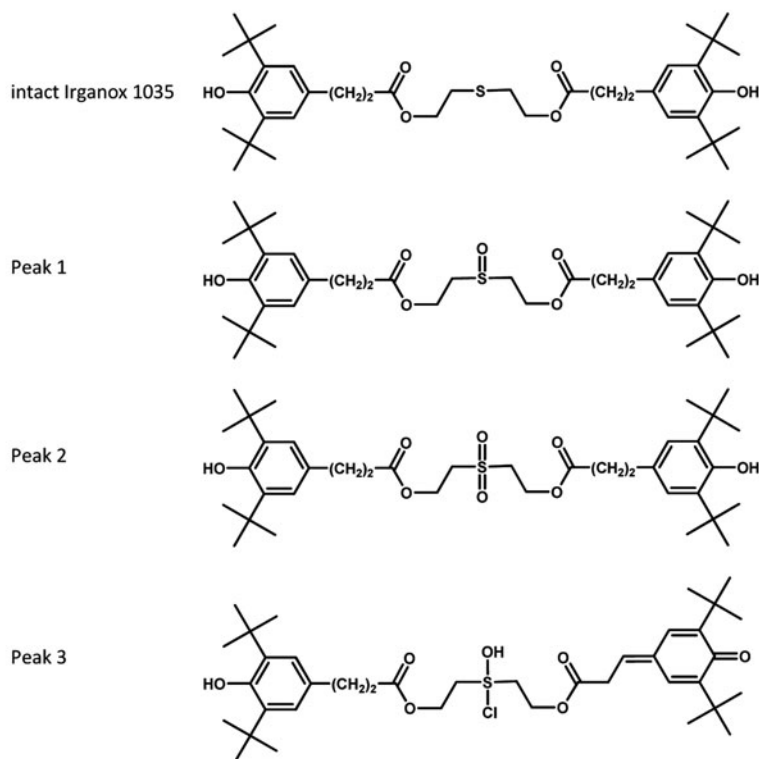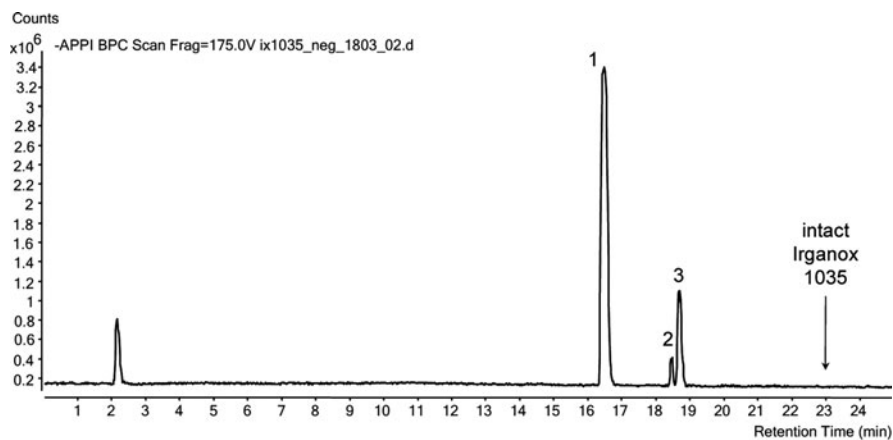
Fig. 5 HPLC-APPI/MS of the stabilizer Irganox 1035 and major degradation products after exposure to chlorinated water (adapted from [43])

speed than hydrophilic analytes. Therefore, a separation of neutral analytes can be achieved on the basis of their hydrophobic properties. Instead of micelles in MEKC, a microemulsion (tiny droplets of a solvent such as octane that is not miscible with

water) stabilized by dodecylsulfate ions that attach to the surface of the droplets and result in a negative charge can be used as the pseudostationary phase (MEEKC).

Regarding CZE for separation of additives for polymers, there are few applications up to now. This is mostly the result of a lack of sufficiently ionizable groups as well as of problems with solubility in carrier electrolytes suitable for CZE. Some preliminary work has been carried out for separation of HALS [18] using a carrier electrolyte of phosphoric acid in methanol, but a fully satisfactory separation of different stabilizers has not yet been achieved.

MEEKC has turned out to be much more promising for separation of hydrophobic polymer additives such as various phenolic antioxidants (Irganox 1024, Irganox 1035, Irganox 1076, Irganox 1010, Irganox 1330, Irgafos 138, Irganox 168, 2,6-di-*tert*.-butyl-4-methylphenol) [44]. The optimized carrier electrolyte consisted of 2.25% (w/w) sodium dodecylsulfate (SDS), 0.75% (w/w) Brij 35, 0.8% (w/w) n-octane, 6.6% (w/w) 1-butanol, 25% (w/w) 2-propanol, and 64.6% (w/w) 10 mM borate buffer (pH 9.2). The addition of 2-propanol was done to manipulate the partitioning of analytes between the borate buffer and the pseudostationary phase. The use of two different surfactants, the anionic SDS and the neutral Brij 35, allowed sufficient stabilization of the microemulsion. Changing the ratio of the two surfactants allowed the manipulation of the charge of the droplets and thereby their velocity. A typical separation of the phenolic antioxidants is shown in Fig. 6.

Nowadays, CE can be combined with MS detection, yielding an instrumentation that is not only suitable for research but can also be used in routine analysis. In this context, a few aspects must be taken into account. Commercially available ESI, APCI, or APPI sources (typically designed for combination with HPLC) require flow rates that are considerably higher than the flow rates in CE. In addition, at the end of the separation capillary the current from the electrophoretic separation has to
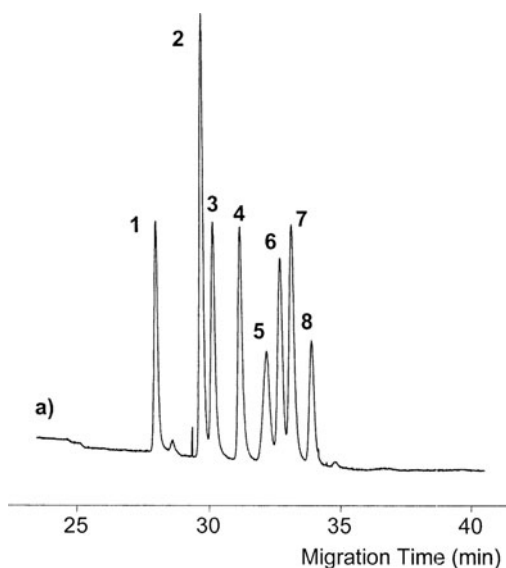

Fig. 6 Separation of stabilizers by MEEKC. Peaks: *1* Irganox 1024, *2* 2,6-di-*tert*-butyl-4-methylphenol, *3* Irganox 1035, *4* Irgafos 38, *5* Irgafos 168, *6* Irganox 1010, *7* Irganox 1330, *8* Irganox 1076. Reprinted from [44] with permission from Elsevier

be grounded and, in the case of ESI, the spray potential must also be applied. For these reasons, the most widely used design for combination of CE with MS is the sheath liquid interface, which is based on a make-up flow at the end of the capillary. Electrical contact is made via the make-up flow.

Another problem encountered for combination of CE and MS is the limited compatibility of components of the carrier electrolyte with the ionization process. ESI in particular can suffer considerably when operated with carrier electrolytes containing less volatile electrolytes. In MEEKC, the carrier electrolytes containing pseudostationary phases are often considered incompatible with ESI. On the other hand, recent work has demonstrated that combination of CE with APPI/MS can avoid a major loss of performance [45].

Up to now, there have been hardly any papers dealing with CE and MS detection for analysis of additives in polymeric materials. Nevertheless, an example of the successful implementation of CE/MS in polymer analysis is the determination of reaction products from the condensation of melamine (M) with formaldehyde (F) in M–F resins. Although this application does not deal with typical additives in polymers, it is a good example of the application of CE/MS for characterization of polymers with respect to their varying properties, and is therefore included here. M–F condensation products such as MF, MF_2, MF_3,... and M_2, M_2F, M_2F_2, M_2F_3,... become protonated under acidic conditions and are efficiently separated in a formic acid-based carrier electrolyte containing 50% acetonitrile. The use of a TOF/MS detector allows the assignment of molecular structures [46]. As can be seen from Fig. 7, even isomers can be separated using CZE.
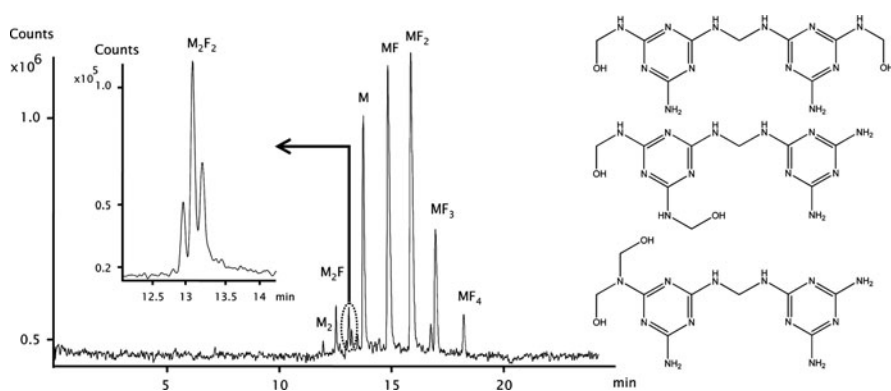

Fig. 7 CZE/MS electropherogram of a melamine (M)/formaldehyde (F) resin showing different reaction products from the condensation of M with F. The *inset* shows the separated isomers of M_2F_2 for which the chemical structures are given on the *right*. Reprinted from [46] with permission from Elsevier

5 Combination of Liquid Chromatography and Pyrolysis-GC/MS

Nowadays, pyrolysis-GC/MS is a routine tool in polymer analysis for identification of the polymer itself as well as for determination of additives that are not sufficiently volatile to be analyzed in their intact forms. Unfortunately, peaks resulting from the polymer may seriously interfere with peaks from additives present at low levels. Furthermore, structurally related additives may yield the same pyrolysis products so that pyrolysis-GC/MS would not be able to differentiate between them. In such cases, the on-line combination of a liquid chromatographic technique with pyrolysis-GC/MS would be an interesting alternative. In such an approach, pyrolysis-GC/MS would act as "detector" for the liquid chromatographic separation. Possible realizations of the combination of liquid chromatography with GC via a programmed temperature vaporizer for elimination of the solvent have been reported various times and have served as the basis for the work of Kaal et al. [47] who demonstrated on-line SEC coupled with pyrolysis-GC/MS for simultaneous polymer characterization and additive analysis. Figure 8 shows the chromatograms for the analysis of polycarbonate containing two additives, Irganox 1076 and Irganox 3114. Two fractions of the polymer peak of the SEC separation were transferred to pyrolysis-GC/MS and showed bisphenol-A as the main peak. Fractions of the later eluting peak containing low molecular weight stabilizers
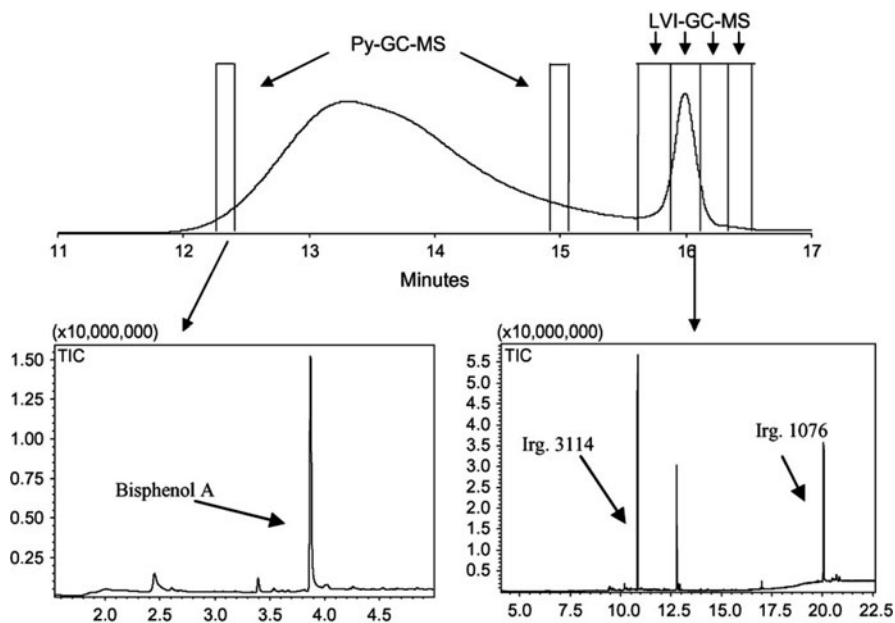
Fig. 8 Simultaneous polymer characterization and additive analysis of a polycarbonate sample using SEC coupled to pyrolysis-GC/MS. *TIC* total ion chromatogram. Reprinted from [47] with permission from Elsevier

were transferred in a similar way and yielded MS signals that allowed a clear identification. Depending on the analytes, the GC injector can operate as simple large-volume injector (LVI) for analytes that are sufficiently volatile, or as pyrolysis injector for nonvolatile analytes. Furthermore, this technique is not restricted to a combination with SEC as liquid chromatographic technique because other techniques like RP or NP chromatography will work as well. Thus, one may think of a range of applications not yet investigated in the area of additive analysis.

6 Direct Mass Spectrometry for Determination of Additives in Polymers

As mentioned in the Introduction, most currently used routine techniques for determination of additives in polymers require dissolution of the polymer for the extraction of analytes from the polymer. These steps may be quite time-consuming and therefore not fully compatible with the requirements of rapid screening procedures. Some alternatives based on novel MS techniques suitable for solid polymer samples have been introduced recently. Some of the approaches are briefly summarized below. They may deliver semiquantitative information rather than quantitative results, but nevertheless they can be very suitable for screening of unknown samples prior to HPLC analysis. It should be made clear that such direct MS measurements give information about additives present in the surface layer of the solid sample, therefore the results may be different from bulk analysis achieved by traditional HPLC analysis after dissolution or extraction of the sample.

6.1 Desorption Electrospray Ionization/Mass Spectrometry

Desorption electrospray ionization (DESI) was developed by Cooks and coworkers [48]. It is based on the flow of a liquid that is converted into an electrospray by applying a high voltage. The charged droplets are directed to the surface of the solid sample under atmospheric pressure. A possible mechanism suggested for the ionization process consists of the impact of the charged droplets on the sample, whereby the analyte is dissolved into the droplets. Subsequently, secondary droplets containing analyte molecules are ejected from the surface and move to the mass analyzer under conditions similar to conventional ESI.

DESI has recently been applied to a set of light stabilizers including Chimassorb 81 (a benzephenone derivative), Tinuvin 326 and 328 (benzotriazole derivatives), and Tinuvin 770 (a sterically hindered amine) in polypropylene samples [49]. These investigations indicated that best results can be achieved with a spray solution of methanol/water/formic acid (80/20/0.1). Calibration curves obtained with polymer samples containing the stabilizers at concentrations of 0.02, 0.05, 0.1, and 0.2% (w/w) yielded satisfactory linearity and values for R^2 better than 0.994. Figure 9

shows the mass spectra of a model polymer sample containing all four additives at a concentration of 0.2% (w/w), of a vinyl liner for an in-ground swimming pool, and of technical polypropylene granules.
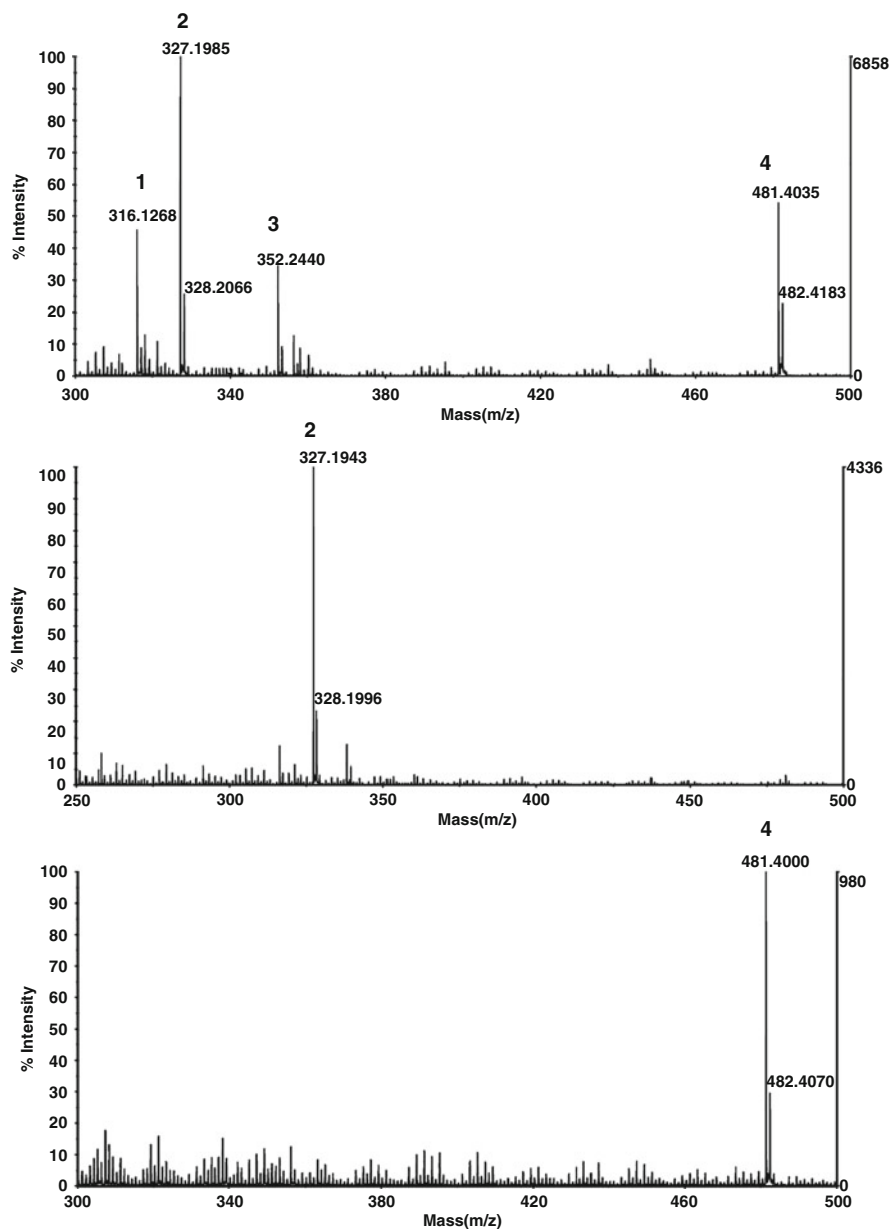

Fig. 9 DESI/MS of (**a**) model sample containing four stabilizers at a concentration level of 0.2%, (**b**) vinyl liner for a swimming pool, and (**c**) technical polymer granule. Analytes: *1* Tinuvin 326, *2* Chimassorb 81, *3* Tinuvin 328, *4* Tinuvin 770. Reprinted from [49] with permission from Springer

6.2 Direct Analysis in Real Time/Mass Spectrometry

The direct analysis in real time (DART) ion source was developed by Cody and Laramee and details were first published in 2005 [50]. Since then, this ion source has become commercially available and consists of a tube of several chambers through which a gas like helium flows. In the first chamber, a glow discharge is generated and produces ions, electrons, and excited state atoms (metastable species) such as $He(2^3S)$. In the second chamber, an applied voltage removes charged species, and only excited state species flow to a third chamber, which can be heated. Afterwards, the excited state species interact with the sample such as a solid polymer (samples in the liquid state can be analyzed as well) at atmospheric pressure to produce and desorb ionized analyte species that are directed to the inlet of the mass analyzer operating under high vacuum.

Ionization of the analyte A by $He(2^3S)$ may occur through Penning ionization:

$$He(2^3S) + A \rightarrow A^+ + He(^1S) + e^-$$

More important may be the following reaction between $He(2^3S)$ and atmospheric moisture, leading to protonated water clusters:

$$He(2^3S) + nH_2O \rightarrow [(H_2O)_{n-1} + H]^+ + OH^- + He(1^1S)$$
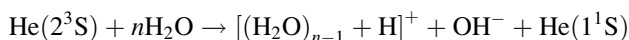
These protonated water clusters may ionize the analyte A by proton transfer:

$$[(H_2O)_n + H]^+ + A \rightarrow [A + H]^+ + nH_2O$$
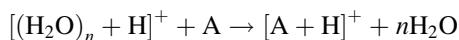
Ammonium adducts $[A+NH_4]^+$ may be observed if ammonia is introduced into the sample region. In addition to the formation of positively charged ions, DART may also generate negatively charged ions, although the relevant mechanisms have not yet been fully investigated.

Recently, Haunschmidt et al. [51] systematically investigated the ionization by DART of various stabilizers. All analytes could be measured in the positive mode as $[A+H^+]$, as A^+, or as $[M+NH_4]^+$ and several could also be measured in the negative mode, yielding $[M-H]^-$ or $[M+O_2]^-$ ions. Generally, the positive mode proved to provide better sensitivities. The applicability to solid polymer samples was tested using laboratory-made polypropylene samples containing various sets of stabilizers. DART also allowed the identification of decomposition products of stabilizers generated due to the elevated temperature of the compounding process. In Fig. 10, the mass spectrum of a polymer sample containing Irgafos 126 and degradation products after compounding at 190 °C is given (to avoid misunderstanding, it is important to mention that the various signals in the mass spectrum do not represent fragment ions generated during the ionization process
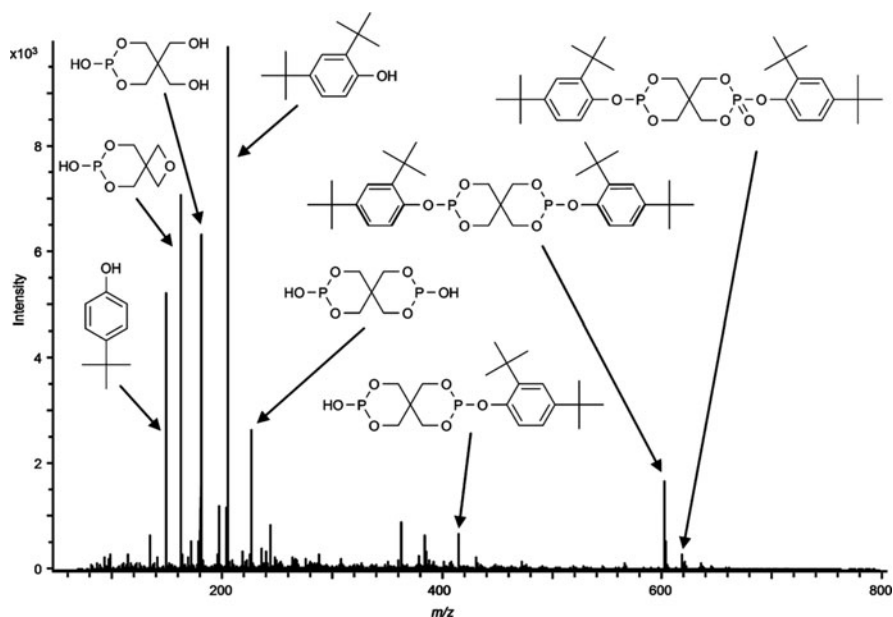
Fig. 10 DART/MS spectrum of a polymer sample containing Irgafos 126 and degradation products after compounding at 190 °C. Reprinted from [51] with permission from The Royal Society of Chemistry

but are indeed caused by degradation of the stabilizer during the compounding process).

It is fair to say that DART/MS of solid polymer samples often delivers semi-quantitative results rather than quantitative results and is most suitable for a quick qualitative screening for the presence of stabilizers in a polymer sample. On the other hand, it has recently been demonstrated that DART is not only suitable for solid sample analysis but can also be used as an MS detection technique for HPLC [52]. In this case, the eluent is not sprayed and vaporized but a liquid jet is formed from which the analytes are ionized by the DART mechanism. Although applications of HPLC-DART to polymer additives have not yet been reported, it could be an attractive additional tool within the range of MS detectors.

6.3 Atmospheric Solid Analysis Probe Technique

The atmospheric solid analysis probe (ASAP) technique is based on an APCI ionization mode. As this mode is widely applicable in polymer additive analysis (see Sect. 3.3), ASAP may be very suitable for use in this area. It uses a traditional APCI source, where the solid sample is positioned into the hot nitrogen gas flowing from the probe, thereby allowing the ionization of analytes by the corona discharge.

The direct qualitative analysis of erucamide, Irganox 1076, Irgafos 168, Irganox 3114, and several brominated flame retardants has been demonstrated by Trimpin et al. [53].

6.4   Other Approaches

Secondary ion mass spectrometry (SIMS) has been investigated for direct analysis of additives in solid samples (see for example the review in [54]) but a detailed discussion would be beyond the scope of this paper.

Last but not least, the potential of solvent-free matrix-assisted laser desorption/ ionization (MALDI) MS has been explored by Trimpin et al. [53] using pre-ground solid mixtures of matrix and sample. Applications so far reported refer to identification of the polymer itself, but the determination of additives should be possible as well.

7   Conclusions

Currently, a range of different chromatographic techniques is available for quantitative analysis of additives and stabilizers in polymeric materials. MS detection has become state-of-the-art for GC, where electron ionization and chemical ionization provide an almost universal ionization of analytes from applications in polymer analysis. Unfortunately, many additives or stabilizers commonly used are not suitable for GC analysis due to insufficient volatility. Therefore, techniques operating in the liquid phase such as HPLC have attained significant importance for separation of various different stabilizers or additives within one run. HPLC has become even more attractive within the last few years due to the availability of highly efficient columns with stationary phases consisting of particles sizes below 2 μm. These stationary phases have increased the peak capacity (number of peaks that can be separated within a certain time window) tremendously and their importance will continue to rise in the near future. Nowadays, atmospheric pressure ionization modes are well established for MS detection in HPLC. Although the applicability is not as universal as ionization sources for GC, some more recent developments like photoionization have resulted in efficient ionization tools for a wide range of structurally different additives and their degradation products in polymers. The increasing availability of reasonably priced high-resolution TOF/ MS analyzers allowing exact mass determination as well as the development of MS/ MS instruments such as quadrupole-TOF or ion trap-TOF make structure elucidation of unknown peaks in non-target analysis quite simple. Detection limits of MS detection are considerably better than for commonly employed UV detectors and will undergo further improvements in the future due to ongoing instrumental developments in MS.

HPLC methods published so far have demonstrated the separation of structurally different additives or stabilizers within a single run. On the other hand, routinely employed methods are often still optimized just for a certain class of analytes so that different HPLC procedures are used side by side to cover the whole range of stabilizers or additives possibly present in real samples. The development of more universal and fully MS-compatible HPLC conditions may be a major challenge in the near future.

A bottleneck for HPLC/MS analysis of additives in polymers may still be the sample preparation step, which can be quite time-consuming and labor-intensive. Furthermore, it can be difficult to prove that extraction of analytes from real samples is quantitative. It is not surprising that direct MS methods for solid polymeric materials are the focus of current research. New ion sources such as DART have become commercially available and complement traditional ion sources for solid samples like MALDI. Some efforts will still be necessary to allow fully quantitative measurements by such direct techniques.

References

1. Reingruber E, Himmelsbach M, Sauer C, Buchberger W (2010) Identification of degradation products of antioxidants in polyolefins by liquid chromatography combined with atmospheric pressure photoionisation mass spectrometry. Polym Degrad Stab 95:740–745
2. Green S, Bai S, Cheatham M, Cong R, Yau W (2010) Determination of antioxidants in polyolefins using total dissolution methodology followed by RPLC. J Sep Sci 33:3455–3462
3. Coulier L, Kaal ER, Tienstra M, Hankemeier T (2005) Identification and quantification of (polymeric) hindered-amine light stabilizers in polymers using pyroylsis-gas chromatography-mass spectrometry and liquid chromatography-ultraviolet absorbance detection-evaporative light scattering detection. J Chromatogr A 1062:227–238
4. Wang FC (2000) Polymer additive analysis by pyrolysis-gas chromatography. IV. Antioxidants. J Chromatogr A 891(2):325–336
5. Barnes KA, Damant AP, Startin JR, Castle L (1995) Qualitative liquid chromatographic-atmospheric pressure chemical ionisation mass spectrometric analysis of polyethylene terephthalate oligomers. J Chromatogr A 712:191–199
6. Vandenburg HJ, Clifford AA, Bartle KD, Carroll J, Newton I, Garden LM, Dean JR, Costley CT (1997) Analytical extraction of additives from polymers. Analyst 122:101R–115R
7. Stiftinger M (2012) PhD Thesis, Johannes-Kepler-University Linz (in preparation)
8. Farajzadeh MA, Eskandar SG, Ranji A, Feyz E (2007) HPLC technique for quantitation of Chimassorb 944, and its evaluation in analysis of real and standard samples of polyolefins. Microchim Acta 159:363–369
9. Vandenburg HJ, Clifford AA, Bartle KD, Carlson RE, Carroll J, Newton ID (1999) A simple solvent selection method for accelerated solvent extraction of additives from polymers. Analyst 124:1707–1710
10. Garrido-Lopez A, Tena MT (2005) Experimental design approach for the optimisation of pressurised fluid extraction of additives from polyethylene films. J Chromatogr A 1099:75–83

11. De Paepe A, Erlandsson B, Östelius J, Gasslander U, Arbin A (2006) An Alternative method for determination of additives in polypropylene using supercritical fluid extraction and enhanced solvent extraction. J Liq Chromatogr Rel Technol 29:1541–1559
12. Vandenburg HJ, Clifford AA, Bartle KD, Carroll J, Newton ID (1999) Comparison of pressurised fluid extraction and microwave assisted extraction with atmospheric pressure methods for extraction of additives from polypropylene. Analyst 124:397–400
13. Marcato B, Vianello M (2000) Microwave-assisted extraction by fast sample preparation for the systematic analysis of additives in polyolefins by high-performance liquid chromatography. J Chromatogr A 869:285–300
14. Dopico Garcia MS, López VJM, Bouza R, Abad MJ, González Soto E, González Rodrıguez MV (2004) Extraction and quantification of antioxidants from low-density polyethylene by microwave energy and liquid chromatography. Anal Chim Acta 521:179–188
15. Smith SH, Taylor LT (2002) Extraction of various additives from polystyrene and their subsequent analysis. Chromatographia 56:165–169
16. Ashraf-Khorassani M, Nazem N, Taylor LT (2003) Feasibility of supercritical fluid extraction with on-line coupling of reversed-phase liquid chromatography for quantitative analysis of polymer additives. J Chromatogr A 995:227–232
17. Thilen M, Shishoo R (2000) Optimization of experimental parameters for the quantification of polymer additives using SFE/HPLC. J Appl Polym Sci 76:938–946
18. Fu C (2010) Diploma Thesis, Johannes-Kepler-University Linz
19. Kim BH, Yang DK, Ok JH (2007) Analysis of polymer additives in high-temperature liquid chromatography. J Chromatogr Sci 45:16–21
20. Noguerol-Cal R, Lopez-Vilarino JM, Gonzalez-Rodriguez MV, Barral-Losada LF (2007) Development of an ultraperformance liquid chromatography method for improved determination of additives in polymeric materials. J Sep Sci 30:2452–2459
21. Gaudin K, Ho-Sung H, Bleton J, Joseph-Charles J, Dallet P, Puig P, Dubost JP (2007) Determination of N, N´-ethylenebisstearamide additive in polymer by normal phase liquid chromatography with evaporative light scattering detection. J Chromatogr A 1167:27–34
22. Raynor MW, Bartle KD, Davies IL, Williams A, Clifford AA, Chalmers JM, Cook BW (1988) Polymer additive characterization by capillary supercritical fluid chromatography/fourier transform infrared microspectrometry. Anal Chem 60:427–433
23. Carrott MJ, Jones DC, Davidson G (1998) Identification and analysis of polymer additives using packed-column supercritical fluid chromatography with APCI mass spectrometric detection. Analyst 123:1827–1833
24. Andersen T, Skuland IL, Holm A, Trones R, Greibrokk T (2004) Temperature-programmed packed capillary liquid chromatography coupled to evaporative light-scattering detection and electrospray ionization time-of-flight mass spectrometry for characterization of high-molecular-mass hindered amine light stabilizers. J Chromatogr A 1029:49–56
25. Noguerol-Cal R, López-Vilarino JM, Fernandez-Martinez G, Gonsales-Rodriquez MV, Barral-Losada LF (2010) Liquid chromatographic methods to analyze hindered amines light stabilizers (HALS) levels to improve safety in polyolefins. J Sep Sci 33:2698–2706
26. Reisinger M (2010) Diploma Thesis, Johannes Kepler-University Linz
27. Haddad PR (2004) Ion chromatography. Anal Bioanal Chem 379:341–343
28. Gill M, Garber MJ, Yousheng H, Jenke D (2010) Development and validation of an HPLC-MS-MS method for quantitating bis (2,2,6,6-tetramethyl-4-piperidyl) sebacate (Tinuvin 770) and a related substance in aqueous extract of plastic materials. J Chromatogr Sci 48:200–207
29. Gonzalez-Rodriguez MV, Dopico-Garcia MS, Noguerol-Cal R, Carballeira-Amarelo T, Lopez-Vilarino JM, Fernandez-Martinez G (2010) Application of liquid chromatography in polymer non-ionic antistatic additives analysis. J Sep Sci 33:3595–3603
30. Larsen BS, Kaiser MA, Botelho M, Wooler GR, Buxton LW (2005) Comparison of pressurized solvent and reflux extraction methods for the determination of perfluorooctanoic acid in polytetrafluoroethylene polymers using LC-MS-MS. Analyst 130:59–62

31. Himmelsbach M, Buchberger W, Reingruber E (2009) Determination of polymer additives by liquid chromatography coupled with mass spectrometry. A comparison of atmospheric pressure photoionization (APPI), atmospheric pressure chemical ionization (APCI), and electrospray ionization (ESI). Polym Degrad Stab 94:1213–1219
32. Schnöller J, Pittenauer E, Hutter H, Allmaier G (2009) Analysis of antioxidants in insulation cladding of copper wire: a comparison of different mass spectrometric techniques (ESI-IT, MALDI-RTOF and RTOF-SIMS). J Mass Spectrom 44:1724–1732
33. Hayen H, Alvarez-Grima MM, Debnath SC, Noordermeer JWM, Karst U (2004) Liquid chromatography/coordination ion spray mass spectrometry for the analysis of rubber vulcanization products. Anal Chem 76:1063–1068
34. Block C, Wynants L, Kelchtermans M, De Boer R, Compernolle F (2006) Identification of polymer additives by liquid chromatography-mass spectrometry. Polym Degrad Stab 91:3163–3173
35. Schlummer M, Brandl F, Mäurer A, van Eldik R (2005) Analysis of flame retardant additives in polymer fractions of waste of electric and electronic equipment (WEEE) by means of HPLC-UV/MS and GPC-HPLC-UV. J Chromatogr A 1064:39–51
36. Desmazieres B, Buchmann W, Terrier P, Tortajada J (2008) APCI interface for LC- and SEC-MS analysis of synthetic polymers: Advantages and limits. Anal Chem 80:783–792
37. Duderstadt RE, Fischer SM (2008) Effect of organic mobile phase composition on signal responses for selected polyalkene additive compounds by liquid chromatography – mass spectrometry. J Chromatogr A 1193:70–78
38. Robb DB, Covey TR, Bruins AP (2000) Atmospheric pressure photoionization: an ionization method for liquid chromatography – mass spectrometry. Anal Chem 72:3653–3659
39. Robb DB, Blades MW (2008) State-of-the-art in atmospheric pressure photoionization for LC/MS. Anal Chim Acta 627:34–49
40. Marchi I, Rudaz S, Veuthey JL (2009) Atmospheric pressure photoionization for coupling liquid chromatography to mass spectrometry: A review. Talanta 78:1–18
41. Hommerson P, Khan AM, Bristow T, Niessen W, de Jong GJ, Somsen GW (2007) Photon-independent gas-phase-ion formation in capillary electrophoresis-mass spectrometry using atmospheric pressure photoionization. Anal Chem 79:5351–5357
42. Reingruber E, Buchberger W (2010) Analysis of polyolefin stabilizers and their degradation products. J Sep Sci 33:3463–3475
43. Pan C (2009) Diploma Thesis, Johannes-Kepler-University Linz
44. Hilder EF, Klampfl CW, Buchberger W, Haddad PR (2001) Separation of hydrophobic polymer additives by microemulsion electrokinetic chromatography. J Chromatogr A 922:293–302
45. Himmelsbach M, Haunschmidt M, Buchberger W, Klampfl CW (2007) Microemulsion electrokinetic chromatography with on-line atmospheric pressure photoionization mass spectrometric detection. Anal Chem 79:1564–1568
46. Vo TDT, Himmelsbach M, Haunschmidt M, Buchberger W, Schwarzinger C, Klampfl CW (2008) Improved analysis of melamine-formaldehyde resins by capillary zone electrophoresis – mass spectrometry using ion-trap and quadrupole-time-of-flight mass spectrometers. J Chromatogr A 1213:83–87
47. Kaal ER, Alkema G, Kurano M, Geissler M, Janssen HG (2007) On-line size exclusion chromatography-pyrolysis-gas chromatography-mass spectrometry for copolymer characterization and additive analysis. J Chromatogr A 1143:182–189
48. Takats Z, Wiseman JM, Gologan B, Cooks RG (2004) Mass spectrometry sampling under ambient conditions with desorption electrospray ionization. Science 306:471–473
49. Reiter SM, Buchberger W, Klampfl CW (2011) Rapid identification and semi-quantitative determination of polymer additives by desorption electrospray ionization/time-of-flight mass spectrometry. Anal Bioanal Chem 400:2317–2322
50. Cody RB, Laramee JA, Durst HD (2005) Versatile new ion source for the analysis of materials in open air under ambient conditions. Anal Chem 77:2297–2302

51. Haunschmidt M, Klampfl CW, Buchberger W, Hertsens R (2010) Rapid identification of stabilisers in polypropylene using time-of-flight mass spectrometry and DART as ion source. Analyst 135:80–85
52. Eberherr W, Buchberger W, Hertsens R, Klampfl CW (2010) Investigations on the coupling of high-performance liquid chromatography to direct analysis in real time mass spectrometry. Anal Chem 82:5792–5796
53. Trimpin S, Wijerathne K, McEwan CN (2009) Rapid methods of polymer and polymer additives identification: Multi-sample solvent-free MALDI, pyrolysis at atmospheric pressure, and atmospheric solids analysis probe mass spectrometry. Anal Chim Acta 654:20–25
54. Weng LT, Chan CM (2006) SSIMS analysis of organics, polymer blends and interfaces. Appl Surf Sci 252:6570–6574

Direct Insertion Probe Mass Spectrometry of Polymers

Jale Hacaloglu

Abstract This chapter reviews advances in the technique of direct insertion probe mass spectrometry (DIP-MS) and its applications in polymer analysis for various purposes. The applications for thermal characterization involve investigation of the thermal stability, degradation products, and decomposition mechanism of complex polymer samples, in particular polymers involving flame retardants, polyphenylene- and poly(phenylene vinylene)-based materials, and coalesced homopolymers and polymer blends. Examples focused on the use of DIP-MS for elucidation of structural characteristics of conducting polymers and thermosets are also given. The great potential of the technique for identification of additives in complex polymer matrices without time-consuming extractions or derivatizations (because components are separated as a function of their volatilities and/or thermal stabilities) is illustrated.

Keywords Direct insertion probe · Mass spectrometry · Polymers · Pyrolysis · Thermal degradation

Contents

J. Hacaloglu
Department of Chemistry, Middle East Technical University, Ankara 06531, Turkey
e-mail: jale@metu.edu.tr

Abbreviations

15-Na	Naphthoxazine
APCI	Atmospheric pressure chemical ionization
ASAP	Atmospheric solids analysis probe
BPAEP	Poly(bisphenyl acryloxyethyl phosphate)
CD	Cyclodextrin
DATE	Decanedioic acid *bis*-(2-thiophen-3-yl-ethyl)ester
DESI	Desorption electrospray ionization
DIP-MS	Direct insertion probe mass spectrometry
DP-MS	Direct pyrolysis mass spectrometry
ESI	Electrospray ionization
FR	Flame retardant
IC	Inclusion compound
MALDI	Matrix assisted laser desorption ionization
OTE	2-(Thiophen-3-yl-)ethyl octanoate
P2VP	Poly(2-vinylpyridine)
P4VP	Poly(4-vinylpyridine)
PANI	Polyaniline
PC	Poly(carbonate)
PCL	Poly(ε-caprolactone)
PEO	Poly(ethylene oxide)
PET	Polyethylene terephthalate
PMMA	Poly(methyl methacrylate)
PMTh	Poly(methyl thiophene)
PPE	Polyphenylene
PPh	Phenolphthalein
PPP	Poly(*p*-phenylene)
PPy	Polypyrrole
PS	Polystyrene
PTh	Polythiophene
PVAc	Poly(vinyl acetate)
PVP	Poly(vinylene phenylene)
TATE	Terephthalic acid *bis*-(2-thiophen-3-yl-ethyl)ester
T_{di}	Initial decomposition temperature
TIC	Total ion current

1   Introduction

Direct insertion probe mass spectrometry, (DIP-MS), a kind of direct pyrolysis MS (DP-MS) technique, has been applied to the analysis of polymers since 1948. Until the introduction of soft ionization techniques such as matrix assisted laser desorption ionization (MALDI) and electrospray ionization (ESI), the application of MS

in polymer analysis was limited to study of degradation prior to mass spectrometric analysis, and to pyrolysis MS techniques [1–3].

Basically, pyrolysis is the thermal degradation of a compound in an inert atmosphere or vacuum. When vibrational excitation, as a result of distribution of thermal energy over all modes of excitation, is greater than the energy of specific bonds, decomposition of the molecule takes place. Temperature and heating rate have significant importance on product distribution. At low temperatures, thermal degradation may be too slow to be useful. On the other hand, at very high temperatures there may be extensive decomposition, generating only very small and nonspecific products. Product distribution is also affected by the heating rate, depending on the kinetics of thermal equilibrium among several vibrational modes. Thus, thermal decomposition of a compound occurs in a reproducible way, producing a fingerprint only at a specific temperature and at a specific heating rate.

Pyrolysis involving gradual heating allows separation of components present in the sample as a function of volatility and/or thermal stability. Vaporization of additives is followed by thermal degradation of high molecular weight components. Pyrolyzate composition changes with temperature when the polymer contains segments with different bond stabilities. This enables determination of precise decomposition mechanisms.

Thermal degradation of polymers may follow a depolymerization mechanism, producing mainly monomer and low molecular weight oligomers. If statistical or random cleavage of the polymer chain takes place, products that may have quite different structure than the monomer are generated. In the presence of thermally labile side chains, generally, two-step decomposition occurs; the first step being elimination of side chains and the second being decomposition of the polymer backbone to form more stable condensed structures. A non-free-radical process involving intermolecular exchange reactions yielding mainly cyclic oligomers may also be involved during thermal degradation. The type and the structure of the polymer determine the major thermal degradation pathways.

Although pyrolysis techniques are widely applied to elucidate thermal stability, degradation products, and decomposition mechanism of a compound, the subsequent MS and tandem MS (MS/MS) characterization of the pyrolyzates is a powerful method for determination of composition, microstructure, and additives of industrial polymers, especially in unknown samples.

In general, primary decomposition mechanisms yield pyrolyzates most representative of the original polymer chain. Measurement of these pyrolyzates is desired when the microstructure of polymers is being studied. Microstructural information is lost when further degradation or recombination of the primary products occurs within the pyrolysis zone. Among the several pyrolysis techniques, DP-MS is the only technique in which secondary and condensation reactions are almost totally avoided and detection of high mass pyrolyzates and unstable thermal degradation products is possible.

In DIP pyrolysis, thermal degradation occurs inside the mass spectrometer and pyrolyzates are rapidly transported from the heating zone to the source region and ionized, almost totally eliminating the possibility of secondary and condensation

reactions. Furthermore, as the high vacuum inside the mass spectrometer favors vaporization, analysis of higher molecular mass pyrolyzates is possible. The rapid detection system of the mass spectrometers also enables the detection of unstable thermal degradation products. Thus, a better understanding of the thermal characteristics, polymerization, crosslinking, and char formation processes can be achieved. However, the direct pyrolysis mass spectra of polymers are almost always very complicated due to concurrent degradation processes and dissociative ionization of the thermal degradation products inside the mass spectrometer. Thus, in DP-MS analysis not only the detection of a peak is important, but also the variation of its intensity as a function of temperature, single ion evolution profiles, or single ion pyrograms.

With the introduction of MALDI and ESI techniques in the late 1980s, enabling ionization of large nonvolatile molecules with limited extent of fragmentation, the use of DP-MS for polymer characterization became somewhat sidelined. On the other hand, numerous insoluble synthetic polymers that have important industrial and biological applications cannot be analyzed by ESI or MALDI-MS due to too high molecular weight and/or polarity or due to lack of functional groups. In the case of DP-MS, almost all types of polymers can be analyzed, even those that are very large or unionizable. Furthermore, analysis of complex solid samples and multicomponent systems are possible without time-consuming extractions or derivatizations because components are separated as a function of their volatilities and/or thermal stabilities. Pyrolysis MS techniques are particularly valuable when detection limits and matrix interference may present limits to the application of common spectroscopic techniques such as nuclear magnetic resonance and infrared spectroscopy.

2 New Techniques

Zhang and coworkers described the development of an on-probe pyrolyzer interfaced to a desorption electrospray ionization (DESI) source as a novel in situ and rapid pyrolysis technique for the analysis of nonvolatile pyrolytic residues by MS and MS/MS analyses [4]. The utility of the technique was demonstrated with the analysis of several model compounds such as peptides, proteins, and synthetic polymers.

The on-probe pyrolyzer was operated either off-line or on-line mode with the DESI source and interfaced with a tandem MS instrument. The pyrolyzer consisted of a membrane heater placed underneath a removable glass slide on which the sample to be pyrolyzed was placed, as shown in Fig. 1. The rate of heating and final pyrolysis temperature, 220°C with the present design, were controlled and measured. The results were in agreement with analyses of nonvolatile pyrolysis products performed either by ESI-MS or MALDI-MS, which were pyrolyzed off-line and required sample extraction and solubilization. It has been determined that, for biological samples, pyrolysis residues of peptides and protein lysozyme retained
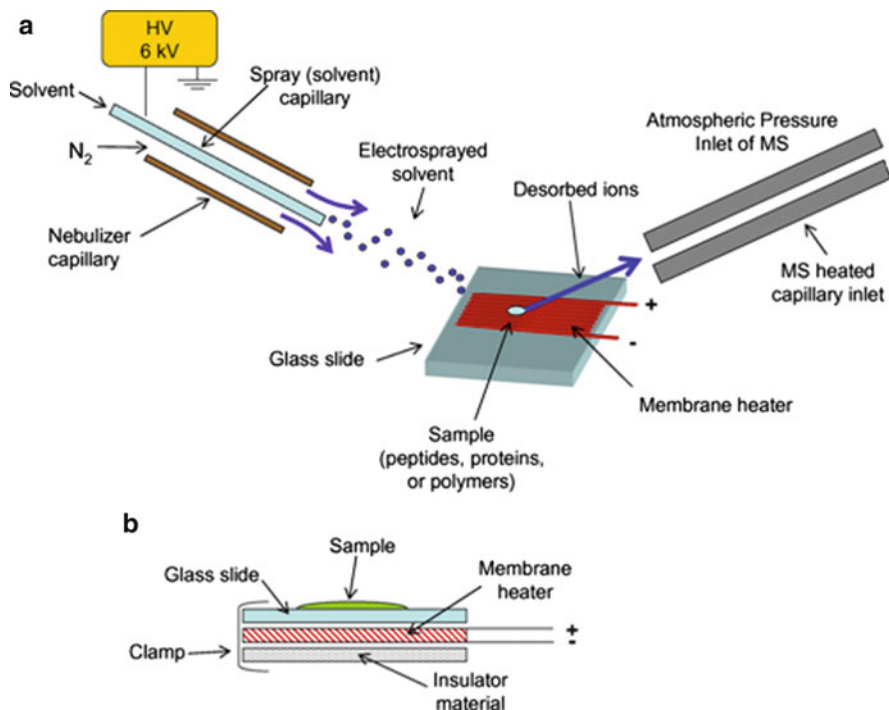
Fig. 1 (a) On-probe pyrolyzer interfaced to the DESI source. (b) Detailed diagram of the on-probe pyrolyzer. Reproduced from [4] with the kind permission of Elsevier

sequence information useful for proteomic-based protein identification. For analysis of the synthetic polymer poly(ethylene glycol), the on-probe pyrolysis DESI-MS system yielded data and information equivalent to previous MALDI-MS analysis, where the use of a matrix compound and cationizing agent were required. Advantages of this system are its simplicity and speed of analysis since the pyrolysis is performed in situ on the DESI source probe and, hence, extraction steps and/or use of matrices are avoided [4].

Whitson et al. developed a simple modification of a commercial quadruple ion trap to permit in situ pyrolysis of synthetic polymers inside an atmospheric pressure chemical ionization (APCI) ion source [5]. A direct probe was inserted into the APCI source and positioned below the corona discharge needle and angled toward the capillary entrance to the ion trap. The temperature was gradually increased from 100 to 700°C. The nature and the thermal stabilities of the hydrophobic and hydrophilic components present in complex amphiphilic copolymers and copolymer blends with different comonomer compositions and extent of crosslinking, yet with similar physical properties, were investigated. Results indicated that direct probe APCI (DP-APCI) mass spectrometry provides a rapid and cost effective means for analysis of thermal stability and chemical composition of complex synthetic polymers that are too large or too complex for direct MS analysis.

Witson and coworkers claimed that, although the traditional direct probe analysis combined with chemical ionization MS and MS/MS allows more precise temperature control and provides a steadier ion current profile and less background noise, thereby leading to more reproducible spectra, DP-APCI conducts pyrolysis at atmospheric pressure, which is more similar to a thermogravimetric analysis experiment and, hence, may provide more useful information about the thermal properties of materials [5].

3 Applications

3.1 Thermal Characterization

3.1.1 Flame Retardants

A wide range of chemicals are added to polymeric materials. As an example, flame retardants (FR) are added to inhibit combustion, smoke, and meet fire safety needs. The changes in the thermal decomposition mechanism and product distribution in the presence of FRs have significant importance, not only for the direction of modifications and determination of application areas of the materials but also for environmental and health aspects. A few studies appear in the literature on DIP-MS analysis of FR resins [6, 7].

DIP-MS was used to elucidate thermal degradation mechanisms of air-cured films of poly(bisphenyl acryloxyethyl phosphate) (BPAEP) blended in different ratios with urethane acrylate to obtain a series of UV-curable FR resins. The results showed that blends have lower initial decomposition temperatures (T_{di}) and higher char residues than pure urethane acrylate, whereas BPAEP has the lowest T_{di} and the highest char residue [6]. The degradation of BPAEP occurred in three steps, involving decomposition of phosphate, ester group and alkyl chain, and of the aromatic structure in the film. UV-cured BPAEP film also degraded in three steps. The first stage was assigned to the decomposition of phosphate and acrylate, the second to the thermal pyrolysis of alkyl chains, and the third stage to the decomposition of some aromatic structures and the formation of poly(phosphoric acid) [6].

DIP-MS was also applied to investigation of the flame retardant mechanism of the copolyester polyethylene terephthalate (PET) phosphorus-containing linked pendant groups [7]. The results suggested that the P–CH$_2$ bond cleavage occurs at pendant groups and that species containing phosphorus volatilize into the gas phase. A flame retardant mechanism was proposed for the gas phase mode of action of the halogen-free copolyester phosphorus-containing linked pendant groups. The yield of char for the copolyester phosphorus-containing linked pendant groups was insignificant relative to neat PET itself, suggesting that the majority of the crucial flame retardant activity of FR-PET is in the gas phase rather than in the condensed phase [7].

3.1.2 Polyphenylenes

Thermal degradation characteristic of polyphenylenes (PPEs) with excellent mechanical, thermal, and thermo-oxidative stability is an important issue for developing a rational technology for its processing and applications. Nur and coworkers applied DIP-MS to investigate the thermal characteristics of graft copolymers of PPE and poly(ε-caprolactone) (PCL) and/or PCL/polystyrene (PS) copolymers prepared by combined controlled polymerization and cross-coupling processes (Scheme 1) [8–11]. It has been determined that the thermal degradation of copolymers of PPE occurred mainly in two steps. In the first step, the decomposition of PCL side chains of poly(p-phenylene) (PPP) **4** occurred at slightly higher temperatures than the pure homopolymer, PCL [10]. In the second stage of pyrolysis, the decomposition of the PPE backbone took place. The evolution of caprolactone monomer or small caprolactone segments left on the phenyl ring was also continued in the temperature region where degradation of the PPP backbone had started. The thermal decomposition of PPP with PS side chains started at higher temperatures than for the PCL analogs [11]. However, it was almost impossible to differentiate product peaks due to the decomposition of the PPE backbone for samples **5** and **6** because of the similarities between the PS chains and PPE backbone.

The gradual heating of PPE-*graft*-PCL/PS copolymers **7** and **8** enabled the determination of the degradation mechanism [11]. The thermally less stable PCL side chains were lost more readily than the PS side chains. A slight increase in

where 〜〜 is poly(e-caprolactone and 〰〰〰 is polystyrene
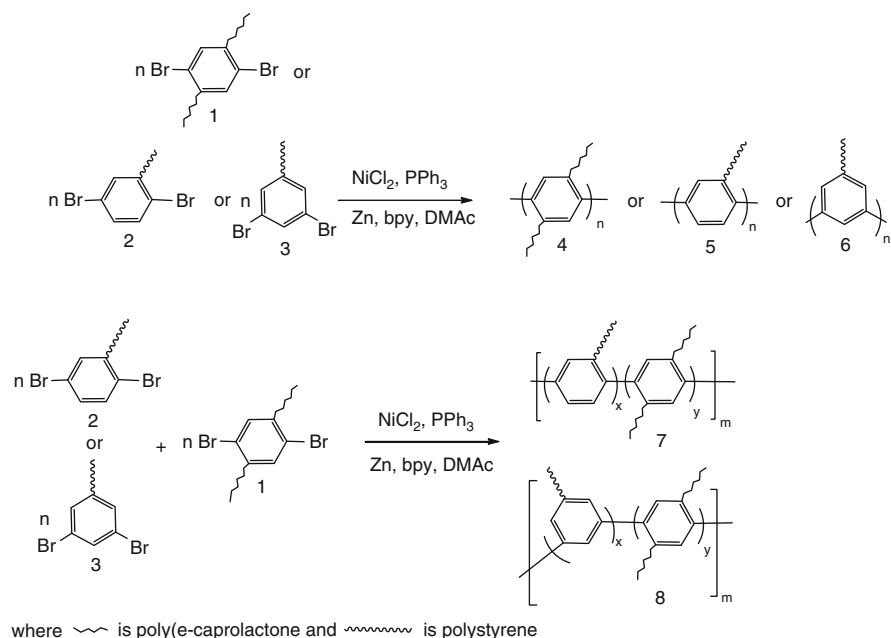
Scheme 1 Polymerization of poly(p-phenylene-*graft*-ε-caprolactone), poly(p-phenylene-*graft*-styrene) and poly(p-phenylene-*graft*-caprolactone)-*co*-(p-phenylene-*graft*-styrene)

thermal stability of PCL chains for PPE-*graft*-PCL/PS copolymers was noted compared to the copolymer PPE-*graft*-PCL due to the interaction between PS and PCL chains. This interaction was stronger when PS chains were linked to the 2-position of the 1, 4-phenylene ring.

The thermal degradation characteristics of new macromonomers PCL and PS with central 4,4′-dicarbaldehyde terphenyl moieties and of poly(phenylene vinylene)s (PPVs) with well-defined ε-caprolactone (PPV-PCL) or polystyrene (PPV-PS) as lateral substituents (Scheme 2) were investigated via DP-MS by
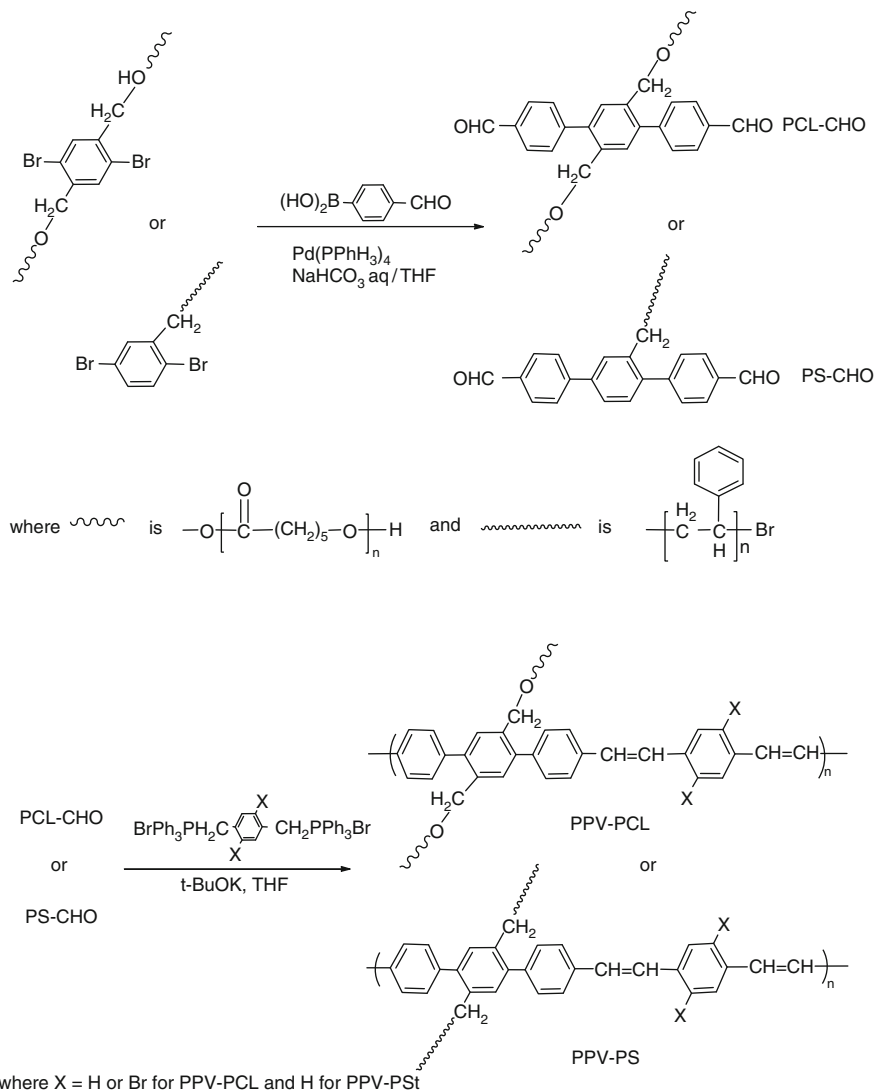
Scheme 2 Polymerization of poly(*p*-phenylene vinylene) with well-defined poly(ε-caprolactone) and polystyrene grafts

the same group [12–15]. The unexpectedly high thermal stability of the macromonomer was attributed to intermolecular acetylation of benzaldehyde, yielding a hemiacetal and causing a crosslinked structure during the pyrolysis. In all the polymers under investigation, decomposition started with degradation of the substituent. The thermal stability of both the substituents (PCL and PS) and the PPV backbone were affected by the thermal stability of the other. The increase in stability of PCL chains was much more pronounced than that detected for PPP-*graft*-PCL copolymer [10, 13]. This pronounced effect was attributed to higher thermal stability of PPV compared to PPP and to the decrease in steric hindrance for PPV with PCL side chains. A slight increase in thermal stability of PS was detected for PPV-PS. This behavior was related to higher thermal stability of the PPV backbone [14, 15]. The thermal stability of the PPV backbone increased in the order PPV-PCL-Br < PPV-PCL < PPV-PS. Figure 2 shows the variation of total ion yield as a function of temperature, and the total ion current (TIC) curves recorded during the DIP-MS analysis of PPV-PCL, Br-substituted PPV with PCL, and PPV with PS. When the thermal stability of the substituent was significantly lower than that of the PPV backbone, as in the case of PPV-PCL and PPV-Br-*graft*-PCL, then the radicals generated at the early stages of pyrolysis coupled before the temperature reached the values necessary for complete decomposition. This in turn yielded a thermally more stable crosslinked structure. The increase in thermal stability was greater when coupling of the radicals generated on the PPV backbone took place.

3.1.3 Coalesced Polymers

Cyclodextrins (CDs) act as hosts in the formation of inclusion compounds (ICs) with various high molecular weight polymers. Once guest polymer chains are
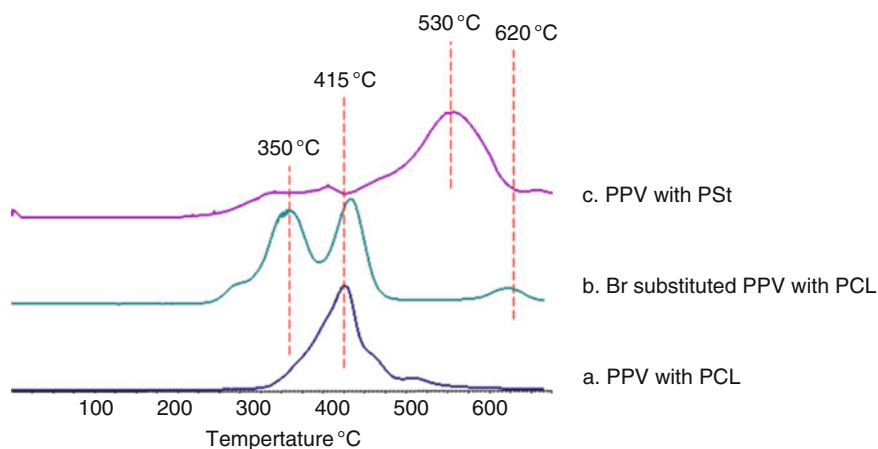
Fig. 2 TIC curves recorded during the DP-MS analysis of (**a**) PPV-*graft*-PCL, (**b**) PPV-Br-*graft*-PCL, and (**c**) PPV-*graft*-PS

included inside the CD cavities, they are forced to adopt highly extended conformations by the narrow host CD channels, and significant improvement in physical properties are observed [16, 17]. Furthermore, coalescing (removal of CD) bulk polymer pairs from their common CD-ICs yields intimately mixed polymer blends [18–22].

In order to elucidate the effect of the coalescing process on the thermal characteristics of intimately mixed polymer blends, DIP-MS analysis of as-received homopolymers, physical blends, coalesced homopolymers, and coalesced blends were carried out. DIP-MS analyses were carried out on intimately mixed binary and ternary blends of poly(vinylacetate) (PVAc), poly(methyl methacrylate) (PMMA), and polycarbonate (PC) (namely PMMA/PVAc, PC/PMMA, and PC/PVAc) and ternary blend PVAc/PC/PMMA obtained by formation of and coalescence from their common ICs with γ-CD. Results indicated that the thermal stability and degradation products of the polymers were affected once the polymers chains are included inside the γ-CD-IC cavities.

DIP-MS observations for PMMA/PVAc blends suggested that the degradation mechanisms for PMMA and PVAc chains in their coalesced blend were significantly altered from those observed in their as-received and solution blended samples [18]. Figure 3 shows the TIC curves and the mass spectra recorded at selected temperatures of physical and intimately mixed PMMA/PVAc blends. The significant decrease in the relative intensity of the MMA peak in the pyrolysis mass spectra of intimately mixed PMMA/PVAc blend can easily be recognized. The inhibition of depolymerization of PMMA chains and the increase in thermal stability of PVAc chains were attributed to the presence of specific molecular interactions between the components of the intimately mixed PMMA/PVAc blend. The intermolecular proton transfer from PVAc to PMMA chains was associated with the close proximity of PMMA and PVAc chains.

Figure 4 shows the TIC curves and the pyrolysis mass spectra recorded at selected temperatures for as-received polymers (PMMA and PC), PC/PMMA physical blend, γ-CD, coalesced homopolymers PMMA and PC, and coalesced PC/PMMA blend. Significant differences in the TIC curves and pyrolysis mass spectra were noted for the coalesced polymers. The results pointed out specific molecular interactions between the PMMA and PC chains, generating an ester–ester interchange reaction between PC and PMMA. Strong evidence for the production of a graft copolymer and low molecular weight PC chains bearing methyl carbonate end groups was observed for the intimately mixed PC/PMMA blend. Furthermore, an exchange reaction between carbonate groups and MMA monomer formed by depolymerization of PMMA above 300°C was suggested due to diffusion of MMA at the interface or even into the PC domains for both coalesced and physical PC/PMMA blends [19].

Drastic changes in the TIC curve and pyrolysis mass spectra were also observed for coalesced PC/PVAc blend compared to the physical blend, as can clearly be seen in Fig. 5 [20]. DIP-MS analyses of coalesced and physical blends of PC and PVAc indicated generation of CH_3COOH by deacetylation of PVAc above 300°C, which decreased the thermal stability of PC chains. This process was determined to
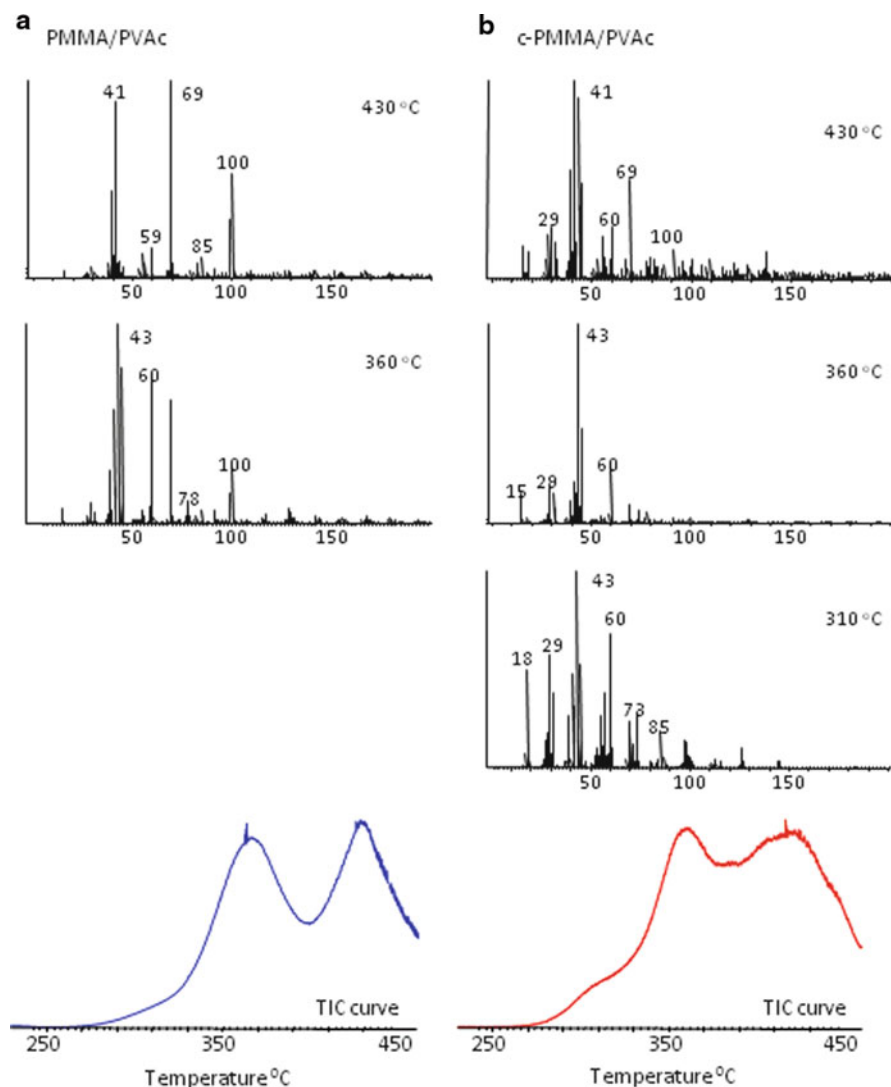
Fig. 3 TIC curves and pyrolysis mass spectra of (**a**) PMMA/PVAc physical blend, (**b**) coalesced PMMA/ PVAc blend

be more effective for the physical blend due to enhanced diffusion of CH_3COOH into the PC domains, where it can further react to produce low molecular weight PC fragments bearing methyl carbonate chain ends.

In the case of PC/PMMA/PVAc ternary blends, significant differences in thermal behavior of intimately mixed blend compared to the co-precipitated physical blend were also noted [21]. Figure 6 shows the TIC curve and the pyrolysis mass spectra recorded during the DP-MS analysis of intimately mixed and
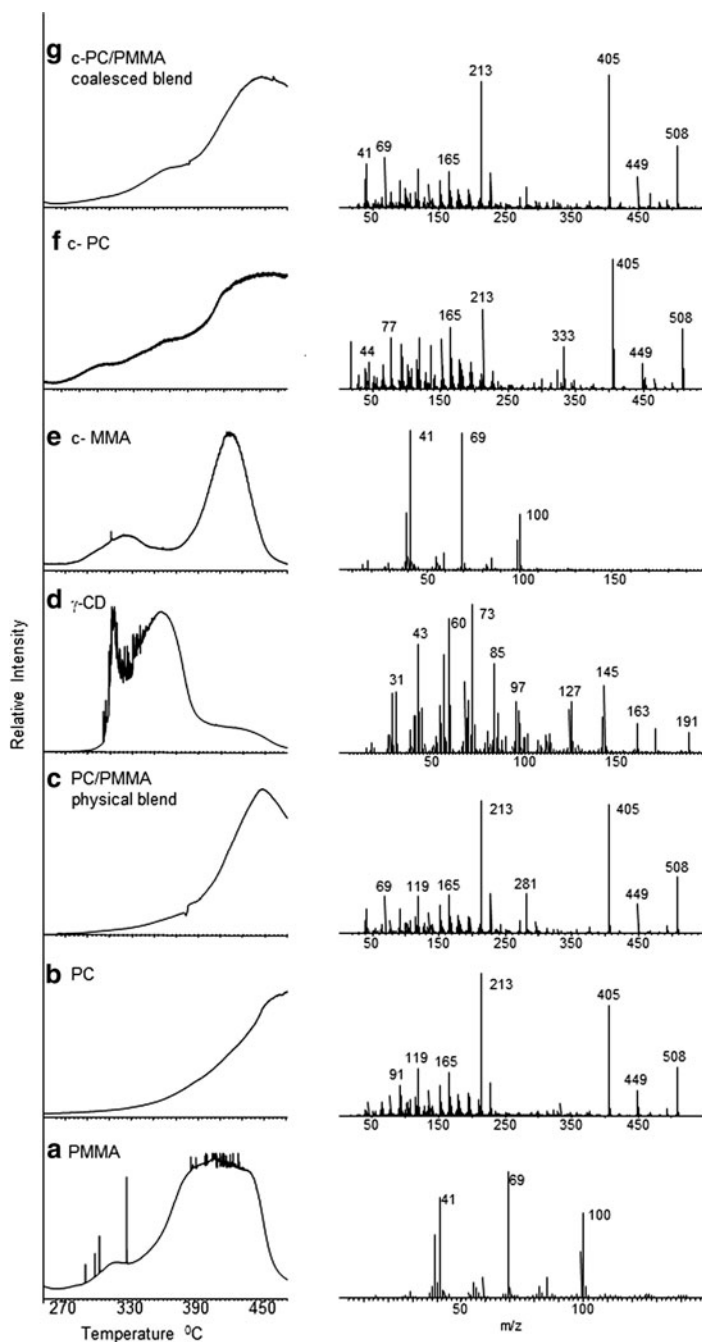
Fig. 4 TIC curves and pyrolysis mass spectra of (**a**) as-received PMMA, (**b**) as-received PC, (**c**) PC/PMMA physical blend, (**d**) γ-CD, (**e**) coalesced PMMA, (**f**) coalesced PC, and (**g**) coalesced PC/PMMA blend. Reproduced from [19] with the kind permission of Elsevier
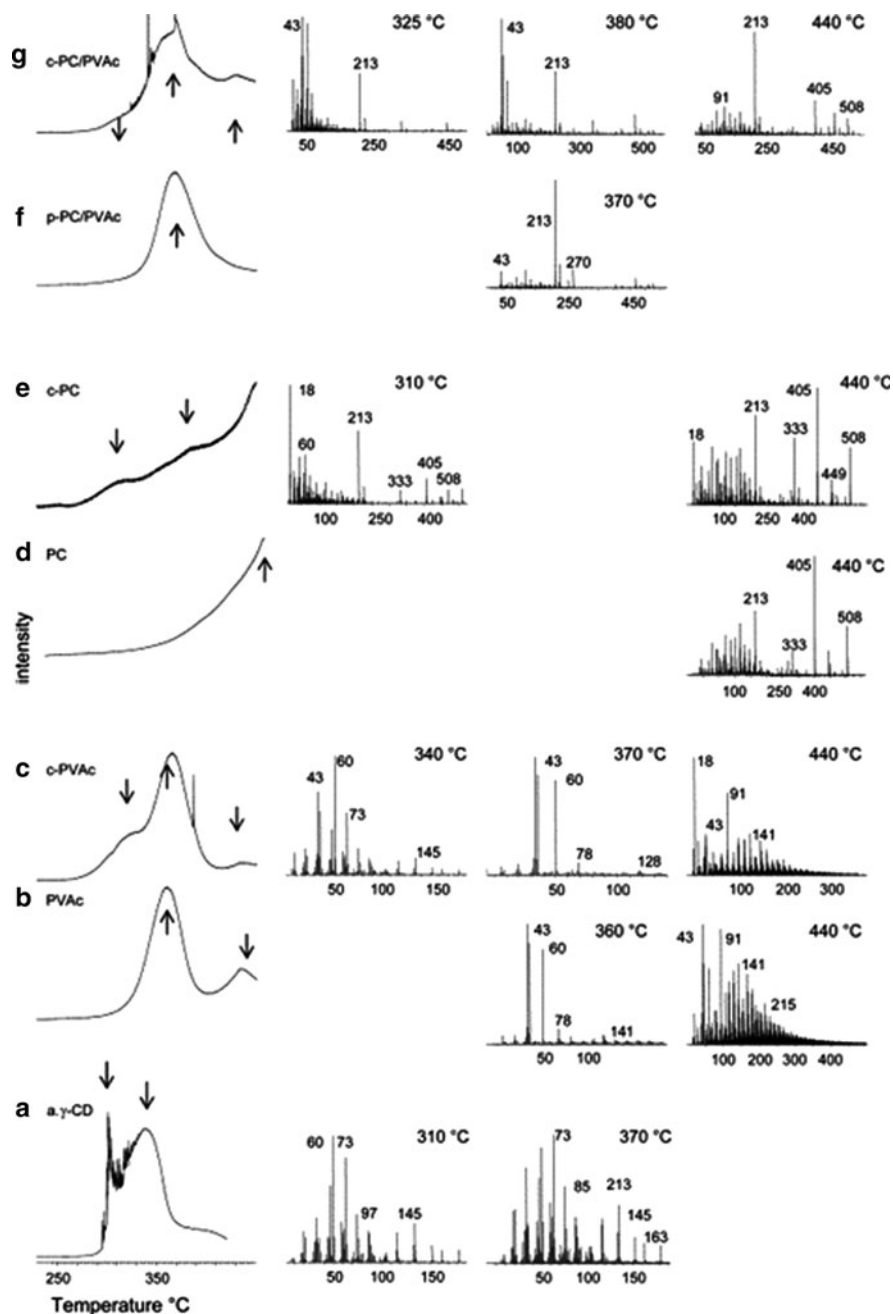
Fig. 5 TIC curves and pyrolysis mass spectra of (**a**) γ-CD, (**b**) as-received PVAc, (**c**) coalesced PVAc, (**d**) as-received-PC, (**e**) coalesced PC, (**f**) PC/PVAc physical mixture, and (**g**) coalesced PC/PVAc blend. Reproduced from [20] with the kind permission of Elsevier
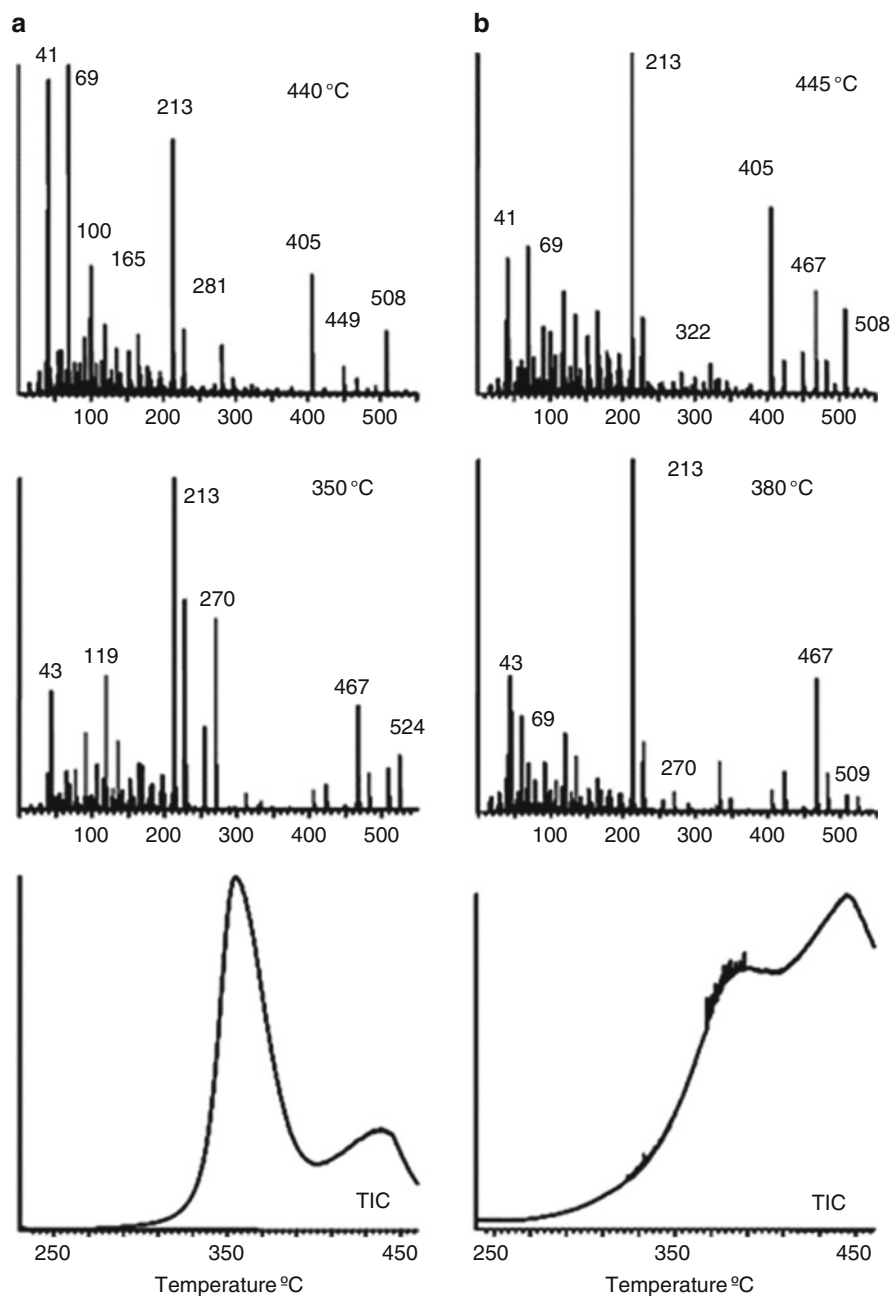
Fig. 6 TIC curves and pyrolysis mass spectra of (**a**) physical PC/PMMA/PVAc and (**b**) coalesced PC/PMMA/PVAc ternary blends. Reproduced from [21] with the kind permission of Elsevier

co-precipitated physical PC/PMMA/PVAc ternary blends. Again, for both coalesced and physical blends, a decrease in the stability of PC was detected and associated with the reactions of CH_3COOH formed by deacetylation of PVAc above 300°C. The decrease in thermal stability of PC chains was less significant for the coalesced ternary blend, indicating that the diffusion of CH_3COOH was either somewhat limited or competed with intermolecular reactions between PMMA and PC and between PMMA and PVAc. The intermolecular reactions were detected, and were associated with their close proximity in the intimately mixed coalesced PC/PMMA/PVAc ternary blend [21].

The formation and characterization of the channel structure of solid IC formed between guest styrene and host γ-CD have also been performed using DIP-MS [22]. The styrene/γ-CD channel-IC was formed in order to perform polymerization of styrene in a confined environment (γ-CD channels). DP-MS studies indicated that once styrene was included in the host γ-CD cavities, the thermal stability of normally volatile bulk styrene shifted to elevated temperatures, much above its boiling point, until the γ-CD host molecules themselves began to degrade at around 300°C. In addition, the thermal degradation of host γ-CD from the styrene/γ-CD channel-IC was observed to be different from that of pure γ-CD due to co-degradation of styrene and γ-CD [22].

3.1.4 Miscellaneous

DP-MS analyses of poly(2-vinylpyridine) (P2VP), poly(4-vinylpyridine) (P4VP), PS-*b*-P2VP, and cobalt-nanofunctional PS-*b*-P2VP have been performed by Elmaci and coworkers [23, 24]. The results revealed that P2VP degraded via a complex degradation mechanism, yielding mainly pyridine and protonated oligomers, whereas depolymerization of P4VP took place in accordance with the general thermal behavior of vinyl polymers, indicating a correlation between the polymer structure and the degradation mechanism. The complex thermal degradation behavior for P2VP was associated with the position of the nitrogen atom in the pyridine ring, with σ-effect [23]. For, PS-*b*-P2VP, decomposition of each unit occurred independently following the degradation pathways for the corresponding homopolymers [24]. On the other hand, upon coordination to cobalt nanoparticles, thermal decomposition of the P2VP blocks was initiated by loss of pyridine units, leaving an unsaturated and/or crosslinked polymer backbone that degraded at relatively high temperatures. Figure 7 shows the single ion evolution profiles of styrene, 2-vinylpyridine dimers, and the $C_{22}H_{17}$ fragment generated by degradation of unsaturated polymer backbone recorded during the DP-MS analysis of PS-*b*-P2VP and cobalt-functional PS-*b*-P2VP.

Sundarrajan et al. studied the thermal degradation of two poly(acyl sulfide) polymers, poly(adipoyl sulfide) and poly(terephthaloyl sulfide), by DP-MS and proposed a thermal degradation mechanism [25]. The structures of pyrolysis products detected in the DP-MS analysis of both poly(adipoyl sulfide) and poly (terephthaloyl sulfide) indicated that the thermal degradation took place mainly
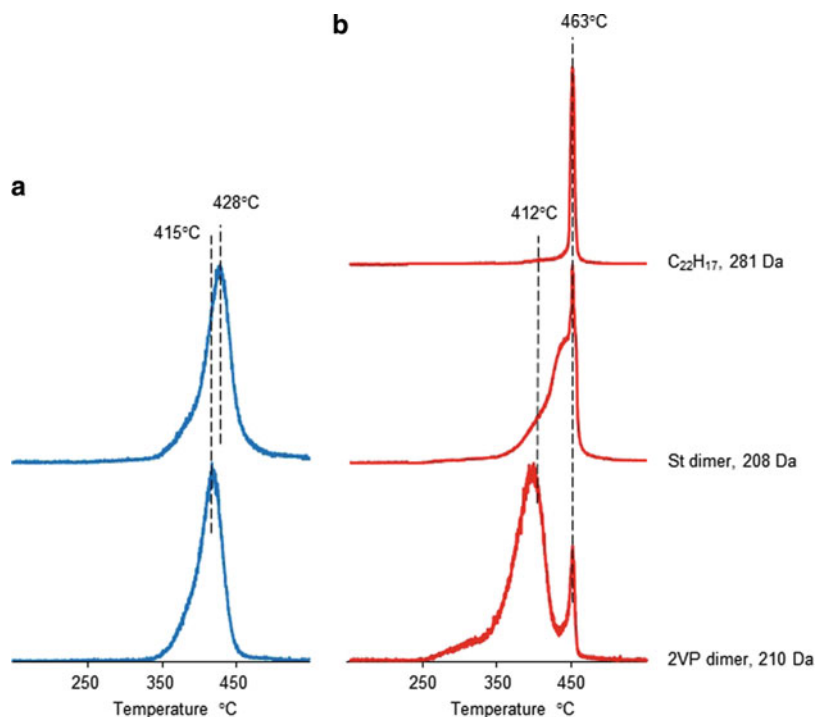
Fig. 7 Single ion evolution profiles of 2-vinylpyridine (*2VP*) and styrene (*St*) dimers and $C_{22}H_{17}$ product for (**a**) PS-*b*-P2VP and (**b**) cobalt-functional PS-*b*-P2VP

through loss of carbon monoxide and carbonyl oxysulfide, leading to the formation of cyclics of repeating units. Linear products with thioacid end groups were formed through hydrogen transfer reactions during the pyrolysis of poly(adipoyl sulfide). In the case of poly(terephthaloyl sulfide), almost equal proportions of linear products with phenyl end groups and cyclic products were generated.

Thermal degradation products of a series of copoly(arylene ether sulfone) s synthesized by nucleophilic condensation of either 4,4′-dichlorodiphenylsulfone or 4,4′-*bis*-(4-chlorophenylsulfonyl) biphenyl, long chain dichloride, with different molar ratios of hydroquinone or dihydroxydiphenylsulfone, were investigated by DP-MS [26]. Pyrolysis products retaining the repeating units of the initial copolymers were formed at the temperature range of 420–470°C. Products containing biphenyl units, formed by the elimination process of SO_2 from diphenyl sulfone bridges were detected in the mass spectra recorded at temperatures above 450°C. On the other hand, products having biphenyl and dibenzofuran moieties, formed by loss of hydrogen atoms from diphenyl ether bridges, were detected above 550°C. The relative intensity of some ions reflected the molar composition of the copolymers analyzed. Cyclic and linear oligomers, with very low molecular mass, that were present in the crude copolymers were also detected by DP-MS [26].

Thermal degradation characteristics of two new classes of polysulfide polymers, poly[1-(phenoxymethyl) ethylene polysulfide] (PPMEP), and poly [1-(phenoxy) ethylene polysulfide] (PPEP), were studied using DP-MS by Ramakrishman and coworkers [27]. The results indicated that the polymers underwent degradation through weak-link scission. The thermal stability of the polysulfide polymers decreased as the number of sulfur atoms in the polysulfide linkage increased. The occurrence of minor levels of monosulfide linkages in poly[1-(phenoxymethyl) ethylene disulfide] and poly[1-(phenoxy) ethylene disulfide] and the minor presence of mono-, di-, and trisulfide linkages in poly[1-(phenoxymethyl) ethylene tetrasulfide] and poly[1-(phenoxy) ethylene tetrasulfide] were ascertained on the basis of DP-MS investigations of these polymers.

Whitson and coworkers applied a direct probe inserted into an APCI MS technique to characterize complex polyurethane samples that cannot be analyzed directly by MS. Separation of thermally desorbed components and thermal degradation products based on their volatilities was obtained. They were able to make distinctions between polymer formulations with variable physical properties due to their different blends [28].

3.2   Structural Characterization

3.2.1   Conducting Polymers

The conducting polymers prepared by electrochemical polymerization methods for the sake of advantages such as simplicity, reproducibility, and control of thickness have poor mechanical and physical properties that create processing problems. Introduction of alkyl groups into the main chain, synthesis of soluble precursors, and preparation of conducting polymer composites, blends, and copolymers have been applied to improve the mechanical characteristics [29–31]. However, a detailed characterization of these hybrid materials by classic spectroscopic techniques is still limited due to the insolubility of the films in common solvents and due to the existence of charges on the polymer backbone.

DIP-MS was applied not only to investigate the effect of dopant on the thermal and structural characteristics of electrochemically prepared polymers such as poly (3-methylthiophene) (PMTh) and polyaniline (PANI) films [32, 33], but also to elucidate the structure of polymer composites synthesized by electrochemical polymerization of pyrrole and thiophene onto electrodes coated with polymers having good mechanical properties and involving pendant pyrrole or thiophene moieties [34–38].

Gozet and coworkers proposed a two-step thermal degradation mechanism for PMTh films doped with PF_6^- and BF_4^-, the first step being the loss of the dopant over a broad temperature range, and the second being the degradation of the polymer backbone to produce segments of various conjugation lengths. Reactions between the dopant and H_2O and polymer were found to be very effective,

especially for PF_6^--doped films, indicating that PF_6^- as a dopant is not very appropriate. Furthermore, DP-MS findings indicated a limited electrochemical reversibility of the transition between the doped and undoped states for PMTh due to decomposition of the polymer and inward diffusion of counterion during dedoping processes for both PF_6^-- and BF_4^--doped polymers [32]. Another example represents the application of DP-MS to the investigation of the thermal degradation of HCl- and HNO_3-doped PANI films [33]. For PANI, three main thermal degradation stages were detected. The first stage was due to removal of dopant, just above 150°C; the second due to loss of low molecular weight oligomers; and the third due to the degradation of polymer backbone and decomposition of the aromatic ring at elevated temperatures. Though weak, peaks due to oligomers up to hexamer were detectable in the pyrolysis mass spectra recorded in the final stage of pyrolysis, where the monomer yield was found to be relatively low. These observations were attributed to a crosslinked structure of the polymer for which depolymerization reactions yielding mainly monomer are not likely. In addition, chlorination and nitrolysis of aniline were detected during the electrochemical polymerization processes, which increased with the electrolysis period [32]. Furthermore, evolution of CO_2 at elevated temperatures during the pyrolysis of HNO_3-doped PANI confirmed oxidation of the polymer film during electrolysis.

A DIP-MS study of the films prepared by electrochemical polymerization of pyrrole onto electrodes coated with thienyl-containing (2,2,6,6,-tetramethylpiperidinyl-1-oxy)-initiated PS samples confirmed the growth of polypyrrole onto the pendant thiophene moiety of PS (Scheme 3) and the degradation of PS films, at least to a certain extent, during electrochemical polymerization of pyrrole [34].
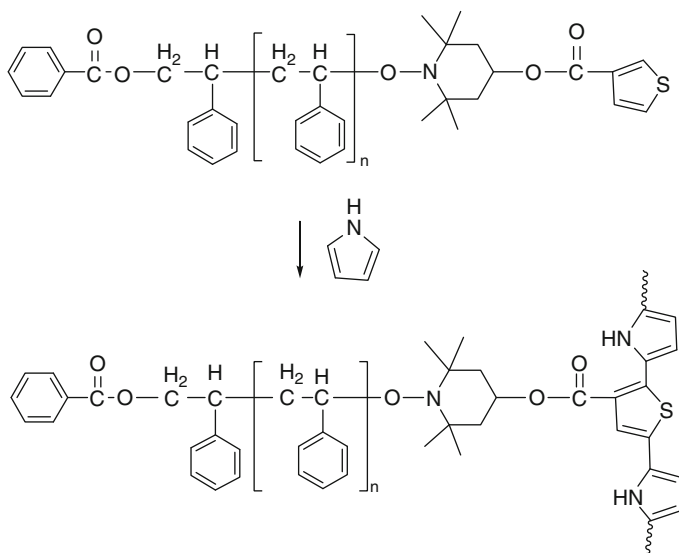
Scheme 3 Growth of polypyrrole onto thiophene moieties of polystyrene

Scheme 4 Electrochemical polymerization of pyrrole on a poly[2-methylbutyl-2-(3-thienyl)acetate]-coated anode through the thiophene moieties
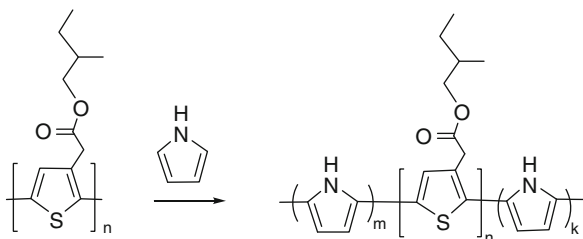
Similarly, the achievement of electrochemical polymerization of pyrrole on a poly[2-methylbutyl-2-(3-thienyl)acetate]-coated anode through the thiophene moieties (Scheme 4), was justified again by DIP-MS results. A slight increase in the thermal stability of poly[2-methylbutyl-2-(3-thienyl)acetate] chains was detected upon growth of pyrrole on pentant thiophene moieties [35].

Aslan and coworkers studied the thermal behavior of copolymers of thiophene with decanedioic acid *bis*-(2-thiophen-3-yl-ethyl)ester (DATE) and terephthalic acid *bis*-(2-thiophen-3-yl-ethyl)ester (TATE) prepared by potentiostatic polymerization via pyrolysis MS [36]. Pyrolysis of the polymer samples prepared by electrochemical oxidation of DATE or TATE in the presence of thiophene indicated an increase in thermal stability of ester linkages compared to the corresponding pure homopolymers PDATE and PTATE and the corresponding mechanical mixtures. Significant differences were detected between the single ion evolution profiles of characteristic thermal degradation products of mechanical mixtures of polythiophene (PTh) and PDATE and PTATE and the corresponding copolymers P(DATE-*co*-Th) and P(TATE-*co*-Th) respectively. The thiophene trimer/monomer peak intensity ratio increased in the order of PTh > P(TATE-*co*-Th) > PTATE and PTh > P(DATE-*co*-Th) > PDATE confirming polymerization of both monomers. Furthermore, detection of peaks due to products involving both thiophene and TATE, and thiophene and DATE, units in the pyrolysis mass spectra recorded at the same temperature region confirmed the growth of thiophene on TATE and DATE backbones and copolymer formation as shown in Scheme 5 [36].

The same group also used DIP-MS to study the thermal characteristics of a new thiophene derivative, 2-(thiophen-3-yl-)ethyl octanoate (OTE), its homopolymer POTE, and copolymer with thiophene P(OTE-*co*-Th) prepared by electrochemical polymerization as given in Scheme 6 [37]. Thermal degradation of the copolymer was started by elimination of side chains, which in turn decreased the stability of polymer matrix. Evolution of thermal degradation products involving thiophene units were detected almost in the same temperature region during the pyrolysis of both PTh and the copolymer, at slightly higher temperatures than the decomposition of PTh backbone of POTE. Dopant evolution occurred at lower temperatures during the pyrolysis of the copolymer compared to the homopolymers, indicating a weaker interaction between the dopant and the polymer. These results indicated that the extent of doping and network structure decreased in the order POTE < P(OTE-*co*-Th) < PTh.

Characterization of electrochemically prepared PANI, polypyrrole (PPy), and their composites or copolymers synthesized either by electrochemical
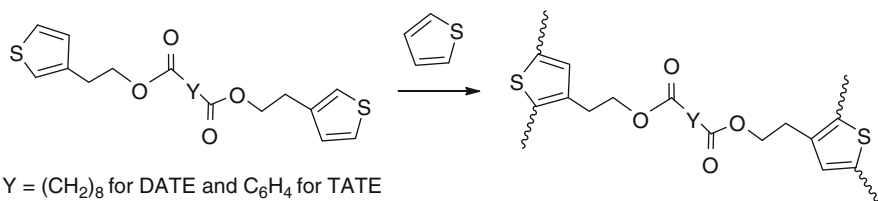
Scheme 5 Electrochemical polymerization of DATE and TATE in the presence of thiophene
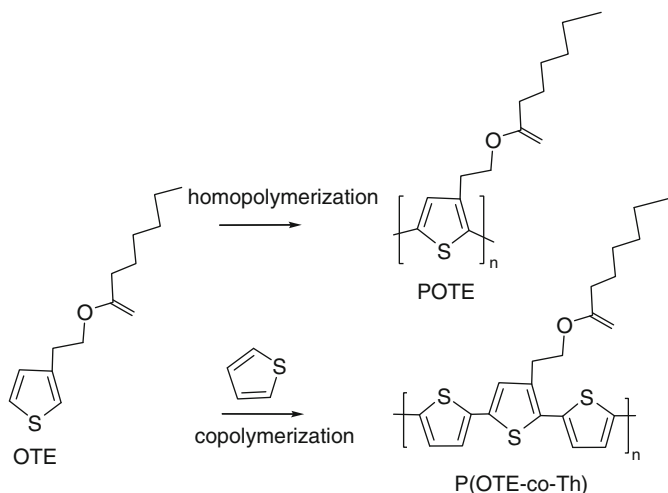
Scheme 6 Preparation of POTE and P(OTE-*co*-Th)

polymerization of pyrrole on PANI-coated electrode (PANI/PPy) or by coating PANI on PPy (PPy/PANI) in H_2SO_4 solutions were performed using DIP-MS [38]. Detection of peaks due to mixed dimers confirmed copolymer formation. However, the results also pointed out some degradation of the polymer first coated on the electrode during the polymerization of the second. Figure 8 shows the SO_2/Py and SO_2/ANI peak intensity ratios detected in the pyrolysis mass spectra of the samples as a function of concentration of H_2SO_4. It is clear that the yield of the products due to the polymer coated first on the electrode diminished to a greater extent. This may be due to degradation of the polymer coated on the electrode during the polymerization of the other polymer, most probably due to the longer period that the coated polymer stayed in the acid solution. Yet, as the effect was greater for PPy, it can also be concluded that PPy is less stable in H_2SO_4 solution.

3.2.2 Thermosets

Significant attention has been paid to the improvement of performance of thermosets for various important industrial applications. Benzoxazines, prepared from
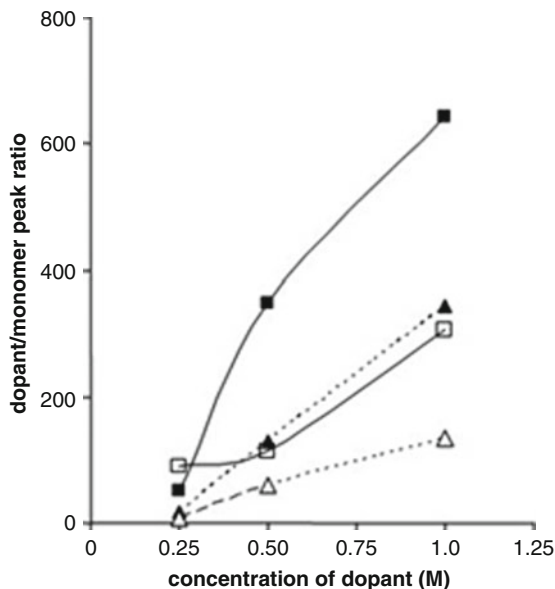
phenols, primary amines, and formaldehyde have been developed as an attractive alternative to epoxies and traditional phenolic resins [39–41]. In order to improve thermal properties of benzoxazines, several studies on the choice of phenols, amines, and reactive functional groups were performed. Additionally, naphthoxazines were synthesized by using hydroxynaphthalenes as phenolic precursor to increase the thermal stability and char yield of the resulting thermosets, polynaphthoxazines [42]. The knowledge of curing and thermal degradation characteristics has crucial importance for the direction of modifications. Few studies have appeared so far in the literature on the use of DIP-MS technique for curing and thermal characterizations of benzoxazines.

DIP-MS analyses of aromatic amine-based naphthoxazine monomer (15-Na) and polynaphthoxazine (Poly15-Na) have been carried out by Koyuncu et al. [43]. The polymerization and degradation mechanisms were proposed for 15-Na and Poly15-Na, respectively. It has been determined that polymerization followed opposing paths, yielding some thermally less stable linkages through which thermally crosslinked Poly15-Na suffered from low thermal stability [43]. The variations in the single ion evolution profiles suggested the presence of units with different thermal stabilities and, thus, different structures (Fig. 9).

Bagheri and coworkers applied DIP-MS to investigate the curing and polymerization mechanisms of phenol- and methyl amine-based benzoxazine monomer, and the thermal decomposition and crosslinking characteristics of the corresponding polybenzoxazine [44]. The curing of the benzoxazine monomer was achieved inside the mass spectrometer with the use of a direct probe. The TIC curve and the mass spectra recorded at each step of curing are shown in Fig. 10. DP-MS findings confirmed the evolution of aniline in the final step of curing. Detection of
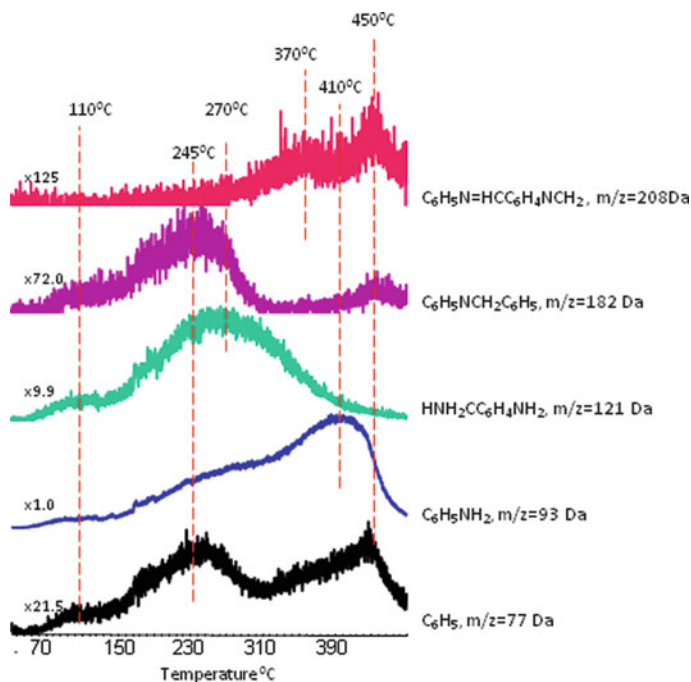
Fig. 9 Single ion evolution profiles of some selected fragments involving N-substituted anilines

units with various thermal stabilities indicated polymerization of the monomer through opposing reaction routes besides the generally accepted one. The evolution of alkyl amines and diamines involving more than three carbon atoms at early stages of pyrolysis and the multistep thermal decomposition process confirmed the coupling of –NCH_2 groups generated by cleavage of oxazine ring. In Fig. 11, the TIC curve and the pyrolysis mass spectra of the polybenzoxazine are given. The significantly high char residue was associated with the crosslinking of fragments and/or polymer backbone generated by the loss of diamine units and side chains.

In a recent study, thermal analyses of polysiloxane and polyetherester containing benzoxazine moieties in the main chain were performed via DIP-MS [45]. Results revealed that the thermal stability and the extent of crosslinking were enhanced when the benzoxazine moieties were separated by thermally more stable units such as siloxanes. However, when the siloxane chain units were long, the possibility of polybenzoxazine growth decreased significantly and benzoxazine moieties were evolved in the temperature range where polysiloxane degradation took place.

3.3 Characterization of Additives in Polymer Matrix

In order to improve and maintain a polymer's superior physical and chemical properties, numerous additives and compounding ingredients are crucial.

Antioxidants, waxes, dyes, and other materials are used to enhance polymer utility or processability. As several additives can be present in commercial polymers, their identification and quantification is complicated. Polymer and polymer additive identification is used for polymer competitive analysis, quality control, environmental and health reasons among others. Numerous analytical methods available for characterization of various chemical aspects of polymers are time consuming for high-throughput analyses because of the necessity of extraction, chromatographic separation, or thermal methods. DIP-MS is one of the few rapid MS analysis methods for direct identification of additives and polymers. In general, the method provides information regardless of the composition or molecular weight of the polymeric material.
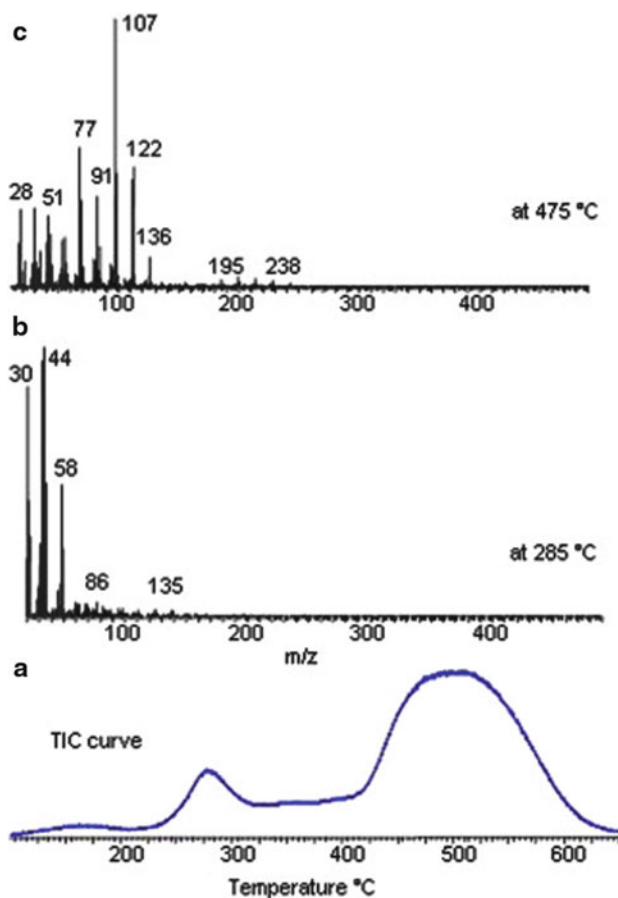
Fig. 11 TIC curve (**a**) and the mass spectra (**b**, **c**) at the maximum of the peaks present in the TIC curve recorded during the pyrolysis of polybenzoxazine. Reproduced from [44] with the kind permission of Elsevier

3.3.1 Analysis of Additives

In the analysis of industrial plastics, it is highly important to identify various additives (softeners; antioxidants; antiozonizing agents, filling oils, crosslinking and vulcanizing agents; heat, light, and radiation stabilizers; and others), and also residual, low molecular weight oligomers, and solvents. Trimpin and coworkers discussed application of atmospheric solid analysis probe (ASAP) MS for direct ambient additive analysis, and polymer identification. ASAP-MS is shown to be useful in additive analysis and for identifying certain polymers regardless of molecular weight [46]. In addition to additive characterization, the ASAP method is also able to identify polymers through the volatiles produced by increasing the temperature of the gas that impinges the sample. As an example, the mass spectrum
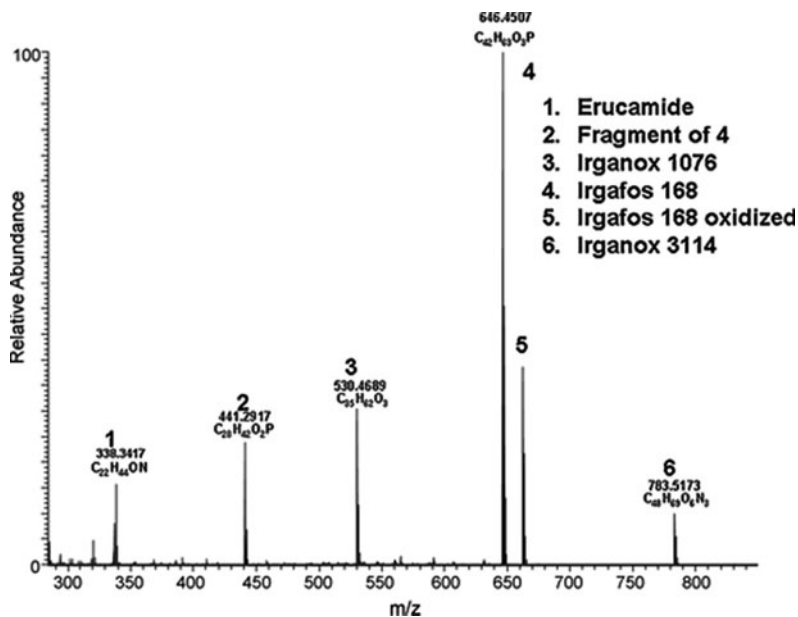
Fig. 12 ASAP mass spectrum of a thread from a polyester shirt obtained using a nitrogen gas temperature of 250°C. At this temperature, the additives are observed without interference by the PET cyclic oligomers. Reproduced from [46] with the kind permission of Elsevier

recorded with the application of ASAP-MS analysis of the additives in a thread from a polyester shirt is given in Fig. 12.

3.3.2 Investigation of Performance and Functionality of Electrospun Polymer Nanofibers

Multifunctional nanofibers and nanowebs with several distinctive characteristics such as a large surface-to-volume ratio and pore sizes in the nano-range are produced by electrospinning of a wide range variety of materials including polymers [47–51]. The functionality of the nanofibers can be improved by incorporating functional additives into the nanofibers during the electrospinning process. CDs, i.e., cyclic oligosaccharides having a toroid-shaped molecular structure, are able to form noncovalent host–guest inclusion complexes (IC) with various molecules [52]. PS, PMMA, and poly(ethylene oxide) (PEO) are suitable fiber matrixes because they are easily electrospun into uniform nanowebs without forming an IC.

Unique characteristics of nanowebs functionalized with CDs, such as potential to be used for enhancement of durability and stability of fragrances and flavors containing fibers, have been determined by DP-MS analyses [52–55].

Menthol was selected as a model fragrance/flavor material and three types of CDs ($\propto$-CD, β-CD and γ-CD) were explored in the studies. To investigate the

interactions of menthol with CDs, DP-MS analyses of PS fibers containing CD-menthol inclusion complexes (CD-menthol-ICs) produced by the electrospinning technique and of each component present were studied and compared [52, 53].

The mass spectra of highly volatile menthol could only be recorded below 50°C, showing diagnostic peaks including the weak molecular ion peak at 156 Da under the high vacuum conditions of the MS. The lack of characteristic peaks of menthol in the pyrolysis mass spectra of PS/menthol fibers indicated that menthol was evaporated from the web after the production of the fibers. On the other hand, during the gradual heating of PS fibers containing CD-menthol-ICs, the release of menthol was detected over a broad temperature range, 100–350°C (Fig. 13). Thus, the achievement of stabilization of menthol for all the PS/CD-menthol-IC webs was confirmed by DP-MS analysis. The extent of low temperature release of menthol, associated with weak interactions with CD, was determined to be lowest for PS/∝-CD-menthol-IC fibers and highest for PS/γ-CD-menthol-IC fibers. The extent of high temperature release of menthol, related to presence of stronger interactions between the menthol and the CD cavity, was comparable for all types of CD-IC webs, i.e., ∝-, β- and γ-CD-menthol ICs. The strength and the extent of CD-menthol complexation determine the durability and temperature stability of menthol in PS fibers. DP-MS results revealed that γ-CD is the best candidate for the stabilization and high temperature release of menthol from PS fibers and pointed out the high potential of electrospun fibers functionalized with CD-ICs for
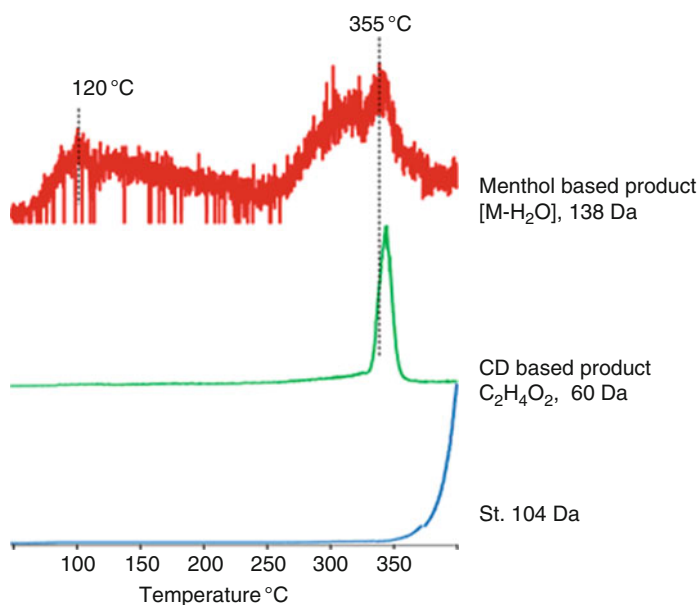
Fig. 13 Single ion evolution profiles of molecular ion for styrene (*St*) (m/z = 104 Da), $C_2H_4O_2$ ion from γ-CD (m/z = 60 Da), and product ion due to loss of H_2O from menthol, (m/z = 138 Da) detected by DIP-MS during the pyrolysis of PS/γ-CD-menthol-IC fiber

enhancement of durability and stability of fragrances/flavors. DP-MS analysis not only confirmed the presence of CDs in PS fibers but also indicated that no significant change in thermal stability and decomposition mechanisms of polymer matrixes occurs in the presence of CDs.

The stability and temperature release profiles of menthol for CD-menthol-IC-functionalized PMMA nanofibers were also investigated by DP-MS [54]. The PMMA nanofibers were electrospun with CD-menthol-ICs using α-CD, β-CD, and γ-CD. In contrast to what was detected for the PS/menthol fibers, DP-MS analysis indicated that the release of menthol from the PMMA/menthol nanofibers without CD occurred at higher temperatures compared to the situation for pure menthol. The retention of menthol at high temperature in PMMA nanofibers was attributed to the strong interactions such as hydrogen bonding between menthol molecules and PMMA chains.

The evaporation of menthol occurred over a very high and a broad temperature range (100–355°C) for PMMA/CD-menthol-IC nanowebs, demonstrating the complexation of menthol with the CD cavity and its high temperature stability. Figure 14 shows the single ion evolution profiles of PMMA and of CD- and menthol-based products recorded during DP-MS analysis of PMMA/menthol nanofibers and CD-menthol-IC functionalized PMMA nanofibers. As the size of CD cavity increased
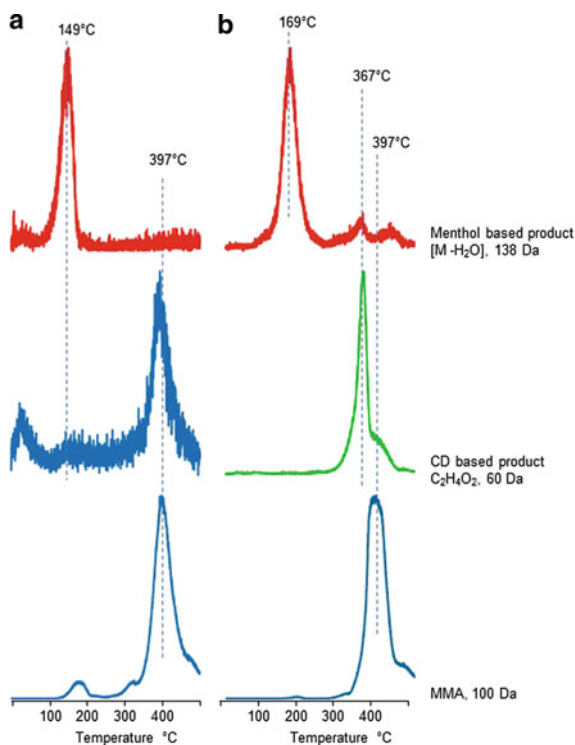
Fig. 14 Single ion evolution profiles of PMMA, CD-based, and menthol-based products recorded during DP-MS analysis of (**a**) PMMA/menthol nanofibers and (**b**) CD-menthol-IC-functionalized PMMA nanofibers

in the order α-CD < β-CD < γ-CD, the thermal evolution of menthol shifted to higher temperatures, suggesting that the strength of interaction between menthol and the CD cavity increases in the same order. The presence of menthol and its high temperature release profiles, as observed by the DP-MS technique, even 10 days after the production of nanofibers, strongly suggests that these PMMA/CD-menthol-IC nanowebs could have attractive applications for the stabilization and sustained release of volatile fragrances/flavors in general.

Recent results on electrospun PEO nanofibers containing CD-menthol-ICs revealed that the solvent system used for the electrospinning process and the type of CD (∝-CD, β-CD, or γ-CD) are very important in obtaining CD-menthol-IC, which ultimately determines the durability and temperature stability of menthol in the PEO nanofibrous web [55]. The results demonstrated that the stability and temperature release of menthol was sustained to a very high and a broad temperature range (100–250°C) for PEO nanowebs containing CD-menthol-IC, whereas the PEO nanofibers without CD and without the CD-menthol complex could not preserve menthol, even during storage. Figure 15 shows the single ion evolution profiles of $[CH_2CH_2O)_2CH_2CH_2]H$ ion ($m/z = 117$ Da), $C_2H_4O_2$ ion ($m/z = 60$ Da), and a fragment due to loss of H_2O from menthol ($m/z = 138$ Da) detected during the pyrolysis of PEO/γ-CD-menthol-IC fiber.

3.3.3 Investigation of Performance of Electrospun Polymer Nanofibers as Molecular Filters

DIP-MS studies have also been applied to explore the use of CD-functionalized electrospun PS nanofibers (PS/CD) as molecular filters and/or nanofilters for filtration, purification, and separation purposes [56, 57]. Again, PS was chosen as a fiber matrix since PS does not form inclusion complexes with CD because the cavity of CD is too narrow to encapsulate atactic PS chains. Thus, the cavity of CD molecules will be empty and able to capture organic molecules. Phenolphthalein is capable of forming inclusion complexes with CD and was chosen as a model organic molecule. PS and PS/CD fibers exposed to phenolphthalein solution were analyzed by DP-MS to investigate the presence of phenolphthalein and its thermal stability in the samples.

The evolution profiles of characteristic thermal degradation products of phenolphthalein, CDs, PS, and PS/CD fibers were compared. For all of the samples, PS- and CD-based products showed identical behaviors to those of the corresponding pure forms. On the other hand, noticeable differences were observed in the evolution profiles of phenolphthalein-based products for PS/CD samples, except for the PS/∝-CD for which the evolution of most of the phenolphthalein occurred independently as in case of the pure form. The evolution of phenolphthalein shifted to higher temperatures for the samples involving β-CD or γ-CD. The trends in the evolution profiles indicated the presence of two different environments and/or interactions of phenolphthalein with CD cavities. When the trends in the evolution profiles are compared, it can be concluded that the strength of interaction between
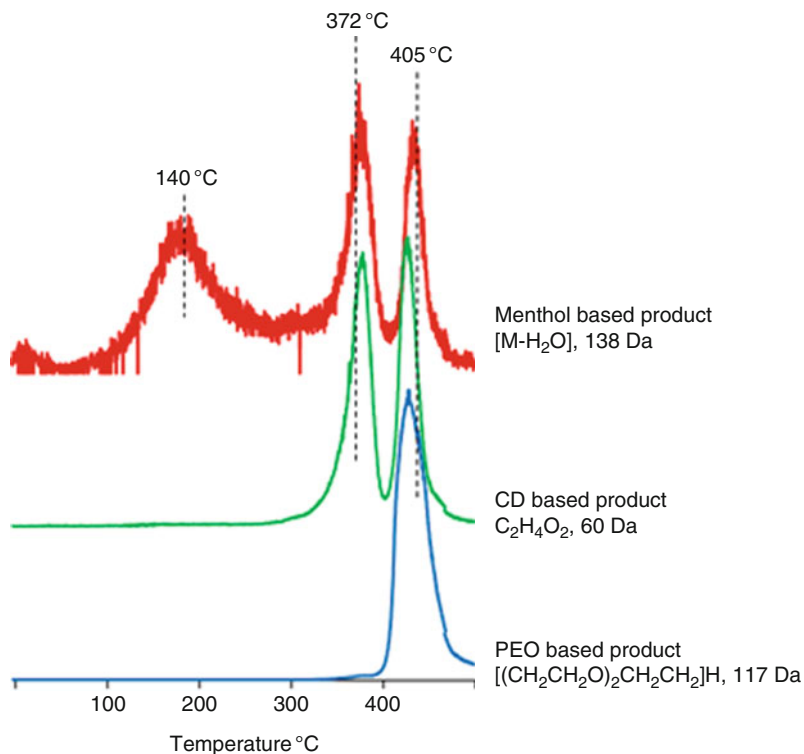
Fig. 15 Single ion evolution profiles of some characteristic fragment ions for PEO, $[CH_2CH_2O)_2CH_2CH_2]H$ ion ($m/z = 117$ Da); for γ-CD, $C_2H_4O_2$ ion ($m/z = 60$ Da); and for menthol product ion due to loss of H_2O, ($m/z = 138$ Da) detected by DIP-MS during the pyrolysis of PEO/γ-CD-menthol-IC fiber

the phenolphthalein molecule and CD cavity was in the order α-CD $< \gamma$-CD $< \beta$-CD, indicating that the size of the CD cavity and the size of the host molecule were crucial for the strength of an inclusion complex. This finding suggests that the binding between the CD cavity and the phenolphthalein is the strongest for β-CD, which was associated with the proper size and shape match between β-CD and phenolphthalein. Figure 16 shows the evolution profiles of the PS-based product, styrene monomer ($m/z = 104$ Da), of phenolphthalein ($m/z = 318$ Da), and of the CD-based product $C_2H_4O_2$ ($m/z = 60$ Da) detected during the pyrolysis of pure samples and the fibers analyzed after the exposure to phenolphthalein solution.

The use of β-CD-functionalized electrospun PMMA nanowebs (PMMA/β-CD) for entrapment of organic waste vapors such as aniline, styrene, and toluene from the environment have also been investigated by DP-MS [58]. Once the guest molecule has been included in the host CD cavity due to a strong interaction between the host and CD, the thermal evaporation and decomposition of the guest
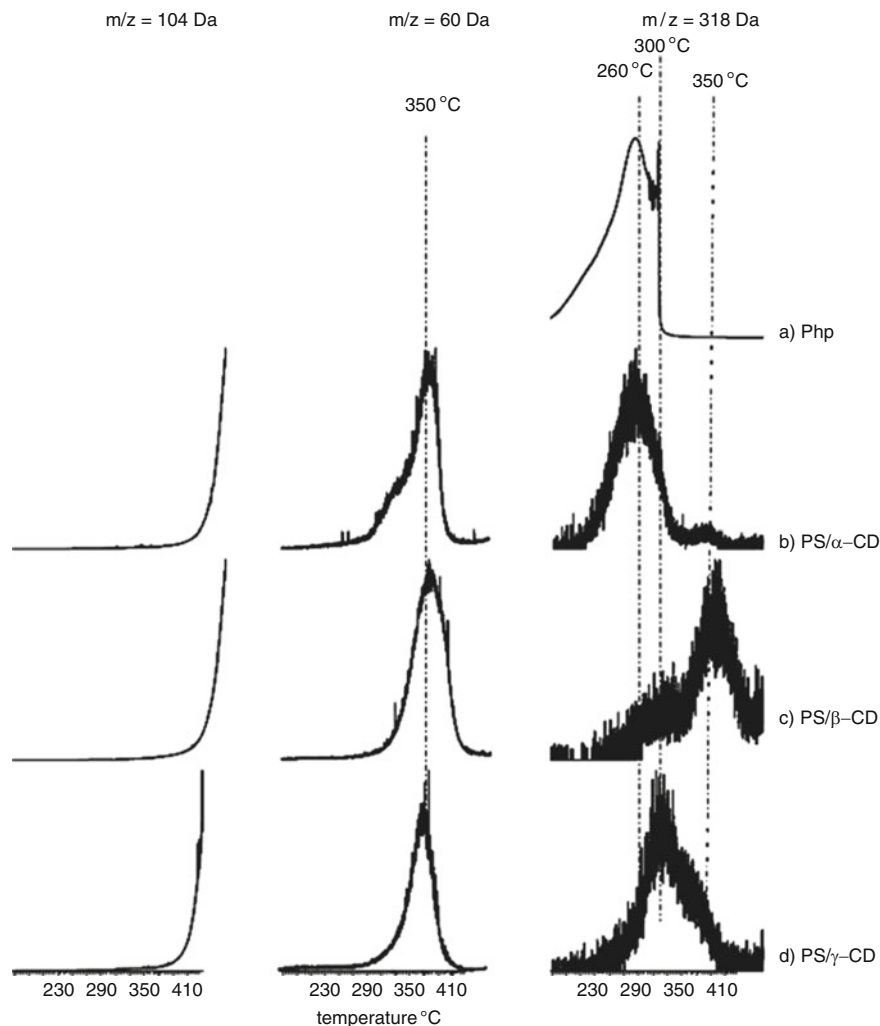
Fig. 16 Evolution profiles of (*from left to right*) PS-based product, monomer ($m/z = 104$ Da); CD-based product, $C_2H_4O_2$ ($m/z = 60$ Da); and phenolphthalein (*Php*) ($m/z = 318$ Da) detected during the pyrolysis of (**a**) pure phenolphthalein, (**b**) PS/α-CD, (**c**) PS/β-CD, and (**d**) PS/γ-CD. Reproduced from [57] with the kind permission of ACS Publications

molecule shifts to higher temperatures. In the study, PMMA nanowebs containing 10, 25, and 50% β-CD were used. As an example, the evolution profiles of MMA monomer ($m/z = 100$ Da), $C_2H_4O_2$ ($m/z = 60$ Da), and aniline ($m/z = 93$ Da) detected during the pyrolysis of PMMA, PMMA/β-CD10, PMMA/β-CD25, and PMMA/β-CD50 nanowebs after exposure to aniline vapor for 1 and 3 h are shown in Fig. 17. Inspection of the evolution profiles of characteristic evolution/decomposition products indicated that trapping of vapor depends both on the
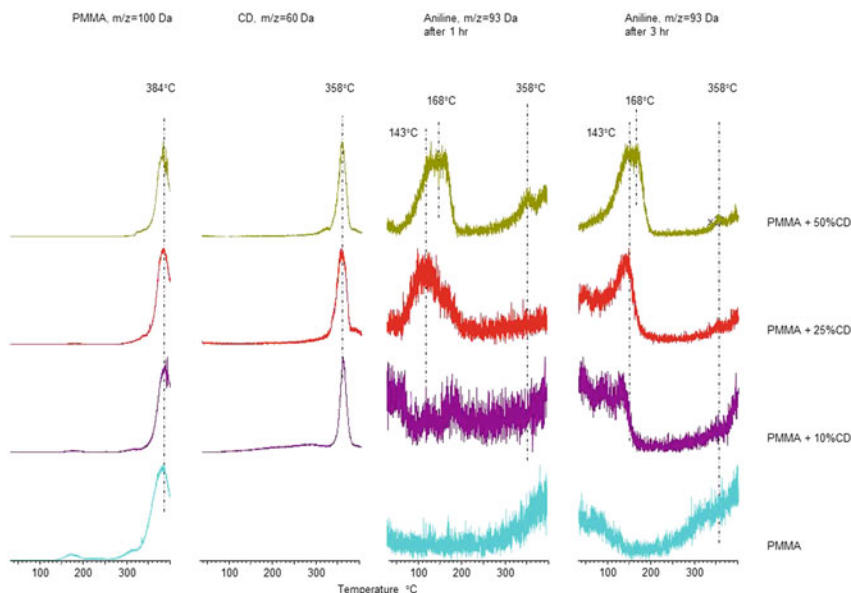
Fig. 17 DP-MS evolution profiles of (*from left to right*) PMMA-based product, monomer (*m/z* = 100 Da); β-CD-based product, $C_2H_4O_2$ (*m/z* = 60 Da); and aniline, C_6H_7N (*m/z* = 93 Da) detected during the pyrolysis of PMMA and PMMA nanowebs containing 10, 25 and 50% of β-CD. Note that the nanofibrous webs were analyzed after exposure to aniline vapor for 1 h and 3 h. Reproduced from [58] with the kind permission of Elsevier

amount of β-CD present in the PMMA nanofibers and on the time period of exposure.

4 Conclusion

DP-MS is the only pyrolysis technique in which secondary and condensation reactions are almost totally avoided and detection of high mass pyrolyzates and unstable thermal degradation products is possible. Thus, a detailed investigation of thermal degradation products and mechanism is possible. Furthermore, as shown in this review, with the use of DIP-MS, analysis of complex solid samples and multicomponent systems is possible without time-consuming extractions or derivatizations because components are separated as a function of their volatilities and/or thermal stabilities. The technique is particularly valuable when detection limits and matrix interference limit the application of common spectroscopic techniques such as nuclear magnetic resonance and infrared spectroscopy. The technique provides a rapid and cost-effective means for analysis of thermal stability and chemical composition of complex synthetic polymers that are too large or too complex for direct MS analysis.

The difficulties in interpretation of quite complex pyrolysis mass spectra due to dissociation of thermal degradation products during ionization, which limits the application of the technique, seem to be resolved with the applications of soft ionization techniques such as APCI and DESI.

The technique will more commonly be applied in the future, not only for investigation of thermal characteristics and additives but also for structural characterization of polymers that are not suitable for analysis with MALDI and ESI-MS techniques.

References

1. Statheropoulos M, Georgakopoulos K, Montaudo G (1991) The interpretation of pyrolysis mass-spectra of polymers using a hybrid software system based on library searching with heuristics. J Anal Appl Pyrol 20:65
2. Statheropoulos M, Georgakopoulos K, Montaudo G (1991) A method for the interpretation of pyrolysis mass-spectra of polyamides. J Anal Appl Pyrol 23:15
3. Qian K, Killinger WE, Casey M (1996) Rapid polymer identification by in-source direct pyrolysis mass spectrometry and library searching techniques. Anal Chem 68:1019
4. Zhang S, Shin YS, Mayer R, Basile F (2007) On-probe pyrolysis desorption electrospray ionization (DESI) mass spectrometry for the analysis of non-volatile pyrolysis products. J Anal Appl Pyrol 80:353
5. Whitson SE, Erdodi G, Kennedy JP, Lattimer RP, Wesdemiotis C (2008) Direct probe-atmospheric pressure chemical ionization mass spectrometry of cross-linked copolymers and copolymer blends. Anal Chem 80:7778
6. Huang Z, Shi W (2006) Thermal behavior and degradation mechanism of poly(bisphenyl acryloxyethyl phosphate) as a UV curable flame-retardant oligomer. Polym Degrad Stab 91:1674
7. Huang NH, Zhang Q, Fan C, Wang JQ (2008) A mechanistic study of flame retardance of novel copolyester phosphorus containing linked pendant groups by TG/XPS/direct Py-MS. Chinese Chem Lett 19:350
8. Yurteri S, Cianga I, Degirmenci M, Yagci Y (2004) Synthesis and characterization of poly(p-phenylene)-graft-poly(epsilon-caprolactone) copolymers by combined ring-opening polymerization and cross-coupling processes. Polym Int 53:1219
9. Yurteri S, Cianga I, Demirel AL, Yagci Y (2005) New polyphenylene-g-polystyrene and polyphenylene-g-polystyrene/poly(epsilon-caprolactone) copolymers by combined controlled polymerization and cross-coupling processes. J Polym Sci A Polym Chem 43:879
10. Nur Y, Yurteri Y, Cianga I, Yagci Y, Hacaloglu J (2007) Thermal degradation of poly(p-phenylene-graft-epsilon-caprolactone) copolymer. Polym Degrad Stab 92:838
11. Nur Y, Yurteri Y, Cianga I, Yagci Y, Hacaloglu J (2007) Pyrolysis of polyphenylenes with PCL or/and PSt side chains. J Anal Appl Pyrol 80:453
12. Colak DG, Cianga I, Yagci Y, Cirpan A, Karasz FE (2007) Novel poly(phenylene vinylenes) with well-defined poly(epsilon-caprolactone) or polystyrene as lateral substituents: synthesis and characterization. Macromolecules 40:5301
13. Nur Y, Colak DE, Chianga I, Yagci Y, Hacaloglu J (2008) Pyrolysis of poly(phenylene vinylene)s with polycaprolactone side chains. Polym Degrad Stab 93:904
14. Nur Y, Colak DE, Chianga I, Yagci Y, Hacaloglu J (2008) Direct pyrolysis mass spectrometry studies on thermal degradation characteristics of poly(phenylene vinylene) with well-defined PSt side chains. J Therm Anal Calorim 94:157

15. Nur Y, Colak DE, Chianga I, Yagci Y, Hacaloglu J (2009) High temperature pyrolysis of poly (phenylene vinylene)s with poly(epsilon-caprolactone) or polystyrene side chains. J Therm Anal Calorim 98:527

16. Bullions TA, Wei M, Porbeni FE, Gerber MJ, Peet J, Balik M, White JL, Tonelli AE (2002) Reorganization of the structures, morphologies, and conformations of bulk polymers via coalescence from polymer-cyclodextrin inclusion compounds. J Polym Sci B Polym Phys 40(10):992

17. Rusa CC, Uyar T, Rusa M, Wang X, Hunt MA, Tonelli AE (2004) An intimate polycarbonate/ poly(methyl methacrylate)/poly(vinyl acetate) ternary blend via coalescence from their common inclusion compound with gamma-cyclodextrin. J Polym Sci B Polym Phys 42(22):4182

18. Uyar T, Aslan E, Tonelli AE, Hacaloglu J (2006) Pyrolysis mass spectrometry analysis of poly (vinyl acetate), poly(methyl methacrylate) and their blend coalesced from inclusion compounds formed with gamma-cyclodextrin. Polym Degrad Stab 91:1

19. Uyar T, Oguz G, Tonelli AE, Hacaloglu J (2006) Thermal degradation processes of poly (carbonate) and poly(methyl methacrylate) in blends coalesced either from their common inclusion compound formed with gamma-cyclodextrin or precipitated from their common solution. Polym Degrad Stab 91:2471

20. Uyar T, Tonelli AE, Hacaloglu J (2006) Thermal degradation of polycarbonate, poly(vinyl acetate) and their blends. Polym Degrad Stab 91:2960

21. Uyar T, Rusa CC, Tonelli AE, Hacaloglu J (2007) Pyrolysis mass spectrometry analysis of polycarbonate/poly(methyl methacrylate)/poly(vinyl acetate) ternary blends. Polym Degrad Stab 92:32

22. Uyar T, El-Shafei A, Wang X, Hacaloglu J, Tonelli AE (2006) The solid channel structure inclusion complex formed between guest styrene and host gamma-cyclodextrin. Incl Phenom Macrocycl Chem 55:109

23. Elmaci A, Hacaloglu J (2009) Thermal degradation of poly(vinylpyridine)s. Polym Degrad Stab 94(4):738

24. Elmaci A, Hacaloglu J, Kayran C, Sakellariou G, Hadjichristidis N (2009) Thermal decomposition of polystyrene-b-poly(2-vinylpyridine) coordinated to co nanoparticles. Polym Degrad Stab 94:2023

25. Sundarrajan S, Srinivasan KSV (2006) Influence of structural factors on degradation product formation: primary pyrolysis products of poly(acyl sulfides) investigated by direct pyrolysis mass spectrometry. Polym Degrad Stab 91:975

26. Samperi F, Puglisi C, Ferreri T, Messina R, Cicala G, Recca A, Restuccia CL, Scamporrino A (2007) Thermal decomposition products of copoly(arylene ether sulfone)s characterized by direct pyrolysis mass spectrometry. Polym Degrad Stab 92:1304

27. Ramakrishnan L, Sivaprakasam K (2009) Synthesis, characterization, thermal degradation, and comparative chain dynamics studies of weak-link polysulfide polymers. J Polym Res 16:623

28. Whitson SE, Wesdemiotis C, Lattimer RP (2010) Characterization of polyurethane formulations by direct probe atmospheric pressure chemical ionization mass spectrometry. Rub Chem Tech 83:35

29. Patil AO, Heeger AJ, Wudl F (1988) Optical properties of conducting polymers. Chem Rev 88:183

30. Hughes M, Shaffer MSP, Renouf AC, Singh C, Chen GZ, Fray DJ, Windle AH (2002) Electrochemical capacitance of nanocomposite films formed by coating aligned arrays of carbon nanotubes with polypyrrole. Adv Mater 14:382

31. Jin S, Liu X, Zhang W, Lu Y, Xue G (2000) Electrochemical copolymerization of pyrrole and styrene. Macromolecules 33:4805

32. Gozet T, Onal AM, Hacaloglu J (2007) Investigation of the effect of dopant on characteristics of poly(3-methyl thiophene) via pyrolysis mass spectrometry. J Macromol Sci Pure Appl Chem 44:259

33. Hacaloglu J, Argin E, Kucukyavuz Z (2008) Characterization of polyaniline via pyrolysis mass spectrometry. J Appl Polym Sci 108:400

34. Papila O, Toppare L, Hacaloglu J (2006) Investigation of copolymers of thiophene-functionalized polystyrene with pyrrole by pyrolysis mass spectrometry. J Macromol Sci Pure Appl Chem 43:655

35. Levent A, Hacaloglu J, Toppare L (2008) Characterization of conducting copolymer of pyrrole via pyrolysis mass spectrometry. J Macromol Sci Pure Appl Chem 45:201

36. Aslan E, Hacaloglu J, Toppare L (2007) A pyrolysis mass spectrometry study of polythiophene copolymers. Polym Degrad Stab 92:822

37. Aslan E, Hacaloglu J, Toppare L (2008) Thermal analysis of a new thiophene derivative and its copolymer. J Therm Anal Calorim 92:839

38. Hacaloglu J, Tezal F, Kücükyavuz Z (2009) The characterization of polyaniline and polypyrrole composites bypyrolysis mass spectrometry. J Appl Polym Sci 133:3130

39. Allen DJ, Ishida H (2006) Physical and mechanical properties of flexible polybenzoxazine resins: effect of aliphatic diamine chain length. J Appl Polym Sci 101(5):2798

40. TakeichiT KT, Agag T (2008) High performance polybenzoxazines as a novel type of phenolic resin. Polym J 40:1121

41. Ghosh NN, Kiskan B, Yagci Y (2007) Polybenzoxazines – new high performance thermosetting resins: synthesis and properties. Prog Polym Sci 32:1344

42. Agag T (2006) Preparation and properties of some thermosets derived from allyl-functional naphthoxazines. J Appl Polym Sci 100:3769

43. Uyar T, Koyuncu Z, Ishida H, Hacaloglu J (2008) Polymerisation and degradation of an aromatic amine-based naphthoxazine. Polym Degrad Stab 93:2096

44. Fam SB, Uyar T, Ishida H, Hacaloglu J (2010) The use of pyrolysis mass spectrometry to investigate polymerization and degradation processes of methyl amine-based benzoxazine. Polym Test 29:520

45. Fam SB, Kiskan B, Aydogan B, Hacaloglu J, Yagcı Y (2011) Thermal degradation of polysiloxane and polyetherester containing benzoxazine moieties in the main chain. J Anal Appl Pyrol 90:155

46. Trimpin S, Wijerathne K, Mc Ewen CN (2009) Rapid methods of polymer and polymer additives identification: multi-sample solvent-free MALDI, pyrolysis at atmospheric pressure, and atmospheric solids analysis probe mass spectrometry. Anal Chim Acta 654:20

47. Greiner A, Wendorff JH (2007) Electrospinning: a fascinating method for the preparation of ultrathin fibres. Angew Chem Int Ed 46:5670

48. Li D, Xia Y (2004) Electrospinning of nanofibers: reinventing the wheel? Adv Mater 16:1151

49. Ren GL, Xu XH, Liu Q, Cheng J, Yuan XY, Wu LL, Wan YZ (2006) Electrospun poly(vinyl alcohol)/glucose oxidase biocomposite membranes for biosensor applications. React Funct Polym 66:1559

50. Teo WE, Ramakrishna S (2006) A review on electrospinning design and nanofibre assemblies. Nanotechnology 17:R89

51. Hedges AR (1998) Industrial applications of cyclodextrins. Chem Rev 98:2035

52. Uyar T, Hacaloglu J, Besenbacher F (2009) Electrospun polystyrene fibers containing high temperature stable volatile fragrance/flavor facilitated by cyclodextrin inclusion complexes. React Funct Polym 69:145

53. Uyar T, Havelund R, Hacaloglu J, Zhou X, Besenbacher F, Kingshott P (2009) The formation and characterization of cyclodextrin functionalized polystyrene nanofibers produced by electrospinning. Nanotechnology 20:125605

54. Uyar T, Nur Y, Hacaloglu J, Besenbacher F (2009) Electrospinning of functional poly(methyl methacrylate) nanofibers containing cyclodextrin-menthol inclusion complexes. Nanotechnology 20:125703

55. Uyar T, Hacaloglu J, Besenbacher F (2011) Electrospun polyethylene oxide (PEO) nanofibers containing cyclodextrin inclusion complex. J Nanosci Nanotechnol 11:3949–3958

56. Uyar T, Havelund R, Nur Y, Hacaloglu J, Besenbacher F, Kingshott P (2009) Molecular filters based on cyclodextrin functionalized electrospun fibers. J Membr Sci 333:129
57. Uyar T, Havelund R, Hacaloglu J, Besenbacher F, Kingshott P (2010) Functional electrospun polystyrene nanofibers incorporating alpha-, beta-, and gamma-cyclodextrins: comparison of molecular filter performance. ACS Nano 4:5121
58. Uyar T, Havelund R, Nur Y, Balan A, Hacaloglu J, Toppare L, Besenbacher F, Kingshott P (2010) Cyclodextrin functionalized poly(methyl methacrylate) (PMMA) electrospun nanofibers for organic vapors waste treatment. J Membr Sci 365:409

Mass Spectrometric Characterization of Oligo- and Polysaccharides and Their Derivatives

Petra Mischnick

Abstract Mass spectrometry has become a key technique for the structural analysis of carbohydrates. Due to their special properties and requirements carbohydrates and especially chemically modified carbohydrates occupy a position between biopolymers and synthetic polymers. Charged analytes can be obtained by adduct formation with appropriate small ions or by various labeling procedures. Besides molecular mass profiling, tandem mass spectrometry can give more detailed structural information including sugar constituents, sequence and interresidue linkage positions, and some information on stereochemistry. Substitution patterns of polysaccharide derivatives are also studied by ESI IT-MS and MALDI ToF-MS. In this review, ion formation of carbohydrates, their chemical modification, fragmentation pathways of various analyte species, and the applicability of MS for quantitative evaluations are discussed. Mainly ESI applications are presented, but where of general significance MALDI-MS applications are also outlined. Examples of application are given, excluding the well-reviewed area of biologically important O- and N-linked glycans. Molecular mass determination and structural analysis of heteroglycans are followed by examples of cellulose and starch derivatives.

Keywords Carbohydrates · Electrospray-ionization mass spectrometry · Fragmentation · Labeling · Matrix-assisted laser desorption/ionization time-of-flight mass spectrometry · Polysaccharides and derivatives

P. Mischnick

Technical University Braunschweig, Institute of Food Chemistry, Schleinitzstr. 20, 38106 Braunschweig, Germany

Department of Fibre and Polymer Technology, Royal Institute of Technology (KTH), Teknikringen 56–58, 10044 Stockholm, Sweden
e-mail: p.mischnick@tu-braunschweig.de

Contents

Abbreviations

AA	Aminobenzoic acid
AB	Aminobenzamide
AEE	Aminobenzoic acid ethyl ester
ANTS	2-Aminonaphthalene-trisulfonic acid
AP	Aminopyridine
APTS	1-Amino-pyrene-trisulfonic acid
CE	Capillary electrophoresis
CID	Collision induced dissociation
CMC	Carboxymethylcellulose
CROP	Cationic ring-opening polymerization
DESI	Desorption electrospray ionization
DHB	Dihydroxybenzoic acid
DHBB	2,5-Dihydroxybenzoic acid/butylamine
DNA	Deoxy ribonucleic acid
DP	Degree of polymerization
ESI	Electrospray ionization
FAB	Fast atom bombardment
FTIC	Fourier transform ion cyclotron
GLC	Gas liquid chromatography
GP	Girard's P [1-(hydrazinocarbonylmethyl)pyridinium chloride]
GPC	Gel permeation chromatography
GT	Girard's T [1-(hydrazinocarbonylmethyl)trimethylammonium chloride]
HABA	2-(4-Hydroxyphenylazo)-benzoic acid

HEC	Hydroxyethyl cellulose
HEMC	Hydroxyethylmethyl cellulose
HPAEC-PAD	High performance anion exchange chromatography-pulsed amperometric detection
HPC	Hydroxypropyl cellulose
HPMC	Hydroxypropylmethyl cellulose
HPSEC-MALLS	High performance size-exclusion chromatography–multi-angle laser light scattering
HPTLC	High performance thin layer chromatography
IEM	Ion evaporation model
IT	Ion trap
LIFD	Laser-induced fluorescence detection
MALDI	Matrix-assisted laser desorption/ionization
MS	Mass spectrometry
NMR	Nuclear magnetic resonance
NP	Normal phase high performance liquid chromatography
PEG	Polyethyleneglycol
PSD	Post-source decay
QIT	Quadrupole ion trap
Q-ToF	Quadrupole time-of-flight mass analyzer
RDA	Retro-Diels–Alder
RP-HPLC	Reversed phase high performance liquid chromatography
SEC	Size-exclusion chromatography
THAP	$2',4',6'$-Trihydroxy-acetophenone
ToF	Time-of-flight
UV	Ultraviolet

1 Introduction

The development of efficient ionization methods for mass spectrometric analysis of large molecules has triggered tremendous progress in structural analysis of biomacromolecules. The inherent properties of these compounds arising from polarity, non-volatility, and chemical instability, and the often limited availability in pure form cause significant analytical challenges. These were overcome first by fast atom bombardment (FAB), and since the late 1980s more efficiently by electrospray ionization (ESI) and matrix-assisted laser desorption/ionization (MALDI). In combination with appropriate mass analyzers such as sector field instruments, quadrupoles, ion traps (IT) and time-of-flight (ToF) tubes, these ionization techniques and their advanced development have been widely applied to biomolecules of oligo- and polymeric size. The combination with tandem mass spectrometry (MS^n) makes these techniques even more attractive, since in addition to the molecular mass measurement, sequence information can be obtained and substituents can be localized. Although for various reasons nucleic acids and

especially proteins and peptides have been preferentially studied, and "proteomics" has even developed into a separate research area, carbohydrates have not been ignored. Unlike proteins, where the nitrogen atoms enable easy and multiple-charged (protonated) ion formation, carbohydrates commonly form sodium adducts at much lower yields. In addition, compared to proteins and peptides, poly- or oligosaccharides show lower surface activity, exhibit higher polarity, are less stable, often show dispersity of molecular mass and chemical structure, and due to many stereochemical centers have isobaric ions, which cannot easily be differentiated by MS.

Nevertheless, carbohydrate analysis has also profited a lot from these methods, and the specific challenges have been tackled. Most of the publications in this field deal with *O*- and *N*-linked glycans from the glycosylation sites of proteins, or with other biologically active molecules, e.g., human milk oligosaccharides [1–5] or everninomicins, a class of complex oligosaccharide antibiotics [6]. Many reviews have reported on the progress in the area of *O*- and *N*-glycan analysis [7–22]. In this chapter, these compounds will only be considered when more general insights and methods are concerned. On the other hand, ESI-MS and MALDI-MS have also been applied for structural analysis of polysaccharides from plants or microorganisms to gain insights into sequences and branching patterns etc. of these less regular biomacromolecules. In addition to application to native compounds, methods for the analysis of the substitution pattern of starch and cellulose derivatives have been developed [23]. Cyclodextrins (cyclic α-1,4-linked glucooligosaccharides) can form inclusion complexes with a wide range of substrates and have many applications, e.g., for encapsulation of drugs. ESI-MS has turned out to be a useful tool for investigating such molecular recognition phenomena, thus providing a powerful means for the analysis of a wide range of host–guest and other non-covalent complexes present in solution [24, 25]. In the case of defined glycoarchitectures such as glycodendrimers, MS is a valuable method for controlling conversion and uniformity [26, 27].

Quantitative aspects are often not emphasized in applications. On the one hand, structural analysis of glycoconjugates is mainly interesting from the qualitative perspective, but on the other hand relative ion intensities in a mass spectrometer cannot simply be translated into sample portions. However, in the field of polysaccharide derivatives the exact quantification of analytes is of high importance. Fundamental studies dealing with the ionization process have revealed several parameters that influence relative ion intensities, and models for calculations and predictions have also been developed [28–30].

Basic aspects like ion formation, labeling of carbohydrates, fragmentation in collision-induced dissociation (CID) processes, and quantifiability will be addressed, completed by examples of application on plant polysaccharides. The high importance of MS for the analysis of substitution patterns of polysaccharide derivatives will be emphasized and, in this context, methods of sample preparation and quantitative aspects will be discussed. The focus is on ESI-MS, but MALDI-MS has often been applied to the same problems and will be considered where reasonable.

It is assumed that the reader is familiar with the basic principles of the ESI and MALDI processes, and with the instrument setup. With respect to (special) MS

techniques [e.g., nanospray, desorption electrospray ionization (DESI), Orbitrap, Fourier transform ion cyclotron (FTIC), ESI-atmospheric pressure ion mobility-ToF MS] and the field of glycoconjugates, the reader is referred to the recent literature [29, 31–34].

2 Carbohydrates as Analytes for Mass Spectrometry

2.1 *Ion Formation of Carbohydrates*

2.1.1 Positively Charged Analytes

A prerequisite for MS analysis is the existence of charged species. Positive and negative ions can be recorded, but the positive mode is more common and therefore preferentially considered here. Carbohydrates are neutral and, except for amino sugars, usually exhibit no basic groups that are available for protonation. More common is, thus, the formation of adducts with metal cations, mainly alkali ions, and preferentially the ubiquitously present sodium ion. Ion yield and consequently the sensitivity of MS depend on appropriate coordination sites. Coordination is accomplished by the oxygen atoms with their non-bonding electron pairs. However, it is not simply a 1:1 complex that is generated with the most basic oxygen, but a multi-coordinated species in which several oxygen atoms interact in a cooperative way with the cation. As a simplified model of glycans, polyethyleneglycol (PEG) can be considered, which (like carbohydrates) exists in oligomeric and polymeric forms, and in open-chain and cyclic forms. For these, it was found by ion mobility measurements and molecular calculations that the complexation constant for sodium adduct formation increases with the number of (CH_2CH_2O) units until it reaches an optimum at the favored coordination number. For sodium, energy minima were found for Na^+-PEG-9, Na^+-PEG-13, and Na^+-PEG-17 with seven or eight oxygen coordination sites [35]. Lithium prefers the coordination number 7, and the larger potassium and caesium ions the coordination number 10 or 11 [36]. The PEG chain "wraps" around the cation and adopts the most favored conformation. These studies refer to solvent-free complexes and are not only a model for MALDI, where ionization mainly occurs in the gas phase in vacuum, but also for ESI, where neutral molecules like common carbohydrates only become sodiated after consecutive Coulomb explosions of the primarily formed charged droplets and evaporation of the solvent [28]. Therefore, it should be emphasized here that the relative intensities of ions observed in the mass spectrometer do not simply reflect the equilibrium in solution, but depend on the surface activities of the analytes [37] and (related to these) on the solvation energies (or desorption energies from the droplets), solvent, droplet size, and instrument parameters affecting the ion transfer. Bahr et al. found a huge change in relative intensities even for neutral unmodified oligosaccharides (maltopentaose) when applying nano-ESI QIT-MS (QIT: quadrupole ion trap) (Fig. 1) [38].
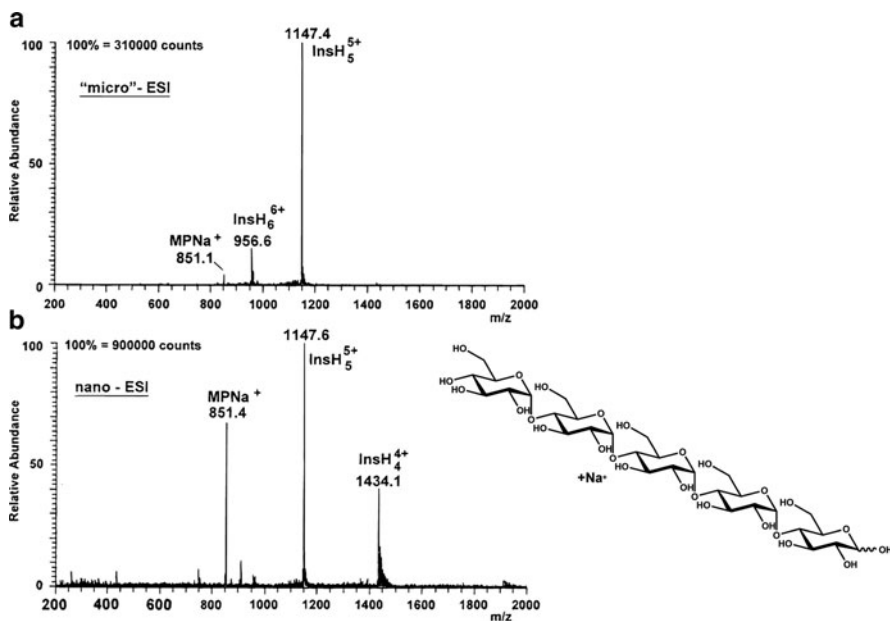
Fig. 1 ESI-MS analysis of a mixture of maltopentaose and insulin (both 5×10^{-6} M) with conventional forced-flow ("micro") (**a**), and nanospray (**b**). The averaged absolute intensities for the base peaks are indicated. Reproduced from [38] with kind permission of the publisher

A nanospray capillary with an orifice diameter of 1–2 μm and a flow rate of <1 μL/min displayed sensitivities which for the maltopentaose was comparable to that of the much more surface active peptide applied together with the maltooligomer. Although surface activity can be regarded as a thermodynamic parameter, reaching the surface requires migration from the interior, which is a kind of kinetic control. At the high field strength of ESI (e.g., 10^6–10^7 V/m) the electrophoretic mobility is the most relevant property in this regard. The effect of this kinetic parameter is obvious from the dependence of the relative signal intensities of competing ions on the capillary voltage (Fig. 2) [30].

Crown ethers, as the cyclic PEG analogs, have also been studied [39, 40]. Comparing adduct formation of a given crown ether (host) in a certain solvent with various cations (guests), e.g., the alkali ions, the experimentally observed ratio of signal strength is in good agreement with the theoretical data calculated from the complexation constants in solution. In comparison with the deviating behavior of the linear tetraglyme (di-*O*-methyl-PEG-4), their lower conformational flexibility obviously mimics a behavior more similar to the solvated state.

Against this background, it is not surprising that disaccharides are detected with higher sensitivity than monosaccharides, which do not exhibit a sufficient number of oxygen atoms in appropriate orientation, although the surface activity of monosaccharides is probably comparable to that of disaccharides. In addition, the disaccharide with its glycosidic linkage has a higher flexibility to adopt the
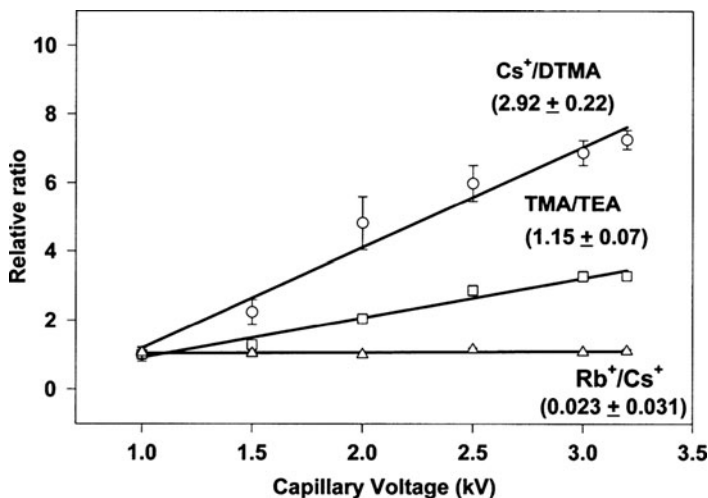
Fig. 2 Voltage dependence of relative signal ratios of various positive ions in ESI-MS. Values were normalized to a ratio of 1 at 1 kV. *DTMA* decyltrimethylammonium iodide, *TMA* tetramethylammonium bromide, *TEA* tetraethylammonium bromide. For details see [30]. Reproduced from [30] with kind permission of the publisher
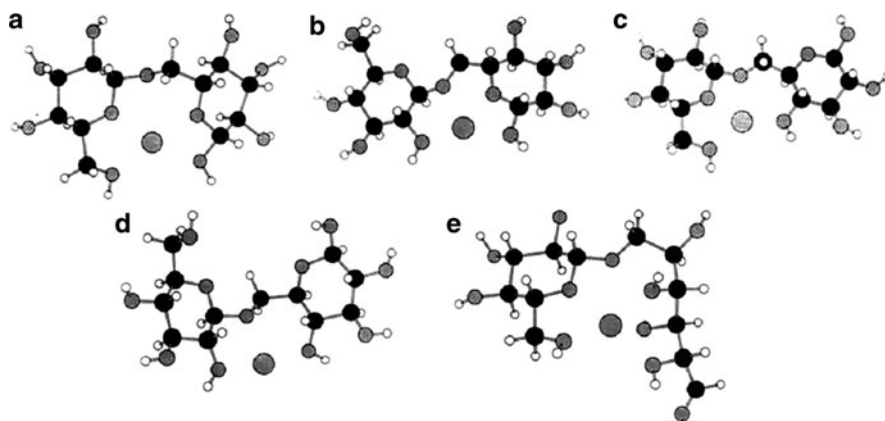
Fig. 3 Structures of lithiated gentiobiose generated from MNDO calculations with $\Delta H_f =$ (**a**) -406, (**b**) -398, (**c**) -400, (**d**) -390, and (**e**) -399 kcal. In (**e**), the disaccharide is opened to the aldehyde form. For details see [41]. Reproduced from [41] with kind permission of the publisher

appropriate conformation required for efficient complexation. Probably for the same reason, reduction of a disaccharide to an alditol glycoside additionally enhances the response in ESI-MS. Hofmeister et al. [41] have studied the coordination site of Li^+ in isomeric disaccharides and open-chain gentiobiose, and showed experimentally and by semi-empirical MNDO (modified neglect of diatomic overlap) molecular orbital calculations that the lithium cation is penta-coordinated between the two sugar rings (Fig. 3).

The location and coordination of the charge-giving cation is also important for the fragmentation of sugar complexes in collision induced dissociation (CID), which will be discussed in Sect. 4.1.

ESI-MS competition experiments with cyclodextrins showed a much larger affinity of the β-cyclodextrin to sodium compared to all other alkali cations, thus demonstrating that it is the size of the cyclic maltooligosaccharide in relation to the cationic radius that drives the formation of the inclusion complex [42], comparable to crown ethers.

Although sodium is ubiquitous, the sample solution is sometimes spiked with sodium salts like sodium acetate [43]. If other adduct types are required, the cations are added as soluble salts, e.g., iodides, chlorides, acetates, trifluoroacetates, perchlorates, or sulfates (less than millimolar concentrations). At high concentrations, slightly acidic protons can be exchanged against Na^+ and clusters with the salt are formed, e.g., $[M + Na + n\ NaOAc]^+$. An increase of sodium adducts with increasing cone (nozzle-skimmer) voltages, but significant in-source fragmentation has been reported by Harvey [44].

Other cations e.g., divalent cations (Mg^{2+}, Ca^{2+}, Mn^{2+}, Co^{2+}, Cu^{2+}) have been studied for their relative complexation ability and cone-voltage-dependent intensities of the different adduct ions formed with maltoheptaose and an high-mannose N-glycan. Beside the $[M + X]^{2+}$ ions, singly charged fragment ions $[M + X^{2+}\text{-(anhydroGlc} + H^+)]$ were observed [45]. Silver adducts have also been applied, especially with the aim to find diagnostically valuable fragmentation pathways. $[M + Ag]^+$ and $[M + 2Ag]^{2+}$ ions have been observed [46].

Variation of counterion is also of interest with respect to stability of the $[M + X]^+$ adduct. In the series of alkali ions, the Li adduct is the most stable, whereas the Cs adduct has the lowest dissociation energy.

A more special application is the coordination with various transition metals under participation of coordinating additives or covalently linked tags, which has been studied by the group of Leary. This approach allows differentiating of diastereoisomers, which is a frequent and important topic in carbohydrate analysis. Established methods in this field, like NMR spectroscopy, are slower and less sensitive, making ESI in combination with tandem MS a promising alternative. Derivatization with diethylenetriamine and complexation with, e.g., Zn^{2+}, differentiates between stereoisomers of hexose (Fig. 4) [48, 49]. *Gluco-*, *galacto-* and *manno-*configuration of the frequently occurring N-acetyl-2-amino-2-deoxy-hexoses have been differentiated by tandem MS of their diaminopropane-cobalt(III) complexes, in which the sugar nitrogen participates in cobalt complexation [47].

For more basic information on models for ESI, the reader is referred to literature on the charged residue model (CRM) of Dole et al. [50], on the ion evaporation model (IEM) of Iribarne and Thomson [51], to reviews summarizing the progress in this field [28, 29, 52], and to monographs [31–33].

2.1.2 Negatively Charged Analytes

Negative ions, directly formed from native carbohydrates, are of less relevance as long as no additional acidic groups like carboxy, sulfate or phosphate groups are
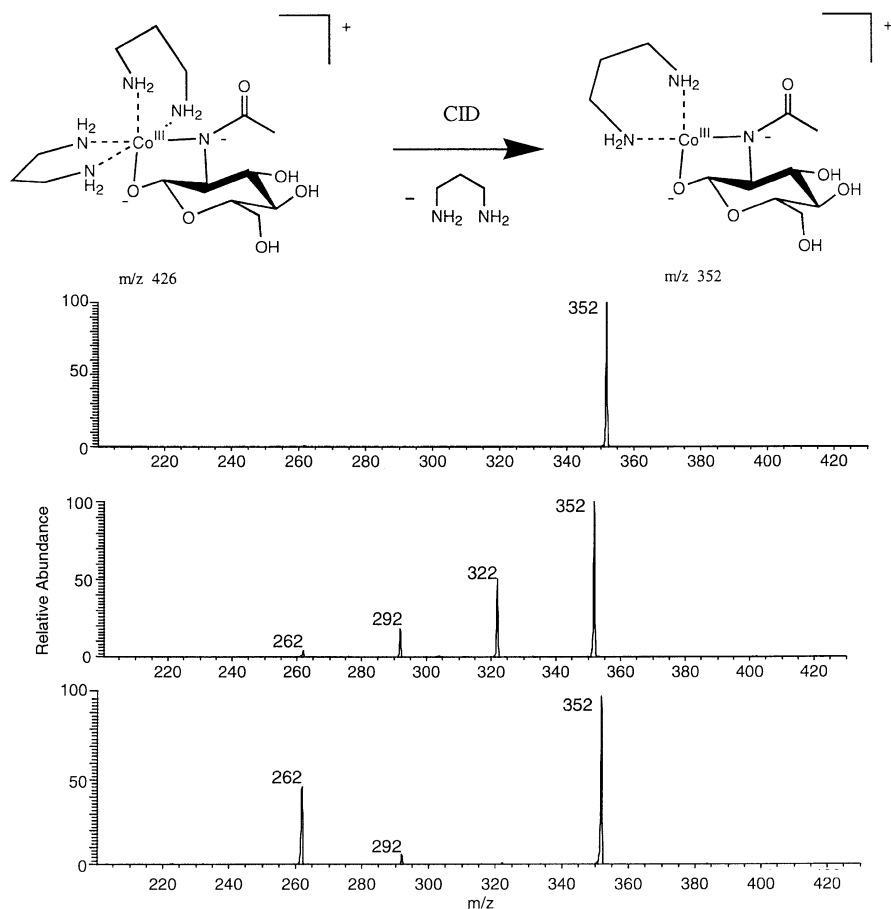
Fig. 4 *Above*: Proposed structures of the Co(DAP)(GlcNAc) complexes *m/z* 426 and 352. *Below*: MS^3 spectra of *m/z* 352 from top to bottom GlcNAc (*A*), GalNAc (*B*) and ManNAc-Co(DAP) (*C*) complexes in MS^2. Reproduced from [47] with kind permission of the publisher

present. Although OH groups in carbohydrates are comparably acidic (pK_a 12–14), this is not acidic enough to form [M-H]$^-$ ions to sufficient extent under normal conditions. These ions are relatively unstable and tend to fragment within the ion source. But again, with respect to selectivity and fragmentation pathways, it is fruitful to generate negatively charged adducts. Harvey found well-polarizable anions such as halogenides (with exception of fluoride), sulfates, phosphates, and nitrates forming stable anionic products with some *N*-glycans, with nitrate giving best stability and sensitivity [53–56]. Both, singly and doubly charged ions were observed, and uronic acid as constituent caused even higher charge states. In studies of neutral oligosaccharides obtained from *N*-glycans, it was found that in the presence of ammonium phosphate (0.5 mM in methanol/water 1:1) more stable [M + H$_2$PO$_4$]$^-$ adducts were formed nearly quantitatively. The fragment spectra of these anion adducts resemble

that of the [M-H]$^-$ ions since the first fragmentation step is the elimination of the corresponding acid, in this case H_3PO_4, thus finally yielding [M-H]$^-$ ions [57]. These negatively charged ions show diagnostically valuable fragmentation behavior without competing mechanisms or rearrangements, thus giving rise to ions presenting unambiguously specific structural features. [1, 2, 58].

2.2   Carbohydrate Derivatives

The physico-chemical properties of carbohydrates are strongly influenced by chemical modification. All parameters affecting ion abundance, such as surface activity, solubility and solvation energy, electron density at O atoms and thus coordination properties, and electrophoretic mobility are either slightly or heavily changed. Furthermore, charged or easily ionizable groups can be introduced by labeling reactions. Surface activity is probably the most decisive factor for the enhanced absolute and higher relative signal intensity of modified carbohydrates in ESI-MS compared to native carbohydrates [37, 38]. In conventional ESI-MS analysis, multiple *O*-alkylation of (oligo)saccharides affects the stepwise increasing response for [M + Na]$^+$ in MS, which is obvious from mixtures of un-, mono-, di- and trisubstituted glucose, where the higher alkylated constituents are increasingly overestimated. This effect becomes less and less pronounced with increasing degree of polymerization (DP) of the corresponding oligosaccharides. Solvation of the OH-rich native or only modestly modified carbohydrates is probably much stronger in commonly used protic solvents (often methanol), since hydrogen bonds can be formed that are of higher bonding energy than van der Waals interactions. With increasing lipo- or amphiphilic character, the analytes become more and more located at the droplet–air interphase, and thus are preferably transferred into the highly charged progenies in subsequent Coulomb explosions. When higher alkyl or hydroxyalkyl residues are introduced, the sensitivity increases further. In the latter case, additional coordinating oxygen atoms are available in the flexible side groups. Also, polar substituents like carboxymethyl groups, which occur as neutral COOH or COONa, enhance the response in ESI-MS. Chemically modified carbohydrates will be treated in more detail in the section on polysaccharide derivatives (Sect. 6).

2.2.1   Labeling of Carbohydrates

A special type of chemical modification is the selective introduction of a label or tag. The tag can exhibit a permanent charge, often a quaternary ammonium group, or an easily ionizable function, e.g., an amino (positive mode), carboxy or sulfonic acid group (negative mode). Besides, most of the tags are chromophors and some tags are also fluorescent, which can be used for parallel detection in the case of liquid chromatography (LC) or capillary electrophoresis (CE) coupling to the ESI mass spectrometer [17, 18, 58]. For a selective reaction, the dormant terminal carbonyl function of the glycan is used. Formation of hydrazones, oximes, and

imines are the most popular reactions, often followed by a reduction to shift reversibly formed intermediates like imines to the stable amines [59–61]. Michael reaction with 1-phenyl-3-methyl-5-pyrazolone has also been applied [62]. Glycan labeling strategies and their applications have been reviewed by several authors, again mainly focusing on glycoconjugate analysis, but of general meaning.

Girard's T [1-(hydrazinocarbonylmethyl)trimethylammonium chloride, GT] and Girard's P reagent [1-(hydrazinocarbonylmethyl)pyridinium chloride, GP] were applied to increase the intensity in MS by hydrazone formation [63, 64] and for performing quantitative measurements [65, 66]. Hydrazones are formed by nucleophilic attack of an acid hydrazide such as GT at the anomeric carbon atom of the reducing sugar, followed by elimination of water (Fig. 5). NMR studies have proved that the product is stabilized as its β-N-glycoside [68]. Thus, no reduction step is necessary to shift the equilibrium to the product side. However, products are acid-sensitive and show the highest stability at neutral pH [67, 69–71].

Another powerful method for labeling of carbohydrates is reductive amination [17, 58]. In this two-step derivatization, an imine is formed by reaction with a primary amine, which is subsequently reduced to the product, usually by NaCNBH$_3$. Some authors [72–74] have studied various parameters that influence the rate and result of the reactions, such as solvent, pH, ratio of reagents, temperature, time, and sample work-up. Selectivity of the reducing agent with respect to the carbonyl function is a crucial point, often not considered [67, 75]. Reductive amination of the carbonyl function is also pH-sensitive [76]. In most cases, large molar excess of amine (up to several 1,000-fold) [77] have been used to avoid twofold reaction of the primary amine and to shift the equilibrium to the imine, which is subsequently reduced to the corresponding aminodeoxyalditol (Fig. 6). Recently, 2-picoline borane has been found to be superior to the cyano compound, since it displays higher reducing selectivity, is nontoxic and does not introduce sodium into the sample [67, 78].
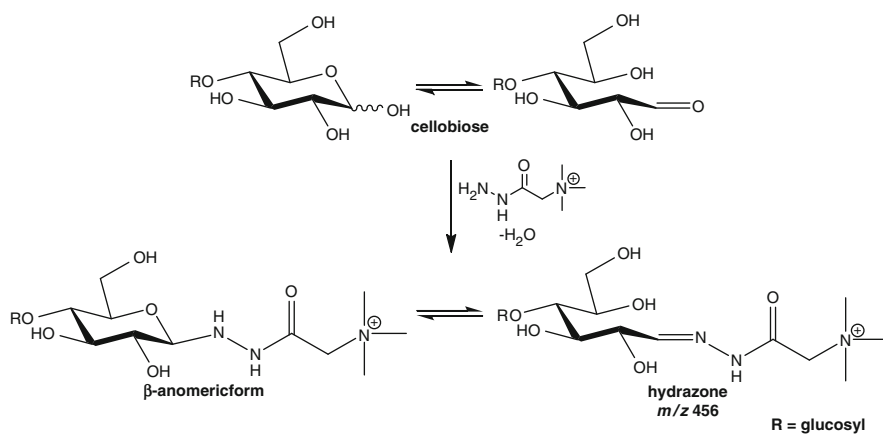
Fig. 5 Hydrazone formation of cellobiose with Girard's T reagent. Reproduced from [67] with kind permission of the publisher
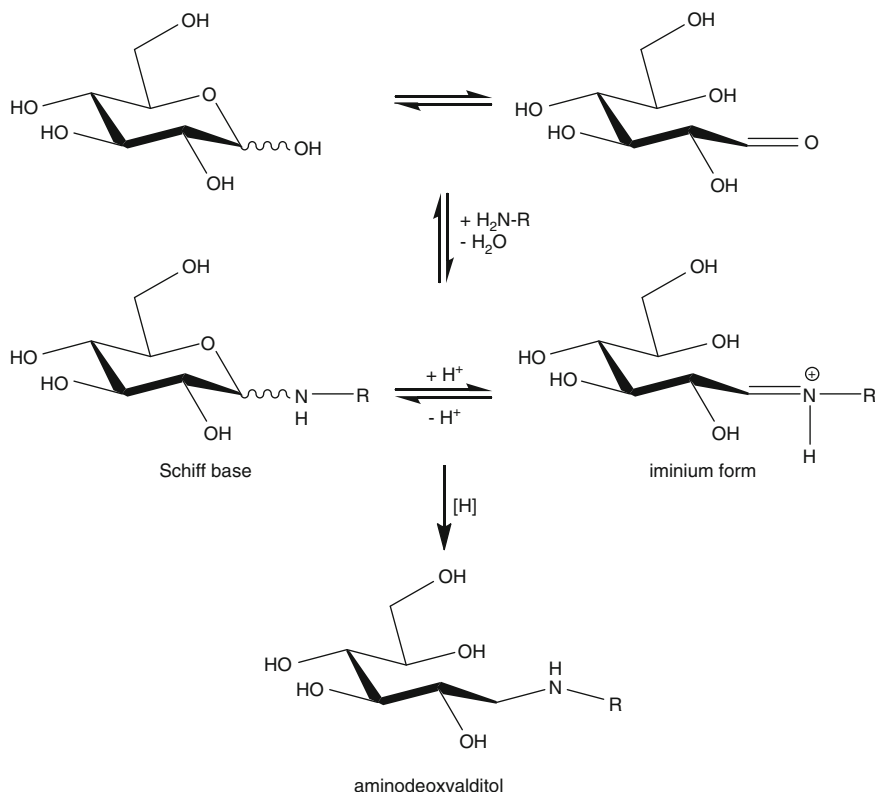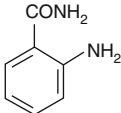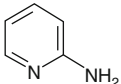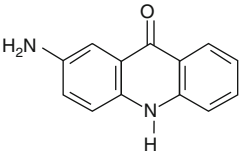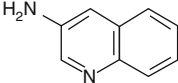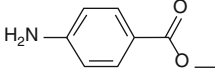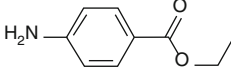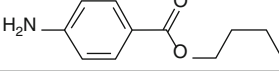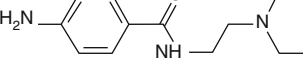
Fig. 6 Reductive amination of glucose. Reproduced from [67] with kind permission of the publisher

Aliphatic amines, functionalized amines like aminoethyl crown ethers, but in most cases aromatic amino reagents have been applied for reductive amination, i.e., 2-amino-pyridine (AP), regiosiomeric aminobenzoic acids (AA), their esters (e.g., ethyl: AEE) and amides (AB), but also polycyclic aromatic amines like 2-aminonaphthalene- (ANTS) and 1-amino-pyrene-trisulfonic acids (APTS). Table 1 shows the structures and mass increments of some common labeling reagents [60]. Acetic acid is usually added to catalyze reductive amination reactions by protonation of the carbonyl group and the intermediate imine, which results in a promotion of the hydride transfer to the iminium ion [79]. However, at too-low a pH, the primary amino function is protonated to too-high an extent. Thus, the reactions have to be performed in an optimal pH range, which depends on the basicity of the amine applied. Sun et al. [76] estimated that the pH should be close to, but not lower than, the pK_a value of the amine applied. Therefore, aromatic deactivated amines are preferably employed because they are less basic than the aliphatic amines and hence show higher reactivity at low pH values. Electron-withdrawing groups in o- or p-positions further decrease the pK_a of the ammonium

Table 1 Common amines applied for labeling by reductive amination. Reproduced from [60] with kind permission of the publisher

No.	Amine	Abbreviation	Mass Increment	Structure
1	2-Aminobenzamide	2-AB	120	
2	2-Aminopyridine	2-AP	78	
3	2-Aminoacridone	2-AMAC	194	
4	3-Aminoquinoline	3-AQ	128	
5	4-Aminobenzoic acid methyl ester	ABME	135	
6	4-Aminobenzoic acid ethyl ester	ABEE	149	
7	4-Aminobenzoic acid n-butyl ester	ABBE	176	
8	4-amino-N-(2-diethylaminoethyl)benzamide	DEAEAB	219	

form, e.g. *o*-aminobenzoic acid (2-AA) has a pK_a of 2.18 [80]. The introduction of acidic groups offers the option of negative ion formation. 2-AA is often used due to its fluorescence and UV activity [72, 81] but also for fragmentation studies in structure analysis of polysaccharides [82–84].

To obtain mass spectra with a high signal-to-noise ratio it is important to remove contaminants such as the excess of reagents, buffer, etc. [58]. MS is therefore often coupled with CE [72, 85, 86] or more commonly with HPLC [87, 88]. Samples are purified by size exclusion chromatography (SEC), precipitation with acetone [89], solid phase extraction [74, 88], or extraction of excess amine with organic solvents [73, 87]. Besides being time-consuming, these steps involve the risk of bias of constituents in a complex mixture.

For the analysis of the substituent distribution of polysaccharide derivatives, the exact quantitative analysis of oligosaccharide mixtures from partial degradation

of the polymer plays a key role. Although the strong influence of hydroxy and methoxy substituents in methyl celluloses on pseudomolecular ion yields of oligosaccharides can be overcome simply by permethylation with methyl iodide-d_3, this approach cannot be applied for hydroxyalkyl derivatives like hydroxyethyl, hydroxypropyl, hydroxyethylmethyl, and hydroxypropylmethyl cellulose (HEC, HPC, HEMC, HPMC). To level off the strong influence of alkoxyalkyl groups on ion formation, amino groups or permanently charged tags have been introduced [90, 91]. These procedures include reductive amination with propyl amine and subsequent quaternization of the nitrogen by methylation (Section 6.2).

3   Molecular Mass Determination

The search for an ionization method that is able to transfer and ionize relatively large polar molecules without decomposition into the gas phase was strongly motivated by the demand for molecular mass information especially of biopolymers. When in the late 1980s MALDI [92, 93] and ESI-MS [94] opened new possibilities compared to FAB-MS, the question arose whether molecular weight distributions could also be determined by these methods. For MALDI ToF-MS, which covers a much wider m/z range, this has been shown to be possible for certain synthetic polymers under appropriate conditions [95]. In the field of biopolymers, polydispersity of molecular mass is only typical for carbohydrates. However, due to the high polarity and limited chemical stability of carbohydrates, there are only a few examples of molecular mass distribution analyses in the higher mass range. In contrast to peptides and proteins, carbohydrates are much less prone to multiply charged ion formation, which could reduce the m/z values.

By means of a SEC-ESI-MS online coupling, the mass spectra of a dextran 5,000 standard with a polydispersity of 1.6 could be successfully obtained by accumulating all spectra recorded during dextran elution [96]. Interestingly, discrete areas of the peak profile showed that dextrans of higher DP were detected as fourfold charged ions ($\Delta m/z = 40.5$), followed by $[M + 3Na]^{3+}$ with a maximum at DP22, $[M + 2Na]^{2+}$ with a maximum at DP15. In the peak maximum, single-charged $[M + Na]^+$ ions were the dominating species with a maximum for DP7 (M 1,152). Up to DP42 could be detected in the subspectra. Direct infusion of this standard provided up to triply charged ions and the highest DP detected was 26. In contrast, mass spectra obtained by MALDI ToF-MS of the spotted SEC fractions showed only single-sodiated adducts, typical for MALDI, but covered about the same mass range. Up to m/z 7,500 was detectable, but due to the high laser power required for desorption of the larger molecules, a plateau of lower m/z fragment ions was observed with increasing intensity. Similar experiments with dextran 12,000 showed fivefold charged ions in SEC-ESI-MS, and the highest m/z detected corresponded to a mass of approximately 9,500, while MALDI-MS could detect up to DP70 (molecular mass 11,358) as $[M + Na]^+$ (Fig. 7). It was also shown that sensitivity and stability can be improved by permethylation, extending the mass range to about 100,000 Da [96]. Whether the
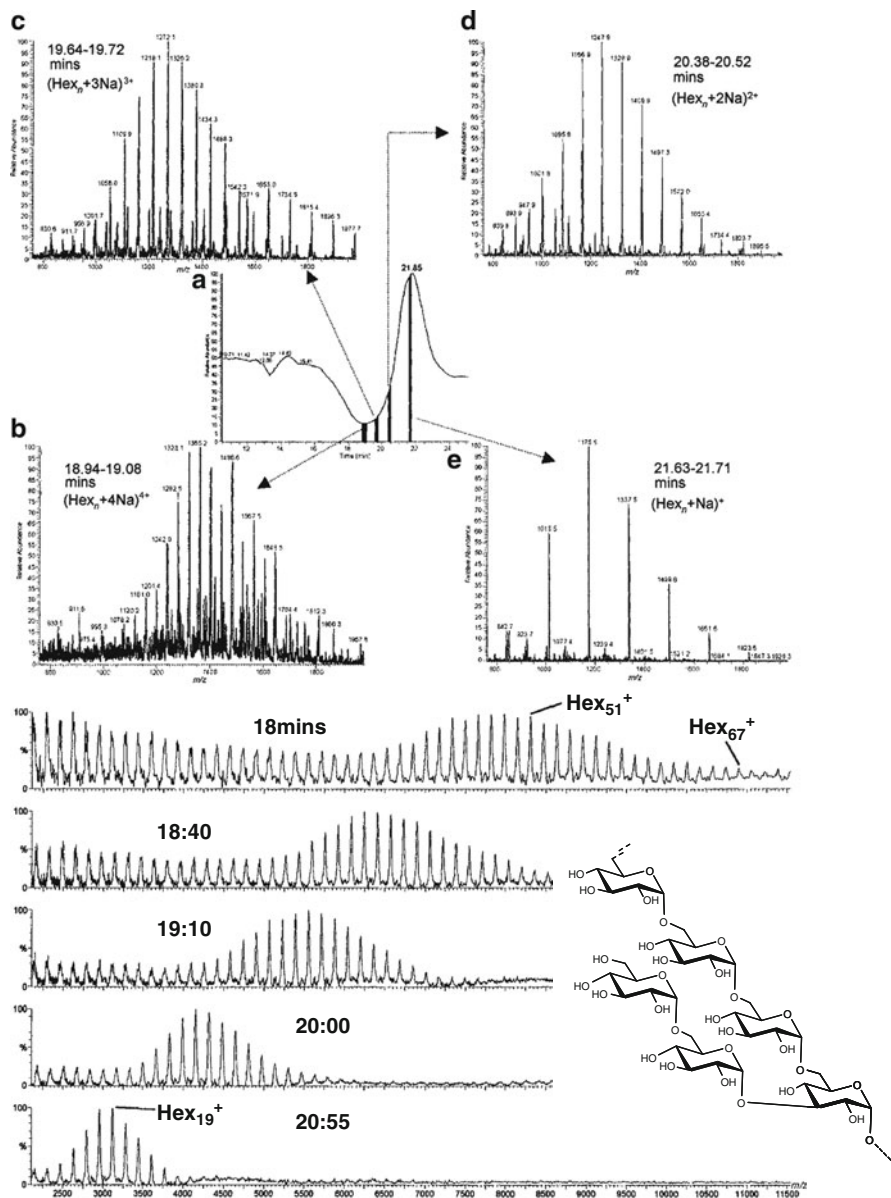
Fig. 7 *Above*: ESI TIC trace (**a**) and mass spectra of dextran 5,000 obtained by SEC-MS. Spectra were generated by summing discrete areas beneath the peak in the TIC trace at elution times of (**b**) 18.94–19.08 min, (**c**) 19.64–19.72 min, (**d**) 20.38–20.52 min, and (**e**) 21.63–21.71 min. *Below*: MALDI mass spectra obtained from manual fractionation of dextran 12,000, following SEC. Reproduced from [96] with kind permission of the publisher

correct molecular weight distribution can be matched by this approach was not proved; however, SEC-MS coupling impressively showed how pre-separation mitigates the competition of analytes in ESI between smaller and larger molecules. On average, seven glucose units complexed one sodium ion under the conditions applied, whereas MALDI leads to single-charged ions.

Since MALDI ToF-MS can cover a wider mass range, most studies in this field have been performed with MALDI. Pre-separation by gel permeation chromatography (GPC) reduces the dispersity of the fractions, which should be no larger than 1.2 to avoid border-discrimination effects [97]. With this restriction, dextran fractions with molecular mass as high as 94,000 (HPSEC-MALLS) could be analyzed (MS: $M_w = 90,000$). Enzymatic digests of hyaluronic acid were analyzed by MALDI-MS up to molecular mass of 15,000, and these data were used for calibration of the GPC system, giving much more realistic results than calibration with chemically and topologically different pullulan and dextran standards [98]. Even better results have been obtained with $2',4',6'$-trihydroxy-acetophenone (THAP) as a matrix [99]. Pullulans of molecular mass up to 47,000 could at least be detected but were no longer resolved. However, in the presence of insulin mixed with polysaccharides of similar average mass, the latter were detected with only 1/1,500 of the protein signal intensity. Degradation products were detected in all polysaccharide spectra and the molecular mass was lower than that determined by SEC. When the signal intensities were corrected for the detection efficiencies in the microchannel plate detector, which decrease with m/z due to decreasing velocity, the distribution was shifted to higher average molecular mass values, and with 10,618 Da came close to the SEC result of 12,000 Da. In contrast to proteins, a much lower matrix-to-analyte ratio was appropriate. Even at a 100:1 ratio (1 nmol/μL matrix, 0.01 nmol/μL analyte) good mass spectra were obtained. Dextrans, polysialic acid, and glycoproteins were also most successfully measured using THAP as matrix. Addition of CsI allowed recording spectra in positive ($[M + Cs]^+$) and negative ($[M + I]^-$) modes. Permethylation strongly improved the sensitivity and reduced discrimination of higher masses, probably partly due to less fragmentation and partly due to better desorption/ionization properties [98].

In 2008, Schnöll-Bitai et al. reported that a non-crystalline matrix, the ionic liquid 2,5-dihydroxybenzoic acid/butylamine (DHBB), was superior to THAP for the MALDI analysis of the molecular mass distribution of pullulans in the mass range of 5,900 to 112,000 Da [100]. Figure 8 shows the mass spectra of two pullulan standards with DHB and DHBB for comparison. $[M + BuNH_3]^+$ ions were detected, and the molecular mass and polydispersity values deviated by 10–25% from the supplier's data. The authors also developed a theory to explain why the liquid character of the matrix should reduce fragmentation compared to a less flexible solid matrix. However, the low polydispersities of ca. 1.1 of the standard samples are also a prerequisite for the comparably low discrimination effects, since narrow distributions facilitate adjustment of the laser power appropriate for all constituents.

Another example is the analysis of fructans, which are extended sucrose-based glycans consisting of 1,2- and 1,6-linked fructofuranosyl residues and various
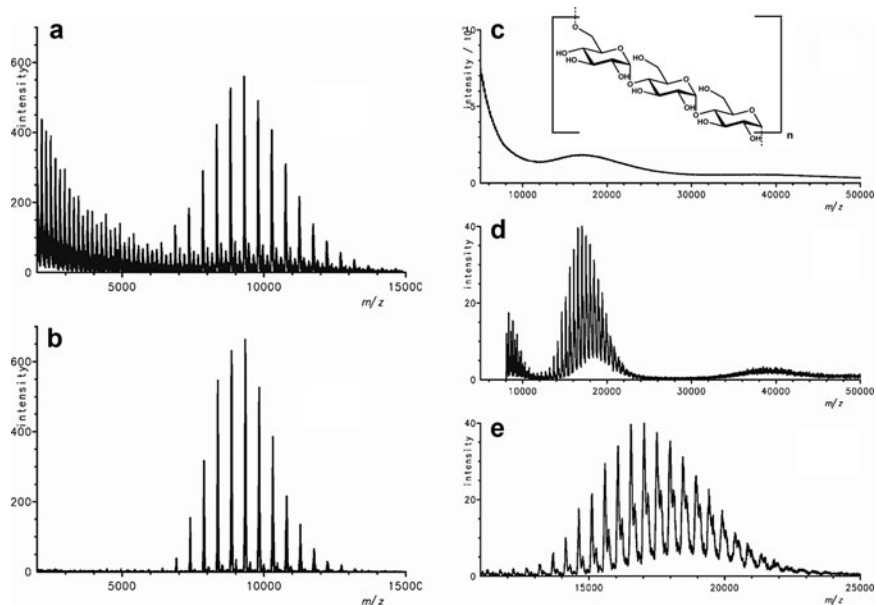
Fig. 8 MALDI-ToF mass spectra of the standard samples pullulan-11,800 (*left*) and pullulan-22,800 (*right*) measured with the matrices DHB (**a**, **c**), and DHBB (2,5-dihydroxybenzoic acid/butylamine) (**b**, **d**, **e**). **e** shows an enlarged part of the smoothed distribution given in **d**. Reproduced from [100] with kind permission of the publisher

molecular weight distributions and branching patterns [101, 102]. Typical fructan-containing plants are dahlia, chicory, artichoke, agave, and onions. Stahl et al. compared DP distributions obtained by MALDI ToF-MS and high performance anion exchange chromatography–pulsed amperometric detection (HPAEC-PAD), and could detect fructooligosaccharides in the mass range of 2,000–6,000 by both methods, while the quantitative signal profiles were different. Interestingly, cell layers of onion tissue could be placed with the matrix on the sample target, giving the same fructan signals. Molecular masses of hemicelluloses have also been analyzed by means of MALDI ToF-MS [103, 104].

4 Structure Analysis

Without any knowledge of the structure of a carbohydrate sample, the molecular weight and molecular weight distribution are of little value. While the constituents of other biopolymers, like the amino acids of proteins, differ in mass, the diversity of glycans is mainly based on isomerism. The existence of five stereocenters – four different positions of alcohol functions and the option of four- or five-membered rings (furanosyl or pyranosyl, respectively) in an aldohexose – means that, at least

theoretically, more than one million isobaric disaccharides can be formulated. Only a very small portion of these exist in nature, e.g., nine disaccharides from D-glucose, one of the 16 possible stereoisomers of aldohexoses (Fig. 9).

Therefore, besides mass profiling, it is also very important to gain insight into linkage and branching patterns, and into the sequence of oligosaccharides. Although chemical sequencing is well established for peptides and DNA, it is almost non-existent in the case of carbohydrates and has only been successful in special cases and for short sequences, e.g., by Svensson oxidation and subsequent β-elimination [105, 106]. Thus, tandem mass spectrometry is a very important and valuable technique for comprehensive structural analysis of oligosaccharides. Metastable fragment ions have been used in the case of MALDI ToF-MS PSD (post-source decay), but fragmentation is nearly non-controllable. Use of a collision cell (MALDI-CID/PSD-ToF-MS) has improved this analysis [107]. ESI coupled to a triple-quadrupole analyzer allows precursor ion selection in a first MS step, CID in the second quad, and mass analysis in the third quad. Ion traps, often used in ESI-MS instruments, can easily accumulate ions of a distinct m/z, and then be used for CID and mass analysis of fragment ions [29]. Helium is most commonly used as collision gas, and the amplitude for excitation can be controlled for efficient fragmentation. As a further important option of this technique, the process can be repeated by isolating and fragmenting daughter ions in the same manner. Thus, generations of fragment spectra can be obtained, as long as abundance of the ions is sufficient and further fragmentation energetically possible, in practice up to MS^4 or MS^5. The competing process is the dissociation of the complexed cation, which makes the carbohydrate "invisible." Nano-ESI-MS is often employed in combination with a Q-ToF (quadrupole and time-of-flight mass analyzer) (CID, as introduced by Jennings [108], or decomposition; some authors use dissociation only for the loss of the charge-giving cation: $[M + X]^+ \rightarrow M + X^+$). For details of instrument set-ups see [29].

Figure 10 summarizes the approach, including optional labeling and/or separation prior to MS and MS^n.

4.1 Fragmentation of Carbohydrates in Tandem MS for Sequencing and Determination of Linkage Pattern

To gain structural information beyond the molecular mass, tandem mass spectrometry is widely applied in glycan analysis. Fragment ions are assigned according to the nomenclature of Domon and Costello [109], who systematically described the positive and negative ions observed by FAB-CID-MS of protonated oligosaccharides (Fig. 11).

To deduce the sequence of an oligosaccharide without being misled by fragment ions of only apparently clear origin, it is very important to know the mechanisms of fragmentation and possible artifact formation. Therefore, similar to studies made
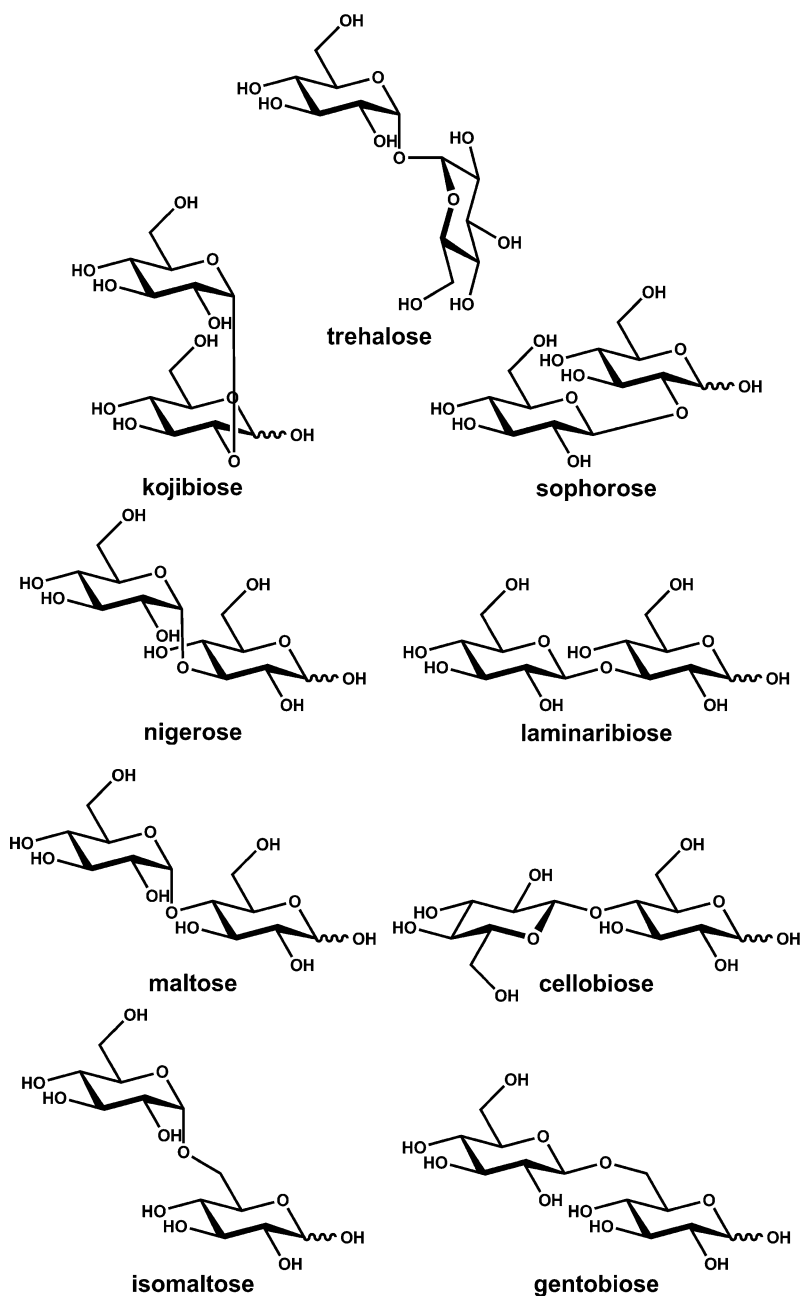
Fig. 9 Structures of nine isomeric disaccharides built from D-glucopyranose
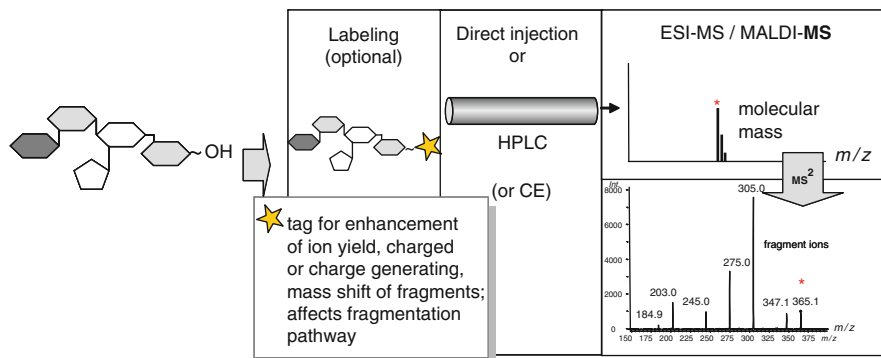
Fig. 10 Sequence analysis of oligosaccharides by (LC)-ESI-MS^n
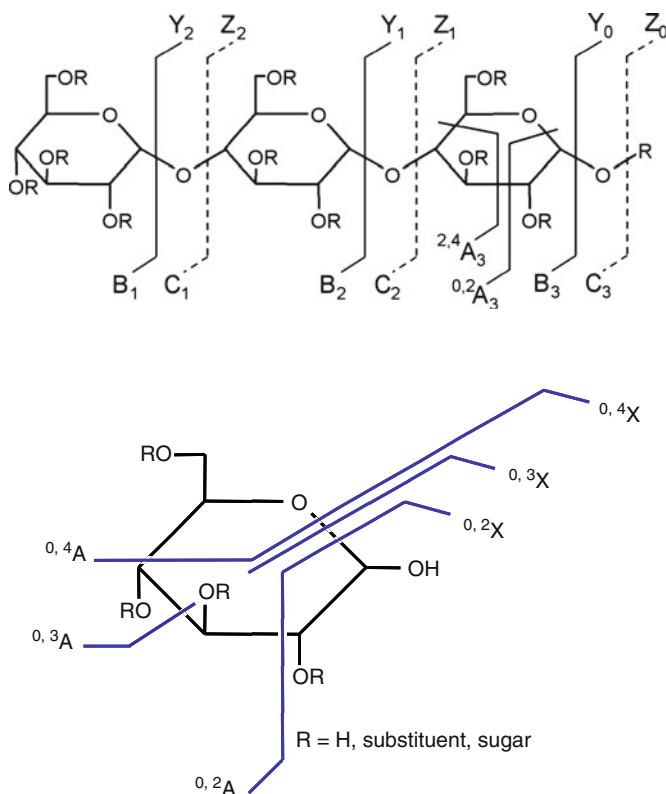
Fig. 11 Nomenclature of fragment ions according to Domon and Costello [109]

decades before for electron impact mass spectra of carbohydrate derivatives, basic studies have been performed with defined model substances for understanding the "rules" of decomposition. Although there are some generally observed fragmentation

patterns of carbohydrates, which are independent of the instrument, charge state, and individual structure (e.g., cleavage of glycosidic linkages), there are on the other hand significant differences controlled by the charge-giving group or counterion, positive or negative ion mode, chemical modification of OH groups, blocking (methyl glycoside) or labeling at the reducing end, solvent, additives, and pH. These differences are of course valuable for extending the choice of diagnostically valuable fragment ions, but at the same time they complicate matters.

4.1.1 Reducing Oligosaccharides

Protonated Oligosaccharides

Protonated oligosaccharides $[M + H]^+$ require the lowest energy for dissociation, and mainly undergo cleavage of the glycosidic linkages. Y and C ions represent protonated shorter oligosaccharides, with the Y-series comprising the reducing side of the starting compound and the C-series the non-reducing side. The complementary B and Z ions differ by 18 Da (H_2O). Differentiation of these ions, which in the case of non-derivatized homoglycans are isomeric, has been achieved by isotopic labeling at the reducing end with ^{18}O [110–112]. In accordance with the linkage stabilities, B and Y fragments usually dominate over C/Z-fragments or are even formed exclusively [113]. Usually, one glycosidic linkage is broken to yield two fragments maintaining the original sequence; however, protonated species can also undergo an "internal loss," where a proton-supported transglycosidation occurs accompanied by loss of one internal anhydroglycose [114–118]. The mechanism is probably similar to a proton-catalyzed transglycosidation, which in the gas phase requires an appropriate sequence and conformation to enable an S_N2-like reaction. For a reductively aminated trisaccharide, Harvey et al. have suggested the pathway shown in Fig. 12 [119, 120]. Although this rearrangement can cause erroneous interpretation, it has also been used to obtain additional information from the substitution patterns of internal residues of trisaccharides [121].

Adducts with Metal Cations

There are marked differences between fragment ions produced from protonated and metal cation-complexed oligosaccharides. In the case of alkali-coordinated oligosaccharides, heterolytic cleavage of the glycosidic bond is always accompanied by proton transfer, so that the part of the molecule that binds the alkali cation is detected, which means usually both parts according to the relative probabilities of retaining the cation. In addition to the B and Y ions, which dominate the positive mode mass spectra of protonated oligosaccharides, A and X fragments from cross-ring cleavages (see Fig. 11) are registered.

The stronger the cation is bound, the higher is the degree of fragmentation, e.g., Li^+ adducts form a higher diversity of fragment ions compared to Cs^+ adducts,
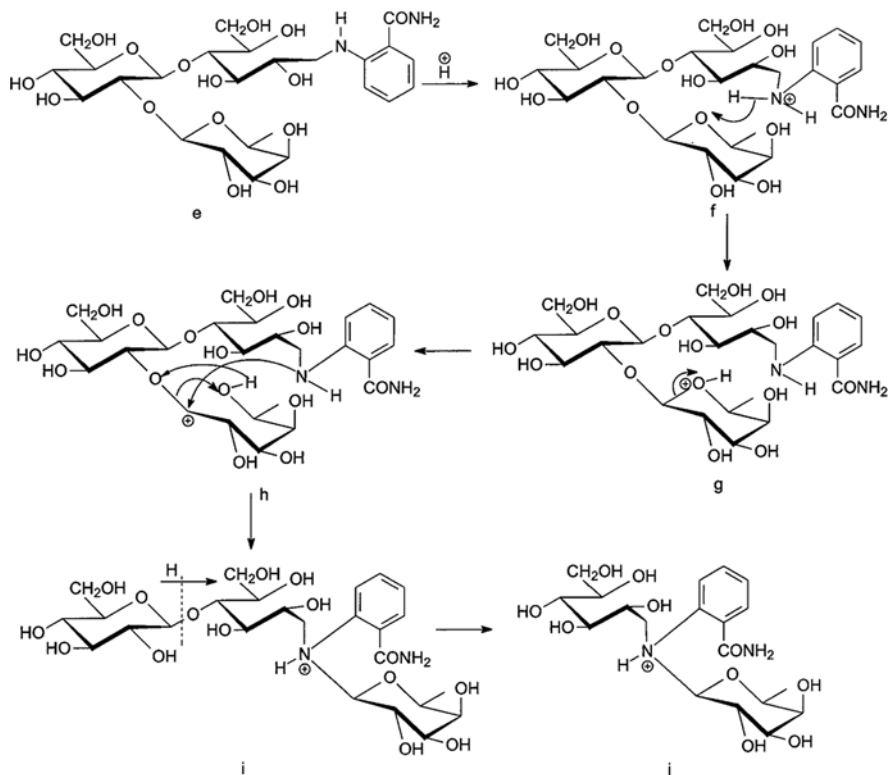
Fig. 12 Mechanism proposed by Harvey et al. for fucose migration during the fragmentation of 2-AB-derivatized 2′-fucosyl-lactose. Reproduced from [119] with kind permission of the publisher

which do not fragment but only dissociate into the carbohydrate and the Cs ion [44]. This is nicely illustrated by comparative MS measurements of a manno-glycan [(GlcNAc)$_2$(Man)$_5$] complexed with Li$^+$, Na$^+$, K$^+$, Rb$^+$, and Cs$^+$ (Fig. 13) by addition of the corresponding iodides (50 ng/µL). Decreasing binding energies of alkali metal ions with increasing size have also been shown by Cancilla et al. [122] and Botek at al. [123].

Cancilla et al. [124] studied the coordination of chitobiose and chitotriose with various alkali metal cations and found decreasing binding with increasing size of the ions. K$^+$ becomes bound more efficiently when extending the di- to the trisaccharide, a phenomenon that has also been observed for inulin, where potassium adducts become increasingly favored over sodium adducts with growing DP. Molecular modeling indicated preferred coordination of the cation by the oxygens of the glycosidic linkage, O-3, O-5′, and O-6′. (Fig. 14) [124]. The results of this study suggest that glycosidic bond cleavages are charge-induced whereas cross-ring cleavages are charge-remote processes. Adams et al. reported fundamental studies of charge-remote fragmentations [125].
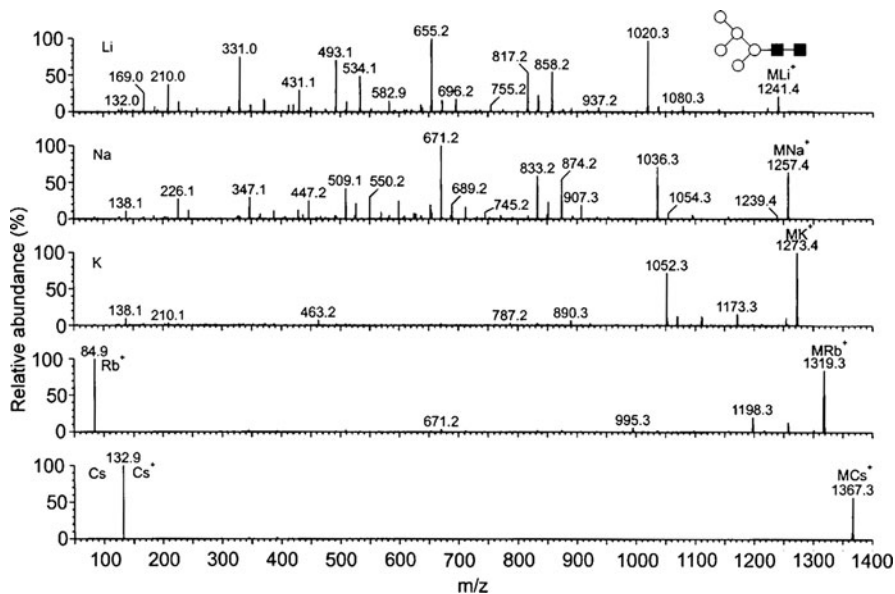
Fig. 13 Comparative ESI-CID-QToF MS measurements of a manno-glycan [(GlcNAc)$_2$(Man)$_5$] complexed with Li$^+$, Na$^+$, K$^+$, Rb$^+$, and Cs$^+$ (from *top* to *bottom*). Reproduced from [44] with kind permission of the publisher

Thus, the most commonly observed [M + Na]$^+$ adducts of reducing oligosaccharides undergo additional cross-ring cleavages, requiring the rupture of two linkages. Depending on which side retains the charge, additional A or X fragments are observed. Since most of these fragmentations start from the reducing end, eliminating small neutral molecules, the A-type are usually favored over X-type ions. The larger fragment has (at comparable chemical structure) the greater affinity to maintain the alkali cation. However, ^{1,5}X ions, which correspond to Y_i fragments bearing C1, and ring oxygen of the next sugar residue ($m/z = Y + 28$) were observed by CID with air as collision gas at 1–2 kV for malto-, manno- and dextranoligosaccharides (MALDI-ToF/ToF-MS) [126]. Primary fragments of sufficient energy undergo further fragmentation. Therefore, many ions are the result of further successive losses. This can be proved by MS^n experiments and has to be considered in the interpretation, e.g., A_i ions formed from Y_j fragment ions only give redundant information, since they all represent the same original reducing end.

The mechanisms of fragmentation have been studied by Hofmeister et al. using isotope-labeled (^{18}O, ^{2}H) model compounds, representing all α- and β-linked positional isomers of disaccharides (see Fig. 9) [41], and were found to follow a retro-aldol cleavage of the ring-opened aldehyde form (Fig. 15). Since a new carbonyl group is formed in this ^{0,2}A-fragmentation (including linkage 0 and 2 of the sugar ring, starting with numbering of linkages with 0 for O-5–C-1, proceeding clockwise), a second retro-aldol reaction can occur in an aldohexose. This reaction splits off $C_2H_4O_2$ (M-60-60) again, yielding ^{2,4}A$_n$. ^{0,3}A-cleavages (M-90) can be
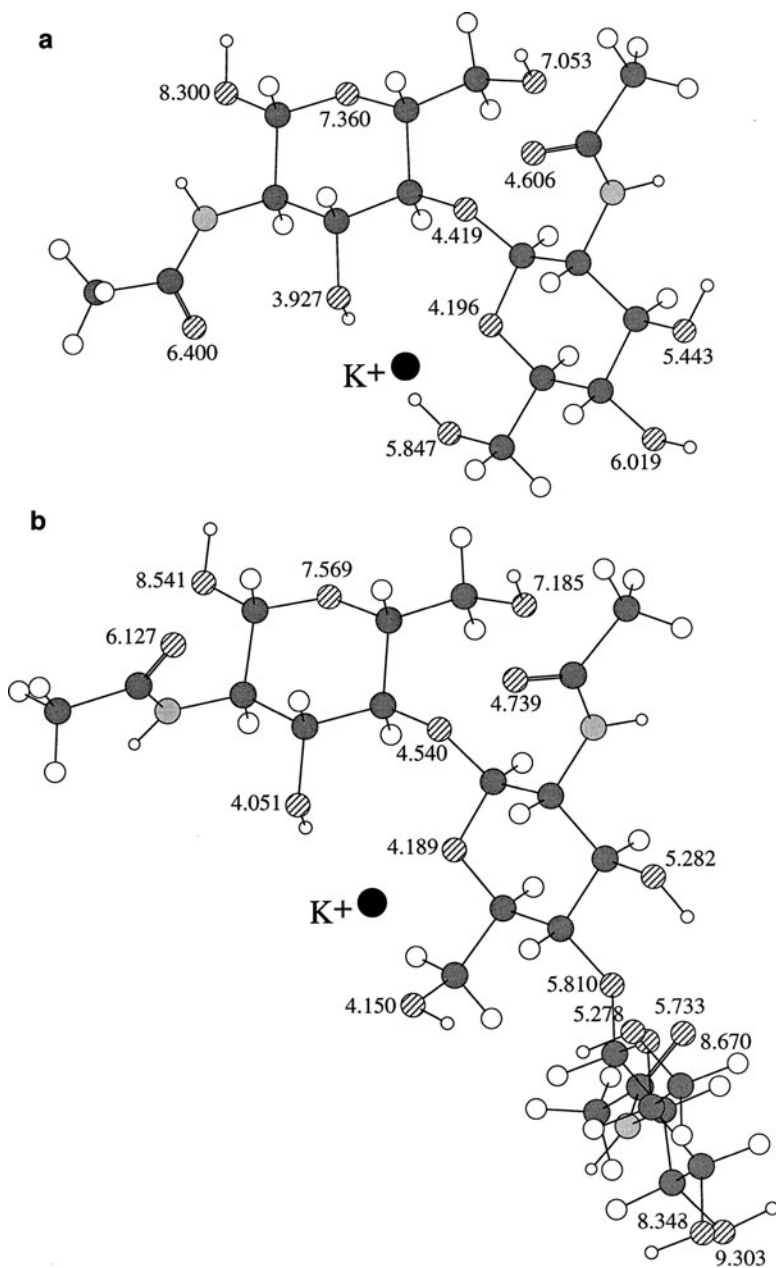
Fig. 14 Coordination of K^+ to chitobiose and chitotriose. Average K^+–O distance is 5.779 Å for chitobiose and 6.220 Å for chitotriose.Reproduced from [124] with kind permission of the publisher
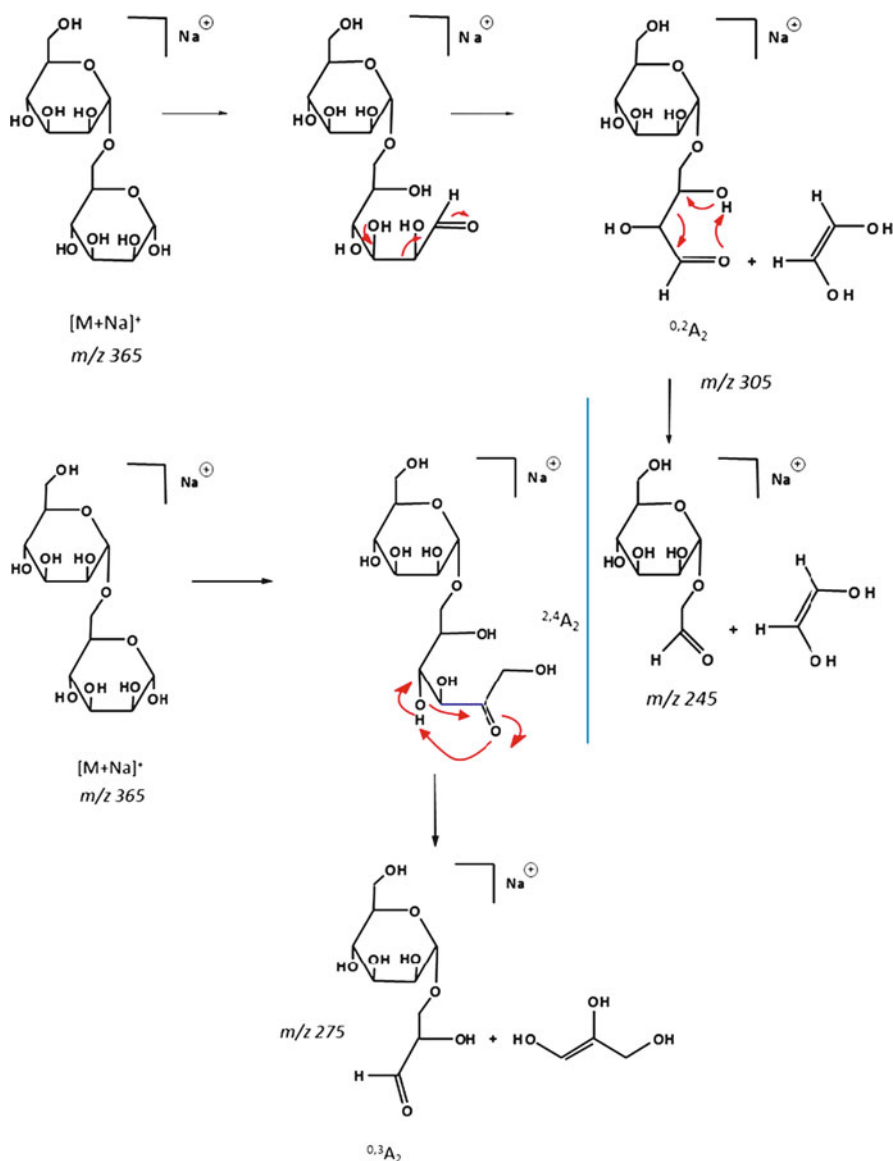
Fig. 15 Fragmentation pathways for a 1,6-linked disaccharide (isomaltose) by subsequent retro-aldol cleavages (^{0,2}A, ^{2,4}A) or after tautomerization to the ketosugar (^{0,3}A); according to Hofmeister [41]

rationalized by a preceding tautomerization to the 2-keto form. Further tauto-merization to the 3-keto isomer could then lead to a precursor for direct formation of ^{2,4}A$_n$. Another plausible retro-ene mechanism for the formation of ^{0,2}A$_n$ [127] has not been confirmed by isotopic labeling studies [41].

Whether these cleavages are observed in the tandem mass spectra depends on the availability of the involved OH group. If this is blocked by other sugars or by substituents, then cleavage is inhibited. Thus, the pattern of fragment ions is of high diagnostic value for the elucidation of linkage positions: M-120 is observed for 1,2-linked aldohexose disaccharides ($^{0,2}X_2$), M-90 for 1,3-linked ($^{0,3}X_2$), a loss of 60 ($^{0,2}A_2$) and 120 u ($^{2,4}A_2$) for 1,4-linked, and of 60, 90 and 120 u for 1,6-linked positional isomers. For pentoses the corresponding fragmentations can be deduced.

Figure 16 shows the ESI-CID mass spectra of the isomeric disaccharides sophorose (glc-β-1,2-glc) and gentiobiose (glc-β-1,6-glc).

Although all mentioned fragmentations can be observed for the 1,6-linked disaccharides, substitution of 2-OH in sophorose only allows the 0,2-cleavage. However, since the second glucosyl residue is linked to the C1-C2-fragment, formally a $^{0,2}X$- instead of the $^{0,2}A$-fragment is observed. Apart from B and Y ions, elimination of water (M-18) and probably formaldehyde (M-30) are observed.

In a similar way, the position of non-sugar substituents can be deduced from shifts in the daughter mass spectra, as will be outlined later (Sects. 5.1 and 6.3) [128–132].

If the molecule is branched, it is usually difficult to differentiate between sugar residue losses of the different branches. The branches are assigned Greek letters α, β, and γ in order of decreasing molecular weight [109], whereas ions resulting from cleavage of the core unit are not designated a Greek letter. The numbering continues in parallel into the branches ("antennae" in the case of glycoconjugates).

In 2004, Garozzo et al. reported on three new fragment ions in the MALDI-ToF/ToF-tandem mass spectra of sodiated ions of well-known human milk oligosaccharides, and suggested a pathway for their formation involving a six-member-ring rearrangement [5]. These fragments were also of high diagnostic value since they allowed the discrimination of linkage positions. These unexpected ions, assigned E, F, and G, are illustrated in Fig. 17.

Each of the ions represents disproportionations of the mother ion since a lactone and a deoxysugar, or an oxo-sugar and an anhydroalditol, are formed from the two aldehydes constituting the disaccharides. All fragmentations are accompanied by additional elimination of HX (HX = ROH or H_2O or NH_2Ac) from position 2 or 4 of the later observed fragment ion. Surprisingly, only the reduced products, but never the oxidized counterparts are observed in the mass spectra. There is no information on whether these structures and mechanisms have been made likely by isotopic labeling studies. But, independent of the pathway, F and G ions are indicative of a glycosyl unit β-linked to the neighboring 3-position, while E was observed for β-1,4-linkages to glucose. It should be kept in mind that these fragments were observed in higher energy MALDI-ToF/ToF-MS/MS experiments, and not in MALDI-PSD mass spectra. Usually, there is no fundamental difference in the fragmentation routes observed by the various tandem MS methods, but only an influence on the extent of fragmentation due to the different energies.

Negative Ions

As described above, negative ions of carbohydrates are obtained with high abundance if appropriate counterions like nitrate or dihydrogenphosphate are added.
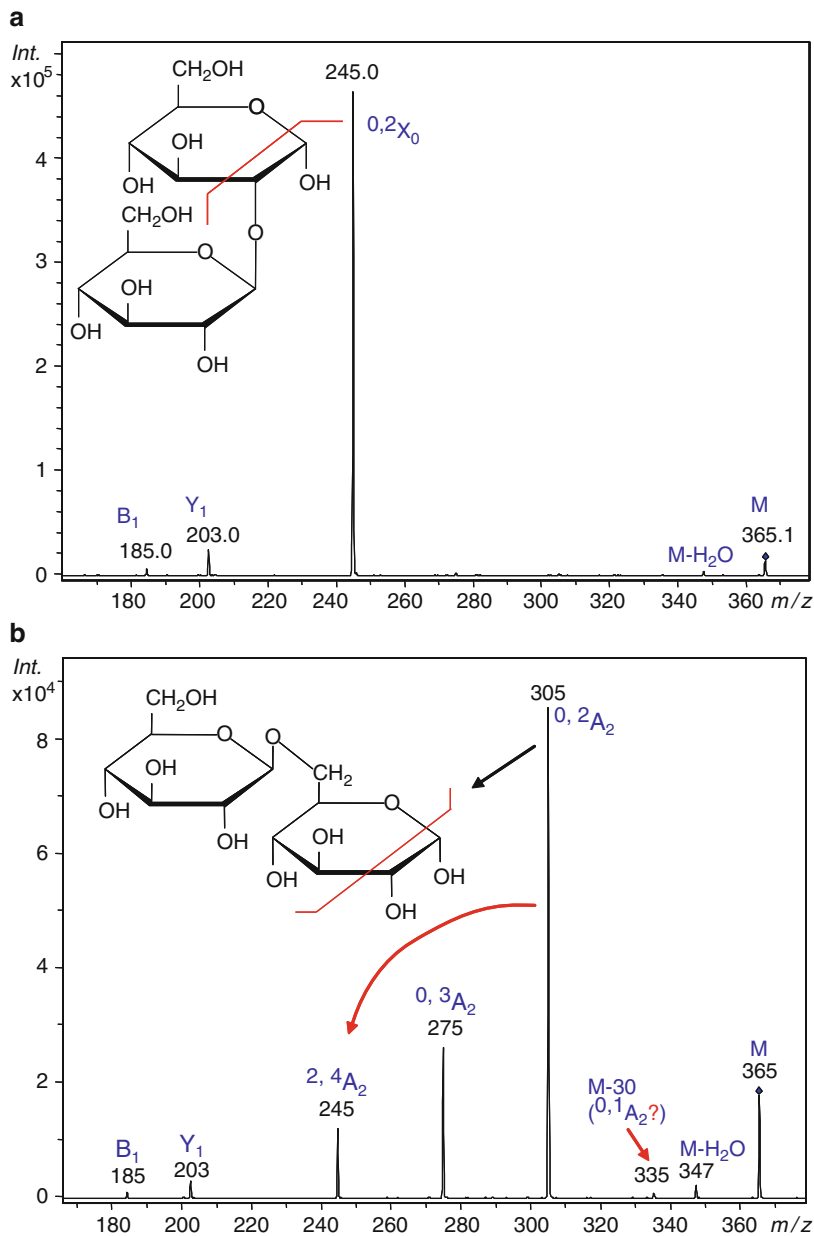
Fig. 16 ESI-CID-MS of sophorose (**a**) and gentiobiose (**b**)

Since elimination of the corresponding acid HY is the first fragmentation step, tandem mass spectra of these $[M + Y]^-$ adducts do not differ significantly from those of the deprotonated oligosaccharides. Principally, negative ions can form the same fragments as positive ions (A, B, C, X, Y, Z), but due to the negative charge as a driving force, other pathways are favored. The negative charge is assumed to be
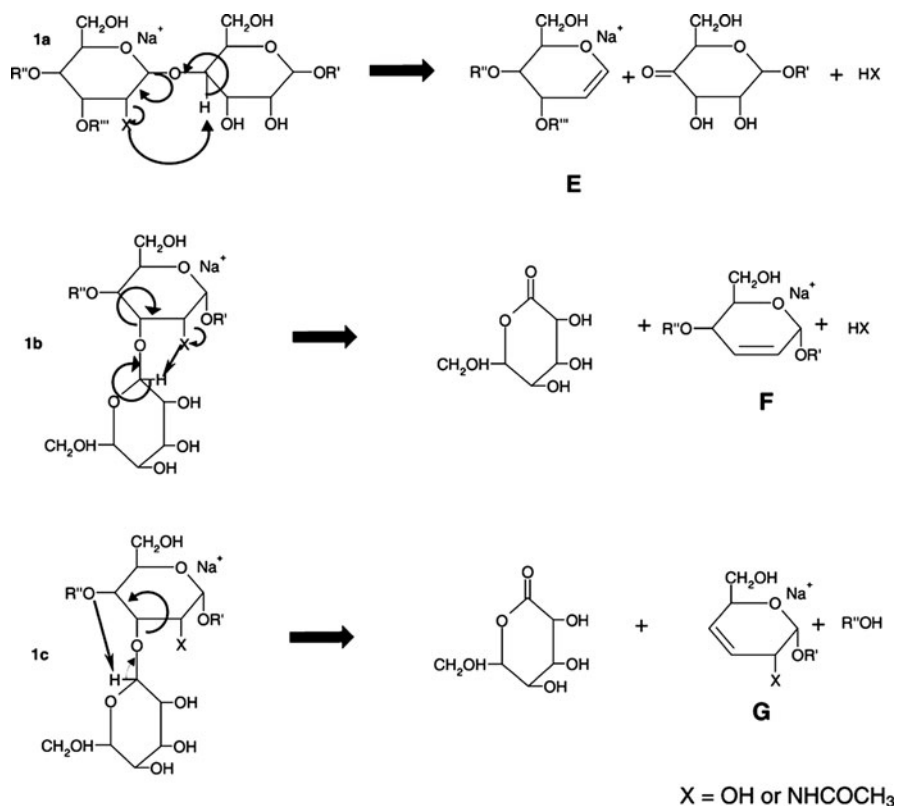
Fig. 17 Formation of E, F and G fragment ions as proposed by Spina et al. F ions are indicative of a 1,3-linkage. Reproduced from [5] with kind permission of the publisher

located at the most acidic position, which often is the hemiacetal function. Thus, the anion formed corresponds to a C_n ion (n = number glycosyl units), which induces consecutive C-type fragmentation probably by electron pair shifts. From the anomeric anion, alcoholates (RO^-) can be pushed out from the 3- and 6-position, while for 4-linked glycosides the negative charge must be located at O-2. Due to this charge-controlled fragmentation, MS^n spectra of deprotonated oligosaccharides can be read "from right to left" and are therefore of high interpretive value, which has been explicitly outlined by Harvey [53–56]. Pfenninger et al. have successfully studied and applied this procedure to human milk oligosaccharides, which have essential biological functions [1, 2]. An example is given in Fig. 18.

4.1.2 Non-Reducing Oligosaccharides

Methyl Glycosides

If the carbohydrate is permethylated or obtained by partial methanolysis from a polysaccharide, the reducing end is blocked. For these methyl glycosides, no
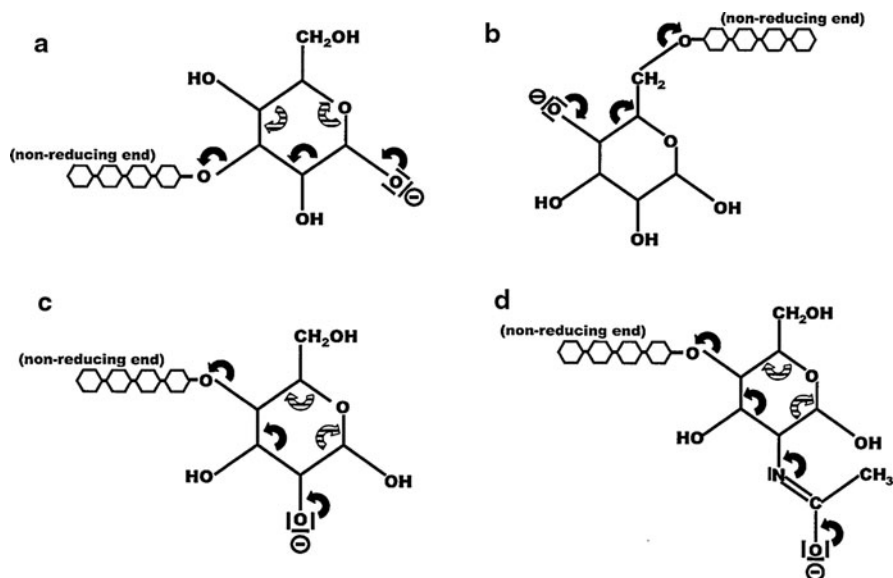
Fig. 18 Consecutive C-type fragmentation of deprotonated oligosaccharides (negative mode) as proposed by Pfenninger et al. [1]; two alternative mechanisms (*black* and *striped arrows*) are shown. Cleavage for 1,3- (**a**), 1,6- (**b**), 1,4-linked hexopyranosides (**c**), and a 4-linked 2-deoxy-*N*-acetylhexosamine (**d**) are shown. Reproduced from [1] with kind permission of the publisher
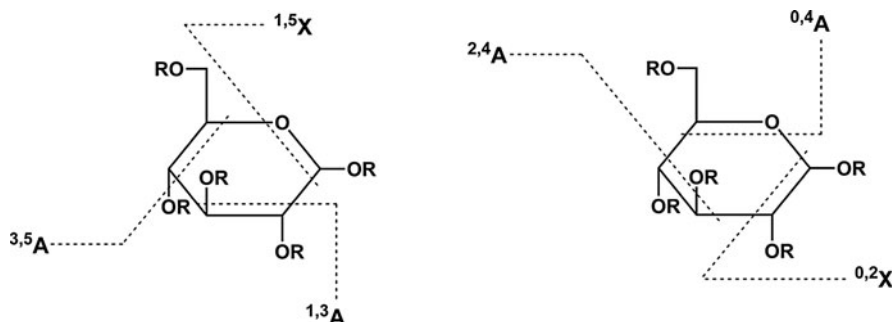
Fig. 19 Proposed pathways for cross-ring cleavages in permethylated oligosaccharides, according to Lemoine et al. [133]

retro-aldol cleavages occur, which is also obvious from the tandem mass spectrum of the non-reducing disaccharide trehalose (structure shown in Fig. 9) [41].

Depending on the collision energy and the gas used, different cross-ring cleavage ions are observed: ^{1,3}A, ^{3,5}A, and ^{1,5}X (Fig. 19, left) [133]. These are formed by charge-remote fragmentation processes at high collision energies and are much more favored if the heavier argon is used rather than helium. At low collision energies, only the more labile glycosidic linkages are cleaved. At 4 kV, pronounced

cross-ring cleavages are observed. Depending on the linkage and branching positions, in addition to the mentioned ^{1,3}A, ^{3,5}A, and ^{1,5}X ions, ^{0,4}A, ^{2,4}A, and ^{0,2}X fragments could be observed (Fig. 19, right). ^{1,5}X ions allow the differentiation of Y and C ions, since they are always related to Y ions with m/z (^{1,5}X$_i$) $= m/z$ (Y$_i$ + 28) [107, 134]. Permethylated oligosaccharides fragmented with argon at high collision energy also showed W ions from C5–C6-cleavages, maintaining the charge on the "right" end of the oligosaccharide and being diagnostic for 1,6-glyclosidic linkages.

Sequencing of Permethylated Carbohydrates

Reinhold and coworkers have thoroughly studied the fragmentation behavior of per-O-methylated di- and higher oligosaccharides comprising various linkage positions and stereochemistry of the hexapyranosyl monomer units (Glc, Gal, Man) [135, 136]. Although Y-type ions are more abundant, they focused on the B-type ions from glycosidic linkage cleavage, which are more informative. The consequence of substitution of hydroxyl group in these permethylated compounds is a proton transfer from C-2 instead of 2-OH to the cleaved part of the glycan. The C $=$ C double bond formed induces a retro-Diels–Alder (RDA) reaction, resulting in a ^{3,5}A fragment ion (Fig. 20). Abundance of these ions strongly depends on the stereochemistry of the pyranose involved. Since, with respect to the dienophile, the Diels–Alder reaction is stereospecifically *syn*, reaction is favored for galactose, which yields *cis*-1,3-dimethoxypropene whereas glucose and mannose derivatives give the *trans*-isomer. The differences in MS^n spectra are reproducible and the relative intensities of various fragments relate to the stereochemistry [136]. Figure 21 illustrates how the different free and permethylated B$_2$ ions obtained from reduced maltotriose undergo further disassembly. Depending on the location of the linked sugar residue, further cross-ring cleavages were observed, probably also the result of RDA reaction after isomerization of the double bond. Comprehensive studies of permethylated oligosaccharide standard compounds resulted in a spectral library, which allows the facile evaluation of structural details including interresidue linkage, monomer identification, anomeric configuration, and branching [137]. An algorithm was developed for this congruent strategy for carbohydrate sequencing [138], requiring up to MS^5 measurements, thus in principle achieving a gas-phase separation of isomer-derived fragments. Based on the knowledge of precursor–product relationships, the individual structures can be deduced [139]. Recently this new tool resulted in a patent [140].

A similar approach has been applied by Mischnick and coworkers for the analysis of isomeric mixtures of partially methylated disaccharides. Also without chromatographic preseparation, the qualitative and quantitative composition of these isomeric mixtures were evaluated from the MS^2 and MS^3 spectra as outlined in Sect. 5.1 [130]. Elucidation was based on the knowledge of the fragmentation pathways of isotope-labeled O-methylated but reducing di- and trisaccharides [131].

Fig. 20 (**a**) Retro-Diels–Alder CID fragmentation of B-type ions from permethylated oligosaccharides. (**b**) Further generic cross-ring cleavages observed for B ions of regioisomeric oligosaccharides (*R* mono- or oligosaccharide substituent). Reproduced from [136] with kind permission of the publisher
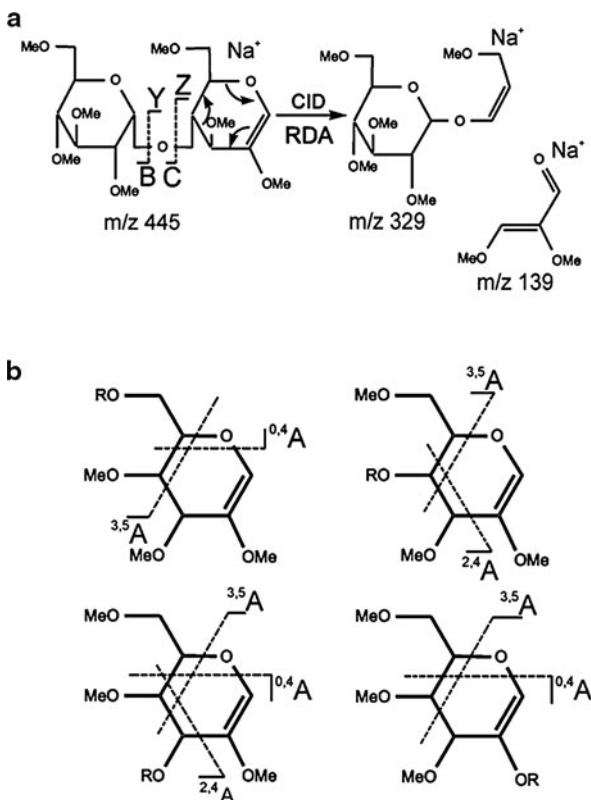
Labeled Compounds

Labeling of the oligosaccharide at the reducing end as described above (Sect. 2.2) can influence the fragmentation behavior differently. It causes a mass shift of Y and Z fragments and thus allows them to be distinguished from the corresponding C and B ions comprising the non-reducing end. In the positive ion mode, these analytes can be protonated due to the basic amino group introduced by reductive amination, but are often sodiated. The label can contain further nitrogen groups, which strongly favors the location of the charge at the tag. Labeling reagents with quaternary ammonium groups like Girard's T or acidic labels like the sulfonic acid reagents ANTS and APTS or AA fix the charge side. This can be advantageous for a straightforward interpretation of the tandem mass spectra with respect to sequence.

However, the observed fragment pattern again strongly depends on whether the molecule is protonated or sodiated. In $[M + H]^+$ of cellooligosaccharides reductively aminated with dimethylamine, the proton is located at the amino group and, consequently, a ladder of Y_i ions ($i = 1, 2, 3 \ldots n$) are detected. In contrast, tandem MS of $[M + Na]^+$ of the same analyte shows daughter ions from cross-ring cleavages, thus indicating that the sodium is (de)located at the carbohydrate
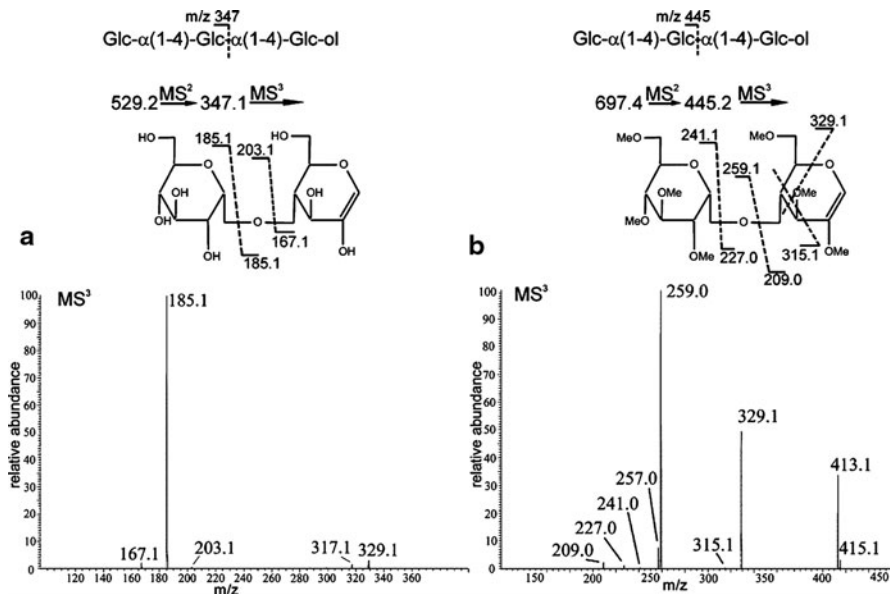
Fig. 21 ESI-MS^3 spectra of B$_2$ ions obtained by MS^2 from (**a**) native and (**b**) *O*-methylated maltotriositol. Reproduced from [136] with kind permission of the publisher

chain, and that the larger aglycon (amino-deoxy-alditol compared to methyl) can be cleaved off (Fig. 22).

These fragments can be separated by one of the various methods mentioned. Although MALDI-MS is very appropriate for profiling the molecular masses of the oligosaccharides in the digest, ESI-MS^n was superior to MALDI-ToF-MS-PSD for unambiguous sequence analysis due to the applicability of MS^3 and MS^4 where MS^2 did not give sufficient structure information. An example of the ESI-MS^2 of a xyloglucan oligomer that contains additional fucosyl-*O*-acetyl-galactose in the side chain is given in Sect. 4.2.1.

Consequently, a free carbonyl side chain is generated, enabling retro-aldol cleavages as outlined above (Fig. 15), for example C$_3$ at *m/z* 527, giving *m/z* 467 and 407, or C$_2$ *m/z* 365 yielding *m/z* 305 and 245, due to the 1,4-linkage. The formation of C fragments has been proved for ^{13}C-cellotriose labeled with dimethylamine [128]. In addition to Y fragments, Y* ions with a Δ*m/z* of 45 are observed at even higher abundance, corresponding to a loss of dimethylamine.

In a comprehensive study, Harvey introduced various tags by reductive amination in a high mannose glycan, and compared the relative ion intensities in ESI-Q-ToF and MALDI ToF-MS (positive ion mode), as well as the fragmentation behavior of the products [60]. There was nearly no difference in the MS^2 spectra for aminobenzoic acid, aminopyridine, and aminoquinoline derivatives, since the label was lost in the primary fragmentation step, indicating that the sodium ion is more probably coordinated to the carbohydrate part (Fig. 23) [60]. Fragmentation differed slightly for aminoacridone and *p*-amino-*N*-(2-diethylaminoethyl)benzamide.
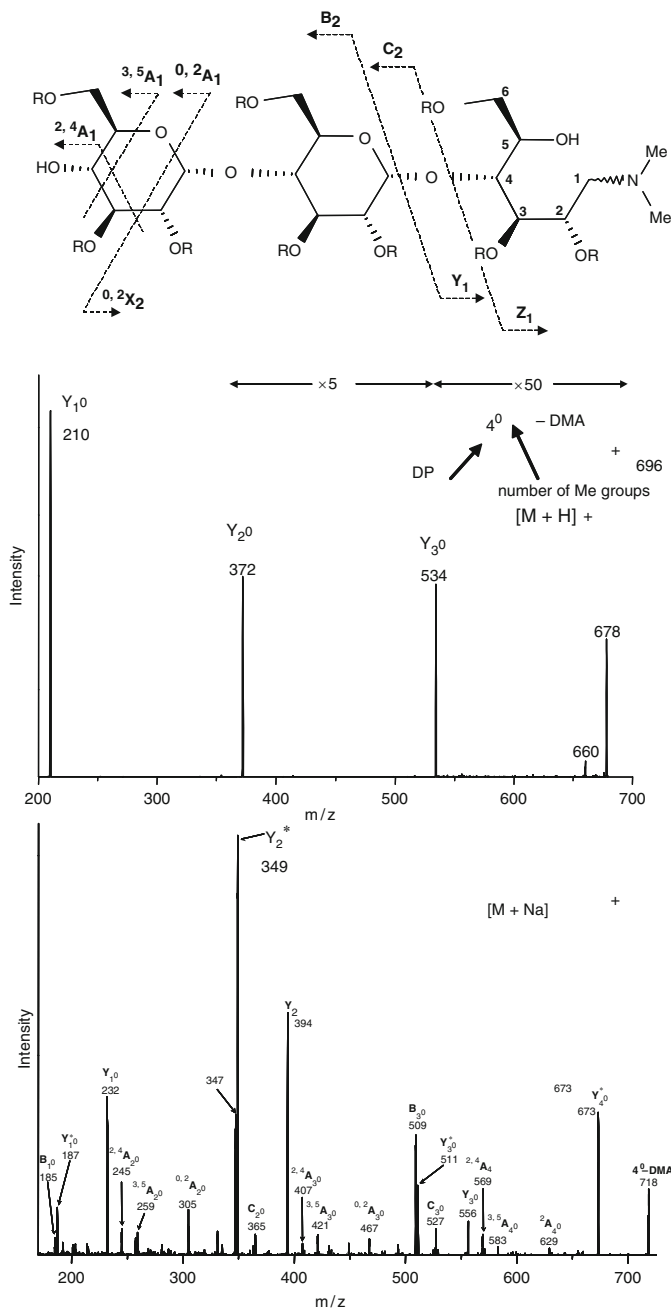
Fig. 22 *Above*: cellotetraose, reductively aminated with dimethylamine (*DMA*). *Below*: ESI CID-MS showing comparison of [M + H]⁺ and [M + Na]⁺ fragmentation. Reproduced from [128] with kind permission of the publisher
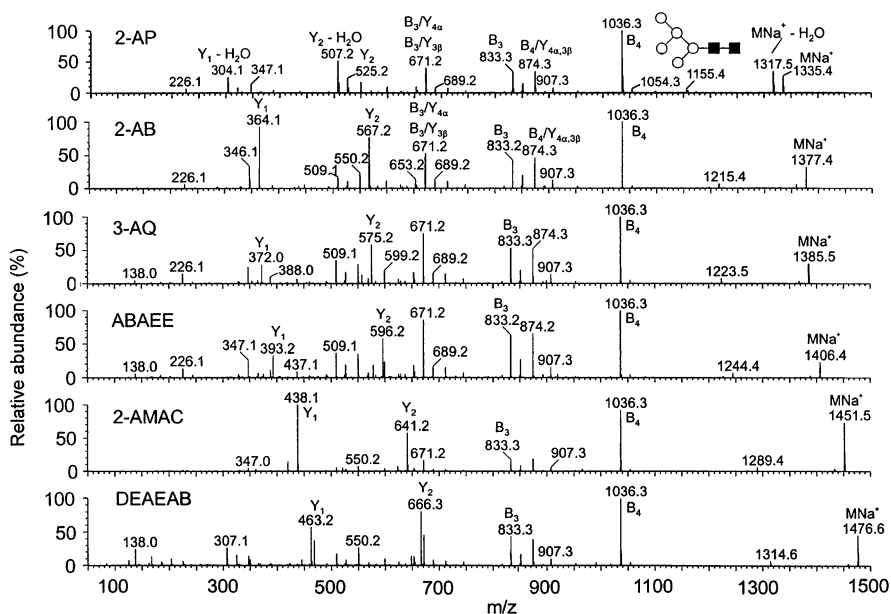
Fig. 23 ESI CID-MS of $[M + Na]^+$ from six derivatives of $(GlcNAc)_2(Man)_5$ obtained by reductive amination with various amines (for abbreviations and formula see Table 1). Reproduced from [60] with kind permission of the publisher. ABAEE = amino-benzoic acid ethyl ester

Negative Ions

Gennaro et al. detected ANTS-derivatized maltooligosaccharides after ion pair reversed phase (RP)-HPLC (NEt_3H^+ as counter ion) as doubly charged ions (two of three SO_3H were dissociated). Under CID conditions, SO_3 is first eliminated, followed by nearly exclusive formation of a "ladder" of Y_i^{2-} fragment ion. (Fig. 24) [88]. Intensity is reported to be enhanced by a factor of 20 for Glc_7-ANTS compared to Glc_7.

Amination without reduction has also been recommended, using *p*-amino-benzoic acid ethyl ester [141]. Instead of the aminodeoxyalditol, an aminosugar is formed because the imine formed from the aldehyde and the amine is "trapped" by aminal formation (see Girard's T labeling in Fig. 5), which is also performed without reduction and yields the β-*N*-glycoside ("closed-ring labeling"). However, this approach requires the reagent in high excess and subsequent purification. About 0.01–10 nmol of substrate was applied for syringe pump injection. Negative ions were studied and behaved similarly to $[M-H]^-$ of unlabeled oligosaccharides, "pushing out" a series of subsequent C ions as described by Pfenninger et al. for negative ion ESI QIT-MS of milk oligosaccharides [1]. Some additional fragments of diagnostic value with respect to the linkage position were detected for these labeled nonreduced compounds. Fragments comprising the labeled end of an oligosaccharide resembled the behavior of corresponding disaccharide derivatives, while fragment
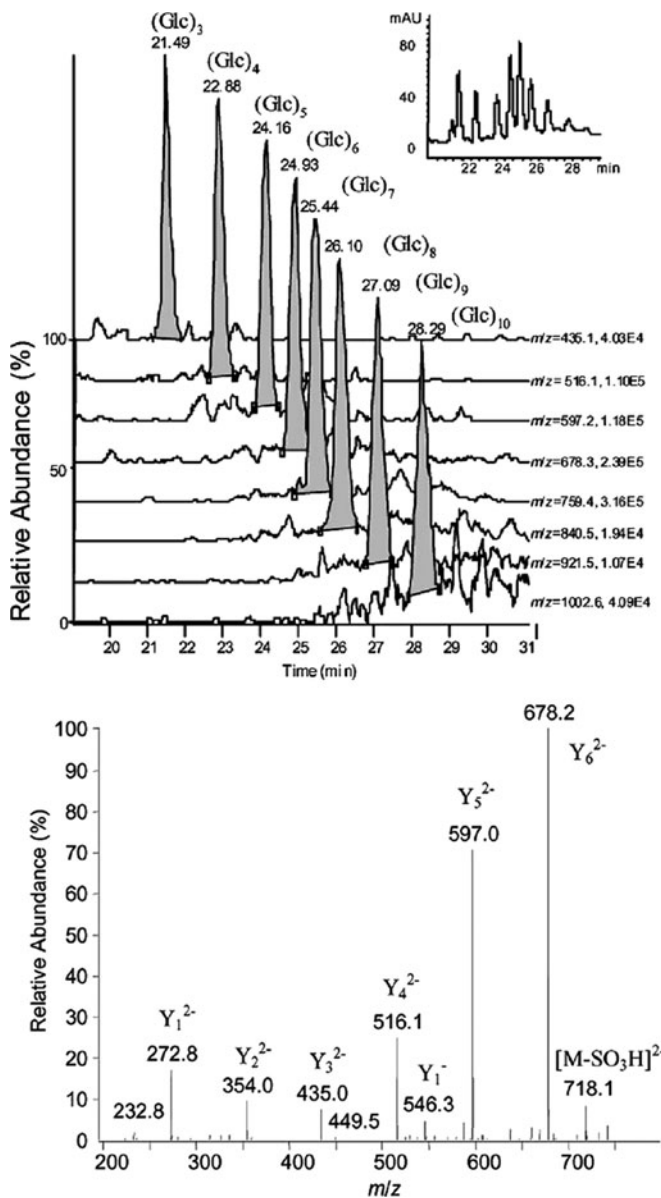
Fig. 24 ANTS-derivatized (8-aminonaphthalene-1,3,6-tri-sulfonic acid) maltooligosaccharides analyzed by LC-ESI-MS. *Above*: Selective ion current chromatogram. *Below*: CID-MS (negative mode) of DP7 (*m/z* 759.4) giving a ladder of Y^{2-} ions after elimination of one sulfonic acid. Reproduced from [88] with kind permission of the publisher

ions involving the other end of the molecule were similar to those of the unlabeled analog. The presence of 2-amino-2-deoxy sugars favored C/Z fragmentation and cross-ring cleavage. Elimination of ROH from position 3 is also favored by 2-amino-2-deoxy sugars [141].

4.2 Applications in Structural Analysis

Literature on structural analysis of carbohydrates by mass spectrometry mainly deals with *O*- and *N*-linked glycans after release from biologically active glycoproteins, and also, but less often, with bacterial lipopolysaccharides and polysaccharides derived from microbes or plants. Human milk oligosaccharides have been extensively studied [1, 2, 5]. The ratio of the comprised sugars, their linkage positions and branching pattern, sequence, and stereochemistry need to be elucidated. Molecular mass and molecular mass distribution, and non-sugar substituents and their location or pattern within the carbohydrate backbone are additional structural features that have to be studied.

What can mass spectrometry contribute to this field? With the "soft" ionization methods ESI and MALDI, information on molecular mass can be obtained at least in a qualitative manner and, as outlined in Sect. 3, limited to a certain mass range and with higher sensitivity and accuracy if coupled with SEC separation.

Substituents can be recognized by the mass shifts they produce. Sequence and linkage positions can be deduced from tandem mass spectra, although it is not generally possible to deduce them unambiguously, especially in complex branched structures. Isotopic labeling, periodate oxidation, or other chemical modifications have been applied in sample preparation for MS analysis to increase the specificity of structure information [43]. Stereochemistry of glycosidic linkages as well as ring size is still mainly deduced from NMR spectra or enzymatic digestibility. Sugar constituents are determined by various chromatographic or electrophoretic methods after hydrolysis of glycosidic linkages, but Reinhold et al. and Leary et al. have demonstrated that even the stereochemistry of isobaric sugar units can be differentiated from their tandem mass spectra if permethylated oligosaccharides are fragmented (Fig. 21) [136–140], or if certain complex-forming additives are applied that are sensitive to the stereochemistry and cause distinct intensity differences in the daughter mass spectra (Fig. 3) [47–49, 142, 143].

Progress in the field of glycobiology has been widely reviewed [7–16] and shall therefore not be outlined in this article. Structural analysis of cell wall polysaccharides or exopolysaccharides from microbes involves special demands, which are different from the popular *O*- and *N*-glycan area. The decisive difference is their dispersity with respect to molecular mass, composition, and branching pattern. Separation into molecularly uniform fractions is no longer possible. Mixtures have to be dealt with and averaged data like relative ratios of sugar constituents, average degree of branching, or average length of certain sequences of side chains have to be determined. Qualitatively, the existence of certain

structural features can be deduced by MS^n methods. Naturally, pretreatment by enzymatic, chemical, and/or separation methods specifies structural information and thus improves the resolution of the final image. This will be demonstrated by a few examples, emphasizing the contribution of mass spectrometry to this area of structure elucidation.

4.2.1 Plant Polysaccharides

Arabinoxylans

Arabinoxylans and arabinogalactans are widespread in plants. Arbinoxylans represent the main so-called hemicelluloses of cereals. They consist of β-1,4-linked xylopyranosyl residues (Xyl*p*, X) with arabinofuranosyl residues (Ara*f*, A) attached to O-2 or O-3 of the xylan backbone (Fig. 25). Other xylans also contain some glucuronic acid and galactose in the side chains. Fractions from acid- and enzyme-hydrolyzed arabinoxylans have been analyzed by SEC-ESI-MS. Thus, fractions eluting in the same mass range, but of different hydrodynamic volume due to different chemical composition (acidic or neutral), could be distinguished. Subsequent fragmentation by CID up to MS^3 gave additional sequence information [95].

For the analysis of the microheterogeneity, Roepstorff et al. [144–146] studied arabinoxylooligosaccharides (AX) up to DP5 derived by enzymatic digestion with endoxylanase prior to and after permethylation by ESI QToF-MS^n. Fragment ions at M-60 ($^{0,2}A_n$) and M-90 ($^{2,4}A_n$) indicated the 1,4-linkage of the pentosan backbone; however, due to the isobaric character of Xyl and Ara, branching patterns could not be deduced directly. After permethylation, mainly B and Y fragments were obtained, but $^{1,5}X$ fragments (corresponding to 4-*O*-formyl derivatives; see Fig. 19) and $^{2,4}A$ and $^{3,5}A$ ions were also formed (Fig. 26) [83, 145]. Further fragmentation (MS^3) of isobaric mixtures of B and Y fragments allowed differentiating branching patterns since the detectable number of methyl groups of a pentosyl unit corresponds to the linkage or branching pattern. However, CID measurements up to MS^4 were required to distinguish positions of Ara linkages unequivocally, while also taking into account information from methylation analysis and NMR spectroscopy [146].
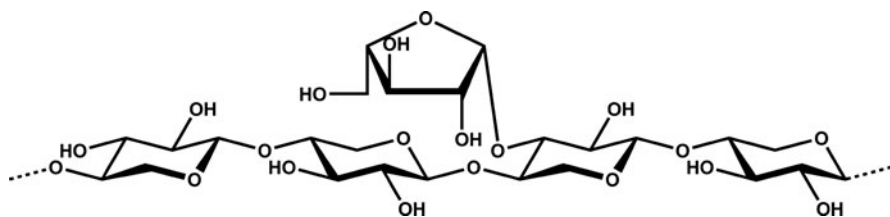
Fig. 25 Structural features of an arabinoxylan
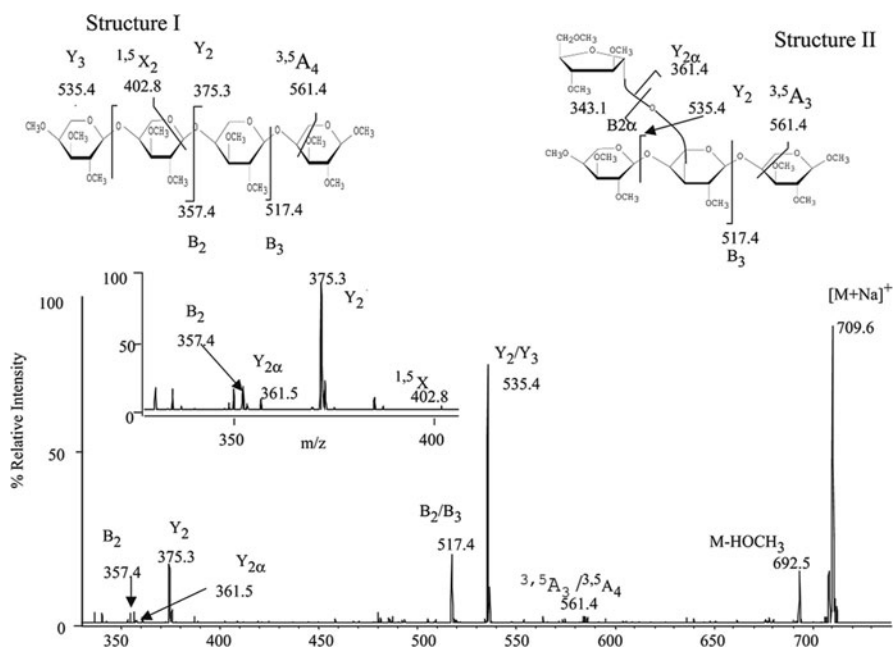
Fig. 26 ESI IT-MS^2 of *m/z* 709.6 obtained from enzymatic hydrolysis of arabinoxylan and subsequent permethylation. *I* and *II* represent possible structures of the tetrasaccharides comprising four pentosyl residues (*I* Xyl$_4$, *II* AraXyl$_3$). Reproduced from [146] with kind permission of the publisher

For more complex mixtures with less restricted options of linkage patterns, labeling and/or chromatographic separation prior to ESI-MS will be necessary to avoid misinterpretation of spectra of isomeric compounds. This has been performed by Maslen et al. [83] who labeled arabinoxylooligomers with *o*-amino-benzoic acid. In addition to ions from glycosidic and cross-ring cleavages, the D, E, F, G, H, and W ions mentioned above were detected (for the nomenclature, see Fig. 17) [5, 126]. These fragments, resulting from elimination and secondary oxidative eliminations from B-ions, indicated the position of arabinosyl residues in the pre-separated isomeric oligosaccharides.

Xyloglucans

Xyloglucans are the main portion of the so-called hemicelluloses of dicotyledons, although their composition depends on the taxonomic family. The xylose residues attached to the β-1,4-linked glucan chain can be capped by galactosyl or additional fucosyl residues. Voragen et al. have analyzed xyloglucan structure in blackcurrants by using different approaches, including online CE- and RP-HPLC-ESI-MS^n and off-line HPAEC-MALDI ToF-MS [147]. The general principle in the

analysis of heteroglycans with a certain diversity of size and chemical structure uses a prefractionation and a chemical or enzymatic partial hydrolysis to oligosaccharides. If enzymes with a known specificity are available, these are very valuable tools for retracing the puzzle pieces obtained to the polymer structure. In the case of xyloglucans, xylan-specific endoglucanases can be applied, which cleave linkages between an unsubstituted and a xylose-substituted glucose in the glucan backbone, thus producing a limited number of specific oligosaccharide building blocks. These can be separated by one of the various methods mentioned. Although MALDI-MS is very appropriate for profiling the molecular masses of the oligosaccharides in the digest, ESI-MS^n was superior to MALDI ToF-MS-PSD for unambiguous sequence analysis due to the applicability of MS^3 and MS^4 where MS^2 did not give sufficient structure information. Figure 27 shows an example of ESI-MS^2 of a xyloglucan oligomer that contains additional fucosyl-*O*-acetyl-galactose in the side chain.

Coupling with capillary electrophoresis (CE), although not often employed, was applied in this case and shown to be superior to LC-ESI-MS. Labeling with a charged tag, APTS, which also allowed laser-induced fluorescence detection (LIFD), was necessary for CE and could solve some problems observed with RP-HPLC.

However, previous knowledge of the structural features of such glycans was considered for interpretation. This is helpful but bears the risk of misinterpretation if unexpected new structural features occur. Data and observations from various methods, their power and limitations, as well as the accumulated knowledge from biology (e.g., specificity of enzymes, relationships of taxonomy and structural
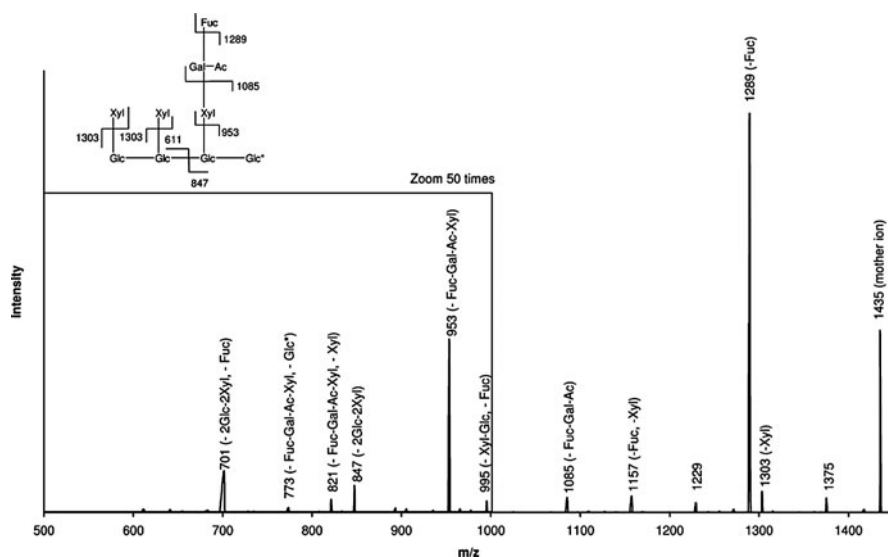
Fig. 27 ESI-MS^2 of a xyloglucan oligosaccharide with fucose and *O*-acetyl-galactose in the side chain (XXFG) obtained from enzymatic degradation of xyloglucan of blackcurrants. Reproduced from [147] with kind permission of the publisher
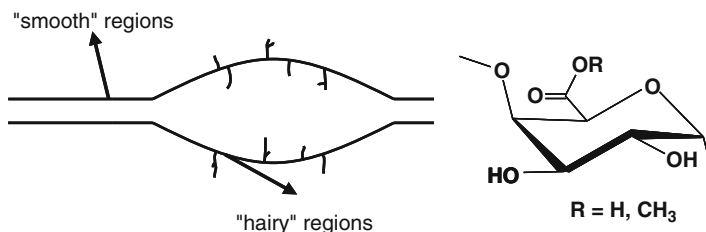
Fig. 28 Schematic structure of pectin. The main chain is constituted of α-1,4-galcturonic acid, which is partially methyl esterified. Gelation mechanism and gel strength depend on the degree of methyl esterification and the distribution of methyl ester groups in the smooth regions

features), chemistry, and instrumental analysis have to be combined in a plausible manner to generate a representative picture of such complex structures of biopolymers. HPEAC-ESI-MS has also been applied to enzymatic digests of legumes [148].

Pectins

Pectins are also ubiquitously occurring, very complex, and important heteropolysaccharides. They are found in the primary cell wall of all plants and form the middle lamella of higher plants. The main chain consists of α-1,4-linked galacturonic acid, which is partially methyl esterified and interrupted by rhamnose residues. Attached to this backbone, arabinans and other oligomeric heteroglycosidic side chains are found ("hairy regions") (Fig. 28).

Therefore, it is not surprising that structural analysis of pectin has profited much from the recent developments in the field of mass spectrometry and other instrumental techniques [149]. As described before, a combination of isolation and fractionation steps, partial degradation by enzymes or chemical methods, labeling, various chromatographic and electrophoretic separations, and finally off-line or online MS and tandem-MS give a more and more detailed insight into the structural features. The methyl esterification pattern could be analyzed after enzymatic digestion by MALDI ToF-MS [149]. Although sequencing is established in the field of proteins/peptides and nucleotides, it is still a challenge in the field of carbohydrates, although the work of Reinhold et al. is an impressing milestone [135–140]. Jensen et al. have reported the initial steps of a solid phase-supported sequencing approach for pectins [150].

5   Quantitative Analysis by Mass Spectrometry

The question of whether data obtained by ESI or MALDI mass spectrometry can be used for quantitative evaluations has already been addressed above with regard to the molecular weight distribution of polysaccharides. Quantitative analysis of

known and available compounds using internal standards, often performed by online-LC-ESI-MS methods, will not be addressed here. However, we will now discuss the conditions under which signal strength can be used to determine the relative composition of a carbohydrate mixture.

The MALDI process is basically more suitable for quantitative measurements than the ESI methodology. Linear relationships of concentration (in a certain matrix) and signal height or area have been found for various compounds [151, 152]. Linearity of the individual response nevertheless requires calibration with the authentic compound or an appropriate internal standard. However, the relative response values in mixtures is of greater relevance for the determination of molar compositions e.g., of oligosaccharides released from O- or N-linked glycans. Therefore, Naven and Harvey studied the relative signal strength of equimolar mixtures of such oligosaccharides (28 pmol of each per target spot) of roughly similar type and covering the mass range from 420 to 2,400 m/z [151]. Although data are usually averaged in MALDI to level the shot-to-shot variations caused by the heterogeneity of the spot (here from 240 shots), standard deviation of a triple determination was in most cases between 7 and 18% when a sector field instrument was coupled to the ion source as mass analyzer (the matrix was 2,5-dihydroxy benzoic acid, DHB). Choice of the matrix had little influence, although for connection with a ToF analyzer, the response of oligosaccharides increased until m/z 1,000 then remained stable but with poor precision. Bias towards the low molecular mass analytes is probably caused by detector saturation through matrix molecules in the lower m/z area.

By labeling with a charge-providing tag, higher intensity and (important for quantitative MS) independency of sodium adduct and avoidance of multiple ion adduct formation is achieved. Powerful reagents are the already mentioned positively charged GT as well as o-aminobenzoic acid (2-AA) for negative mode MS. Kim et al. applied this procedure to oligosaccharides released from neutral N-linked glycans, and proved the method with an equimolar mixture of gluco- and mannooligosaccharides [65, 66]. Evaluation of signal areas but not of heights from MALDI ToF-mass spectra of GT-labeled oligosaccharides agreed well with data obtained by normal phase (NP)-HPLC of the 2-AA labeled mixture (using fluorescence detection) as reference method. Although 100 pmol of substance was required for HPLC, only 20 pmol was necessary for MS analysis [65].

In a similar approach, quantification of a roughly equimolar mixture of glucose up to maltohexaose was carried out [152a]. The exact composition of the maltooligosaccharides was determined by HPTLC (high performance thin layer chromatography) of the 2-AA-labeled compounds. Sample spots for MALDI-ToF-MS contained about 10 pmol of each constituent of the GT-labeled mixture. Matrix and the laser power were varied, with HABA [2-(4-hydroxyphenylazo)-benzoic acid] turning out to be the most appropriate matrix, although the laser power was adjusted significantly above the usually recommended threshold of ion formation (Fig. 29, left). For ESI IT-MS, a mixture containing ca. 160 pmol/μL of each compound was applied using a syringe pump (200 μL/h), and instrument parameters as target mass and, related to this, RF amplitude and capillary exit
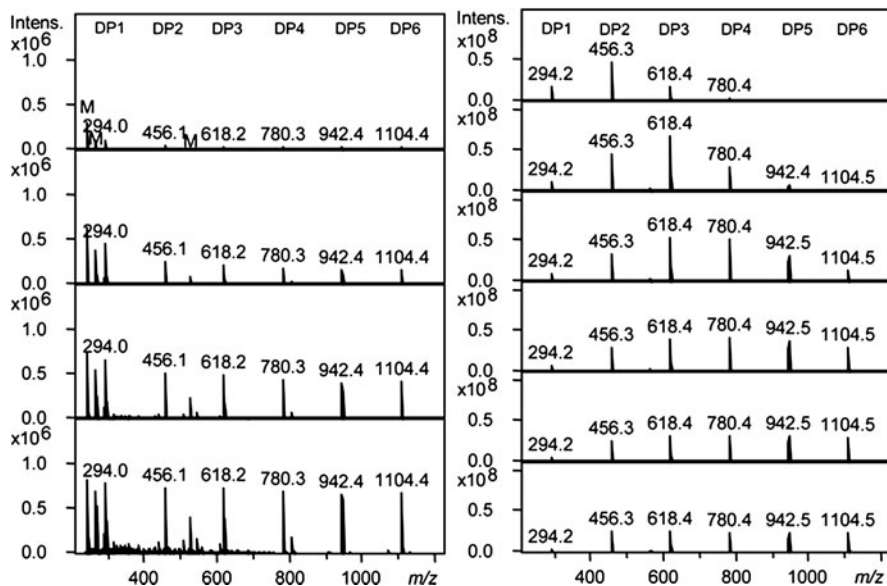
Fig. 29 Quantitative mass spectrometric analysis (positive mode) of a mixture of maltooligosaccharides (*DP1–DP6*), labeled with Girard's T (see Fig. 5). *Left*: MALDI ToF mass spectra with HABA [2-(4-hydroxyphenylazo)-benzoic acid] as matrix under variation of the laser power (45, 50, 55, and 60%, *top* to *bottom*); *M* matrix signals. *Right*: ESI IT mass spectra under variation of the target mass from *m/z* of DP1 to DP6 (*top* to *bottom*)

voltage were varied. Best results were obtained at highest target mass, i.e., *m/z* of DP 6, for the GT-labeled maltooligosaccharides (Fig. 29, right). Average deviation compared to the reference method (HPTLC) was 1–2% under these conditions. Only slight differences were observed for area and height evaluations.

5.1 Tandem Mass Spectrometry for Quantification

Tandem mass spectrometry opens a chance for quantification of isobaric mixtures, which are not separated in the mother spectrum. This is a very typical problem in carbohydrate analysis, since many constituents only differ in stereochemistry or are regioisomers with different patterns of the same functional groups or substituents, as in polysaccharide derivatives. With the exception of bacterial lipopolysaccharides, which beside the core region consist of repeating units of oligomeric size, polysaccharides show a high diversity with respect to the distribution of their building bricks, branching pattern, side chain length, and substituents like acetyl or sulfate groups. On the other hand, structural diversity is not simply random, since enzymes involved in the biosynthesis act with certain selectivity, and often various topological patterns exist. Since various enzymes are available, nature produces

different types of basically the same polysaccharides, e.g., alginates, galactomannans, pectins, or carrageenans, in random, regular, or block-like patterns.

Analysis of such patterns usually involves partial degradation to oligosaccharides, which can be performed in a more or a less selective manner, using various enzymes or chemical methods, most commonly acid hydrolysis. Chromatographic separation of oligosaccharides obtained by such procedures is limited due to the high complexity, which rapidly increases with DP. A nice example of how tandem MS can help to elucidate the composition of isobars in such mixtures has been reported by Haebel et al. [153]. They analyzed the qualitative and quantitative composition of oligosaccharides derived from partially deacetylated chitin by enzymatic digestion (Fig. 30). These hetero-chitooligosaccharides D_nA_m (D = GlcNH$_2$, A = GlcNAc) were chromatographically fractionated and the isomeric mixtures analyzed by MALDI linear ion trap-MS, using CID up to MS^3. As usually applied in the analysis of polysaccharide derivatives [23], chemical uniformity of the chitooligomers was achieved by N-acetylation with Ac$_2$O-d_6. Thus, the originally present and later introduced acetyl groups can be differentiated by $\Delta m/z$ of 3. By reductive amination with 3-acetylamino-6-aminoacridine, derivatives were generated that exclusively produced Y fragments, always bearing the protonated tag. (Fig. 31) [153]. From their pattern and from additional MS^3 experiments, the contribution of individual sequences to
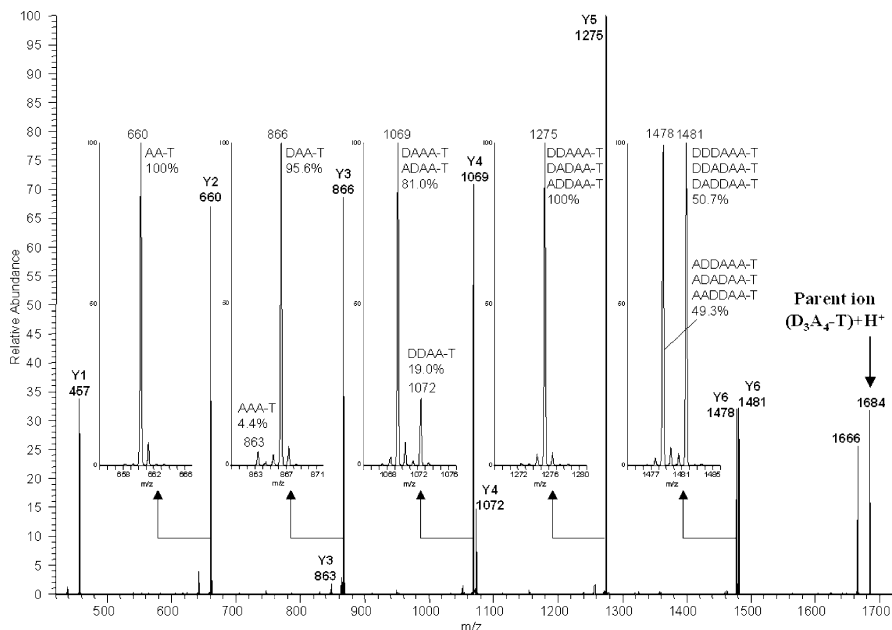
Fig. 30 MALDI LIT-CID-MS spectrum of [M + H]$^+$of isobaric mixture of N-perdeuteroacetylated D3A4-T chitooligosaccharides at m/z 1,684. D GlcNAc-d_3 from GlcNH$_2$, A GlcNAc, T tag = 3-N-acetyl-aminoacridine. Quantitative evaluation is outlined in Fig. 31. Reproduced from [153] with kind permission of the publisher
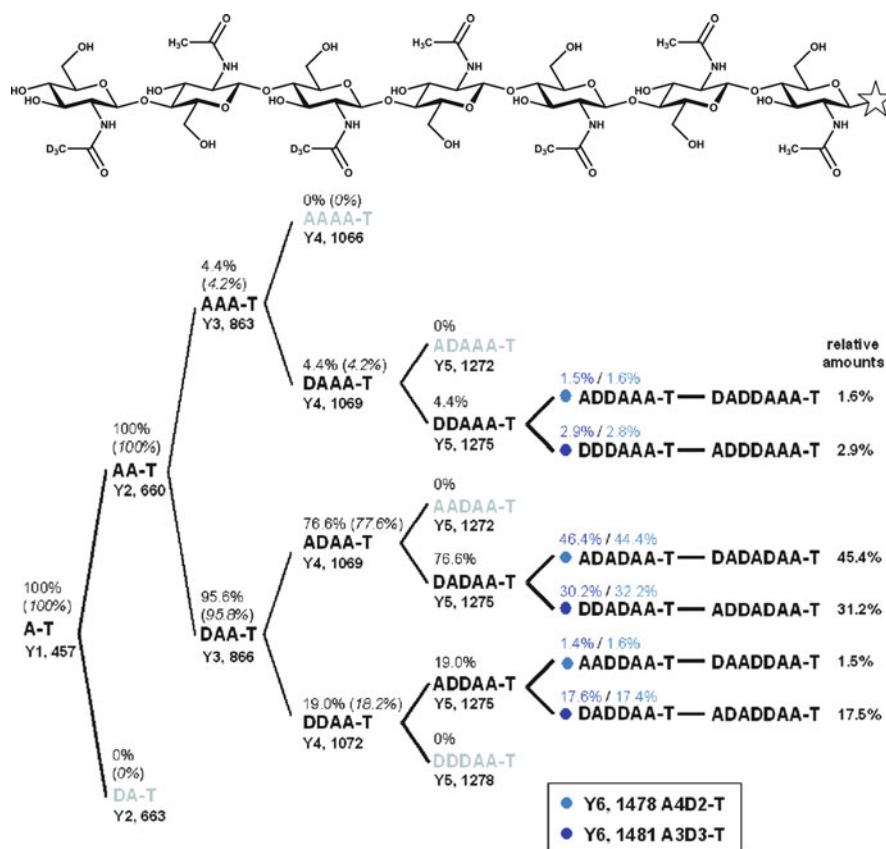
Fig. 31 Quantitative sequencing procedure for a mixture of D3A4 isomers. The structure of the main constituent (DADADAA-T) after *N*-acetylation-d_3 of D units is shown *above*. Sequences that may be excluded due to the absence of a peak at the corresponding mass are printed in gray. Results were obtained from MS^2 spectra (shown in Fig. 30) and from the MS^3 spectra of the two Y_6 fragments at *m/z* 1,481 and 1,478 (not shown). Reproduced in modified form from [153] with kind permission of the publisher

isobaric mixtures could be determined up to DP 8 and were shown to consist of an equal number of Glc*NAc* and Glc*NH$_2$* (D$_4$A$_4$) sequences. However, due to selectivity of the enzyme applied, 96% of this mixture comprised only eight of the theoretically possible 70 different sequences with individual contributions of between 2 and 34%.

Another example deals with the elucidation of the complete monomer composition of methyl amylose or cellulose (Fig. 32) by ESI IT-MS^2 and by MS^3 of maltose or cellobiose derivatives obtained after permethylation with MeI-d_3 and subsequent partial hydrolysis [130].

Based on ESI IT-MS^n studies with regioselectively *O*-methyl/*O*-deuteromethyl maltoses, ions could be assigned to certain glucose fragments [131]. By combining
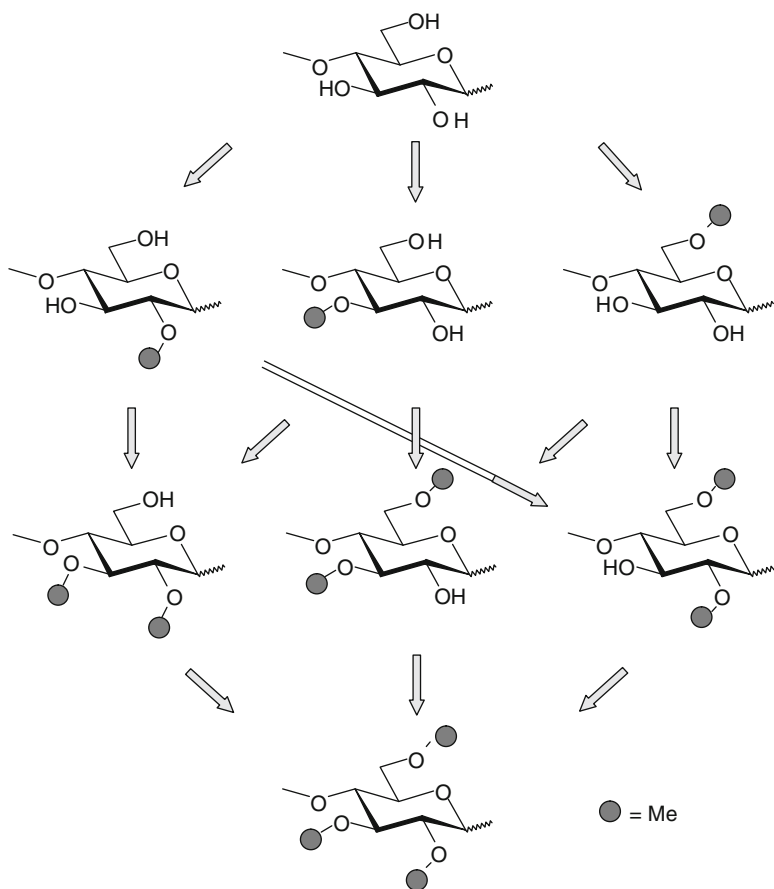
Fig. 32 Eight monomers with different methylation patterns present in a 1,4-glucan after partial *O*-methylation

the data obtained for the isotopic patterns of the various fragment ions, all molar ratios of the eight different glucosyl units present in methyl cellulose could be calculated. Since no total hydrolysis is required, as it is for chromatographic or electrophoretic separation and determination of these eight constituents, this approach can be regarded as an independent reference method.

Figure 33 illustrates the evaluation of the mass spectra for a monosubstituted dimer bearing one CH_3 and six CD_3 groups. The *m/z* of $[M + Na]^+$ is 464. The Y_1 fragment ion of the CID-MS presents the reducing part of the disaccharide. The 1:1 ratio of the intensities at *m/z* 251 and 254 indicates that the methyl group is located with the same probability at both units of the dimer. The ratio of the abundances of the $^{0,2}A_2$ ions reflects the probabilities of a CH_3-group at O-2 and O-3, or O-6. Elimination of methanol from Y_1 is known to involve RO-3. Thus, the ratio of
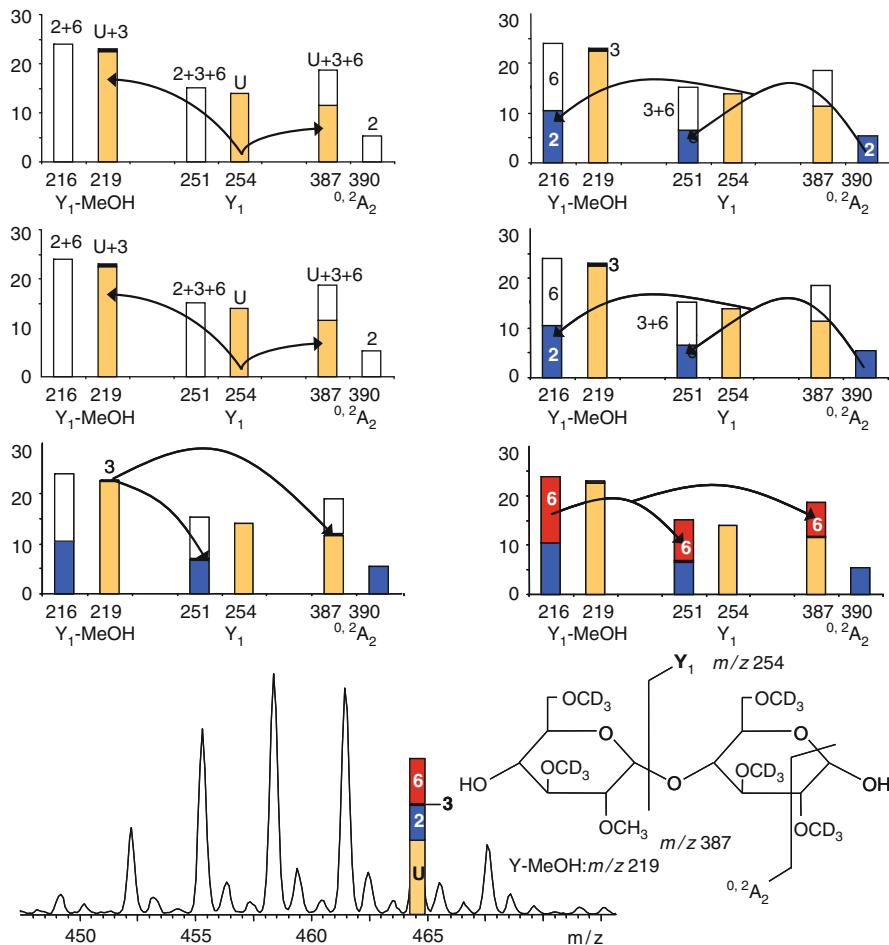
Fig. 33 Evaluation of the monomer composition of the monosubstituted fraction of *O*Me/*O*Me-*d₃* disaccharides obtained from methyl amylose. As an example, the step-by-step-distributions of the signal intensity of the penta-*O*-methyl-*d₃*-mono-*O*-methyl-dimer ([M + Na]⁺ *m/z* 464) on non- (50%), 2-, 3- and 6-*O*-monosubstitution are shown *above*. *U* unsubstituted. Reproduced in modified form from [130] with kind permission of the publisher

O-3- to (*O*-2 + *O*-6)-substitution can be calculated from these fragments. Finally, each signal of the MS¹ spectrum (Fig. 34a) is distributed to the contributing isomeric methyl patterns. Since information obtained by MS² (Fig. 34c) is not sufficient for all isobaric mixtures, MS³ is performed (Fig. 34e, f). For this fragmentation, Li⁺ adducts are required (Fig. 34b, d) because Na⁺ adducts dissociate at the collision energy required, as outlined above (Fig. 35). Finally, all data are summed and the complete monomer composition of methylcelluloses, methylamylose or methylcyclodextrin is obtained. For details see [130].
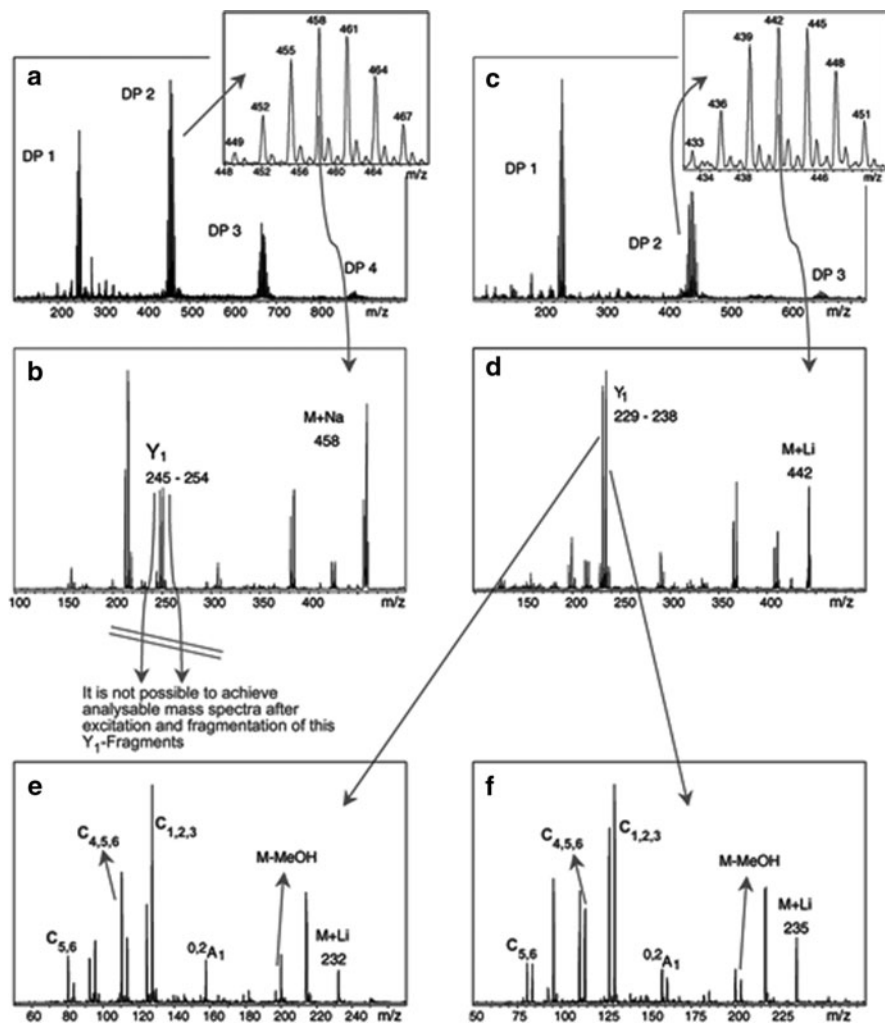
Fig. 34 ESI-MS^n of *O*Me/*O*Me-*d₃* disaccharides obtained from methyl amylose. ESI-MS of [M + Na]$^+$ and [M + Li]$^+$ (**a, c**), ESI-MS^2 of dimers with 3 Me and 3 Me-*d₃* of Na$^+$ and Li$^+$ adducts (**b, d**), and ESI-MS^3 of Y₁ at *m/z* 232 (**e**), and ESI-MS^3 of Y₁ at *m/z* 235 (**f**). For fragment evaluation see Fig. 35. Reproduced from [130] with kind permission of the publisher

6 Polysaccharide Derivatives

Polysaccharide derivatives, i.e., glycans with non-sugar substituents, are produced both naturally and chemically. Sulfates are common functional groups, e.g., in glycosaminoglycans (e.g., heparin, chondroitin sulfate) and algae polysaccharides (e.g., carrageenan, agar); phosphate esters occur in bacterial lipopolysaccharides or in potato starch; acetate groups are known from hemicelluloses (galactoglucomannan,
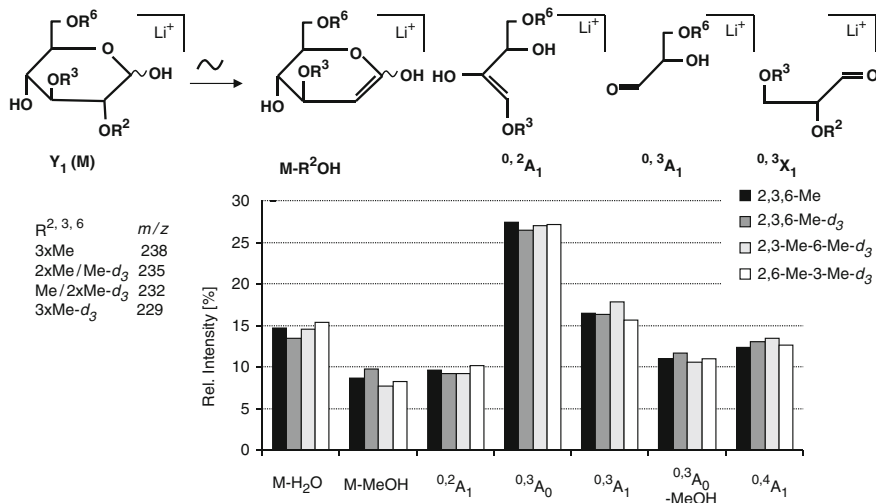
Fig. 35 ESI CID-MS[3] of Y_1 (Li-adduct) obtained from 2,3,6-O-methylated disaccharides in MS[2] experiment (see Fig. 34d–f). Fragment structures and relative ion intensities obtained from regioselectively O-Me-d_3 isomers as the basis for quantitative methyl pattern evaluation are shown. For details see [130]

xylan), acemannan from Aloe vera, or xanthan produced by *Xanthomonas campestris*. Methyl ethers are found in the terminal glucuronic acid of xylans, in cell wall polysaccharides of *Chlorella vulgaris* [154, 155], or in various bacterial and fungal polysaccharides, e.g., 2-O-methyl-mannose in mucoralean extracellular polysaccharides [156, 157]. On the other hand, chemical modification of widely available polysaccharides, especially cellulose and starch, is performed on an industrial scale [23, 158–160]. Less abundant glycans such as galactomannans (guar, locust bean gum) or dextrans have also been functionalized by chemical transformation [161].

Chemically modified polysaccharides can be considered as semisynthetic copolymers of high complexity. In addition to the dispersity of the starting material (e.g., concerning their molecular weight), chemical dispersity is established in the modification process. Distribution of substituents has to be considered on various structural levels, which will be outlined here using cellulose as an example. In the glucosyl unit, three different OH groups are available in positions 2, 3, and 6 (see Fig. 32). The distribution in the next dimension, the cellulose chain, depends on the content and arrangement of non-, mono-, di- and trisubstituted monomer residues. If all units of the chain are equally accessible during the reaction, a random pattern is obtained. Depending on the reaction system (homogeneous, heterogeneous, protic, aprotic etc.) and the interactions between primary substituents and remaining OH-groups or reagent, the pattern can deviate from the random model in various ways. Related to this heterogeneity of second order, a heterogeneity of first order also exists, i.e., along the polymer chains within the material (third dimension). Although the material can be fractionated with respect to the heterogeneity of first order, the second order heterogeneity is located on

single macromolecules and therefore only analyzable after partial depolymerization [23, 162–167]. The latter can be achieved either by chemical or enzymatic degradation [121, 128, 168, 169].

Method development to gain detailed knowledge of the substituent distributions in all these dimensions is mainly motivated by the fact that the properties of such compounds, e.g., solubility, degradability, or flocculation points in thermoreversible gelation (and the dynamics of these processes), are affected by the chemical structure of the material. Within this very challenging field of structure analysis, MS has always been a very important instrumental method and is still of high potential. Due to the lack of standard compounds, GLC/electron impact (EI) MS is usually applied in monomer analysis because it allows elucidation of the substitution pattern in glucose-based derivatives due to characteristic shifts of fragment ions [23, 170].

The development of soft ionization methods has enabled the analysis of less volatile oligomeric analytes, giving information about the probabilities of various domains in the chains, i.e., the distribution in the chain. Since basic aspects of the ionization processes, labeling, quantification, tandem MS, and fragmentation mechanisms have already been addressed above, this section will focus on the application of these methods to cellulose and starch derivatives to illustrate the high value of MS for this field of carbohydrate analysis [171].

6.1 Methyl Ethers

Methyl ethers are not only important commercial products derived from cellulose and are used as adhesives and thickeners, but are also appropriate model compounds for analytical method development because the methyl group is chemically stable, small, neutral, and available in isotope-labeled version. Therefore, several basic studies, including MS, have been performed on methyl ethers of cellulose [128, 130, 166, 167, 169, 171, 172], amylose [164], starch [121], and dextrans [173].

Analysis of the substitution pattern in the polymer chain of such methyl glucans has been tackled by the following four-step approach:

1. Perdeuteromethylation, which makes the compound chemically uniform, but allows differentiation of original and introduced methyl groups. This is also a prerequisite for the next step.
2. Partial random degradation, which can be performed by aqueous hydrolysis or methanolysis.
3. Mass spectrometric analysis by FAB- [162, 174], ESI- [167, 169, 173] or MALDI ToF-MS (3) [128, 129, 162].
4. Quantitative evaluation of MS data and comparison of the substituent distributions in a certain oligosaccharide fraction with the theoretical distribution calculated from the monomer data, determined independently (Fig. 36).
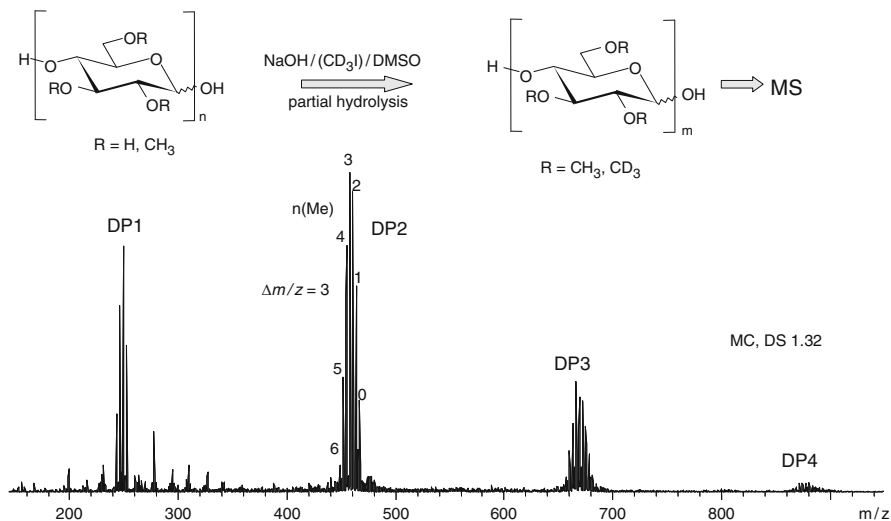
Fig. 36 Sample preparation (*above*) and ESI-MS (*below*) of methyl cellulose (DS 1.32) for analysis of the substituent distribution along the polymer chain. (DP2 is shown in extended scale in Figs. 33 and 34). Quantifiability of signal abundances is proved by perdeuteromethylation, giving chemically uniform analytes in a narrow *m/z* range. Methyl pattern of each DP is calculated and compared with the random distribution for the glucose constituents present (compare Fig. 32) [23, 162, 174]

With respect to MS, the most important point in this analytical approach is the quantifiability of the constituents of a certain DP on the basis of signal strength. It is not essential to quantify the relative portions of oligomers, although it would be of additional value to control the randomness and degree of partial depolymerization. In contrast, this is of higher importance for enzymatically digested cellulose or starch ethers.

In the case of methyl ethers, the required quantifiability is achieved by permethylation with MeI-d_3, to get a chemically uniform, isotope-labeled product. The *m/z*-range for the oligomers obtained by partial hydrolysis of these compounds is 449–467 for DP2, 653–680 for DP3, and 857–893 for DP4, which means an appropriate mass range for ESI IT-MS. The signals within these oligomer fractions differ by *m/z* 3, and thus are of sufficient similarity that they are not discriminated by the ionization process or the mass analyzer, but just differing enough to avoid significant overlapping of ^{13}C-related isotopic signals of compounds with various degrees of methylation. At DP4, the relative intensity of the $[M + Na + 3]^+$ ion, which is isobaric with the next higher deuterated homolog, is 2.77% of the main peak or 1.77% of the total intensity (Fig. 37). Since this overlap extends throughout the whole pattern, the final distortion is not significant at this DP and not even very pronounced at DP 9 as long as the distribution is not very narrow or bimodal.

$m/z = 857.4$

$C_{36}H_{66}O_{21}^{+}$	
M[%]	64.07
M+1[%]	25.94
M+2[%]	7.88
M+3[%]	1.77
M+4[%]	0.34
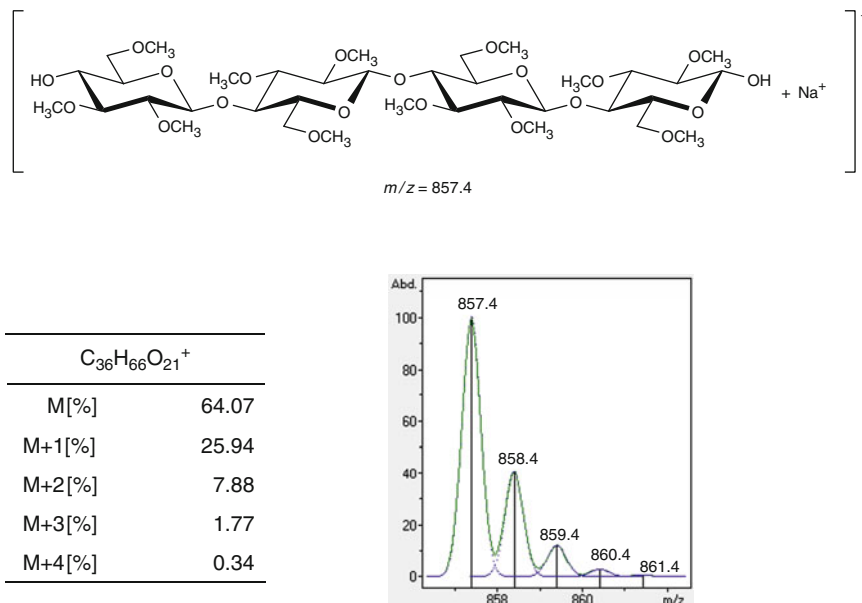
Fig. 37 Isotope composition of tetrakis[2,3,6-tri-O-methyl]-cellotetraose

Although in the pioneer work in this field (still employing FAB-MS), correction for the abundant noise was an important factor in evaluation [162, 174], this is often not necessary for the much higher quality ESI and MALDI mass spectra. However, for ions of low intensity at the profile borders, this can be critical, depending on the S/N ratio. One has also to decide whether to summarize the ^{13}C-isotope peaks at $[M + Na]^{+}$, $[M + Na + 1]^{+}$, and $[M + Na + 2]^{+}$ for each signal, or to use only the base peak for evaluation. To sum up all these intensities could average the contribution of noise, but at the same time could impair the quality of small signals, since their isotopic sister ions often strongly deviate from theory due to decreasing S/N ratio. Therefore, as long as all compounds within a set for quantitative evaluation comprise the same C number, as is the case for O-methyl-O-methyl-d_3-oligoglycosides, and the $[M + Na]^{+}$ signal is the most abundant, then quantitative evaluation is best based on these main peaks. The situation is different when the number of C atoms, and thus the relative ratios of isotope peaks, differs within a certain DP, as is the case for hydroxyalkylmethyl ethers (see Sect. 6.2). By this approach, various types and extents of deviation from calculated patterns have been determined for methyl polysaccharides [23, 162].

Higher oligomers are only present in lower amounts in a partially degraded polysaccharide derivative and are discriminated in ESI-MS by direct infusion with a syringe pump due to the facts outlined above. To record mass spectra of good quality for these higher homologs, LC-ESI-MS can be applied. The coupling with

the chromatographic system allows ionization of each set of analytes of the same DP without competition by compounds with higher surface activity or electrophoretic mobility, and at the same time enables automation. The continuously recorded mass spectra are accumulated for the DP-corresponding intervals. Separation should not be optimized with respect to fast elution and narrow peaks, since broad peaks eluting over a longer time period allow recording and summing of more mass spectra, and thus enhance the sensitivity and quality of the data. The scan range should be programmed for each DP according to the *m/z* range of interest. To detect the analytes independently by UV detector, a chromophor was introduced by reductive amination with *m*-amino benzoic acid (3-AA) [172].

6.2 Hydroxyalkyl Methyl Ethers

Cellulose derivatives other than methyl ethers have also been transformed to *O*-methyl-*O*-methyl-*d₃*-celluloses. This approach was applicable to cellulose acetates [175] and sulfates [176]. In the case of hydroxyalkyl methyl ethers such as hydroxyethyl methyl cellulose (HEMC), and the corresponding hydroxypropyl derivative (HPMC), which are widely applied in the construction, pharmacy, and food areas, this is impossible because the substituent also bears a free OH group. These hydroxyl groups will undergo the same transformations as (or like?) the remaining OH of the cellulose backbone and, as a consequence, the chemical and mass differences will be maintained. In addition, some of the OH groups are already methylated. Therefore, permethylation or perdeuteromethylation are the methods of choice to increase, at least chemical uniformity of the compounds. However, since hydroxyalkyl and methoxyalkyl groups are flexible, and alter polarity and sodium complexation ability, oligosaccharides bearing these groups are extremely overrepresented in ESI mass spectra. Therefore, a permanent cationic group has been introduced by reductive amination with *n*-propylamine and subsequent permethylation. In ESI-MS, a decreasing trend in degree of substitution (DS)/DP was still observed. DS should be constant over all DPs and resemble the average DS of the sample if all steps of the analytical procedure (partial degradation, derivatization, work-up, MS analysis) are free of discrimination. MALDI-MS gave representative results for HEMCs, HPMS, and HECs [90, 91, 177].

In Fig. 38, the ESI-IT-mass spectrum of an *O*-deuteriomethylated partially hydrolyzed HEMC is compared with those recorded after reductive amination and subsequent quaternization. Total abundance and S/N ratio is stepwise enhanced. Correct quantitative evaluation of the hydroxyethyl pattern was only possible using the MALDI ToF mass spectra.

The methyl pattern and hydroxyalkyl pattern are analyzed independently. Although for conservation of the methyl pattern permethylation with MeI-*d₃* is necessary, the sensitivity for the analysis of the hydroxyalkyl pattern can be enhanced by using permethylation, since all oligosaccharides representing a certain number of hydroxyalkyl groups are then concentrated in one peak rather than being split into several peaks with various ratios of Me and Me-*d₃*. Other labels, described
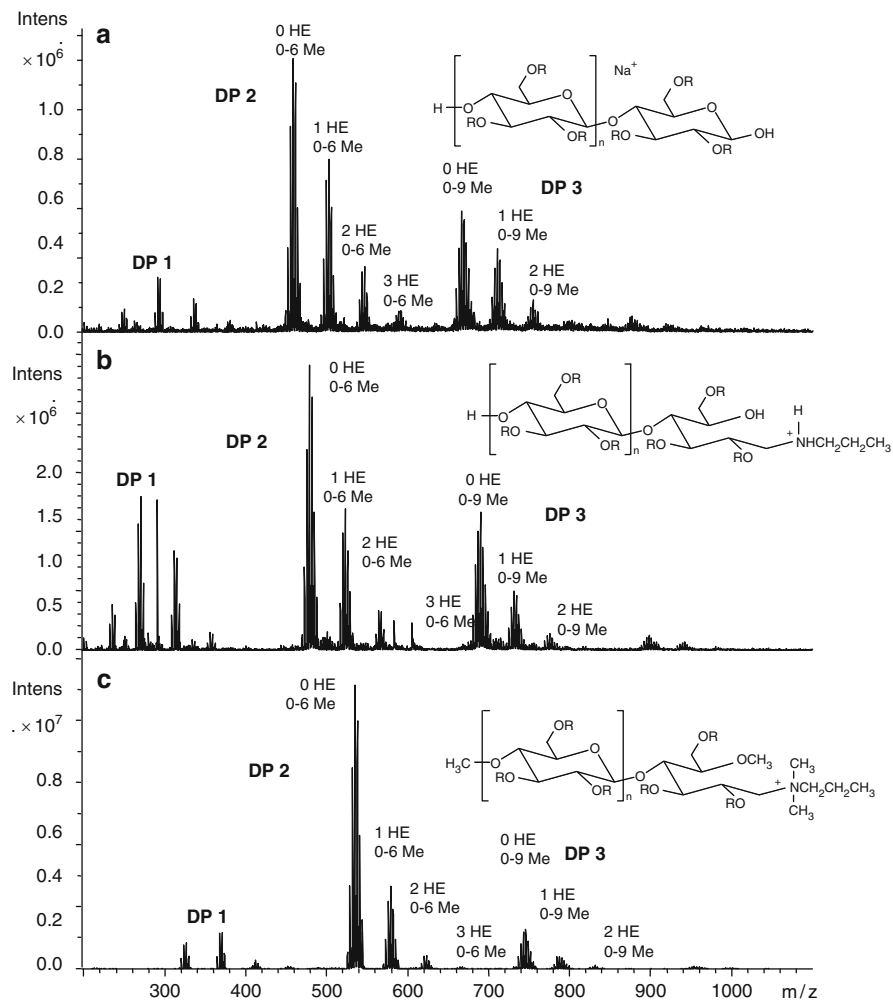
Fig. 38 ESI-IT-MS of hydroxyethylmethylcellulose (HEMC). The sample was perdeutero-methylated and partially hydrolyzed (**a**), reductively aminated (**b**), and quaternized with MeI (**c**). The number of hydroxyethyl (*HE*) and methyl (*Me*) groups are shown. For explanation see text or for more details [91]. Reproduced in modified form from [91] with kind permission of the publisher

above, can also be introduced instead of labeling with an aliphatic amine and additional quaternization.

6.2.1 Quantitative Evaluation

Since the isotopic pattern slightly shifts with increasing number of C atoms, the question of whether quantitative evaluation should be based on the main signal

	Me6						HEme6
	$C_{25}H_{52}NO_{10}^+$	$C_{27}H_{56}NO_{11}^+$	$C_{29}H_{60}NO_{12}^+$	$C_{31}H_{64}NO_{13}^+$	$C_{33}H_{68}NO_{14}^+$	$C_{35}H_{72}NO_{15}^+$	$C_{37}H_{76}NO_{16}^+$
m/z (M)	526.36	570.38	614.41	658.43	702.46	746.49	790.52
M [%]	73.87	72.09	70.36	68.66	67.02	65.40	63.83
M+1 [%]	20.97	22.09	23.13	24.12	25.05	25.91	26.73
M+2 [%]	4.39	4.90	5.42	5.95	6.48	7.02	7.56
M+3 [%]	0.68	0.81	0.95	1.10	1.25	1.43	1.60
M+4 [%]	0.09	0.12	0.14	0.17	0.20	0.24	0.28

Fig. 39 Isotope composition of cellobiose derivatives with various numbers of methyl (*Me*) and methoxyethyl (*HEme*) groups as prepared from HEMC for the analysis of the substituent distribution in the polymer chain, according to Adden et al. [91] (see also Fig. 38)

only, or whether ^{13}C isotope peaks should be included, is of higher relevance for these mixed ethers. In the case of *O*-methylated hydroxyethyl ethers, the number of C atoms range from nine [n(HE) $= 0$] to 15 [n(HE) $= 3$ per glucosyl unit; n is theoretically unlimited because the substituent can undergo tandem reactions]. As a consequence for DP 2, the first ion with n(HE) $= 0$ represents 73.87% of the total ions, and for n(HE) $= 6$, it represents only 63.83% of all isotope peaks. All other signals [n(HE) $= 1\ldots5$] lie in between (see Fig. 39). Therefore, it is important to sum up the isotope peaks at least at M $+ 1$ and M $+ 2$ for these derivatives [corresponding to 99.23% (Me$_6$) of the total ion abundance, and to 98.12% (HEme$_6$), respectively as shown in Fig. 39]. This can be achieved by taking the values from the mass spectrum, but, if smaller peaks are not accurately measured, by calculating the entire intensity from the base peak using the known isotopic composition. If necessary, overlapping of [M $+ 3$]$^+$ isotope peaks with the next higher [M]$^+$ must be corrected by subtraction of the calculated amount to avoid a distortion in favor of higher deuteromethylated isomers of a certain DP profile.

6.3   Application of Enzymes

Enzymes have also been applied in combination with MS to analyze the substituent pattern in cellulose and starch derivatives [23, 112, 132, 178–186]. Degradability

decreases with increasing number of substituents, since they interfere with the formation of the active complex. However, at the same DS and for a given enzyme, digestibility strongly depends on the location of the substituents on the various hierarchical structure levels. MS is again a very valuable tool for the study of oligosaccharides released by enzymes. Patterns can be analyzed in the same manner as described above for chemically degraded glycans. In contrast to the latter, not only the DS, but also the DP pattern is of interest here. As is obvious from what has been outlined above, MALDI-MS is superior to ESI-MS in this respect, but derivatization can improve ESI-MS, enabling quantitative evaluation under appropriate conditions.

To elucidate the enzyme specificity, i.e., in which positions substituents are accepted at the cleavage site, tandem MS is of high value. Fragmentation provides information about the number and position at the reducing end. For example, unsubstituted residues of the n-mer derived from a 1,4-glucan like starch or cellulose will give $^{0,2}A_n$ (M-60) and subsequent $^{2,4}A_n$ (M-120). One methyl group at the new reducing end (position -1 in the active complex) causes a loss of 194 instead of 180u to form B_{n-1}. Location of this methyl group at O-6 can be recognized from a loss of 60 and, subsequently, a shift to -74. Location at O-2 will shift the first cross-ring cleavage to M-74, followed by a loss of 60, while blocking of 3-OH suppresses A-fragment formation (see Figs. 15 and 16). To differentiate overlapping patterns and avoid erroneous interpretation, separation is required. However, due to the enzymes' specificity, substitution at the cleavage site is usually very restricted. Enebro et al. applied a different approach for this type of position analysis. The oligosaccharides obtained by enzymatic digestion from carboxymethylcellulose (CMC) were permethylated, after the end groups had been reduced to alditols, and after total methanolysis analyzed by LC/ESI-MS^2. CID mass spectra of the non-carboxymethyl-substituted glucitol (Fig. 40a) showed subsequent losses of $3 \times$ MeOH. Diagnostically more valuable fragmentations were induced by the free OH at C4 between C3–C4 and C4–C5 of the alditol. Carboxymethylation at O-6 induced a shift for the C4–C6 fragment from m/z 125 t to m/z 183 (Fig. 40b). For the 2- and 3-O-carboxymethyl isomers, the C1–C4 fragment was shifted from m/z 196 to m/z 254 (Fig. 40c, d). These two secondary ethers could not be unambiguously differentiated from the tandem mass spectra, but the independent assignment agreed with an assumed higher probability of ROH elimination from position 3 (m/z 196 and m/z 228 are higher for 3-O-CM than for 2-O-CM). Thus it was found that one of the enzymes (endoglucanases) tolerated carboxymethyl groups at O-6, and another only at O-3, while position 2 was not substituted at all in the released reducing units [132].

Cationic starches [O-(2-hydroxy)propyl-3-trimethylammonium] have also been studied by ESI-MS-CID after exhaustive enzymatic degradation [112]. Due to multiple charged state of the oligosaccharides released, up to fourfold substituted dodecamers (DP12) were detected (Fig. 41). Tandem MS and evaluation of the fragmentation pathway by ^{2}H and ^{18}O labeling allowed differentiation of more homogeneous and more heterogeneous modification of the starch granules under various cationization conditions. H–D exchange of OH indicated that in the first
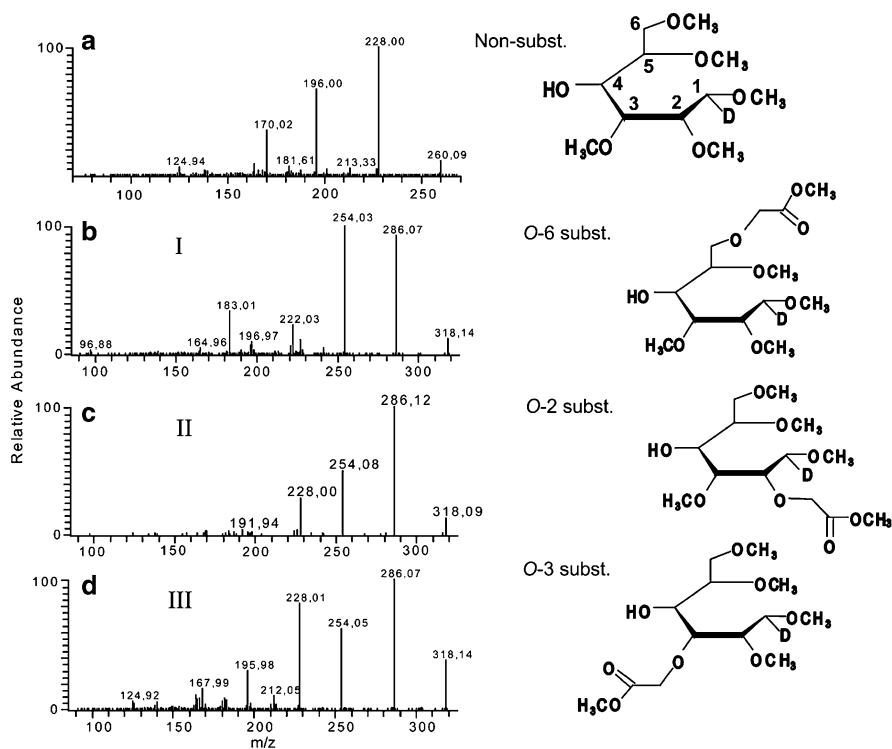
Fig. 40 ESI CID-MS ([M + Li]$^+$) of 1,2,3,5,6-penta-*O*-methyl- D-glucitols-1-*d* (**a**) and isomeric 2-, 3- and 6-mono-*O*-methoxycarbonyl-tetra-*O*-methyl-D-glucitols-1-*d* (**b**, **c**, **d**, respectively) obtained from CMC by partial degradation (here acid hydrolysis), reduction with NaBD$_4$, permethylation, and methanolysis. The position of the carboxymethyl group as shown in the formulae can be deduced from certain fragment shifts of **b**, **c**, and **d** compared to **a**. For details see text. Reproduced from [132] with kind permission of the publisher

loss of 60 u, two exchangeable H, i.e. from OH, are involved (shift of Δ*m/z* to 62), The second loss is only shifted from 60 to 61 u, which means that one H is abstracted from a C–H (Fig. 42). ESI-MS^2 of the isolated monosubstituted cationic maltotrioses, the main products from enzymic digestion (see Fig. 41), proved that no substitution is tolerated at the new formed reducing glucosyl unit (i.e., at the −1 cleavage site) by the α-amylase (from *B. licheniformis*) as has been found for methyl starches [179]. From the fragment ratios of the shifted B and Y ions it is evident that the cationic substituent is mainly located at the inner glucosyl unit and to a less extent at the new non-reducing end.

One has to keep in mind that in contrast to charge-remote fragmentations of sodiated molecules, only those fragments bearing the covalently linked charged substituent – and thus only shifted ions – can be observed. While B$_2$ comprises the maltotriose isomers functionalized at the terminal and the inner 1,4-linked glucosyl residue, Y$_2$ is only observable for the latter.
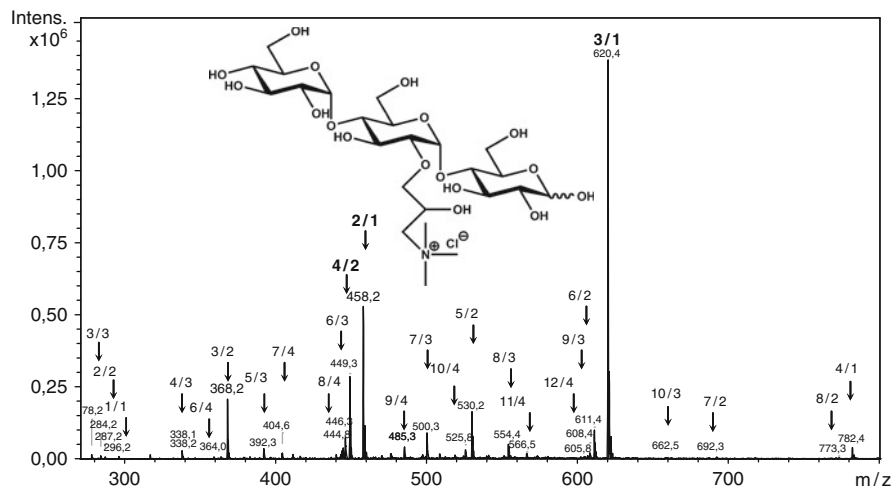
Fig. 41 ESI-MS and ESI-MS^2 of O-(2-hydroxypropyl-3-trimethylammonium) maltooligosaccharides obtained from cationic starch (DS 0.24) by enzymatic hydrolysis with α-amylase and amyloglucosidase. Signals are assigned with the DP (*first number*), and the number of cationic substituents (*n, second number*). The main product (3/1) is a monosubstituted maltotriose, for which a structure example is given. Fragmentation of 3/1 is shown in Fig. 42

Therefore, the enhanced B_2/Y_2 ratio and the occurrence of B_1 in the daughter spectrum of the monosubstituted maltotriose undoubtedly indicate the acceptance of substitution at the +1 and +2 cleavage sites of the *exo*-enzyme amyloglucosidase. With respect to the *endo*-enzyme α-amylase, tolerance of substitution at the −2 and −3 cleavage sites can be revealed from the ESI-CID-MS data. Cationic starches have also been studied by HPAEC-MS after enzymic hydrolysis [178].

6.4   Carbohydrate-Based Block Copolymers: Determination of Block Length

Another semisynthetic type of oligo- or polysaccharide is presented by copolymers prepared by cationic ring-opening polymerization (CROP) from cyclodextrin derivatives as macromonomers. In nature, block structures can be produced by certain enzymes, e.g., in alginates. These polyuronic acids are formed by postmodification of a β-1,4-D-mannuronan by inversion at C-5, thus forming α-1,4-guluronic acids which, depending on the type of enzyme, can be distributed in random, regular, or block-like patterns [23, 162].

No real multiblock polysaccharide structures can be established using chemical modification, and the number of monomer patterns from the eight possible ones (see Fig. 32) can only be reduced by temporary protection of one or two OH
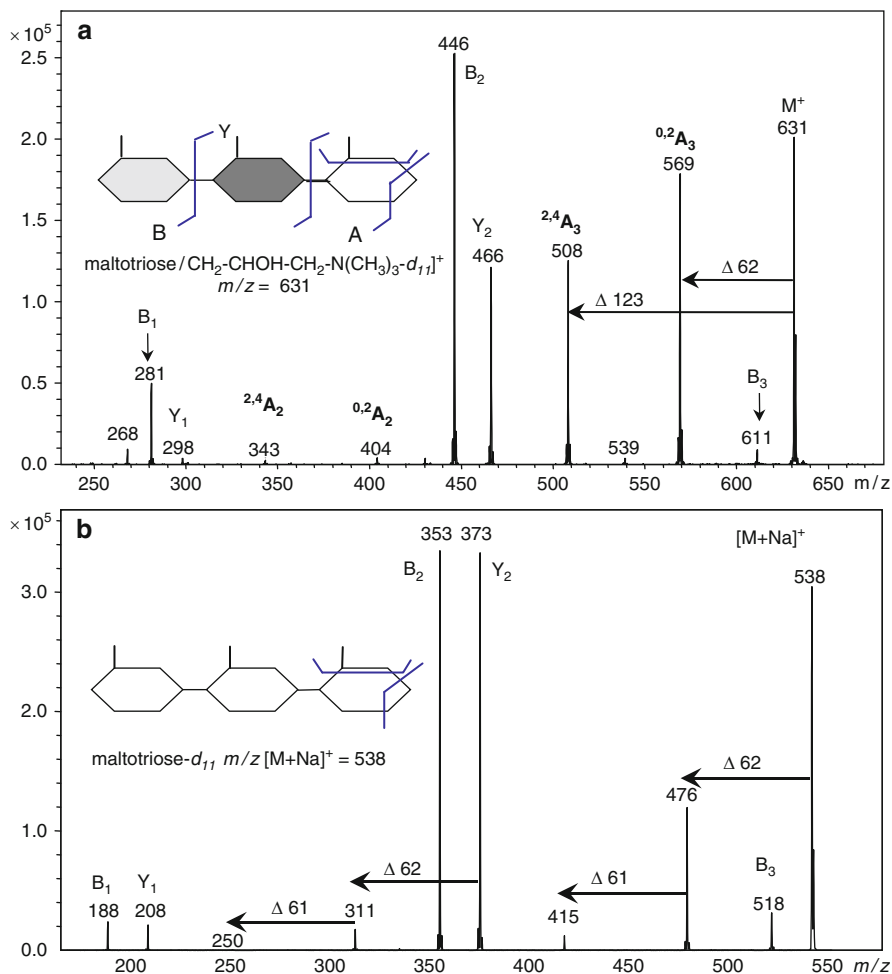
Fig. 42 ESI-MS^2 of (**a**) the mono-*O*-(2-hydroxy-3-trimethylammonium)propyl-maltotriose (3/1 in Fig. 40) obtained from cationic starch (DS 0.24) by enzymic degradation in D$_2$O and (**b**) of maltotriose

positions. However, since block structures are of great interest for model studies of e.g. gelation properties, cyclodextrin derivatives have been applied as macromonomers. Heptakis[2,3,6-tri-*O*-methyl]-cyclomaltoheptaose (A$_7$) and heptakis[2,3,6-tri-*O*-methyl-*d$_3$*]-cyclomaltoheptaose (B$_7$) were polymerized using various catalysts [186–188]. In addition to NMR spectroscopy, MS is also a very powerful method for analyzing the block length of such products. The polymer obtained was partially degraded and the oligomeric products measured with ESI-MS. From the ratio of AA, AB/BA, and BB dimers the average block lengths were calculated. In an early stage of the reaction the block length was 14 (2 × 7), as
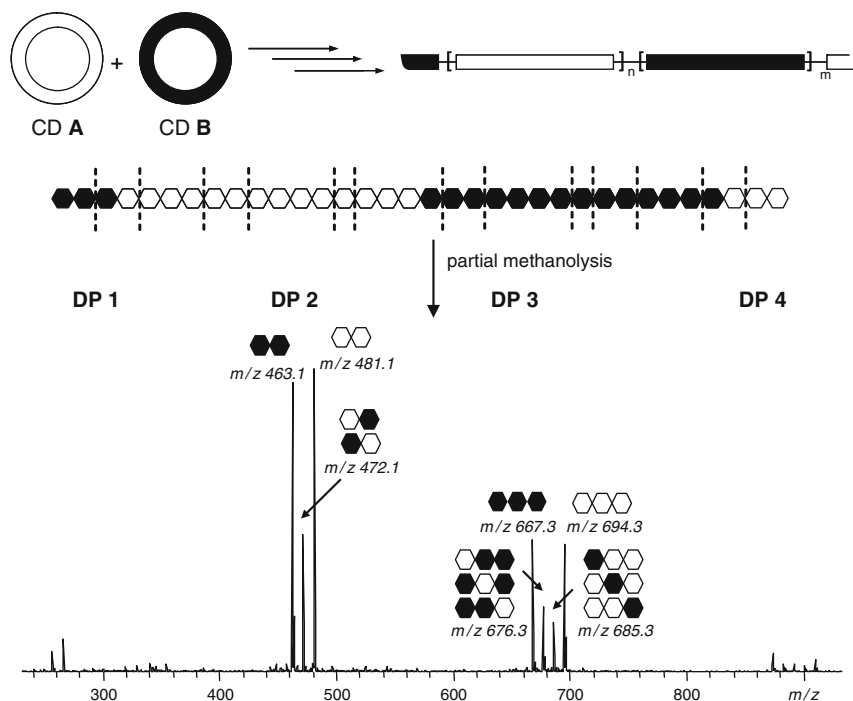
Fig. 43 *Above*: Synthesis of multiblock glucan derivatives by cationic ring-opening polymerization of cyclodextrins as macromonomers. *Below*: Principle of determination of block length in $(A_nB_m)_x$ copolymers by ESI-MS according to Bösch et al. (for details see [186–188])

expected from theory. However, block length rapidly decreased because transglycosidation randomized the original block structure in a competing process, which dominated as soon as the substrate had been consumed. Figure 43 shows the corresponding reaction, MS, and evaluation scheme.

With respect to the accuracy of this method, two sources of error must be emphasized. First of all, in the case of incomplete conversion, residual substrate must be carefully removed, since its partial hydrolysis will produce only AA and BB sequences and thus cause too-high apparent block lengths. Second, the new glucosidic linkages formed in the polymerization process preferably show β-configuration, while the starting material is α-linked. However, hydrolysis rates for α- and β-glycosides are different [189]. Faster cleavage of β-linkages will cause enrichment of homogeneous AA and BB α-rich dimers at a high degree of degradation; consequently the block lengths are observed too high. Therefore, short and harsh hydrolysis conditions should be applied to suppress selectivity. Furthermore, it should be mentioned that end groups are neglected in the calculation of block length. Therefore, the DP must be high enough to justify this. Otherwise, terminal residues should be labeled for differentiation from the inner chain residues.

7 Conclusion and Outlook

Impressive progress has been achieved in mass spectrometric analysis of complex carbohydrates during the last decades. On the instrumental side, speed, sensitivity, and resolution have increased at the same time as detailed knowledge on fragmentation mechanisms has been gained. How fragmentation pathways can be influenced by, e.g., appropriate labeling procedures or complexation has been established. In addition, in the popular and important field of glycoconjugate analysis, significant progress has been achieved for plant and bacterial polysaccharides. The analysis of substituent distribution in polysaccharide derivatives has also immensely profited from these new possibilities. It is expected that this trend will continue during the coming years, generating algorithms for automated data evaluation, improving quantifiability, and refining techniques for separation and differentiation of isobars and isomers, e.g., by making use of the topological effects on ion mobility. Such progress will allow more differentiated and higher throughput analysis, which could produce sufficient data for the statistical evaluation of substitution patterns in complex mixtures of polysaccharide derivatives. Further development of complexing agents and labeling procedures for specific fragmentation pathways in CID will probably improve and extend the applicability of sequence analysis, still a tedious and challenging endeavor.

References

1. Pfenninger A, Karas M, Finke B, Stahl B (2002) Structural analysis of underivatized neutral human milk oligosaccharides in the negative ion mode by nano-electrospray MS^n (part 1: methodology). J Am Soc Mass Spectrom 13:1331–1340
2. Pfenninger A, Karas M, Finke B, Stahl B (2002) Structural analysis of underivatized neutral human milk oligosaccharides in the negative ion mode by nano-electrospray MS^n (part 2: application to isomeric mixtures). J Am Soc Mass Spectrom 13:1341–1348
3. Schmid D, Behnke B, Metzger J, Kuhn R (2002) Nano-HPLC-mass spectrometry and MEKC for the analysis of oligosaccharides from human milk. Biomed Chromatrogr 16:151–156
4. Dreisewerd K, Kölbl S, Peter-Katalinic J, Berkenkamp S, Pohlentz G (2006) Analysis of native milk oligosaccharides directly from thin-layer chromatography plates by matrix –assisted laser desorption/ionization orthogonal time-of-flight mass spectrometry with a glycerol matrix. J Am Soc Mass Spectrom 17:139–150
5. Spina E, Sturiale L, Romeo D, Impallomeni G, Garozzo D, Waidelich D, Glueckmann M (2004) New fragmentation mechanisms in matrix-assisted laser desorption/ionization time-of-flight/time-of-flight tandem mass spectrometry of carbohydrates. Rapid Commun Mass Spectrom 18:392–398
6. Chen G, Pramanik BN, Bartner PK, Saksena AK, Gross ML (2002) Multiple-stage mass spectrometric analysis of complex oligosaccharide antibiotics (everninomicins) in a quadrupole ion trap. J Am Soc Mass Spectrom 13:1313–1321

7. Harvey DJ (2011) Analysis of carbohydrates and glycoconjugates by matrix-assisted laser desorption/ionization mass spectrometry: an update for the period 2005–2006. Mass Spectrom Rev 30:1–100

8. Harvey DJ (2009) Analysis of carbohydrates and glycoconjugates by matrix-assisted laser desorption/ionization mass spectrometry: an update for 2003–2004. Mass Spectrom Rev 28:273–361

9. Harvey DJ (2008) Analysis of carbohydrates and glycoconjugates by matrix-assisted laser desorption/ionization mass spectrometry: an update covering the period 2001–2002. Mass Spectrom Rev 27:125–201

10. Harvey DJ (2006) Analysis of carbohydrates and glycoconjugates by matrix-assisted laser desorption/ionization mass spectrometry: an update covering the period 1999–2000. Mass Spectrom Rev 25:595–662

11. Kirsch S, Bindila L (2009) Nano-LC and HPLC-chip-ESI-MS: an emerging technique for glycobioanalysis. Bioanalysis 1:1307–1327

12. Huhn C, Selman MHJ, Ruhaak LR, Deelder AM, Wuhrer M (2009) IgG glycosylation analysis. Proteomics 9:882–913

13. Ruhaak LR, Deelder AM, Wuhrer M (2009) Oligosaccharide analysis by graphitized carbon liquid chromatography-mass spectrometry. Anal Bioanal Chem 394:163–174

14. Grice ID, Wilson JC (2009) Analytical approaches towards the structural characterization of microbial wall glycopolymers. In: Moran AP, Holst O, Brennan PJ, von Itzstein M (eds) Microbial glycobiology: structures, relevance and applications. Academic, Oxford, pp 233–252

15. Harvey DJ (2005) Structural determination of N-linked glycans by matrix-assisted laser desorption/ionization and electrospray ionization mass spectrometry. Proteomics 5:1774–1786

16. Harvey DJ (2005) Proteomic analysis of glycosylation: structural determination of N- and O-linked glycans by mass spectrometry. Proteomics 2:87–101

17. Harvey DJ (1999) Matrix-assisted laser desorption/ionization mass spectrometry of carbohydrates. Mass Spectrom Rev 18:349–450

18. Harvey DJ (2003) Matrix-assisted laser desorption/ionization mass spectrometry of carbohydrates and glycoconjugates. Int J Mass Spectrom 226:1–35

19. Zaia J (2004) Mass spectrometry of oligosaccharides. Mass Spectrom Rev 23:161–227

20. Jang-Lee J, North SJ, Sutton-Smith M, Goldberg D, Panico M, Morris H, Haslam S, Dell A (2006) Glycomic profiling of cells and tissues by mass spectrometry: fingerprinting and sequencing methodologies. Methods Enzymol 415:59–86

21. Haslam SM, North SJ, Dell A (2006) Mass spectrometric analysis of N- and O-glycosylation of tissues and cells. Curr Opin Struct Biol 16:584–591

22. Campa C, Coslovi A, Flamigni A, Rossi M (2006) Overview on advances in capillary electrophoresis-mass spectrometry of carbohydrates: a tabulated review. Electrophoresis 27:2027–2050

23. Mischnick P, Momcilovic D (2010) Structure analysis of starch and cellulose derivatives. Adv Carbohydr Chem Biochem 64:117–210

24. Short LC, Syage JA (2008) Electrospray photoionization (ESPI) liquid chromatography/ mass spectrometry for the simultaneous analysis of cyclodextrin and pharmaceuticals and their binding interactions. Rapid Commun Mass Spectrom 22:541–548

25. Zhang H, Zhang H, Qu C, Bai L, Ding L (2007) Fluorimetric and mass spectrometric study of the interaction of β-cyclodextrin and osthole. Spectrochim Acta A Mol Biomol Spectrosc 68A:474–477

26. Kensinger RD, Yowler BC, Benesi AJ, Schengrund C-L (2004) Synthesis of novel, multivalent glycodendrimers as ligands for HIV-1 gp120. Bioconjug Chem 15:349–358

27. Han S, Yoshida T, Uryu T (2007) Synthesis of a new polylysine-dendritic oligosaccharide with alkyl spacer having peptide linkage. Carbohydr Polym 69:436–444

28. Kebarle P, Verkerk UH (2009) Electrospray: from ions in solution to ions in the gas phase: what we know now. Mass Spectrom Rev 28:898–917, and references cited herein

29. Rodrigues JA, Taylor AM, Sumpton DP, Reynolds JC, Pickford R, Thomas-Oates J (2007) Mass spectrometry of carbohydrates: newer aspects. Adv Carbohydr Chem Biochem 62:58–141

30. Zhou S, Cook KC (2001) A mechanistic study of electrospray mass spectrometry: charge gradients within electrospray droplets and their influence on ion response. J Am Soc Mass Spectrom 12:206–214

31. Cole RB (2010) Electrospray and MALDI mass spectrometry, 2nd edn. Wiley-VCH, Weinheim

32. De Hoffmann E, Stroobant V (2007) Mass spectrometry, 3rd edn. Wiley-VCH, Weinheim

33. Hillenkamp F, Peter-Katalinic J (eds) (2007) MALDI MS. Wiley-VCH, Weinheim

34. Clowers BH, Dwivedi P, Steiner WE, Hill HH Jr (2005) Separation of sodiated isobaric disaccharides and trisaccharides using electrospray ionization atmospheric pressure ion mobility-time of flight mass spectrometry. J Am Soc Mass Spectrom 16:660–669

35. Von Helden G, Wyttenbach T, Bowers MT (1995) Inclusion of a MALDI ion source in the ion chromatography technique: conformational information on polymer and biomolecular ions. Int J Mass Spectrom Ion Proc 146(147):349–364

36. Wyttenbach T, Von Helden G, Bowers MT (1997) Conformations of alkali ion cationized polyethers in the gas phase: polyethylene glycol and bis[(benzo-15-crown-5)-15-ylmethyl] pimelate. Int J Mass Spectrom Ion Proc 165(166):377–390

37. Schmidt A, Karas M, Dülcks T (2003) Effect of different solution flow rates on analyte ion signals in nano-ESI MS, or: when does ESI turn into nano-ESI? J Am Chem Soc Mass Spectrom 14:492–500

38. Bahr U, Pfenninger A, Karas M, Stahl B (1997) High-sensitivity analysis of neutral underivatized oligosaccharides by nanoelectrospray mass spectrometry. Anal Chem 69:4530–4535

39. Blair SM, Kempen EC, Brodbelt JS (1998) Determination of binding selectivities in host-guest complexation by electrospray/quadrupole ion trap mass spectrometry. J Am Soc Mass Spectrom 9:1049–1059, and references cited herein

40. Lee S, Wyttenbach T, Von Helden G (1995) Gas phase conformations of Li+, Na+, K+, and Cs + complexes with 18-crown-6. J Am Chem Soc 117:10159–101560

41. Hofmeister GE, Zhou Z, Leary JA (1991) Linkage position determination in lithium-cationized disaccharides: tandem mass spectrometry and semiempirical calculations. J Am Chem Soc 113:5964–5970

42. Reale S, Teixido E, De Angelis F (2005) Study of alkali metal cations binding selectivity of β-cyclodextrin by ESI-MS. Ann Chim 95:375–381

43. Reinhold VN, Reinhold BB, Costello CE (1995) Carbohydrate molecular weight profiling; sequence, linkages, and branching data: ES-MS and CID. Anal Chem 67:1772–1784

44. Harvey DJ (2000) Collison-induced fragmentation of underivatized N-linked carbohydrates ionized by electrospray. J Mass Spectrom 35:1178–1190

45. Harvey DJ (2001) Ionization and collision-induced fragmentation of N-linked and related carbohydrates using divalent cations. J Am Soc Mass Spectrom 12:926–937

46. Harvey DJ (2005) Ionization and fragmentation of N-linked glycans as silver adducts by electrospray mass spectrometry. Rapid Commun Mass Spectrom 19:484–492

47. Desaire H, Leary JA (1999) Differentiation of diastereomeric N-acetylhexosamine monosaccharides using ion trap tandem mass spectrometry. Anal Chem 71:1997–2002

48. Gaucher SP, Leary JA (1998) Stereochemical differentiation of mannose, glucose, galactose, and talose using zinc(II) diethylenetriamine and ESI-ion trap mass spectrometry. Anal Chem 70:3009–3014

49. Desaire H, Laevell MD, Leary JA (2002) Solvent effects in tandem mass spectrometry: mechanistic studies indicating how a change in solvent conditions an pH can dramatically alter CID spectra. J Org Chem 67:3693–3699

50. Dole M, Mack LL, Hines RL, Mobley RC, Ferguson LS, Alice MB (1968) Molecular beams of macroions. J Chem Phys 49:2240–2249

51. Iribarne JV, Thomson BA (1976) On the evaporation of small ions from charged droplets. J Chem Phys 64:2287–2294

52. Kebarle P, Tang L (1993) From ions in solution to ions in the gas phase. Anal Chem 65: A972–A986
53. Harvey DJ (2005) Fragmentation of negative ions from carbohydrates: part 1. use of nitrate and other anionic adducts for the productions of negative ion electrospray spectra from N-linked carbohydrates. J Am Soc Mass Spectrom 16:622–630
54. Harvey DJ (2005) Fragmentation of negative ions from carbohydrates: part 2. Fragmentation of high-mannose N-linked glycans. J Am Soc Mass Spectrom 16:631–646
55. Harvey DJ (2005) Fragmentation of negative ions from carbohydrates: part 3. Fragmentation of hybrid and complex N-linked. J Am Soc Mass Spectrom 16:647–659
56. Harvey DJ, Jaeken J, Butler M, Armitage AJ, Rudd PM, Dwek RA (2010) Fragmentation of negative ions from N-linked carbohydrates: Part 4. Fragmentation of complex glycans lacking substitution on the 6-antenna. J Am Soc Mass Spectrom 45:528–535
57. Harvey DJ, Royle L, Radcliffe CM, Rudd PM, Dwek RA (2008) Structural and quantitative analysis of N-linked glycans by matrix-assisted laser desorption ionization and negative ion nanospray mass spectrometry. Anal Biochem 376:44–60
58. Lamari FN, Kuhn R, Karamanos NK (2003) Derivatization of carbohydrates for chromatographic, electrophoretic and mass spectrometric structure analysis. J Chromatogr B 793:15–36
59. Ruhaak LR, Zauner G, Huhn C, Bruggink C, Deelder AM, Wuhrer M (2010) Glycan labeling strategies and their use in identification and quantification. Anal Bioanal Chem 397:3457–3481
60. Harvey DJ (2000) Electrospray mass spectrometry and fragmentation of N-linked carbohydrates derivatized at the reducing terminus. J Am Soc Mass Spectrom 11:900–915
61. Nicotra F, Cipolla L, Peri F, Ferla BL, Redaelli C, Derek H (2007) Chemoselective neoglycosylation. Adv Carbohydr Chem Biochem 61:353–398
62. You J, Sheng X, Ding D, Sun Z, Suo Y, Wang H, Li Y (2008) Detection of carbohydrates using new labeling reagent 1-(2-naphthyl)-3-methyl-5-pyrazolone by capillary zone electrophoresis with absorbance (UV). Anal Chim Acta 609:66–75
63. Gouw JW, Burgers PC, Trikoupis MA, Terlouw JK (2002) Derivatization of small oligosaccharides prior to analysis by matrix-assisted laser desorption/ionization using glycidyltrimethylammonium chloride and Girard's reagent T. Rapid Commun Mass Spectrom 16:905–912
64. Naven TJP, Harvey DJ (1996) Cationic derivatization of oligosaccharides with Girard's T reagent for improved performance in matrix-assisted laser desorption/ionization and electrospray mass spectrometry. Rapid Commun Mass Spectrom 10:829–834
65. Gil G-C, Kim Y-G, Kim B-G (2008) A relative and absolute quantification of neutral N-linked oligosaccharides using modification with carboxymethyl trimethylammonium hydrazide and matrix-assisted laser desorption/ionization time-of-flight mass spectrometry. Anal Biochem 379:45–59
66. Jang K-S, Kim Y-G, Gil G-C, Park S-H, Kim B-G (2009) Mass spectrometric quantification of neutral and sialylated N-glycans from a recombinant therapeutic glycoprotein produced in the two Chinese hamster ovary cell lines. Anal Biochem 386:228–236
67. Unterieser I, Mischnick P (2011) Labeling of oligosaccharides for quantitative mass spectrometry. Carbohydr Res 346:68–75
68. Takeda Y (1979) Determination of sugar hydrazide and hydrazone structures in solution. Carbohydr Res 77:9–23
69. Girard A, Sandulesco G (1936) Sur une nouvelle série de réactifs du groupe carbonyle, leur utilisation à l'extraction des substances cétoniques et à la caractérisation microchimique des aldéhydes et cétones. Helv Chim Acta 19:1095–1107
70. Gudmundsdottir AV, Nitz M (2007) Hydrolysis rates of 1-glucosyl-2-benzoylhydrazines in aqueous solution. Carbohydr Res 342:749–752
71. Gudmundsdottir AV, Paul CE, Nitz M (2009) Stability studies of hydrazide and hydroxylamine-based glycoconjugates in aqueous solution. Carbohydr Res 344:278–284
72. Sato K, Sato K, Okubo A, Yamazaki S (1998) Optimization of derivatization with 2-aminobenzoic acid for determination of monosaccharide composition by capillary electrophoresis. Anal Biochem 262:195–197

73. Zhang Y, Huang L-J, Wang Z-F (2007) A sensitive derivatization method for the determination of the sugar composition after pre-column reductive amination with 3-amino-9-ethylcarbazole (AEC) by high-performance liquid chromatography. Chin J Chem 25:1522–1528
74. Bigge JC, Patel TP, Bruce JA, Goulding PN, Charles SM, Parekh RB (1995) Nonselective and efficient fluorescent labeling of glycans using 2-amino benzamide and anthranilic acid. Anal Biochem 230:229–238
75. Borch RF, Bernstein MD, Durst HD (1971) Cyanohydridoborate anion as a selective reducing agent. J Am Chem Soc 93:2897–2904
76. Sun Z, Wei Z, Wei K (2009) A model for predicting the optimal conditions for labeling the carbohydrates with the amine derivatives by reductive amination. Lett Org Chem 6:549–551
77. Xia B, Feasley CL, Sachdev GP, Smith DF, Cummings RD (2009) Glycan reductive isotope labeling for quantitative glycomics. Anal Biochem 387:162–170
78. Ruhaak LR, Steenvoorden E, Koeleman CAM, Deelden AM, Wuhrer M (2010) 2-Picoline-borane: a non-toxic reducing agent for oligosaccharide labeling by reductive. Proteomics 10:2330–2336
79. Schellenberg KA (1963) The synthesis of secondary and tertiary amines by borohydride reduction1. J Org Chem 28:3259–3261
80. Zapala L, Kalembkiewicz J, Sitarz-Palczak E (2009) Studies on equilibrium of anthranilic acid in aqueous solutions and in two-phase systems: aromatic solvent-water. Biophys Chem 140:91–98
81. Anumula KR, Dhume ST (1998) High resolution and high sensitivity methods for oligosaccharide mapping and characterization by normal phase high performance liquid chromatography following derivatization with highly fluorescent anthranilic acid. Glycobiology 8:685–694
82. Harvey DJ (2005) Halogeno-substituted 2-aminobenzoic acid derivatives for negative ion fragmentation studies of N-linked carbohydrates. Rapid Commun Mass Spectrom 19:397–400
83. Maslen SL, Goubet F, Adam A, Dupree P, Stephens E (2007) Structure elucidation of arabinoxylan isomers by normal phase HPLC-MALDI-TOF/TOF-MS/MS. Carbohydr Res 342:724–735
84. Harvey DJ (2005) Collision-induced fragmentation of negative ions from N-linked glycans derivatized with 2-aminobenzoic acid. J Mass Spectrom 40:642–653
85. Gennaro LA, Delaney J, Vouros P, Harvey DJ, Domon B (2002) Capillary electrophoresis/electrospray ion trap mass spectrometry for the analysis of negatively charged derivatized and underivatized glycans. Rapid Commun Mass Spectrom 16:192–200
86. Doliška A, Strnad S, Ribitsch V, Kleinschek K, Willför S, Saake B (2009) Analysis of galactoglucomannans from spruce wood by capillary electrophoresis. Cellulose 16:1089–1097
87. Yuen CT, Gee CK, Jones C (2002) High-performance liquid chromatographic profiling of fluorescent labelled N-glycans on glycoproteins. Biomed Chromatogr 16:247–254
88. Gennaro LA, Harvey DJ, Vouros P (2003) Reversed-phase ion-pairing liquid chromatography/ion trap mass spectrometry for the analysis of negatively charged, derivatized glycans. Rapid Commun Mass Spectrom 17:1528–1534
89. Pabst M, Kolarich D, Pöltl G, Dalik T, Lubec G, Hofinger A, Altmann F (2009) Comparison of fluorescent labels for oligosaccharides and introduction of a new postlabeling purification method. Anal Biochem 384:263–273
90. Adden R, Müller R, Mischnick P (2006) Analysis of the substituent distribution in the glucosyl units and along the polymer chain of hydroxypropylmethylcelluloses and statistical evaluation. Cellulose 13:459–476
91. Adden R, Niedner W, Müller R, Mischnick P (2006) Comprehensive analysis of the substituent distribution in the glucosyl units and along the polymer chain of hydroxylethylmethylcelluloses and statistical evaluation. Anal Chem 78:1146–1157
92. Karas M, Hillenkamp F (1988) Laser desorption ionization of proteins with molecular masses exceeding 10,000 daltons. Anal Chem 60:2299–2301

93. Tanaka K, Ido Y, Akita S, Yoshida Y, Yoshida T, Matsuo T (1988) Protein and polymer analyses up to m/z 100,000 by laser ionization time-of-flight mass spectrometry. Rapid Commun Mass Spectrom 2:151–153

94. Fenn JB, Mann M, Meng CK, Wong SF (1989) Electrospray ionization for mass spectrometry of large biomolecules. Science 246(4926):64–71

95. Nielen MWF (1999) MALDI time-of-flight mass spectrometry of synthetic polymers. Mass Spectrom Rev 18:309–344

96. Deery MJ, Stimson E, Chappell CG (2001) Size exclusion chromatography/mass spectrometry applied to the analysis of polysaccharides. Rapid Commun Mass Spectrom 15:2273–2283

97. Garozzo D, Impallomeni G, Spina E, Sturiale L, Zanetti F (1995) Matrix-assisted laser desorption/ionization mass spectrometry of polysaccharides. Rapid Commun Mass Spectrom 9:937–941

98. Yeung B, Marecak D (1999) Molecular weight determination of hyaluronic acid by gel filtration chromatrography coupled to matrix-assisted laser desorption ionizaton mass spectrometry. J Chromatogr A 852:573–581

99. Hsu N-Y, Yang W-B, Wong C-H, Lee Y-C, Lee RT, Wang Y-S, Chen C-H (2007) Matrix-assisted laser desorption/ionization mass spectrometry of polysaccharides with 2',4',6'-trihydroxyacetophenone as matrix. Rapid Commun Mass Spectrom 21:2137–2146

100. Schnöll-Bitai I, Ullmer R, Hrebicek T, Rizzi A, Lacik I (2008) Characterization of the molecualr mass distribution of pullulans by matrix-assisted laser desorption/ionization time-of-flight mass spectrometry using 2,5-dihydroxy-benzoic acid butylamine (DHBB) as liquid matrix. Rapid Commun Mass Spectrom 22:2961–2970

101. Stahl B, Linos A, Karas M, Hillenkamp F, Streup M (1997) Analysis of fructans from higher plants by matrix-assisted laser desorption/ioniszation mass spectrometry. Anal Biochem 246:195–204

102. Haská L, Nyman M, Andersson R (2008) Distribution and characterisation of fructan in wheat milling fractions. J Cereal Sci 48:768–774

103. Jacobs A, Dahlman O (2001) Characterization of the molar masses of hemicelluloses from wood and pulps employing size exclusion chromatography and matrix-assisted laser desorption ionization time-of-flight mass spectrometry. Biomacromolecules 2:894–905

104. Jacobs A, Lundqvist J, Stålbrand H, Tjerneld F, Dahlman O (2002) Characterization of water-soluble hemicelluloses from spruce and aspen employing SEC/MALDI mass spectroscopy. Carbohydr Res 337:711–717

105. Kenne L, Lönngren J, Svensson S (1973) A new method for specific degradation of polysaccharides. Acta Chem Scan 27:3692–3698

106. Jansson PE, Kenne L, Lindberg B, Ljunggren H, Lonngren J, Ruden U, Svensson S (1977) Demonstration of an octasaccharide repeating unit in the extracellular polysaccharide of Rhizobium meliloti by sequential degradation. J Am Chem Soc 99:3812–3815

107. Spina E, Cozzolino R, Ryan E, Garozzo D (2000) Sequencing of oligosaccharides by collision-induced dissociation matrix-assisted laser desorption/ionization mass spectrometry. J Mass Spectrom 35:1042–1048

108. Jennings K (1968) Collision-induced decompositions of aromatic molecular ions. Int J Mass Spectrom Ion Phys 1:227–235

109. Domon B, Costello CE (1988) A systematic nomenclature for carbohydrate fragmentations in FAB-MS/MS spectra of glycoconjugates. Glycoconjugate J 5:397–409

110. Garozzo G, Impallomeni E, Spina E, Green BN, Hutton T (1991) Linkage analysis in disaccharides by electrospray mass spectrometry. Carbohydr Res 221:253–257

111. Friedl CH, Lochnit G, Geyer R, Karas M, Bahr U (2000) Elucidation of zwitterionic sugar cores from glycosphingolipids by nanoelectrospray ionization-ion-trap mass spectrometry. Anal Biochem 284:279–287

112. Tüting W, Wegemann K, Mischnick P (2004) Enzymatic degradation and electrospray tandem mass spectrometry as tools for determining the structure of cationic starches prepared by wet and dry methods. Carbohydr Res 339:637–648

113. Viseux N, de Hoffmann E, Domon B (1998) Structural assignment of permethylated oligosaccharide subunits using sequential tandem mass spectrometry. Anal Chem 70:4951–4959

114. McNeil M (1983) Elimination of internal glycosyl residues during chemical ionization-mass spectrometry of per-O-alkylated oligosaccharide-alditols. Carbohydr Res 123:31–40

115. Kovácik V, Hirsch J, Kovác P, Heerma W, Thomas-Oates J, Haverkamp J (1995) Oligosaccharide characterization using collision-induced dissociation fast atom bombardment mass spectrometry. J Mass Spectrom 30:949–958

116. Brüll LP, Heerma W, Thomas-Oates J, Haverkamp J, Kovácik V, Kovác P (1997) Loss of internal 1 → 6 substituted monosaccharide residues from underivatized and per-O-methylated trisaccharides. J Am Soc Mass Spectrom 8:43–49

117. Brüll LP, Kovácik V, Thomas-Oates J, Heerma W, Haverkamp J (1998) Sodium-cationized oligosaccharides do not appear to undergo 'internal residue loss' rearrangement processes on tandem mass spectrometry. Rapid Commun Mass Spectrom 12:1520–1532

118. Ernst B, Müller DR, Richter WJ (1997) False sugar sequence ions in electrospray tandem mass spectrometry of underivatized sialyl-Lewis-type oligosaccharides. Int J Mass Spectrom Ion Proc 160:283–290

119. Harvey DJ, Mattu TS, Wormald MR, Royle L, Dwek A, Rudd PM (2002) "Internal residue loss": rearrangements occurring during the fragmentation of carbohydrates derivatized at the reducing terminus. Anal Chem 74:734–774

120. Ma Y-L, Vedernikova I, Van den Heuvel H, Claeys M (2000) Internal glucose residue loss in protonated O-diglycosyl flavonoids upon low-energy collision-induced dissociation. J Am Soc Mass Spectrom 11:136–144

121. Van der Burgt YEM, Bergsma J, Bleeker IP, Mijland PJHC, Van der Kerk-van HA, Kamerling JP, Vliegenthart JFG (2000) FAB CIDMS:MS analysis of partially methylated maltotrioses derived from methylated amylose: a study of the substituent distribution. Carbohydr Res 329:341–349

122. Cancilla MT, Penn SG, Caroll JA, Lebrilla CB (1996) Coordination of alkali metals to oligosaccharides dictates fragmentation behavior in matrix assisted laser desorption ionization/Fourier transform mass spectrometry. J Am Chem Soc 118:6736–6745

123. Botek E, Debrun JL, Hakim B, Morin-Allory L (2001) Attachment of alkali cations on β-D-glucopyranose: matrix-assisted laser desorption/ionization time-of-flight studies and ab initio calculations. Rapid Commun Mass Spectrom 15:273–276

124. Cancilla MT, Wong AW, Voss LR, Lebrilla CB (1999) Fragmentation reactions in the mass spectrometry analysis of neutral oligosaccharides. Anal Chem 71:3206–3218

125. Adams J (1990) Charge-remote fragmentations: analytical applications and fundamental studies. Mass Spectrom Rev 9:141–186

126. Mechref Y, Novotny V, Krishnan C (2003) Structural characterization of oligosaccharides using MALDI-TOF/TOF tandem mass spectrometry. Anal Chem 75:4895–4903

127. Spengler B, Dolce JW, Cotter RJ (1990) Infrared laser desorption mass spectrometry of oligosaccharides: fragmentation mechanisms and isomer analysis. Anal Chem 62:1731–1737

128. Momcilovic D, Schagerlöf H, Wittgren B, Wahlund K-G, Brinkmalm G (2005) Improved chemical analysis of cellulsoe ethers using dialkylamine derivatization and mass spectrometry. Anal Chem 77:2948–2959

129. Momcilovic D, Schagerlöf H, Röme D, Jörntén-Karlsoon M, Karlsson K-E, Wittgren B, Tjerneld F, Wahlund K-G, Brinkmalm G (2005) Novel derivatisation using dimethylamine for tandem mass spectrometric structure analysis of enzymatically and acidically depolymerised methyl cellulose. Biomacromolecules 6:2793–2799

130. Adden R, Mischnick P (2005) A novel method for the analysis of the substitution pattern of O-methyl- α- and β-1,4-glucans by means of electrospray ionisation-mass spectrometry/collision induced dissociation. Int J Mass Spectrom 242:63–73

131. Tüting W, Adden R, Mischnick P (2004) Fragmentation pattern of regioselectively O-methylated maltooligosaccharides in electrospray ionisation-mass spectrometry/collision induced dissociation. Int J Mass Spectrom 232:107–115

132. Enebro J, Momcilovic D, Siika-aho M, Karlsson S (2009) Liquid chromatography combined with mass spectrometry for investigation of endoglucanase selectivity on carboxymethyl cellulose. Carbohydr Res 344:2173–2181

133. Lemoine J, Fournet B, Despeyroux D, Jennings KR, Rosenberg R, de Hoffmann E (1993) Collision-induced dissociation of alkali metal cationized and permethylated oligosaccharides: influence of the collision energy and of the collision gas for the assignment of linkage position. J Am Soc Mass Spectrom 4:197–203

134. Muzikar J, Mechref Y, Huang Y, Novotny MV (2004) Enhanced post-source decay and cross-ring fragmentation of oligosaccharides facilitated by conversion to amino derivatives. Rapid Commun Mass Spectrom 18:1513–1518

135. Sheeley DM, Reinhold VN (1998) Structural characterization of carbohydrate sequence, linkage, and branching in quadrupole ion trap mass spectrometer: neutral oligosaccahrides and N-linkes glycans. Anal Chem 70:3053–3059

136. Ashline D, Singh S, Hanneman A, Reinhold V (2005) Congruent strategies for carbohydrate sequencing. 1. Mining structural details by MS^n. Anal Chem 77:6250–6262

137. Zhang H, Singh S, Reinhold VN (2005) Congruent strategies for carbohydrate sequencing. 2. FragLib: an MS^n spectral library. Anal Chem 77:6263–6270

138. Lapadula AJ, Hatcher PJ, Hanneman AJ, Ashline DJ, Zhang H, Reinhold VN (2005) Congruent strategies for carbohydrate sequencing. 3. OSCAR: an algorithm for assigning oligosaccharide topology from MS^n data. Anal Chem 77:6271–6279

139. Ashline DJ, Lapadula AJ, Liu Y-H, Lin M, Grace M, Pramanik B, Reinhold VN (2007) Carbohydrae structural isomers analyzed by sequential mass spectrometry. Anal Chem 79:3830–3842

140. Reinhold VN, Lapadula AJ, Ashline DJ, Zhang H (2008) Systems and methods for sequencing carbohydrates by mass spectrometry. PCT International Patent Application WO 2008027599 A2

141. Cheng HL, Her GR (2002) Determination of linkages of linear and branched oligosaccharides using closed-ring-chromophore labeling and negative ion trap mass spectrometry. J Am Soc Mass Spectrom 13:1322–1330

142. Sible EM, Brimmer SP, Leary JA (1997) Interaction of first row transition metals with a 1–3, a 1–6 mannotriose, and conserved trimannosyl core oligosaccharides: a comparative electrospray ionization study of doubly and singly charged complexes. J Am Chem Soc 8:32–42

143. König SR, Leary JA (1998) Evidence for linkage position determination in cobalt coordinated pentasaccharides using ion trap mass spectrometry. J Am Chem Soc Mass Spectrom 9:1125–1134

144. Matamoros Fernandéz LE, Obel N, Scheller HV, Roepstorff P (2004) Differentiation of isomeric oligosaccharide structures by ESI tandem MS and GC-MS. Carbohydr Res 339:655–664

145. Matamoros Fernandéz LE, Obel N, Scheller HV, Roepstorff P (2003) Characterization of plant oligosaccharides by matrix-assisted laser desorption/ionization and electrospray mass spectrometry. J Mass Spectrom 38:427–437

146. Matamoros Fernandéz LE, Sorensen HR, Jorgensen C, Pedersen S, Meyer AS, Roepstorff P (2007) Characterization of oligosaccharides from industrial fermentation residues by matrix-assisted laser desorption/ionization, electrospray mass spectrometry, and gas chromatography mass spectrometry. Mol Biotechnol 35:149–160

147. Hilz H, De Jong LE, Mabel MA, Schols HA, Voragen AGJ (2006) A comparison of liquid chromatography, capillary electrophoresis, and mass spectrometry methods to determine xyloglucan structures in black currants. J Chromatogr A 1133:275–286

148. Okatch H, Torto N, Armateifio J (2003) Characterisation of legumes by enzymatic hydrolysis, microdialysis sampling, and micro-high-performance anion-exchange chromatrography with electrospray ionization mass spectrometry. J Chromatogr A 992:67–74

149. Körner R, Limberg G, Mikkelsen JD, Roepstorff P (1998) Characterization of enzymatic pectin digests by matrix-assisted laser desorption/ionization mass spectrometry. J Mass Spectrom 33:836–842

150. Guillaumie F, Justesen SFL, Mutenda KE, Roepstorff P, Jensen KJ, Thomas ORT (2006) Fractionation, solid-phase immobilization and chemical degradation of long pectin oligogalacturonides. Initial steps towards sequencing of oligosaccharides. Carbohydr Res 341:118–129

151. Naven TJP, Harvey DJ (1996) Effect of structure on the signal strength of oligosaccharides in matrix-assisted laser desorption/ionization mass spectrometry on time-of-flight and magnetic sector instruments. Rapid Commun Mass Spectrom 10:1361–1366

152. Harvey DJ (1993) Quantitative aspects of the matrix-assisted laser desorption mass spectrometry of complex oligosaccharides. Rapid Commun Mass Spectrom 7:614–619

152a. Unterieser I, Cuers J, Voiges K, Enebro J, Mischnick P (2011) Quantitative aspects in electrospray ionization ion trap and matrix-assisted laser desorption/ionization time-of-flight mass spectrometry of maltooligosaccharides. Rap Commun Mass Spectrom 25:2201–2208. DOI:10.1002/rcm.5105

153. Haebel S, Bahrke S, Peter MG (2007) Quantitative sequencing of complex mixtures of heterochitooligosaccharides by vMALDI linear ion trap mass spectrometry. Anal Chem 79:5557–5566

154. Ogawa K, Yamaura M, Maruyama I (1994) Isolation and identification of 3-O-methyl-D-galactose as a constituent of a neutral polysaccharides of C*hlorella vulgaris*. Biosci Biotech Biochem 58:942–944

155. Ogawa K, Yamaura M, Maruyama I (1997) Isolation and identification of 2-O-methyl-L-rhamnose and 3-O-methyl-L-rhamnose as constituents of an acidic polysaccharide of C*hlorella vulgaris*. Biosci Biotech Biochem 61:539–540

156. Aspinall GO (1982) The polysaccharides. Academic, New York

157. De Ruiter GA, Bruggen-van V, der Lugt AW, Mischnick P, Smid P, Van Boom JH, Notermans SH, Rombouts FM (1994) 2-O-methyl-D-mannose residues are immunodominant in extracellular polysaccharides of Mucor racemosus and related molds. J Biol Chem 269:4299–4306

158. Dönges R (1990) Non-ionic cellulose ethers. Brit Polym J 23:315–326

159. Klemm D, Philipp B, Heinze T, Heinze U, Wagenknecht W (1998) Comprehensive cellulose chemistry: vol 1 fundamentals and analytical methods, vol 2 functionalization of cellulose. Wiley VCH, Weinheim

160. Wurzburg OB (ed) (1986) Modified starches: properties and uses. CRC, Boca Raton

161. Heinze T, Liebert T, Heublein B, Hornig S (2006) Functional polymers based on dextrans. Adv Polym Sci 205:199–291

162. Mischnick P, Kühn G (1996) Correlation between reaction conditions and primary structure: model studies on methyl amylose. Carbohydr Res 290:199–207

163. Mischnick P, Hennig C (2001) A new model for the substitution patterns in the polymer chain of polysaccharide derivatives. Biomacromolecules 2:180–184

164. Adden R, Müller R, Mischnick P (2006) Fractionation of methyl cellulose according to polarity - a tool to differentiate first and second order heterogeneity of the substituent distribution. Macromol Chem Phys 207:954–965

165. Mischnick P, Adden R (2008) Fractionation of polysaccharide derivatives and subsequent analysis to differentiate heterogeneities on various hierarchical levels. Macromol Symp 262:1–7

166. Mischnick P (2001) Challenges in structure analysis of polysaccharide derivatives. Cellulose 8:245–257

167. Mischnick P, Heinrich J, Gohdes M, Wilke O, Rogmann N (2000) Structure analysis of 1,4-glucan derivatives macromol. Chem Phys 201:1985–1995

168. Adden R, Melander C, Brinkmalm G, Gorton L, Mischnick P (2006) New approaches to the analysis of enzymatically hydrolyzed methyl cellulose. part 1. Investigation of structural parameters on the extent of degradation. Biomacromolecules 7:1399–1409
169. Melander C, Adden R, Brinkmalm G, Gorton L, Mischnick P (2006) New approaches to the analysis of enzymatically hydrolyzed methyl cellulose. Part 2. Comparison of various enzyme preparations. Biomacromolecules 7:1410–1421
170. Kochetkov NK, Chizov OS (1971) Mass spectrometry of carbohydrate derivatives. Adv Carbohydr Chem 21:29–38
171. Mischnick P, Niedner W, Adden R (2005) Possibilities of mass spectrometry and tandem-mass spectrometry in the analysis of cellulose ethers. Macromol Symp 223:67–77
172. Cuers J, Unterieser I, Adden R, Rinken M, Mischnick P (2011) Analysis of the substituent pattern in cellulose ethers by quantitative HPLC-ESI-MS. Abstracts SCM5, Amsterdam
173. Vollmer A, Voiges K, Bork C, Fiege K, Cuber K, Mischnick P (2009) Comprehensive analysis of the substitution pattern in dextran ethers with respect to the reaction conditions. Anal Bioanal Chem 395:1749–1768
174. Arisz P, Kauw HJJ, Boon JJ (1995) Substituent distribution along the cellulose backbone in O-methylcelluloses using GC and FAB MS for monomer and oligomer analysis. Carbohydr Res 271:1–14
175. Heinrich J, Mischnick P (1999) Determination of the substitution pattern in the polymer chain of cellulose acetates. J Polym Sci A Polym Chem 37:3011–3016
176. Gohdes M, Mischnick P (1998) Determination of the substitution pattern in the polymer chain of cellulose sulfates. Carbohydr Res 309:109–115
177. Adden R, Müller R, Brinkmalm G, Ehrler R, Mischnick P (2006) Comprehensive analysis of the substituent distribution in hydroxyethyl celluloses by quantitative MALDI-TOF-MS. Macromol Biosci 6:435–444
178. Richardson S, Nilsson G, Cohen A, Momcilovic D, Brinkmalm G, Gorton L (2003) Enzyme-aided investigation of the substituent distribution in cationic potato amylopectin starch. Anal Chem 75:6499–6508
179. Mischnick P (2001) Selectivity in enzymic degradation of methyl amylose. Starch/Stärke 53:110–120
180. Momcilovic D, Wittgren B, Wahlund K-G, Karlsson J, Brinkmalm G (2003) Sample preparation effects in matrix-assisted laser desorption/ionisation time-of-flight mass spectrometry of partially depolymerized carboxymethyl cellulose. Rapid Commun Mass Spectrom 17:1107–1115
181. Enebro J, Karlsson S (2006) Improved matrix-assisted laser desorption/ionisation time-of-flight mass spectrometry of carboxymethylcellulose. Rapid Commun Mass Spectrom 20:3693–3698
182. Schagerlöf U, Schagerlöf H, Momcilovic D, Brinkmalm G, Tjerneld F (2007) Endoglucanase sensitivity for substituents in methyl cellulose hydrolysis studied using MALDI-TOFMS for oligosaccharide analysis and structural analysis of enzyme active sites. Biomacromolecules 8:2358–2365
183. Enebro J, Momcilovic D, Siika-aho M, Karlsson S (2007) A new approach for studying correlations between the chemical structure and the rheological properties in carboxymethyl cellulose. Biomacromolecules 8:3253–3257
184. Enebro J, Momcilovic D, Siika-aho M, Karlsson S (2009) Investigation of endoglucanase selectivity on carboxymethyl cellulose by mass spectrometric techniques. Cellulose 16:271–280
185. Momcilovic D, Wittgren B, Wahlund K-G, Karlsson J, Brinkmalm G (2003) Sample preparation effects in matrix-assisted laser desorption/ionisation time-of-flight mass spectrometry of partially depolymerised methyl cellulose. Rapid Commun Mass Spectrom 17:1116–1124

186. Adden R, Bösch A, Mischnick P (2004) Novel possibilities by cationic ring-opening polymerisation of cyclodextrin derivatives: preparation of a copolymer bearing block-like sequences of Tri-*O*-methyl-glucosyl units. Macromol Chem Phys 205:2072–2079
187. Bösch A, Nimtz M, Mischnick P (2006) Mechanistic studies on cationic ring-opening polymerization of cyclodextrin derivatives using various Lewis acids. Cellulose 13:493–507
188. Bösch A, Mischnick P (2007) Bifunctional building blocks for glyco-architectures by TiCl₄-promoted ring opening of cyclodextrin derivatives. Biomacromolecules 8:2311–2320
189. Capon B (1969) Mechanism in carbohydrate chemistry. Chem Rev 69:407–498

Electrospray Ionization–Mass Spectrometry for Molecular Level Understanding of Polymer Degradation

Minna Hakkarainen

Abstract The stability and durability of polymeric materials under different external influences (e.g., sunlight, humidity, heat, chemicals, or microorganisms) is of outmost importance in applications such as coatings, building materials, and automotive parts, whereas a rapidly degradable material is preferable in temporary short-term applications. There are considerable economic and environmental benefits if we can design polymers for short or long lifetimes as well as prevent the release of harmful substances from the materials during their lifetime. The recent developments in mass spectrometric techniques facilitate possibilities for molecular level characterization of the changes taking place in the polymer matrix as well as for identification of the released degradation products. This review presents an overview of the application of electrospray ionization–mass spectrometry (ESI-MS) for the analysis of polymer degradation. The great potential of the technique for revealing detailed insights into the degradative reactions taking place is demonstrated with examples ranging from degradable polymers and biomaterials to degradation of coatings, paints, polymer electrolyte membranes, food packaging, and materials in the nuclear industry.

M. Hakkarainen (✉)
Department of Fibre and Polymer Technology, School of Chemical Science and Engineering, Royal Institute of Technology (KTH), 100 44 Stockholm, Sweden
e-mail: minna@polymer.kth.se

Contents

Abbreviations

APCI-MS	Atmospheric pressure chemical ionization–mass spectrometry
a-PHB	Atactic poly(3-hydroxybutyrate)
APPI-MS	Atmospheric pressure photoionization–mass spectrometry
ATC	Acetyl tributyl citrate
BPA	Bisphenol A
CE	Capillary electrophoresis
CL	Caprolactone
CPLA	Cyclic polylactide
DESI-MS	Desorption ionization–mass spectrometry
EHA	2-Ethylhexyl-(4-dimethylamino)benzoate
EPR	Electron paramagnetic resonance
ESBO	Epoxidized soybean oil
ESI-MS	Electrospray ionization–mass spectrometry
FTIR	Fourier transform infrared
GC-MS	Gas chromatography–mass spectrometry
HALS	Hindered amine light stabilizer
HPLC	High performance liquid chromatography
ITX	Isopropylthioxanthone
LA	Lactide
LC	Liquid chromatography
MALDI	Matrix-assisted laser desorption ionization
MS	Mass spectrometry

MS^n	Multistage mass spectrometry
NMR	Nuclear magnetic resonance
PA	Polyacrylate
PBTA	Poly(1,4-butylene terephthalate)-*co*-(1,4-butylene adipate)
PCL	Polycaprolactone
PDLA	Poly(D-lactide)
PDXO	Poly(1,5-dioxepan-2-one)
PEG	Poly(ethylene glycol)
PHA	Polyhydroxyalkanoate
PHB	Poly(3-hydroxybutyrate)
PHBV	Poly(3-hydroxybutyrate-*co*-3-hydroxyvalerate)
PLA	Polylactide
PLLA	Poly(L-lactide)
PMMA	Polymethacrylate
PP-R	Polypropylene random copolymer
PTMG	Poly(tetramethylene glycol)
PVC	Poly(vinyl chloride)
TELNR	Telechelic epoxidized liquid natural rubber
TOF	Time-of-flight
UPLC	Ultra-performance liquid chromatography

1 Introduction

Depending on the application, the ideal lifetime of a polymeric product could vary from weeks to years. The stability and durability of polymeric materials during thermo-or photo-oxidation or under other external influences is of outmost importance in applications such as coatings, building materials, and automotive parts, whereas a rapidly degradable material is preferable in temporary short-time applications. There are considerable economic and environmental benefits if we can design polymers for short or long lifetimes as well as prevent the release of harmful substances from the materials during their lifetime. Mass spectrometry (MS) allows analysis of polymer microstructures, end-groups and molecular weights of the individual chains, information not obtained by other techniques. In polymer degradation studies, developments in mass spectrometric techniques can provide us with molecular level information about the smallest changes taking place in the polymeric materials as well as about the identity of the formed degradation products. During their lifecycle, polymeric materials are subjected to different harmful environments including high temperatures, chemicals, oxygen, sunlight, microorganisms, and/or humidity. Degradative reactions can take place during synthesis and processing of the materials and later during, e.g., the use outdoors or in contact with food, body fluids, or other corrosive liquids. Here the utilization of novel mass spectrometric techniques could provide better understanding of the influence of various environmental parameters on different polymeric

materials as well as an understanding of the stabilization mechanisms of antioxidants and light stabilizers. This in turn will provide tools for the development of materials for optimum lifetimes, whether we desire stable and durable materials or environmentally benign degradable materials.

In the 1980s it became possible to ionize large molecules into the gas phase, and soft ionization techniques like matrix-assisted laser desorption ionization–mass spectrometry (MALDI-MS) and electrospray ionization–mass spectrometry (ESI-MS) appeared. Recent developments in these techniques and MS of polymers in general have been reviewed in several papers [1–3]. Even though MALDI-MS has been more widely utilized for polymer characterization, in some applications ESI-MS poses advantages over MALDI-MS. It is easier to interface ESI-MS with separation techniques like liquid chromatography (LC) to provide both MS-based structural information, separation of the compound mixtures, and quantitative information from the LC analysis. ESI-MS analysis has also been shown to be more effective than MALDI-MS for determination of end-groups due to lower noise levels, absence of matrix ion interferences at lower m/z region and more effective ionization [4], and there are already many examples of the utilization of ESI–tandem mass spectrometry (ESI-MS/MS) and LC-ESI-MS/MS for the end-group characterization [5, 6]. ESI-MS has been applied for structural characterization of polymers in a number of studies, including monitoring of reaction pathways and detection of degradation reactions taking place during synthesis [7, 8]. Another very interesting and increasingly important application is the characterization of different biopolymers as well as their derivatives and hydrolysates [9, 10]. ESI-MS has not yet been widely utilized in polymer degradation studies even though the potential of the technique is great. In many cases, polymers are aged or used in different aqueous solutions, which could be analyzed by ESI-MS directly or after concentration and/or purification steps. This review presents an overview of the application of ESI-MS for the analysis of polymer degradation. The great power of the technique in providing deeper understanding of the degradation reactions is demonstrated with examples ranging from degradable polymers and biomaterials to degradation of coatings, paints, polymer electrolyte membranes, food packaging, and materials in the nuclear industry.

2 Degradation of Degradable Polymers and Biomaterials

Aliphatic polyesters are among the most promising materials for tissue engineering and degradable packaging applications. In both cases, the thorough understanding of degradation mechanisms, lifetime prediction and mapping of low molecular weight migrants is of outmost importance to ensure the safe use of the materials and their complete degradation to environmentally friendly products. Gas chromatography–mass spectrometry (GC-MS) [11, 12] and LC [13] have been successfully applied for identification and quantification of hydrolysis and biodegradation products. Both of these methods have their own advantages and limitations.

ESI-MS has emerged as an alternative effective and rapid tool for structural characterization of polyesters and copolyesters [14]. It also allows mapping of the whole water-soluble degradation product patterns up to molecular weights of 2,000 Da. Interesting ESI-MS work has also been performed to understand the molecular level structures of complex natural polyesters like suberin [15] and of linear and branched poly(ω-hydroxyacid) esters from plant cutins [16]. The main advantage of ESI-MS is the ease of sample preparation as the aging water can in many cases be directly analyzed after, e.g., addition of methanol. The technique also allows the analysis of longer water-soluble oligomers.

2.1 Side Reactions and Degradation During Synthesis of Polyesters

The physical properties of bacterial polyhydroxyalkanoates (PHA)s can be changed by addition of acids of different lengths. ESI-MS analysis has made it possible to show the incorporation of longer hydroxyacid units into the PHA chain during bacterial synthesis [17]. The analysis proved that PHAs could be synthesized from odd carbon atom *n*-alkanoic acids ranging from heptanoic to heptadecanoic acid. Ether bond fragmentation resulting in unsaturated end-groups was shown to take place during ring-opening polymerization of poly(1,5-dioxepan-2-one) (PDXO) at temperatures above 140 °C [18]. The formed double bonds could be further utilized for synthesis of crosslinked PDXO. ESI-MS also demonstrated the formation of vinyl ether end-groups during Na_2CO_3 promoted polymerization of poly(ethylene glycol) (PEG) [19].

Recently, a quantitative method for direct determination of residual monomers after polyester synthesis by ESI-MS was proposed [20]. This method allowed rapid quantification of terephthalic acid and sebacic acid after synthesis of copolyesters. Methanol was used to extract the monomers and 1,12-dodecanedioic acid was utilized as internal standard. The method was validated by comparing the obtained results with high performance liquid chromatography (HPLC) analysis. The detection limits were between 0.01 and 0.03 ppm. ESI-MS also showed that cyclization had taken place during synthesis of hydroxylated hyperbranched polyesters of fourth and fifth generation [21]. These cyclic structures were not detectable by nuclear magnetic resonance (NMR).

LC-MS and ESI-MS/MS methods were developed for the determination of low molecular weight cyclic polylactides (CPLA), which are formed as side-products during synthesis of polylactide (PLA) and could also be added to modify material properties [22]. The introduction of these cyclic compounds into the human body through migration from PLA biomaterials is undesirable as they may have negative effects such as lowering of the activity of pyruvate kinase and lactic hydrogenase. Linear and CPLA oligomers and their solvolysis products were also characterized by ESI-MS [23]. The study showed that solvolysis of the cyclic oligomers took
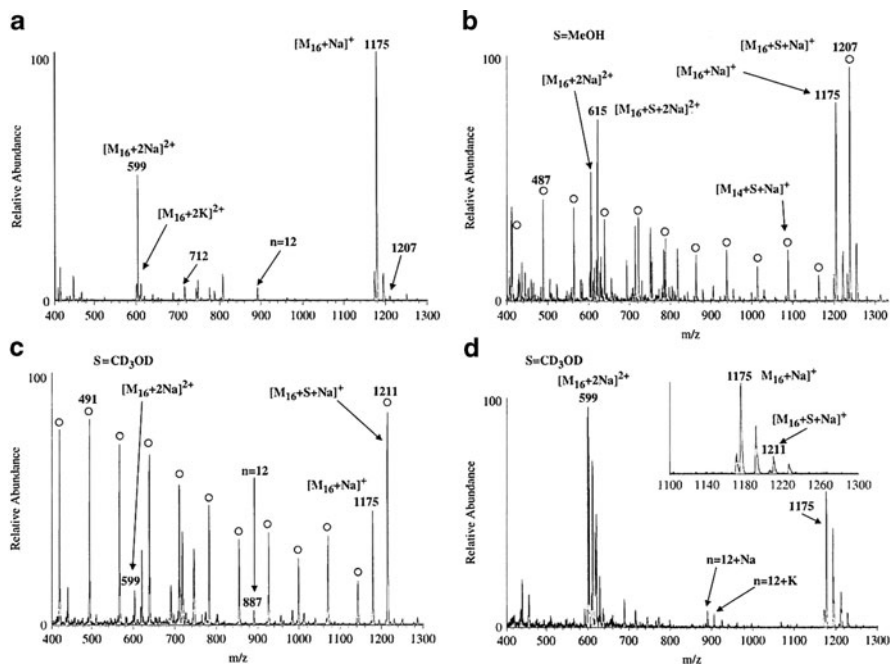
Fig. 1 ESI-MS spectrum obtained immediately after dissolving uniform CPLA ($n = 16$) in anhydrous MeOH (**a**). ESI spectrum of the solution after having been left standing for 1 day in anhydrous MeOH (**b**), CD$_3$OD (**c**), or 1/1 H$_2$O/CD$_3$OD (**d**). Reprinted from [23] with permission. Copyright 2006 John Wiley & Sons

place during overnight contact with anhydrous methanol and after shorter contact at an elevated temperature. This reaction resulted in appearance of methylated linear oligomers in the ESI-MS spectra (see Fig. 1). The reaction was, however, impeded by the presence of even small amounts of water. The presence of cyclic structures in poly(butylene adipate-*co*-butylene terephthalate) copolymers was also shown by LC-MS and LC-MS^n [24]. During aging in aqueous tetrabutylammonium hydroxide/methanol solution, these oligomers underwent methanol trans-esterification and formed linear oligomers with methyl ester end groups.

2.2 Effect of Copolymer Microstructure and Composition on Hydrolytic Degradation

ESI-MS clearly demonstrated the effect of microstructure and composition on the hydrolytic degradation pathways of polyesters and revealed molecular level information concerning the degradation process and susceptibility of different ester bonds [25]. The hydrolytic degradation of glycolide/caprolactone copolymer in

pH 7.4 phosphate buffer showed that not only the copolymer composition but also the microstructure influenced the degradation process. The ester bonds between the different monomer units seemed to be more susceptible to hydrolysis, leading to higher hydrolysis rate for more random copolymers, which could be partly related to the degree of crystallinity in the samples. The combination of high-resolution NMR spectroscopy and ESI-MS allowed detailed molecular level mapping of the degradation processes and release of degradation products from glycolide/caprolactone copolymers [26]. The influence of copolymer structure and crystallinity was evaluated in the compositions ranging from 70/30 to 30/70 glycolide/caprolactone. With the help of ESI-MS it was possible to follow in detail at molecular level the accumulation and/or further hydrolysis of water-soluble degradation products with different compositions and sequence distributions. The changes in the distribution of different oligomers during hydrolysis were demonstrated by illustrative planar projections.

The large effect of polymer architecture together with hydrophilicity of the monomeric building blocks was also clearly shown by ESI-MS analysis of hydrolysis products of different polycaprolactone (PCL) and PDXO copolymers [27]. In the case of the DXO–PCL–DXO triblock copolymers, the hydrophilic DXO blocks were rapidly hydrolyzed and released to the aging water, whereas the hydrolysis rate for the PCL blocks was similar to that for the PCL homopolymer. The more random distribution of the "weak" DXO linkages on the other hand also accelerated the hydrolysis of PCL sequences. This is clearly demonstrated in Fig. 2, which shows an expansion of the region m/z 1,040–1,320 from the mass spectra of the hydrolysis products of multi-and triblock copolymers. In the case of the triblock copolymer, the main hydrolysis products were the linear DXO oligomers, while mixed CL/DXO oligomers were released from the more random multiblock structures. The hydrophilicity of the building blocks is important for controlling the hydrolysis rate because it both regulates the water uptake by the materials and largely influences the water solubility of the resulting hydrolysis products.

2.3 Effect of Crosslinking on Hydrolytic Degradation

Following the hydrolysis process of crosslinked materials is complicated as the possible analyses are limited by the non-solubility of the material. Here, ESI-MS analysis of the water soluble products proved to be a valuable tool [28]. The hydrolytic degradation of crosslinked CL and/or DXO networks was followed and the results clearly showed differences in the hydrolytic degradation rate depending on the copolymer composition. At low degrees of degradation, the products patterns mainly consisted of linear CL and/or DXO oligomers, while at later stages oligomers with attached crosslinking agent were detected showing the point where the network structure started to disrupt. Figures 3 and 4 show, as an example, the water-soluble product patterns for crosslinked PCL homopolymer at low degree of degradation and at a later stage where oligomers with crosslinking
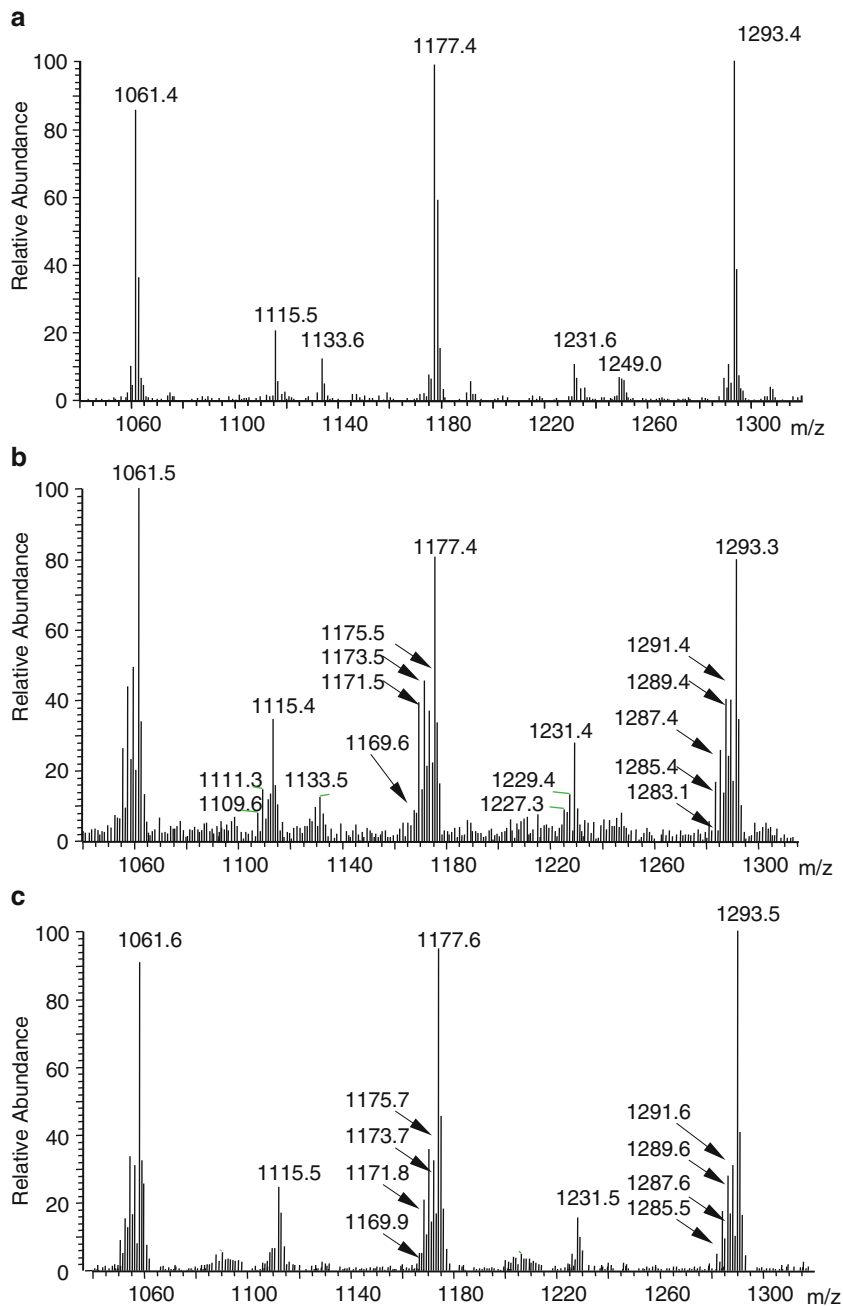
Fig. 2 Expanded region *m/z* 1,040–1,320 of the ESI-MS spectra of degradation products from
(**a**) 60/40 CL/DXO triblock copolymer, (**b**) 60/40 CL/DXO multiblock copolymer, and (**c**) 75/25
CL/DXO multiblock copolymer. Reprinted from [27] with permission. Copyright 2008 American
Chemical Society
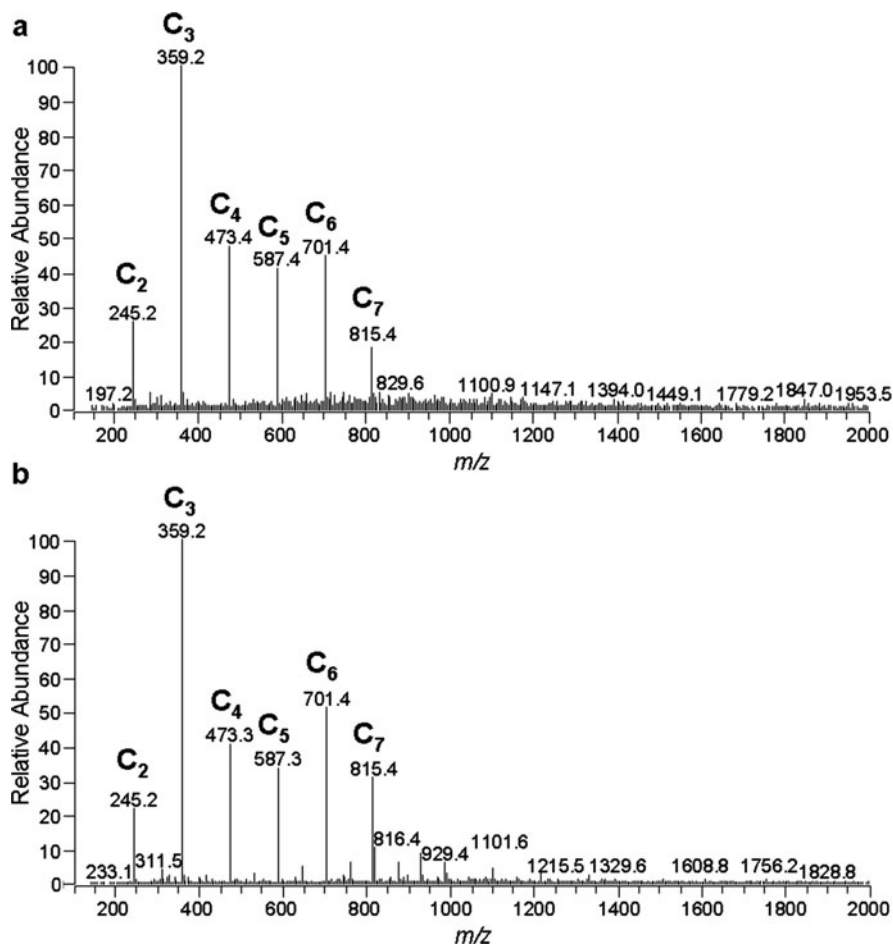
Fig. 3 Negative ESI-MS spectra of hydrolysis products from crosslinked PCL after (**a**) 1 day and (**b**) 21 days of hydrolysis in water at 37 °C showing linear caprolactone oligomers from dimer to heptamer. Reprinted from [29] with permission. Copyright 2008 John Wiley & Sons

agent are also detected. In another study PCL with acrylate end groups was crosslinked with amino-telechelic poly(tetrahydrofuran) and the in vitro degradation of the crosslinked PCL was evaluated by ESI-MS [28].

2.4 Effect of Blending on Hydrolytic Degradation

Several studies have applied ESI-MS to map the degradation process of PLA and different PLA modifications. Each material modification potentially affects the degradability, degradation rate, and degradation product patterns, which makes it
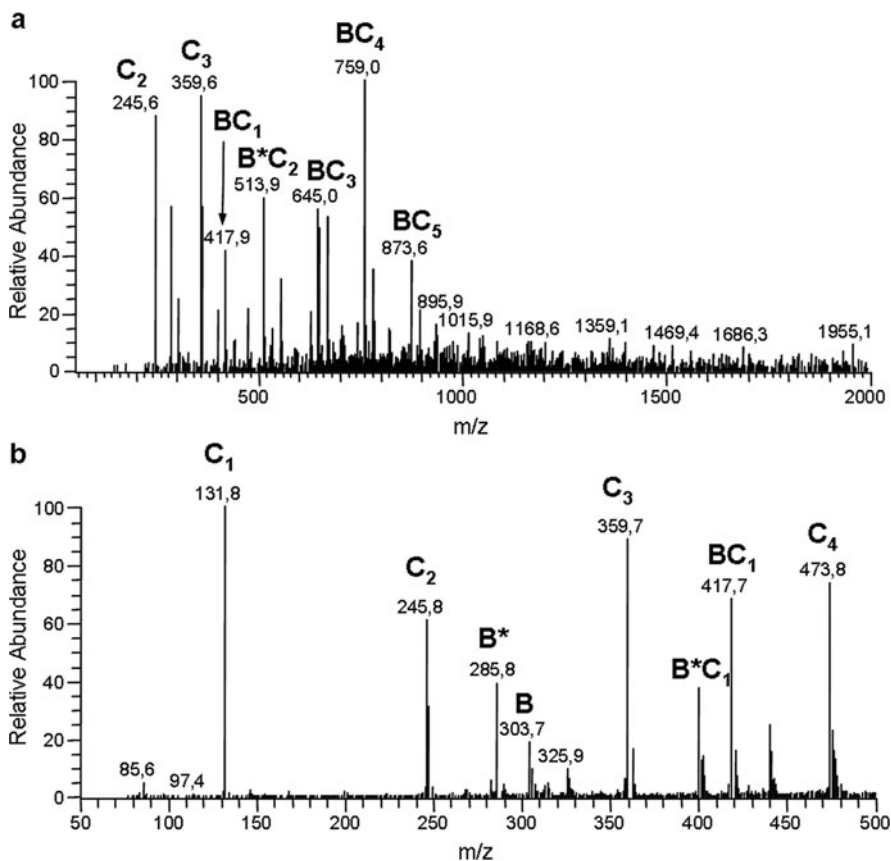
Fig. 4 Negative ESI-MS spectra of hydrolysis products from crosslinked PCL after 147 days of hydrolysis in water at 37 °C showing linear caprolactone oligomers as well as oligomers with the attached crosslinking agent (2,2′-bis(e-caprolactone-4-yl): (**a**) *m/z* 150–2,000 and (**b**) *m/z* 50–500. Reprinted from [28] with permission. Copyright 2008 John Wiley & Sons

crucial for the safe use of the materials to establish these relationships. The addition of new components in most cases introduces new migrants, or at least influences the product pattern and release rate of degradation products [30]. Interestingly, ESI-MS revealed that even modification with similar chemical structures could introduce important changes in the product patterns. As an example, the hydrolysis of PLA stereocomplex formed by blending of poly(L-lactide) (PLLA) and poly(D-lactide) (PDLA) resulted in the formation of shorter and more acidic lactic acid oligomers as degradation products [31]. Figure 5 presents ESI-MS spectra of hydrolysis products from PLLA and PLA stereocomplex. The spectra clearly show the differences in the product patterns. Even though the stereocomplex material was more stable than the plain PLLA and demonstrated much smaller mass loss during aging, the higher acidity of the released hydrolysis products led to a larger pH
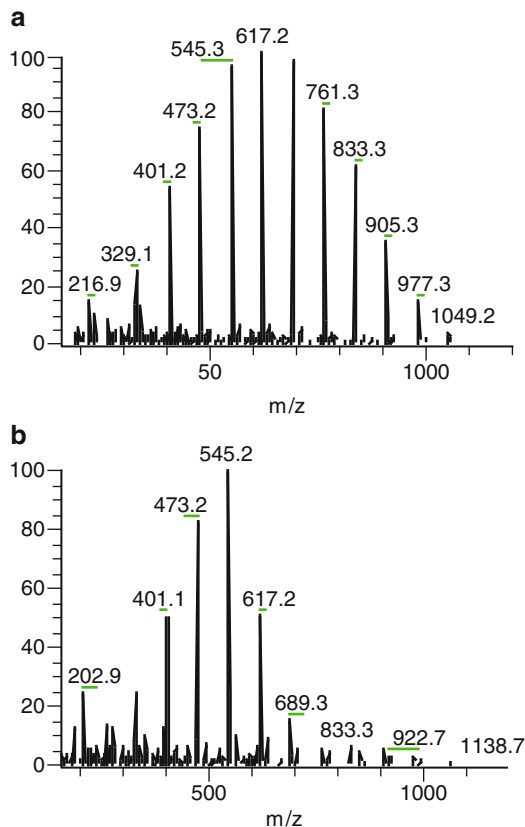
Fig. 5 Positive ESI-MS spectra showing the water-soluble degradation products of (**a**) PLLA and (**b**) PLLA/PDLA after hydrolysis in water for 13 weeks at 60 °C. Reprinted from [31] with permission. Copyright 2010 American Chemical Society

decrease for the stereocomplex material. Addition of plasticizers based on linear and cyclic lactic acids did not change the water-soluble product patterns, but ESI-MS showed significant differences in the release rate of these additives and the appearance of detectable water-soluble products [32]. The linear additives were water-soluble and started to migrate from the materials immediately after immersion in water. The cyclic structures on the other hand had first to be hydrolyzed before they could migrate into water.

In another study, a hydrophobic acetyl tributyl citrate (ATC) ester plasticizer was added to PLA [33]. The hydrophobic plasticizer partially prevented water-uptake by the materials and protected the PLA matrix against hydrolytic degradation. However, even though the water solubility of ATC is low, it was already detected in the aging solution by ESI-MS after 1 day of aging at 37 °C or 60 °C. On prolonged aging, hydrolysis of the plasticizer took place and various plasticizer degradation products were detected.

2.5   Effect of Substituents and Surface Modification on Hydrolytic Degradation

Hydrophilic material modification usually leads to faster hydrolysis rate, whereas hydrophobic modifications naturally decrease the degradation rate. ESI-MS analysis revealed that hydrophilic surface modification of PLA by acrylic acid accelerated the degradation rate and totally changed the water-soluble product patterns, which contained lactic acid and mixed acrylic acid grafted lactic acid oligomers [34]. Figure 6 illustrates the complex degradation product patterns after 28 days of hydrolytic degradation at 37 °C, which can be compared to the relatively simple pattern usually observed after hydrolysis of PLA (See Fig. 5a). For the surface-modified material, ESI-MS showed the appearance of water-soluble products already after 1 day at 60 °C or after 7 days at 37 °C. After hydrolysis of plain PLLA, the first water-soluble degradation products were detected after considerably longer aging times of 28 and 133 days at 60 °C and 37 °C, respectively. This effect can be partly due to the larger water uptake for the more hydrophilic material causing accelerated hydrolysis of the PLA matrix, but an even more important parameter is the high water solubility of the degradation products containing grafted acrylic acid. ESI-MS analysis also showed that hydrolytic degradation of hexyl-substituted PLAs led to the formation of oligoesters, and at later stages lactic acid and nontoxic 2-hydroxyoctanoic acid were formed [35].

2.6   Effect of Porosity on Hydrolytic Degradation

Acidic degradation products that are trapped into biomedical products can catalyze the hydrolysis process and lead to faster hydrolysis rates for thick specimens than for thin ones [36]. It could, thus, be expected that the hydrolysis of porous polyester scaffolds could proceed at lower rates compared to nonporous solid scaffolds [37]. Porosity and pore size were found to regulate the degradation rate and release rate of water-soluble degradation products from PLA scaffolds with over 90% porosity [38]. As expected, the solid PLA scaffolds had faster hydrolysis rates compared to the porous scaffolds and the hydrolysis rate decreased with decreasing pore size. This was also clearly reflected by the distribution of the oligomeric degradation product patterns determined by ESI-MS. However, somewhat unexpectedly, degradation products were detected earlier in the case of thicker solid PLA scaffolds, where the products could be trapped inside the films and their release into the aging solution could be delayed. Instead, the release of water-soluble products from the porous samples with very thin pore walls was delayed. This was attributed to the additional migration pathway within the porous structures and possible trapping of the hydrolysis products inside isolated pores.

Fig. 6 ESI-MS spectra showing the complex water-soluble product pattern after hydrolysis of acrylic acid grafted polylactide for 28 days at 37 °C): (**a**) *m/z* 200–2,000 and (**b**) *m/z* 200–1,000. Reprinted from [34] with permission. Copyright 2010 American Chemical Society
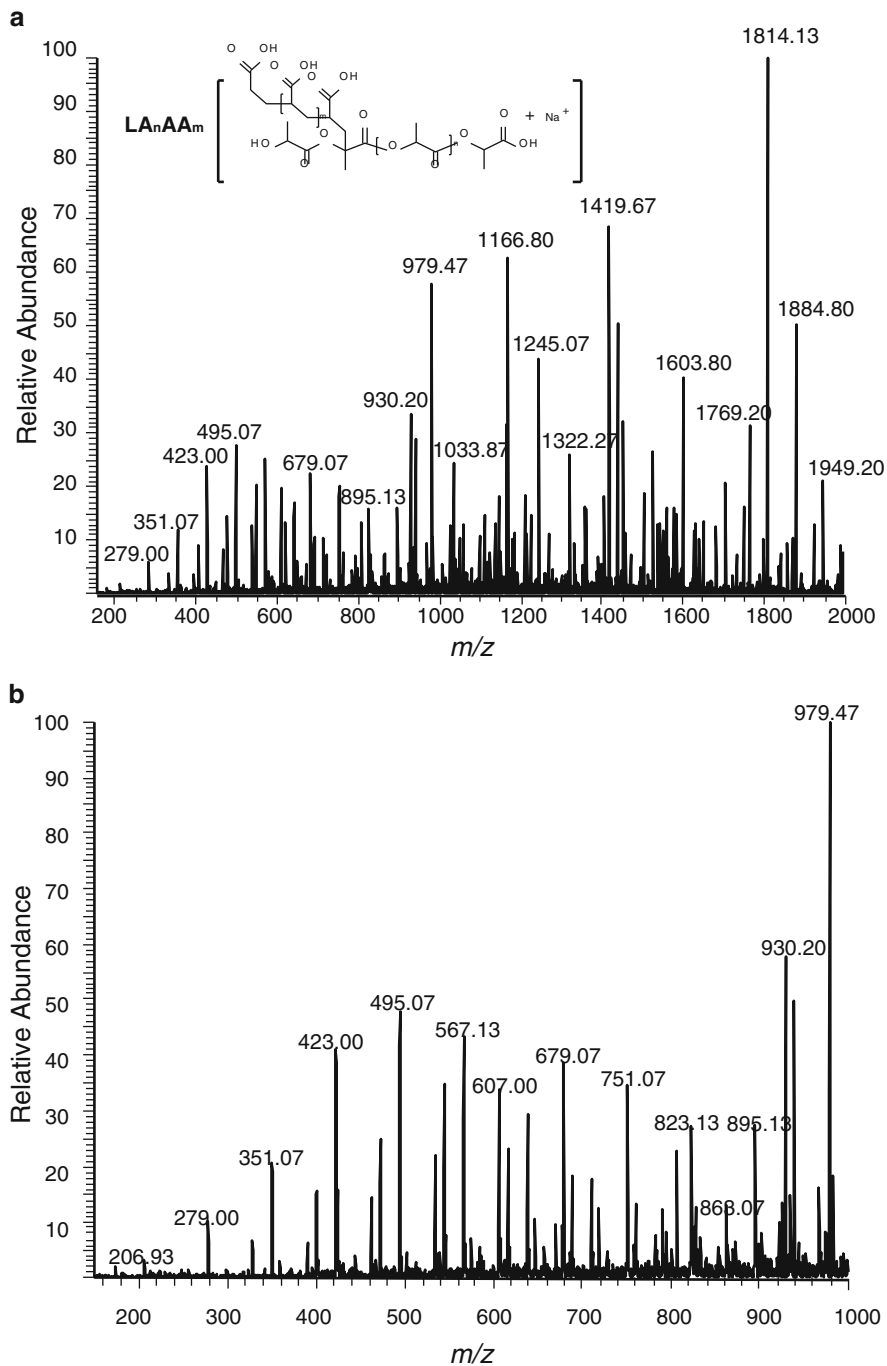
2.7   Biodegradation

Only a few studies so far have utilized ESI-MS for establishing biodegradation mechanisms of aliphatic or aliphatic–aromatic polyesters. The great potential of the technique is, however, clearly demonstrated by these studies. Formation of oligomers with up to seven repeating units was shown by ESI-MS, and atmospheric pressure chemical ionization–mass spectrometry (APCI-MS) analysis of enzymatically hydrolyzed blends of poly(3-hydroxybutyrate-*co*-3-hydroxyvalerate) (PHBV) and atactic poly(3-hydroxybutyrate) (a-PHB) [39]. The HPLC analysis of same samples only allowed identification of 3-hydroxybutyric acid and its dimer. Bioassimilation of water-soluble a-PHB oligomers ranging from dimer to dodecamer was also followed by ESI-MS [40]. These oligomers are analogous to PHB hydrolysis products. With the help of the ESI-MS analysis, utilization of these oligomers by two PHB degrading (*Alcaligenes faecalis* T1 and *Comamonas* sp) and one non-PHB degrading (*Ralstonia eutropha* H16) bacteria was shown, clearly indicating the total biodegradability of PHB in suitable natural environments. Poly(1,4-butylene terephthalate)-*co*-(1,4-butylene adipate) (PBTA) was aged in sandy soil for up to 22 months [41]. Even though PBTA is compostable under industrial composting processes, only limited degradability was shown in standardized sandy soil where disintegration and partial mineralization of PBTA was observed. The total mass loss after 22 months was only around 50%. After aging, the low molecular weight fraction was collected from size-exclusion chromatography analysis and further analyzed by ESI-MS. ESI-MS showed the retention of aromatic oligomers in the low molecular weight fractions, indicating preferential degradation of the aliphatic units. Phytotoxicity studies, however, indicated no visible damage or inhibitory effects on radish, cress and monocotyledonous oat.

HPLC-ESI-MS was utilized to study the enzymatic degradation process of poly (butylene succinate-*co*-butylene sebacate) and poly(butylene succinate-*co*-butylene adipate) with different compositions by lipase from *Mucor miehei* or *Rhizopus arrhizus* [42]. The hydrolysis resulted in a mixture of water-soluble oligomers. The sequence distribution of the oligomers with same molecular weight and monomer composition could be determined by HPLC-ESI-MS/MS analysis. The results clearly indicated preferential cleavage of ester bonds in the order sebacic, succinic and adipic ester bonds, starting from the most susceptible bond. The results gave indication that lipase catalysis was also active in aqueous solution, which was explained by the hydrophobic effect induced by the aliphatic units in the polyesters. In another study, enzymatic degradation of 2,2′-bis(2-oxazoline)-linked PCL by pancreatic enzymes was followed by HPLC-ESI-MS/MS [43]. With the help of HPLC-ESI-MS/MS the degradation was shown to proceed by surface erosion through hydrolysis of ester bonds, while amide bonds were mainly left intact. A large number of oligomers, altogether 80, were identified with *m/z* values up to 1,350. MS and MS^2 spectra of selected degradation products are shown in Fig. 7. HPLC-ESI-MS/MS was demonstrated to be a rapid and very useful technique for

Fig. 7 Mass spectra of selected enzymatic degradation products from crosslinked PCL. (**a**) MS spectrum of the compounds eluting at retention time 19.78 min and having m/z 719, (**b**) MS^2 spectrum of the same compound, and (**c**) MS^2 spectrum of the compounds eluting at 21.56 min. Reprinted from [43] with permission. Copyright 2008 John Wiley & Sons
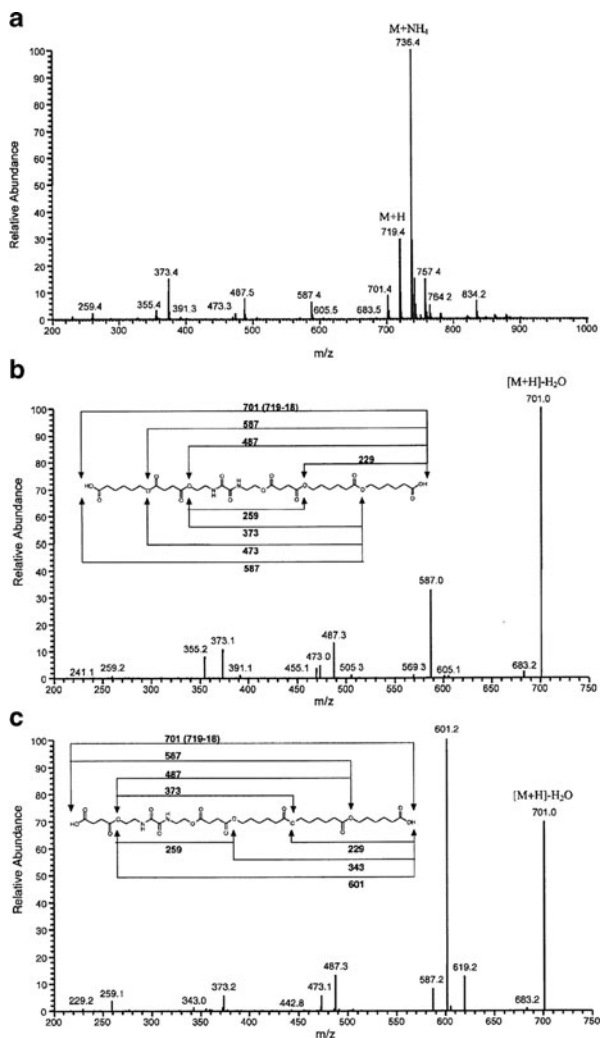
mapping the enzymatic degradation process at different stages, which is difficult to achieve by other techniques.

Enzymatic degradation of polyester amides based on natural amino acids, such as lysine and leucine, was performed by serine proteases (α-chymotrypsin) and proteinase K [44]. The water-soluble degradation products were analyzed by LC-ESI-TOF-MS. Tracking the release of degradation products showed that both α-chymotrypsin and proteinase K had esterase and amidase activity. The polymer was found to degrade at a steady rate in the presence of both enzymes, while the polymer was remarkably stable towards pure chemical hydrolysis. Aerobic biodegradation of PEG was evaluated in wastewater and seawater [45]. The molecular weight of the studied PEGs varied from 250 up to 60,000 g/mol. All the PEGs were

totally biodegraded during 65 days in freshwater media, while the degradation in seawater proceeded much more slowly. With the help of LC-ESI-MS and MALDI-TOF-MS analysis, significant differences in degradation mechanisms could be shown depending on the molecular weight of the materials.

3 Analysis of Medical Materials, Devices and Toys

Medical materials and toys are groups of materials where, for safety reasons, total control is needed over the type and content of low molecular weight compounds. These include compounds intentionally added to achieve certain properties as well as compounds formed due to degradation during synthesis, processing and, for example, sterilization of materials. The formation of ethylene glycol in ethylene oxide-sterilized medical devices is well known. A LC-MS/MS method was developed for detection of residual ethylene glycol in sterilized polymers [46]. In the method, an ammonium adduct of ethylene glycol was detected in the presence of ammonium acetate buffer and methanol. The method allowed quantification of ethylene glycol at levels down to 0.06 μg/mL. The potential of the method was demonstrated by analysis of ethylene glycol in sterilized polyethylene terephthalate fabrics for heart valve sewing rings. Dental composites are suspected of degradation during their lifetime in the oral environment. This degradation can lead to release of potentially toxic compounds such as bisphenol A (BPA). BPA diglycidyl methacrylate (BisGMA) was attached to a porous silicon oxide surface and this simplified model system was subjected to aging in an aqueous environment [47]. With the help of LC-ESI-MS, leaching of BisGMA and several other degradation products containing the BPA moiety were detected after aging of the materials for 2 weeks. No pure BPA was detected, but it could be formed later as a result of further degradation of the released degradation products.

N-Nitrosamines are a group of chemical compounds that can be formed during vulcanization of rubber in the presence of additives such as carbamate accelerators. The presence of *N*-nitrosamine in teats, soothers and child care articles is regulated by Commission Directive 93/11/EEC. LC-MS/MS was proposed and tested as a powerful technique for detection and identification of these compounds in rubber and elastomer teats and soothers [48]. The LC-MS/MS method was developed and validated for simultaneous determination of eight *N*-nitrosamines released into artificial saliva from rubber teats and soothers.

4 Degradation of Coatings and Paints

The application of polymer coatings on different substrate surfaces has great importance both for esthetic reasons and for corrosion protection. Understanding the microstructure of the coating and changes taking place when subjected to

environmental conditions is essential for development of improved coating materials. Polymethacrylates (PMMA), polyacrylates (PA), and polyesters are used in coating and paint formulations where the long-term properties and environmental stability are crucial parameters. In a series of studies, ESI-MS was utilized to fingerprint the degradation of PMMA under different environmental or accelerated conditions (95 °C and/or UV radiation) [49, 50]. ESI-MS analysis of degradation products of saturated and unsaturated poly(methyl methacrylate) model compounds revealed for the first time that PMMA degradation does not exclusively proceed via radical intermediates. The product analysis showed the formation of ethylene oxide-type end-groups after aging of unsaturated model compounds formed by the reaction of oxygen with the vinyl terminal groups. These end-groups were further rearranged under expulsion of formaldehyde and 2-oxo-propanoic acid. The corresponding saturated compounds were stable during the same time period up to 10 months. Combination with UV radiation accelerated the degradation process and resulted also in some degradation of the saturated compounds. Figure 8 shows the ESI-MS spectra and demonstrates the evolution of
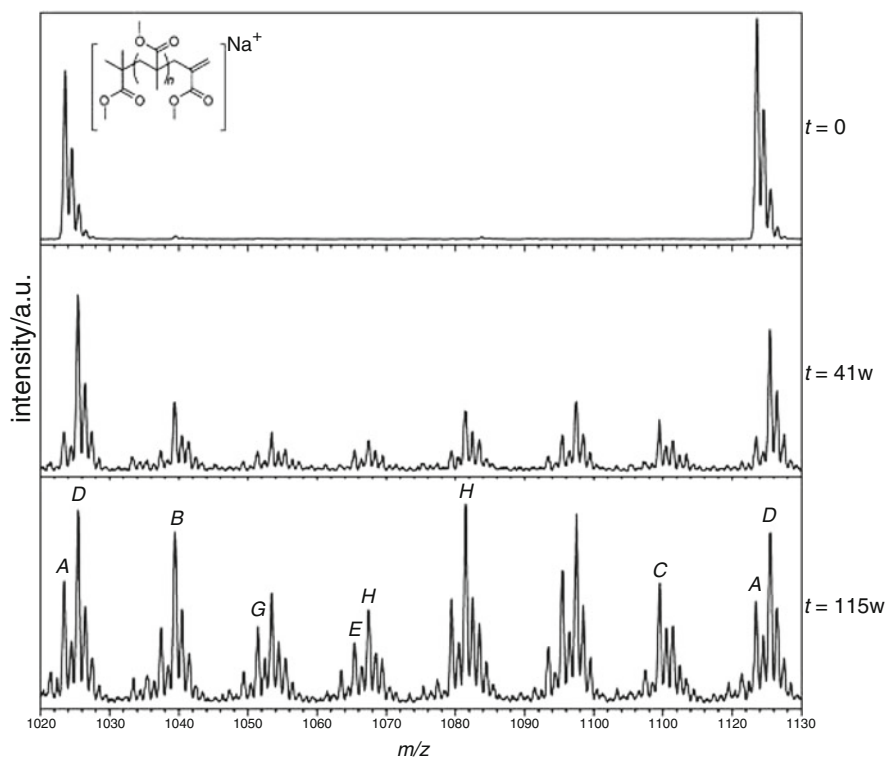
Fig. 8 ESI-MS spectra of vinyl terminated PMMA model compounds before ($t = 0$) and after 41 and 115 weeks of thermal aging at 95 °C. Reprinted from [50] with permission. Copyright 2010 John Wiley & Sons

degradation products as a function of thermal aging of unsaturated PMMA. It was further shown that butyl substituents were lost during the aging, leading to acid side groups [51]. The magnitude of this reaction was related to the side-chain structure as the reaction was more prominent for the compounds with *tert*-butyl groups compared to *n*-butyl groups. Acrylic polymers are also widely used in the artistic field as well as in conservation and restoration. Nano-ESI-MS was shown to be an excellent tool for identifying and characterizing additives such as PEG and poly (propylene glycol) in acrylic paints [52]. Degradation of an isopolyester based on isophthalic acid, glycols, maleic anhydride, cobalt dimethyl aniline and styrene as a crosslinking agent was studied in alkaline environment to simulate aggressive outdoor environments [53]. The LC-ESI-MS analysis showed leaching of low molecular weight compounds such as isophthalic acid from the material to the aging medium.

5   Migration from Food Packaging

Migration studies have an important role in ensuring the safety of polymer packaging in contact with different foodstuffs during storage and processing of food inside the polymer package. Gas chromatography and LC often coupled to a mass spectrometer have been applied in numerous studies for the identification of various migrants from polymer packaging, food simulants and/or real foods. ESI-MS has emerged as an attractive compliment to these analyses. It can be utilized alone for rapid direct analysis of liquid samples such as food simulants or it can be utilized as a detector for LC. A big advantage of ESI-MS compared to GC-MS or HPLC is that it can be applied for rapid screening of unknown compounds because it is less selective concerning the volatility and polarity of the compounds to be identified, which facilitates the detection of unknown non-intentionally added compounds in food packaging.

5.1   Direct Electrospray Ionization–Mass Spectrometry Analysis

Direct ESI-MS analysis of food simulants was recently demonstrated as a useful tool for studying migration from polymer packaging to food simulants [54]. The complexity of the resulting ESI-MS spectra clearly correlated with overall migration values. Compared to GC-MS analysis of the same samples, migrants with lower volatility could be detected. including polymer additives such as low molecular weight PEG. Figure 9 shows ESI-MS spectra of the compounds that migrated from random polypropylene copolymer (PP-R) to different food simulants during 1 h of microwave heating in contact with food simulants including water, 10% ethanol, 96% ethanol and 90/10 isooctane/ethanol. In addition, comparison of the ESI-MS spectra of the migrants from PP-R after 1 h of conventional heating and 1 h
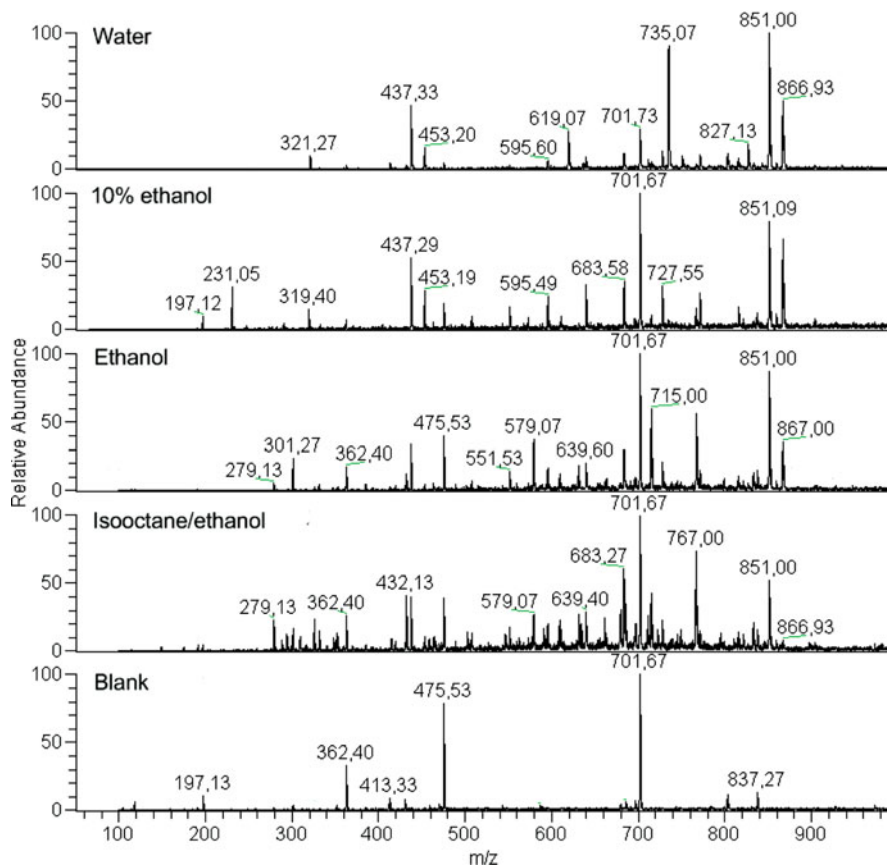
Fig. 9 ESI-MS spectra showing the compounds that migrated from PP-R into water, 10% ethanol, ethanol, and 90/10 isooctane food simulants during 1 h of microwave heating. The blank sample consisted of 90/10 isooctane/ethanol, which was microwave heated for 1 h at 80 °C. Reprinted from [54] with permission. Copyright 2011 American Chemical Society

of microwave heating clearly showed that significant antioxidant degradation took place during microwave heating in contact with fatty food simulants (Fig. 10). This degradation did not take place or was insignificant during heating at the same temperature without the microwaves. In another study, the large overall migration values during storage of PLA in contact with 96% ethanol food simulant could be explained because the ESI-MS showed migration of cyclic oligomers from PLA to ethanol. Due to solubility limitations, these compounds did not migrate to the other studied food simulants (water, 3% acetic acid, 10% ethanol and isooctane), which agreed with the considerably lower overall migration values (Bor, Alin, and Hakkarainen; unpublished results). The study also showed the higher stability of stereocomplex PLA in comparison with the regular PLLA during storage in contact with the food simulants.
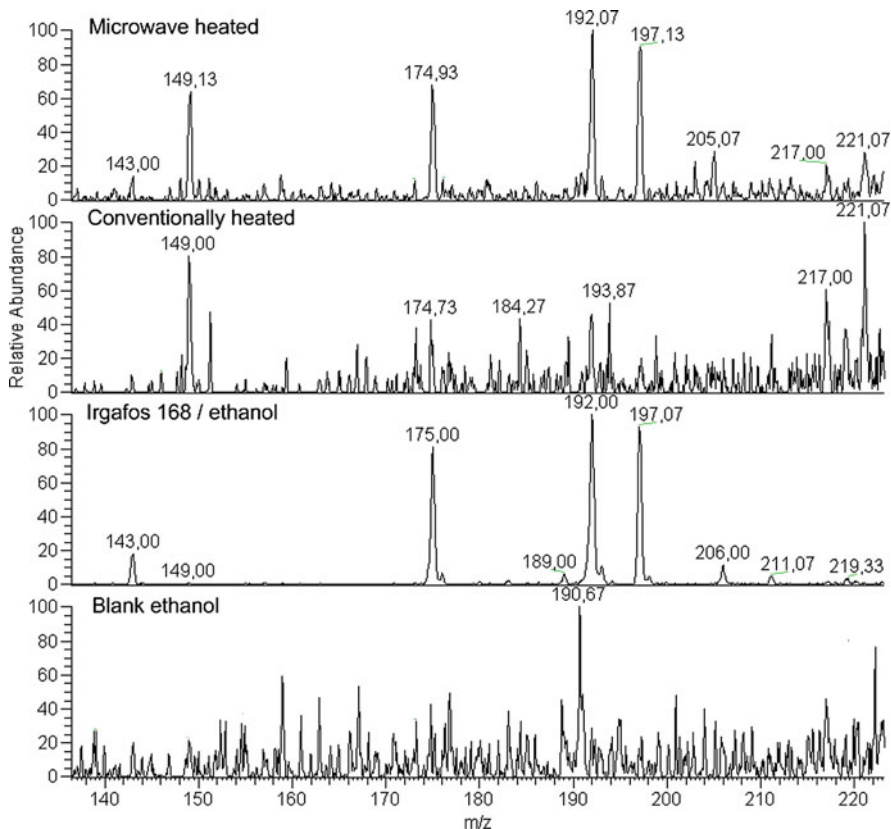
Fig. 10 ESI-MS spectra of (from *top* to *bottom*) 90/10 isooctane/ethanol extract of PP-R heated with microwaves, 90/10 isooctane/ethanol extract of PP-R heated conventionally, microwave-heated standard of Irgafos 168 (in ethanol), and conventionally heated ethanol blank sample. Samples and standard were heated for 1 h at 80 °C. The spectrum of microwave-heated PP-R have peaks corresponding to the degradation products from Irgafos 168. Reprinted from [54] with permission. Copyright 2011 American Chemical Society

5.2 Liquid Chromatography–Electrospray Ionization–Mass Spectrometry Analysis

Several studies utilized LC-ESI-MS for determination of various polymer additives or contaminants migrating from polymeric food packaging. The migration of the potential endocrine disrupter BPA from baby bottles into aqueous food simulants was studied by LC-ESI-MS [55]. The study showed that temperature was an important factor in controlling the migration of BPA from plastic bottles to water. However, the BPA released was decreased after repeated sterilization and use

cycles, indicating that the initial BPA release is due to residual BPA in the bottles and not caused by polymer degradation in hot water. LC coupled with negative ion ESI-MS/MS was also compared with positive ion ESI-MS for identification of bisphenolic migrants from can coatings [56]. LC-ESI-MS analysis in combination with elemental and NMR analysis allowed the identification of two compounds, which co-eluted with BPA and disturbed the LC analysis, as oxidized forms of epoxy can coating monomer.

Epoxidized soybean oil (ESBO) is a commonly used plasticizer/stabilizer in, e.g., polyvinyl chloride. It is used especially in food closure gaskets for metal lids and could migrate from them into the food in sealed glass jars. The main product of poly(vinyl chloride) (PVC) degradation, HCl, could react with ESBO to produce mono-and polychlorohydrins with unknown health effects. A method based on ultra-performance liquid chromatography (UPLC) coupled to ESI-MS was developed and allowed the detection of trace amounts of chlorohydrins in foodstuffs originating from ESBO [57]. Several potential mono-and dichlorohydrins were separated and identified, some of which were also detected in commercial foods at low concentrations. In another study, migration of polyadipates and their degradation products (also potential migrants from polyvinyl chloride used in lid gaskets of glass jars) into different food simulants was determined by LC-ESI-TOF-MS [58]. The direct determination of the polyadipate oligomers was complicated due to the large number of detected peaks. However, a rapid method for determination of adipic acid after alkaline hydrolysis was developed. In addition, a LC-ESI-MS/MS method was developed for the detection of different phthalates in milk and milk products including infant formulas [59]. Before analysis, the phthalates were extracted by organic solvent and separated from the milk fats.

Low level ink photo-initiator residues were determined by LC-ESI-MS/MS in milk packaged in carton or plastic [60]. The developed quantitative method allowed simultaneous quantification of several photo-initiator residues including, e.g., benzophenone, isopropylthioxanthone (ITX), 2-ethylhexyl-(4-dimethylamino)benzoate (EHA) and others. The method was applied to analysis of real samples of different fat contents and showed that benzophenone and ITX were the most important contaminants in these samples. GC-MS, LC-ESI-MS and LC-atmospheric pressure photoionization (APPI)-MS/MS were also utilized for identification of ink photo-initiators in packaged beverages [61]. Altogether, 40 packages and liquid foods were analyzed and benzophenone was found to be a common contaminant in most of the studied samples. UPLC-ESI-TOF-MS demonstrated strong potential as a screening tool for identification of adhesive compounds from polymer packaging [62]. Several acrylic adhesive formulations were extracted and analyzed by UPLC-TOF-MS. The possibility of obtaining full-mass spectra as well as fragmentation of each single-mass provides a powerful tool, even for analysis of a wide range of other unknown compounds in other complex sample matrixes.

6 Analysis of Antioxidants, Light Stabilizers, and Flame Retardants

In many applications, polymers need to be effectively stabilized against thermo-oxidative and/or photo-oxidative degradation. Considerable savings could be achieved through development of more effective antioxidants and light stabilizers. One step is a better understanding of the stabilization mechanisms. Hindered amine light stabilizers (HALS) are among the most effective antioxidants for polymeric systems. However, how they function in polymeric materials is still not totally understood. ESI-MS/MS was applied as a new tool for structural identification of standard HALS and its modifications formed through oxidation to better understand the mechanisms of stabilization [63]. In addition, the HALS species present in an extract from polyester-based coil coating were identified. With the help of MS/MS some degradation products were also identified. Figure 11 shows the ESI-MS/MS spectra conducted on $[M + H]^+$ ions of four different HALS. It was shown that all the studied piperidine-based HALS produced m/z 123 upon fragmentation. This ion could thus be utilized during analysis of extracts from polymers. ESI-MS was shown to be a very promising technique that could be more widely applied in the coatings industry to elucidate stabilization mechanisms and to develop improved formulations with optimized type and concentration of HALS.

ESI-MS was utilized for evaluating the mechanism of stabilization of chlorinated PVC by pentaerythritol/calcium-zinc stearate mixtures [64]. After aging at 185 °C under 40 rpm for 4 or 12 min, a significant number of reactions were detected and ESI-MS results indicated that oligomerization and chlorination of pentaerythritol had taken place. This indicates that pentaerythritol reacts with HCl, removing its harmful catalytic effect on PVC. It was also shown that addition of pentaerythritol considerably improved the stabilization effect of calcium and zinc stearates, but only exhibited a slight stabilizing effect if added alone. A LC-ESI-MS/MS method was developed and presented for the analysis organophosphorus flame retardants and plasticizers in wastewater samples [65]. This method allowed the determination of 11 different organophosphorus compounds with quantification limits after a solid-phase extraction concentration step of 3–80 ng/L. Direct LC-ESI-MS/MS analysis without a concentrations step allowed the detection of compounds in the low microgram per liter range, which in many cases is adequate. The method was successfully applied for the analysis of a municipal wastewater sample in which six phosphoric acid triesters were detected. LC-ESI-MS/MS was also shown suitable for the analysis of phthalates in house dust [66].

7 Radiation Effects on Polymers in the Nuclear Industry

PVC, polyurethanes and polyethers are frequently used in the nuclear industry where they are radiolyzed and as a result could undergo degradative processes. In a series of papers, the radiation effects on polyethers and polyether urethanes were evaluated.
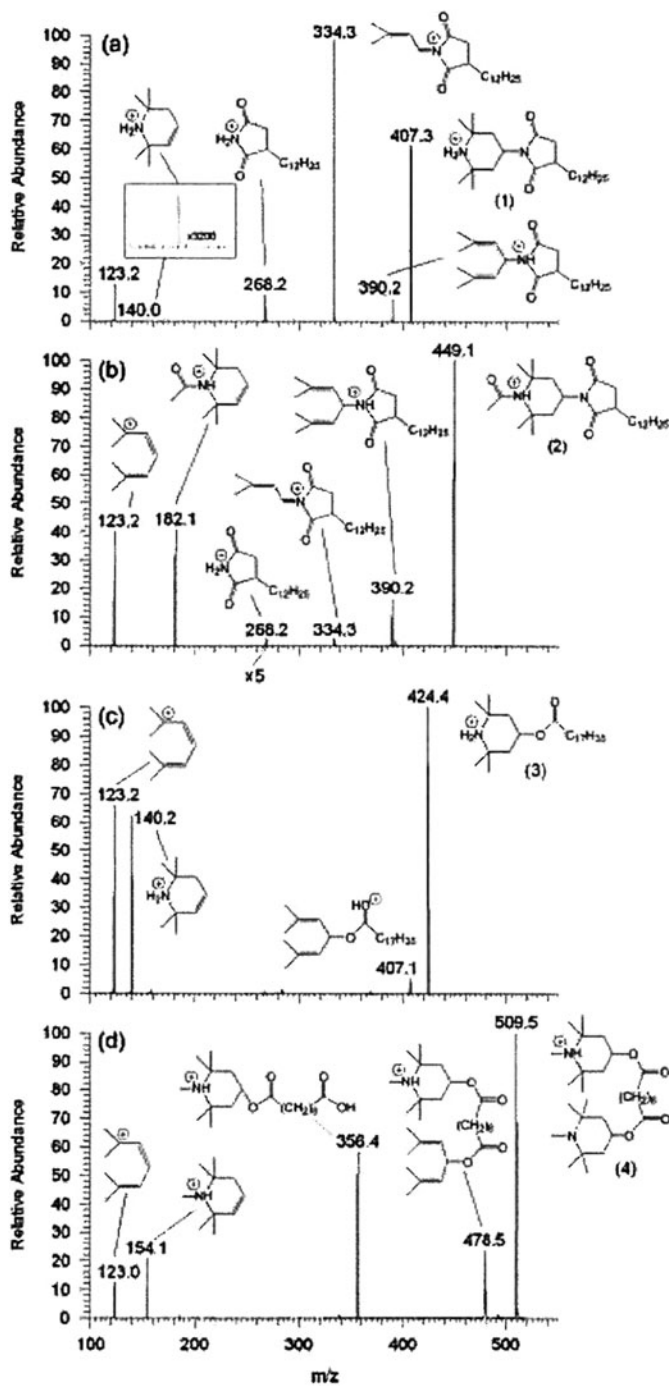
Fig. 11 ESI-MS/MS spectra conducted on [M + H]⁺ ion of (**a**) HALS SANDUVOR 3055, (**b**) HALS SADUVOR 3058, (**c**) HALS CYASORB 3853, and (**d**) HALS TINUVIN 292 using a linear ion-trap mass spectrometer. Reprinted from [63] with permission. Copyright 2010 John Wiley & Sons

ESI-MS provided new insights into the degradation mechanisms of these materials. Aromatic polyether urethanes were subjected to high-energy radiation under oxygen atmosphere to predict the long-term behavior during a nuclear waste storage [67]. ESI-MS together with electron paramagnetic resonance (EPR) and Fourier transform infrared spectroscopy (FTIR) were utilized to propose an accurate degradation mechanism, which was then utilized to develop a predictive model of what would happen under long-term radio-oxidation. It was found that degradation mainly occurred at urethane bonds and in polyether soft segments, which resulted in the formation of formates, alcohols and carboxylic acids as stable degradation products. In addition to chain scission, crosslinking was a competing reaction during radiation.

Radiation effects were further evaluated with the help of low molecular weight model polyether–poly(tetramethylene glycol) (PTMG) and a degradation mechanism was proposed [68]. Figure 12 shows examples of ESI-MS mass spectra obtained after analysis of pristine and irradiated samples at different doses. For the pristine samples, the most intense peaks corresponded to the initial mass distribution of the oligomeric PTMG compounds. After irradiation, the mass spectra became more complex as many new peaks appeared, resulting in mass spectra with around 700 peaks representing both single and multiply charged ions. The most intense series of degradation products were identified with the help of ESI-MS and FTIR as formates and crosslinked species. Radiolysis of polyurethanes was further studied by ESI-MS and desorption electrospray ionization mass spectrometry (DESI-MS) [69]. The surface analysis of the irradiated polyurethane by DESI-MS revealed similar products as the analysis of methanol extracts by ESI-MS. The sensitivity of DESI-MS was lower, but nevertheless it allowed the analysis of irradiation products directly on the polymer surface without any sample preparation. The analysis also showed that similar degradation products are formed at the surface and in the bulk of the materials.
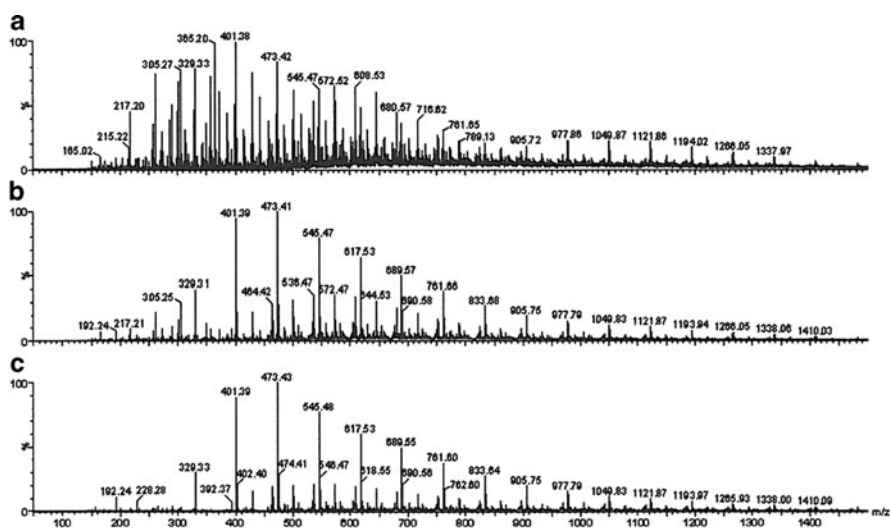
Fig. 12 ESI-MS analysis of PTMG after 380 kGy (**a**) and 94 kGy (**b**) doses of irradiation as well as the original spectra (**c**). Reprinted from [68] with permission. Copyright 2011 Elsevier

8 Degradation of Polymer Electrolyte Membranes

The polymer electrolyte membranes are susceptible to degradation caused by hydroxyl and peroxyl radicals formed by (electro)chemical side reactions. Understanding these processes and prevention of polymer electrolyte membrane degradation are crucial for the development of improved future membranes. In two interesting studies, LC-ESI-MS/MS and ESI-MS were applied for the analysis of degradation products from polymer electrolyte membrane fuel cells [70, 71]. The authors performed systematic method development for separation and identification of structurally similar compounds, such as 4-hydroxybenzoic acid, isophthalic acid, terephthalic acid, 4-hydrobenzaldehyde and 4-formylbenzoic acid. In addition, screening for unknown compounds in the product water of the fuel cell was performed by LC-MS. The developed ESI-MS method could be very valuable for real-time in situ membrane degradation product monitoring. This could allow the identification of relationships between fuel cell operating parameters and the resulting degradation products, giving insights into the membrane processes.

9 Structural Analysis and Recycling Through Controlled Degradation

A rapid method leading to complete hydrolytic degradation of polyester urethane acrylates was developed by utilizing a microwave instrument [72]. The method was applied in order to understand the structure and hydrolytic degradation of poly(2-hydroxylethyl methacrylate), poly(L-lactide-*co*-glycolide) diol and their copolymers. The degradation products were collected quantitatively and analyzed by NMR, size exclusion chromatography and HPLC-ESI-TOF-MS to elucidate the structure and hydrolysis process of these crosslinked materials. In another study, a recycling method for waste tires, causing considerable environmental pollution, was developed and evaluated. In a search for an effective recycling method, natural rubber was oxidized with the help of sodium tungstate, acetic acid, and hydrogen peroxide to prepare telechelic epoxidized liquid natural rubber (TELNR) [73]. With the help of ESI-MS analysis it was proposed that the catalysis proceeds via a tungstic anion, which is a mononuclear tungsten peroxo-species with a coordinated peracetyl/acetyl group.

10 Future Perspectives

ESI-MS has emerged as a relatively new tool for polymer degradation analysis. ESI-MS has already in many studies been utilized for structural characterization of polymers, including analysis of chemical structures and end-groups as well as copolymer microstructures, but its application to polymer degradation studies is

still scarce. The potential of the technique is, however, enormous as demonstrated by the examples summarized in this review. Wider utilization of ESI-MS, and mass spectrometric tools in general, for tracking the molecular level changes taking place in polymers during different stages of their lifecycle could significantly contribute to faster development of better functioning and more sustainable polymeric materials. Further development of instruments interfaced with ESI-MS will probably allow detection of broaden ranges of products, and utilization of mass analyzers such as Fourier transform ion cyclotron resonance will further enhance the possibilities. In numerous applications, ESI-MS can offer improved understanding of polymers and their long-term properties as well as the interactions between polymers and their environment. This will further promote the development of polymers for controlled optimum life times, whether we require materials with improved long-term properties and durability, or environmentally benign degradable polymers.

References

1. Hart-Smith G, Barner-Kowollik C (2010) Contemporary mass spectrometry and the analysis of synthetic polymers: trends, techniques and untapped potential. Trends Polymer Sci 211: 1507–1529
2. Weidner SM, Trimpin S (2008) Mass spectrometry of synthetic polymers. Anal Chem 80:4349–4361
3. Weidner SM, Trimpin S (2010) Mass spectrometry of synthetic polymers. Anal Chem 82:4811–4829
4. Hart-Smith G, Lammens M, Du Prez FE, Guilhaus M (2009) ATRP poly(acrylate) star formation: a comparative study between MALDI and ESI MS mass spectrometry. Polymer 50:1986–2000
5. Jackson AT, Slade SE, Thalassinos K, Scrivens JH (2008) End-group characterization of poly (propylene glycol)s by means of electrospray ionization-tandem mass spectrometry (ESI-MS/MS). Anal Bioanal Chem 392:643–650
6. Song J, van Velde JW, Vertommen LLT, Smith DF, Heeren RMA, van den Brink OF (2010) End-group analysis by methacrylic (co)polymers by LC-ESI-MS2. Macromolecules 44:1319–1326
7. Szablan Z, Lovestad TM, Davis TP, Stenzel MH, Barner-Kowollik C (2007) Mapping free radical reactivity: a high-resolution electrospray ionization-mass spectrometry study of photoinitiation processes in methyl methacrylate free radical polymerization. Macromolecules 40:26–39
8. Hart-Smith G, Lovestad TM, Davis TP, Stenzel MH, Barner-Kowollik C (2007) Mapping formation pathways and end group patterns of stimuli-responsive polymer systems via high-resolution electrospray ionization mass spectrometry. Biomacromolecules 8:2404–2415
9. Richardson S, Cohen A, Gorton L (2001) High-performance anion-exchange chromatography-electrospray mass spectrometry for investigation of substituent distribution in hydroxy-propylated potato amylopectin starch. J Chromatogr A 917:111–121
10. Cerqueira MA, Souza BWS, Simoes J, Teixeira JA, Domingues MRM, Coimbra MA, Vicente AA (2011) Structural and thermal characterization of galactomannans from non-conventional sources. Carbohydr Polym 83:179–185

11. Hakkarainen M, Albertsson A-C, Karlsson S (1996) Weight losses and molecular weight changes correlated with the evolution of hydroxyacids in simulated in vivo degradation of homo-and copolymers of PLA and PGA. Polym Degrad Stab 52:283–291
12. Hakkarainen M, Albertsson A-C (2002) Heterogenous biodegradation of polycaprolactone – low molecular weight products and surface changes. Macromol Chem Phys 203:1357–1363
13. Codari F, Moscatelli D, Storti G, Morbidelli M (2010) Characterization of low-molecular-weight PLA using HPLC. Macromol Mater Eng 295:58–66
14. Adamus G (2009) Molecular level structure of (R, S)-3-hydroxybutyrate/(R, S)-3-hydroxy-4-ethoxybutyrate copolyesters with dissimilar architecture. Macromolecules 42:4547–4557
15. Graca J, Santos S (2006) Linear aliphatic dimeric esters from cork suberin. Biomacromolecules 7:2003–2010
16. Graca J, Lamosa P (2010) Linear and branched poly(ω-hydroxyacid) esters in plant cutins. J Agric Food Sci 58:9666–9674
17. Barbuzzi T, Giuffraida M, Impallomeni G, Carnazza S, Ferreri A, Guglielmino SPP, Ballistreri A (2004) Microbial synthesis of poly(3-hydroxyalkanoates) by *Pseudomonas aeruginosa* from fatty acids: identification of higher monomer units and structural characterization. Biomacromolecules 5:2469–2478
18. Höglund A, Albertsson A-C (2008) Spontaneous crosslinking of poly(1,5-dioxepan-2-one) originating from ether bond fragmentation. J Polym Sci A Polym Chem 46:7258–7267
19. Harrison JJ, Onopchenko A, Cheng MT, Chan CY (2000) Vinyl ether end-groups in poly (ethylene glycol)s from the Na2CO3-promoted degradation of 1,3-dioxolan-2-one polymers. J Polym Sci A Polym Chem 38:152–160
20. Rizzarelli P, Zampino D, Ferreri L, Impallomeni G (2011) Direct electrospray ionization mass spectrometry quantitative analysis of sebacic and terepthalic acids in biodegradable polymers. Anal Chem 83:654–660
21. Murillo EA, Vallejo PP, Lopez BL (2010) Characterization of hydroxylated hyperbranched polyesters of fourth and fifth generation. e-polymers 120:112
22. Osaka I, Yoshimoto A, Watanabe M, Takama M, Murakami M, Kawasaki H, Arakawa R (2008) J Chromatogr B 870:247–250
23. Osaka I, Watanabe M, Takama M, Murakami M, Arakawa R (2006) Characterization of linear and cyclic polylactic acids and their solvolysis products by electrospray ionization mass spectrometry. J Mass Spectrom 41:1369–1377
24. Song J, Siskova A, Simons MG, Kowalski WJ, Kowalczuk MM, van den Brink OF (2011) LC-multistage mass spectrometry for the characterization of poly(butylenes adipate-co-butylene terephthalate) copolyester. J Am Soc Mass Spectrom 22:641–648
25. Li S, Dobrzynski P, Kasperczyk J, Bero M, Braud C, Vert M (2005) Structure–property relationships of copolymers obtained by ring-opening polymerization of glycolide and e-caprolactone. Part 2. Influence of composition and chain microstructure on the hydrolytic degradation. Biomacromolecules 6:489–497
26. Kasperczyk J, Li S, Jaworska J, Dobrzynski P, Vert M (2008) Degradation of copolymers obtained by ring-opening polymerization of glycolide and e-caprolactone: a high resolution NMR and ESI-MS study. Polym Degrad Stab 93:990–999
27. Hakkarainen M, Adamus G, Höglund A, Kowalczuk M, Albertsson A-C (2008) ESI-MS reveals the influence of hydrophilicity and architecture on the water-soluble degradation product patterns of biodegradable homo- and copolyesters of 1,5-dioxepan-2-one and ε-caprolactone. Macromolecules 41:3547–3554
28. Höglund A, Hakkarainen M, Kowalczuk M, Adamus G, Albertsson A-C (2008) Fingerprinting the degradation product patterns of different polyester-ether networks by electrospray ionization mass spectrometry. J Polym Sci A Polym Chem 46:4617–4629
29. Theiler S, Teske M, Keul H, Sternberg K, Moller M (2010) Synthesis, characterization and in vitro degradation of 3D-microstructured poly(epsilon-caprolactone) resins. Polym Chem 1:1215–1225

30. Hakkarainen M (2002) Aliphatic polyesters: abiotic and biotic degradation and degradation products. Adv Polym Sci 157:113–138

31. Andersson SR, Hakkarainen M, Inkinen S, Södergård A, Albertsson A-C (2010) Polylactide stereocomplexation leads to higher hydrolytic stability but more acidic hydrolysis product pattern. Biomacromolecules 11:1067–1073

32. Andersson SR, Hakkarainen M, Albertsson A-C (2010) Tuning the polylactide hydrolysis rate by plasticizer architecture and hydrophilicity without introducing new migrants. Biomacromolecules 11:3617–3623

33. Höglund A, Hakkarainen M, Albertsson A-C (2010) Migration and hydrolysis of hydrophobic polylactide plasticizer. Biomacromolecules 11:277–283

34. Höglund A, Hakkarainen M, Edlund U, Albertsson A-C (2010) Surface modification changes the degradation process and degradation product pattern of polylactide. Langmuir 26:378–383

35. Trimaille T, Möller M (2006) Poly(hexyl-substituted lactides): novel injectable hydrophobic drug delivery systems. J Biomed Mater Res 80A:55–65

36. Li SM, Garreau H, Vert M (1990) Structure–property relationships in the case of the degradation of massive aliphatic poly-(α-hydroxy acids) in aqueous media. J Mater Sci Mater Med 1:123–130

37. Höglund A, Hakkarainen M, Albertsson A-C (2007) Degradation Profile of poly (ε-caprolactone) – the influence of macroscopic and macromolecular biomaterial design. J Macromol Sci A 44:1041–1046

38. Odelius K, Höglund A, Kumar S, Hakkarainen M, Ghosh AK, Bhatnagar N, Albertsson A-C (2011) Porosity and pore size regulate the degradation product profile of polylactide. Biomacromolecules 12:1250–1258

39. Scandola M, Focarete ML, Adamus G, Sikorska W, Baranowska I, Swierczek S, Gnatowski M, Kowalczuk M, Jedlinski Z (1997) Polymer blends of natural poly(3-hydroxybutyrate-co-3-hydroxyvalerate) and a synthetic atactic poly(3-hydroxybutyrate). Characterization and biodegradation studies. Macromolecules 30:2568–2574

40. Focarete ML, Scandola M, Jendrossek D, Adamus G, Sikorska W, Kowalczuk M (1999) Bioassimilation of atactic poly[(R, S)-3-hydroxybutyrate] oligomers by selected bacterial strains. Macromolecules 32:4814–4818

41. Rychter P, Kawalec M, Sobota M, Kurcok P, Kowalczuk M (2010) Study of aliphatic-aromatic copolyester degradation in sandy soil and its ecotoxicological impact. Biomacromolecules 11:839–847

42. Raizzarelli P, Impallomeni G (2004) Evidence of selective hydrolysis of aliphatic copolyesters induced by lipase catalysis. Biomacromolecules 5:433–444

43. Pulkkinen M, Palmgren JJ, Auriola S, Malin M, Seppälä J, Järvinen K (2008) Rapid Commun Mass Spectrom 22:121–129

44. Ghaffar A, Draaisma GJJ, Mihov G, Dias AA, Schoenmakers J, van der Wal SJ (2011) Monitoring the in vitro enzyme-mediated degradation of degradable poly(ester amide) for controlled drug delivery by LC-ToF-MS. Biomacromolecules. doi:10.1021/bm200709r

45. Bernhard M, Eubeler JP, Zok S, Knepper TP (2008) Aerobic biodegradation of polyethylene glycols of different molecular weights in wastewater and seawater. Water Res 42:4791–4801

46. Hari PR, Naseerali CP, Sreenivasan K (2009) A sensitive estimation of residual ethylene glycol in ethylene oxide sterilized medical devices by HPLC with electrospray ionization mass spectrometric detection. J Chromatogr B 877:328–332

47. Koin PJ, Kilislioglu A, Zhou M, Drummond JL, Hanley L (2008) Analysis of the degradation of a model dental composite. J Dent Res 87:661–665

48. Sung JH, Kwak IS, Park SK, Kim HI, Lim HS, Park HJ, Kim SH (2010) Liquid chromatography-tandem mass spectrometry determination of N-nitrosamines released from rubber or elastomer teats and soothers. Food Addit Contam 27:1745–1754

49. Bennet F, Lovestead TM, Barker PJ, Davis TP, Stenzel MH, Berner-Kowollik C (2007) Degradation of poly(methyl methacrylate) model compounds at constant elevated temperature

studied via high resolution electrospray ionization mass spectrometry (ESI-MS). Macromol Rapid Commun 28:1593–1600

50. Bennet F, Hart-Smith G, Gruendling T, Davis TP, Barker PJ, Barner-Kowoolik C (2010) Macromol Chem Phys 211:1083–1097

51. Soeriyadi AH, Bennet F, Whittaker MR, Barker PJ, Barner-Kowollik C, Davis TP (2011) Degradation of poly(butyl methacrylate) model compounds studied via high-resolution electrospray ionization mass spectrometry. J Polym Sci A Polym Chem 49:848–861

52. Hoogland FG, Boon JJ (2009) Development of MALDI-MS and nano-ESI-MS methodology for the full identification of poly(ethylene glycol) additives in artists' acrylic paints. Int J Mass Spectrom 284:66–71

53. Raghavan D, Egwim K (2000) Degradation of polyester film in alkali solution. J Appl Polym Sci 78:2454–2463

54. Alin M, Hakkarainen M (2011) Microwave heating causes rapid degradation of antioxidants in polypropylene packaging, leading to greatly increased specific migration to food simulants as shown by ESI-MS and GC-MS. J Agric Food Chem 59:5418–5427

55. Maragou NC, Makri A, Lampi EN, Thomaidis NS, Koupparis MA (2008) Migration of bisphenol A from polycarbonate baby bottles under real use conditions. Food Addit Contam 25:373–383

56. Ackerman LK, Noonan GO, Begley TH, Mazzola EP (2011) Accurate mass and nuclear magnetic resonance identification of bisphenolic can coating migrants and their interference with liquid chromatography/tandem mass spectrometric analysis of bisphenol A+. Rapid Commun Mass Spectrom 25:1336–1342

57. Suman M, De Dominicis E, Commissati I (2010) Trace detection of the chlorohydrins of epoxidized soybean oil in foodstuffs by UPLC-ESI-MS/MS. J Mass Spectrom 45:996–1002

58. Driffield M, Bradley EL, Harmer N, Castle L, Klump S, Mottier P (2010) Determination of polyadipates migrating from lid gaskets of glass jars. Hydrolysis to adipic acid and measurements by LC-MS/MS. Food Addit Contam 27:1487–1495

59. Sorensen LK (2006) Determination of phthalates in milk and milk products by liquid chromatography/tandem mass spectrometry. Rapid Commun Mass Spectrom 20:1135–1143

60. Shen D-X, Lian H-Z, Ding T, Xu J-Z, Shen C-Y (2009) Determination of low-level ink photoinitiator residues in packaged milk by solid-phase extraction and LC-ESI/MS/MS using triple-quadrupole mass analyzer. Anal Bioanal Chem 395:2359–2370

61. Sagratini G, Caprioli G, Crstalli G, Giardina D, Ricciutelli M, Volpini R, Zuo Y, Vittori S (2008) Determination of ink photoinitiators in packaged beverages by gas chromatography–mass spectrometry and liquid chromatography-mass spectrometry. J Chromatogr A 1194:213–220

62. Canellas E, Nerin C, Moore R, Silcock P (2010) New UPLC coupled to mass spectrometry approaches for screening of non-volatile compounds as potential migrants from adhesives used in food packaging materials. Anal Chim Acta 666:62–69

63. Lowe TA, Paine MRL, Marshall DL, Hich LA, Boge JA, Barker PJ, Blanksby SJ (2010) Structural identification of hindered amine light stabilizers in coil coatings using electrospray ionization tandem mass spectrometry. J Mass Spectrom 45:486–495

64. Liao X, He B, Chen X (2011) Chlorinated poly(vinyl chloride) stabilization by pentaerythritol/calcium-zinc stearate mixtures: the fate of pentaerythritol. J Vinyl Addit Technol 17:1–8

65. Rodil R, Quintana JB, Reemtsma T (2005) Liquid chromatography-tandem mass spectrometry determination of nonionic organophosphorus flame retardants and plasticizers in wastewater samples. Anal Chem 77:3083–3089

66. Abb M, Heinrich T, Sorkau E, Lorenz W (2009) Phthalates in house dust. Environ Int 35:965–970

67. Dannoux A, Esnouf S, Amekraz B, Dauvois V, Moulin C (2008) Degradation mechanism of poly(ether-urethane) estane ® induced by high-energy radiation. II. Oxidation effects. J Polym Sci B Polym Phys 46:861–878

68. Aymes-Chodur C, Dannoux A, Dauvois V, Esnouf S (2011) Radiation effects on a linear model compound for polyethers. Polym Degrad Stab 96:1225–1235
69. Bonnaire N, Dannoux A, Pernelle C, Amekraz B, Moulin C (2010) On the use of electrospray ionization and desorption electrospray ionization mass spectrometry for bulk and surface polymer analysis. Appl Spectrosc 64:810–818
70. Zedda M, Tuerk J, Teutenberg T, Peil S, Schmidt TC (2009) A strategy for the systematic development of a liquid chromatographic mass spectrometric screening method for polymer electrolyte membrane degradation products using isocratic and gradient phase optimized liquid chromatography. J Chromatogr A 1216:8910–8917
71. Zedda M, Tuerk J, Peil S, Schmidt TC (2010) Determination of polymer electrolyte membrane (PEM) degradation products in fuel cell water using electrospray ionization tandem mass spectrometry. Rapid Commun Mass Spectrom 24:3531–3538
72. Ghaffar A, Verschuren PG, Geenevasen JAJ, Handels T, Berard J, Plum B, Dias AA, Schoenmakers PJ, Van der Wal SJ (2011) Fast in vitro hydrolytic degradation of polyester urethane acrylate biomaterials: structure elucidation, separation and quantification of degradation products. J Chromatogr A 1218:449–458
73. Zhang J, Zhou Q, Jiang X-H, Du A-K, Zhao T, van Kasteren WY-Z (2010) Oxidation of natural rubber using a sodium tungstate/acetic acid/hydrogen peroxide catalytic system. Polym Degrad Stab 95:1077–1082

Index